Investigating several putative mitochondrial pumps in *Saccharomyces cerevisiae*

by

Md Deen Islam

A Thesis Submitted to the Faculty of Graduate Studies of

The University of Manitoba

in partial fulfilment of the requirements of the degree of

MASTER OF SCIENCE

Department of Microbiology

University of Manitoba

Winnipeg

Copyright © 2021 by Md Deen Islam

Abstract

Resistance to antifungal drugs is an increasingly significant clinical problem. The most common antifungal resistance encountered is efflux pump-mediated resistance. Members of the major facilitator superfamily (MFS) are more prevalent than the ATP-binding cassette (ABC) multidrug transporters among *Saccharomyces cerevisiae* and clinically important fungi. Even though fungi can withstand various environmental selective pressures due to their ecological, morphological, and biological plasticity, there is no established association of antifungal resistance with fungal mitochondrial MFS. Here, we have hypothesized that fungal mitochondria will contain efflux pumps of the major facilitator superfamily (MFS) that could participate in antimicrobial resistance. We are interested in investigating this phenomenon in fungal mitochondria. In one approach, we have cloned and expressed a set of *S. cerevisiae* transporters of the MFS namely Transporter of Polyamines (Tpo1 to Tpo5) and Hexose transporter (Hxt5), some of which are localized in mitochondria, in an *Escherichia coli* expression system. Following optimization of expression in *E. coli*, we have carried out the functional analysis of these putative pumps to determine the specific substrates using mitochondria-targeting antibiotics. We have shown chloramphenicol (CAP) and erythromycin (ERY) as potential substrates of Tpo1 and Tpo3 using indirect assays (antibiotic susceptibility testing). However, we were unable to establish if these proteins were efflux pumps using a direct ethidium bromide (EtBr) accumulation assay. In another approach, we have examined *S. cerevisiae* BY4741 strains that each are missing one of the pumps from Tpo1 to Tpo4. We tested if the absence of a pump causes increased susceptibility to antibiotics. We have shown that Tpo3 is likely involved in protecting yeast cells from CAP and ERY, and this is supported by qualitative results measuring growth phenotype and quantitative results of growth kinetics. Finally, we could demonstrate evidence for efflux of EtBr by *Neurospora crassa* wild-

type (WT) mitochondria, but EtBr efflux could not be shown for *S. cerevisiae* BY4741 mitochondria. We anticipate our study is a starting point for future *in-vivo* models to look into mitochondrial drug accumulation and efflux-mediated resistance in fungi.

Acknowledgements

I would like to dedicate this work to my mother Anowara Begum, who has single-handedly brought me up. Thank you ‘Ma’ for believing in me and letting me come this far away from you. I would also like to acknowledge my wife Sabrin Bashar for being there for me during the good and bad times of my master's life.

This work could not have been possible without the support of my supervisor Dr. Court, without her endless patience and care in guiding me I would have been lost. She made me feel independent while planning my experiment and courageous on how to face failures. So thank you for being my supervisor and having me in your lab. I would like to thank my advisory committee members, Dr. Ayush Kumar and Dr. Denice Bay. Thank you for your suggestions and for allowing me to use your lab equipment and materials.

I would like to thank the funding agencies that made this work possible. The present work was funded by the Natural Science and Engineering Council of Canada (NSERC) grants awarded to Deborah Court. Moreover, Md Deen Islam was supported by the Govt. of Manitoba (Manitoba Government Scholarship), Faculty of Graduate Studies (University of Manitoba Graduate Fellowship) and (Manitoba Graduate Enhancement of Tri-Council Stipends) at the University of Manitoba.

I would also like to thank my only partner in research from Court lab, Jason Dubyna for his company, suggestions and supports. My sincere gratitude to the summer students, Nicole Rutbeek, Kelsey Weshnoweski, Erwin Taguiam, Sabrine Mahmoud and Michael Adeyemi for your kind help.

I would like to acknowledge all the professors, staff and graduate students of the Dept. of Microbiology for being very helpful and welcoming during my stay at the dept. It was a wonderful time to cherish the memories for.

Table of Contents

Abstract II

Acknowledgements IV

Table of Contents VI

List of Tables XI

List of Figures XII

List of Abbreviations……..XIV

List of Copyrighted Material for Which Permission has Been Granted XVIII

Chapter 1: Review of literature..... 2

1 Introduction..... 2

1.1 Environmental influence on fungi and mitochondrial evolution..... 2

1.1.1 Environmental selective pressure..... 2

1.1.2 Mitochondrial evolution (Endosymbiosis)..... 3

1.1.2.1 Comparison of mtDNA and bacterial DNA.....……. 4

1.1.2.2 Physiological functions of mitochondria..... 5

1.1.2.3 Distribution and composition of mitochondrial membrane proteins..... 6

1.2 Drug efflux pumps in antifungal resistance and their prevalence..... **6**

1.2.1 Types of drug efflux pump proteins in *S. cerevisiae*..... 6

1.2.2 MFS superfamily and conserved sequence motifs..... 8

1.2.3 Plausibility of finding drug EPs in clinical fungal mitochondria..... 14

1.2.4 Prevalence of MFS compared to ABC transporters..... 15

1.2.5 The relevance of the non-clinical fungal DHA to those of the clinical fungi..... 17

1.3 Characterization of the Transporter of polyamines (Tpo) of *S. cerevisiae*..... 19

1.3.1 Physiological functions of Tpo proteins..... 19

1.3.2 Cellular localization of Tpo proteins in *S. cerevisiae*..... 20

1.3.3 HeXose Transporter (Hxt5) of *S. cerevisiae*..... 22

1.3.4 Phylogenetic relationship of Tpo and Hxt proteins..... 24

1.3.5 Implications of the Tpo proteins in drug resistance..... 24

1.3.6 Substrate range of Tpo1..... 27

1.3.7 Homologues of Tpo1 from Prokaryotes (*E. coli*) and eukaryotes (*Homo sapiens*)..... 27

1.4 Mitochondria targeting drugs……..... 28

1.5 Research gap..... 32

1.6 Hypothesis..... 33

1.7 Objectives..... 33

Chapter 2: Methods and Materials..... 35

2.1 Search for putative MFS efflux pumps in fungi and creation of yeast deletion mutants...35

2.1.1 Analysis of yeast strains lacking putative pumps..... 36

2.1.1.1 Selection media..... 36

2.1.1.2 Chemicals..... 36

2.1.1.3 Antibiotic susceptibility assays..... 37

2.1.2 EtBr efflux from fungal mitochondria..... 38

2.1.2.1 *N. crassa* mitochondria extraction..... 38

2.1.2.2 *S. cerevisiae* mitochondria extraction.....…….... 38

2.1.2.3 EtBr efflux assay..... 39

2.2 Expression and examination of the putative drug efflux pumps in bacteria..... 47

2.2.1 Oligonucleotides, plasmids, bacterial strains, and growth conditions..... 47

2.2.2 Extraction of genomic DNA (gDNA) and plasmid..... 47

2.2.3 Construction and cloning of putative efflux pump genes..... 47

2.2.4 Expression and detection of Tpo proteins..... 48

2.2.5 Functional analysis of the Tpo proteins..... 49

2.2.5.1 Antibiotic susceptibility testing assay..... 49

2.2.5.2 EtBr accumulation assay..... 50

Chapter 3: To search for potential candidates of MFS drug efflux pumps and to demonstrate efflux of EtBr, a model compound, from fungal mitochondria. 52

3.1 Introduction..... 52

3.2 Results..... 53

3.2.1 Predicted structural similarity among yeast Tpo1 and homologues in *E. coli* and humans..... 53

3.2.2 Analysis of yeast strains lacking putative pumps..... 56

3.2.2.1 Growth kinetics at the non-selective conditions..... 56

3.2.2.2 Growth kinetics analysis using spot plating..... 58

3.2.2.2.1 Response to Chloramphenicol..... 58

3.2.2.2.2 Response to Erythromycin..... 61

3.2.2.2.3 Response to Tetracycline..... 63

3.2.2.3 Effect of growth medium on the antibiotic response..... 67

3.2.2.4 Analysis of growth kinetics in the presence of antibiotics, using 96-well plating..... 69

3.2.2.4.1 Response to Chloramphenicol..... 69

3.2.2.4.2 Response to Tetracycline..... 73

3.2.3 EtBr efflux from fungal mitochondria..... 76

3.2.3.1 EtBr efflux from *N. crassa* mitochondria..... 76

3.2.3.2 EtBr efflux from *S. cerevisiae* mitochondria..... 80

3.3 Discussion..... 83

Chapter 4: To express and examine the putative mitochondrial MFS drug efflux pumps in bacteria in order to study their specificity and mode of action……..... 92

4.1 Introduction..... 92

4.2 Results..... 93

4.2.1 Cloning of *TPO* genes..... 93

4.2.2 Expression of Tpo proteins..... 100

4.2.2.1 Optimization of expression parameters..... 100

4.2.2.2 Detection of the expressed protein..... 104

4.2.3 Functional analysis of putative pumps..... 110

4.2.3.1 Response to Chloramphenicol..... 110

4.2.3.2 Response to Erythromycin..... 113

4.2.4 EtBr accumulation assay using cloned *E. coli* 117

4.3 Discussion..... 120

Chapter 5……..…… 127

5.1 Conclusion..... 128

5.2 Future directions..... 129

5.3 Significance of this study..... 131

6. Appendix 1: Supporting Information for Chapter 1 132

7. Appendix 2: Supporting Information for Chapter 2 136

8. Appendix 3: Supporting Information for Chapter 3..... 144

9. Appendix 4: Supporting Information for Chapter 4..... 146

10. References 148

List of Tables

Table 1.1 Occurrence of putative efflux transporters in a few clinical and non-clinical fungi.…16

Table 1.2 Characteristic properties of the Tpo proteins and Hxt5……..… 23

Table 1.3 All the mitochondria-targeted potential antibiotics with their mode of action are listed in the table below…….. 30

Table 2.1 Commercially obtained deletion mutants……...…….. 35

Table 2.2 List of strains used in this study……..……. 40

Table 2.3 List of plasmids used in this study……...……...…….... 41

Table 2.4 List of oligonucleotides (primers) and PCR reactions used in this study……..….. 42

Table 4.1 All the constructs created with the circular polymerase extension cloning (CPEC) method are listed in the table below……...….. 97

Table 4.2 Summary of conditions tested for the expression of native and commercially codon-optimized proteins……..….. 101

Table 4.3 Strategies adopted in this study to address the toxicity of the Tpo proteins expression in *E. coli*…….. 123

Table 6.1 The list of antifungal substrates of Tpo1…… 132

Table 6.2 The list of herbicide substrates of Tpo1…….…… 134

Table 7.1 The composition of a modified LB medium……..…… 136

Table 7.2 Parameters tested for protein expression in this study……...…..….. 137

Table 9.1 Glycosylation percentage of the Tpo proteins and Hxt5……...……. 146

Table 9.2 The Codon Adaptation Index (CAI) of the Tpo proteins and Hxt5……...…… 146

Table 9.3 Distribution of cysteine residues (C) among the Tpo proteins and Hxt5……..……. 147

List of Figures

Figure 1.1 Yeast multidrug efflux transporters……..… 7

Figure 1.2 Conserved sequence motif of DHA1 and DHA2 among the Tpo proteins of *S. cerevisiae*, prokaryotes, and eukaryotes……...…… 13

Figure 1.3 A radial phylogenetic tree demonstrating the clustering of DHA1 transporters from the *S. cerevisiae* S288C to the DHA1 of eight clinically important fungal species……..... 18

Figure 1.4 The involvement of transporters of polyamine (Tpo) in polyamine regulation and their localization in the *S. cerevisiae* cell…….. 21

Figure 1.5 Evolutionary relationships of Tpo proteins……..….. 25

Figure 3.1 The homology modelling and structural prediction of Tpo1, and alignment to TETRAN and YajR showing a conserved sequence motif of three amino acid residues……. 54

Figure 3.2 Growth of wild-type (BY4741) and deletion strains under non-selective conditions…….……. 57

Figure 3.3 Growth of BY4741 and deletion mutants in the presence of chloramphenicol (CAP)…… 59

Figure 3.4 Growth of BY4741 and deletion mutants in the presence of erythromycin..……. 61

Figure 3.5 Growth of BY4741 and the deletion mutants ΔTPO1-2 (A) and ΔTPO3-4 (B) in the presence of tetracycline……..……... 64

Figure 3.6 Role of growth media on the mitochondrial response to antibiotics……..... 68

Figure 3.7 Growth of BY4741 and deletion mutants in the presence of Chloramphenicol……...…… 71

Figure 3.8 Growth of BY4741 and deletion mutants in the presence of Tetracycline……..... 75

Figure 3.9 Optimization of EtBr efflux from *N. crassa* mitochondria……..…..……. 79

Figure 3.10 Optimization of EtBr efflux from *S. cerevisiae* mitochondria……..... 82

Figure 4.1 A schematic diagram of the Circular Polymerase Extension Cloning (CPEC) mechanism for cloning an individual gene…….…….. 94

Figure 4.2 Cloning in the expression vector pET21b(+)……...……. 96

Figure 4.3 Cloning in the expression vector pMS119EH. A) The pMS119EH vector design…….……... 99

Figure 4.4 Comparison of growth of E. coli C43 expressing codon-optimized proteins from pET vectors…….…… 102

Figure 4.5 Determining the optimum concentration of IPTG for induction of *TPO1*……... 104

Figure 4.6 Workflow for testing expression in *E. coli*……...…...…. 105

Figure 4.7 SDS-PAGE analysis of proteins produced in induced and un-induced cells……. 109

Figure 4.8 Growth of wild-type C43 and the Tpo1- or Tpo3-expressing strains in the presence of Chloramphenicol……. 112

Figure 4.9 Growth of wild-type C43 and the Tpo1- or Tpo3-expressing strains in the presence of Erythromycin…….. 115

Figure 4.10 Ethidium bromide accumulation assay of cells with pMS119EH-based constructs…… 119

Figure 8.1 EtBr fluorescence in the presence and absence of membrane potential in *N. crassa* mitochondria……..…. 144

Figure 8.2 Yeast WT_BY4741 were grown in YPG with and without 3% ethanol…...…...… 145

List of Abbreviations

AACs	ADP/ATP carriers
ABC	ATP-binding cassette
ACT	amino acid/choline transporter
ADP	adenosine diphosphate
AMP	antimicrobial peptide
ARS	autonomously replicating sequence
ATP	adenosine triphosphate
a. u.	arbitrary unit
BCRP	breast cancer resistance protein
bp	base pair
BR	biological replicate
BSA	bovine serum albumin
$Ca2^{+}$	Calcium
CAP	chloramphenicol
CCCP	carbonyl cyanide m-chlorophenyl hydrazone
CFW	calcofluor white
CI	confidence interval
CLSI	clinical and laboratory standards institute
COX	cyclooxygenase
CPEC	circular polymerase extension cloning
CSC	cancer stem cell
DHA	drug:H+ antiporter

DOX	doxorubicin
DTT	dithiothreitol
EP	efflux pump
ER	endoplasmic reticulum
ERY	erythromycin
EtBr	ethidium bromide
FGSC	fungal genetics stock centre
gDNA	genomic DNA
GFP	green fluorescent protein
Hxt	hexose transporter
IB	inclusion bodies
IPTG	isopropyl β-D-1-thiogalactopyranoside
LB	Luria-Bertani medium
M	molar
MCS	multiple cloning site
Mdm	mitochondrial division and morphology protein
MDR	multi-drug resistance
MFS	major facilitator superfamily
MIC	minimum inhibitory concentration
mito	mitochondria
MIM	mitochondrial inner membrane
mM	mili molar
MOM	mitochondrial outer membrane

MP	membrane protein
MRP1	multidrug resistance-associated protein
mtDNA	mitochondrial DNA
NBD	nucleotide-binding domain
nm	nano meter
NSAID	non-steroidal anti-inflammatory drug
OD	optical density
Opt.	optimized
ORF	open reading frame
PAGE	polyacrylamide gel electrophoresis
PBS	phosphate-buffered saline
PCR	polymerase chain reaction
PUT	putrescine
qRT-PCR	quantitative real-time PCR
RFU	relative fluorescence unit
rRNA	ribosomal ribonucleic acid
SC	synthetic complete
SC150	*Saccharomyces cerevisiae* 150
SDHI	succinate dehydrogenase inhibitor
SDS	sodium dodecyl sulphate
SEM	standard error mean
SGD	*Saccharomyces* Genome Database
SPD	spermidine

SPM	spermine
STL	sugar transporter-like protein
TB	terrific broth medium
TBS	tris-buffered saline
TCA	tricarboxylic acid cycle
TET	tetracycline
TETRAN	tetracycline transporter-like protein
TMS	transmembrane segment
Tpo	transporter of polyamines
tRNA	transfer ribonucleic acid
UV	ultraviolet
VDAC	voltage-dependent anion-selective channel
VM	vogel’s medium
WB	western blot
WGD	whole-genome duplication
WT	wild-type
YPD	yeast peptone dextrose medium
YPG	yeast peptone glycerol medium
β-ME	beta- mercaptoethanol
ΔΨm	membrane potential
ΔPor	delta porin
μm	micrometre
μM	micro-molar

List of Copyrighted Material for Which Permission has Been Granted

Costa C., Dias P. J., Sá-Correia I., Teixeira M. C. 2014. MFS multidrug transporters in pathogenic fungi: do they have a real clinical impact? *Front. Physiol.* **5:**197 with permission from the authors as per Copyright and License information:

> ‘This is an open-access article distributed under the terms of the Creative Commons Attribution License (CC BY). The use, distribution or reproduction in other forums is permitted, provided the original author(s) or licensor are credited and that the original publication in this journal is cited, in accordance with accepted academic practice. No use, distribution or reproduction is permitted which does not comply with these terms.’

CHAPTER 1

Chapter 1: Review of literature

1. Introduction

Antifungal drug resistance is increasing recently, and a serious burden on public health management. Resistance develops against a variety of unrelated compounds because of the frequent and prolonged use of antifungals to plants, animals, and human fungal infections. There are 4 main resistance mechanisms in fungi to deal with antifungals (Fisher et al., 2018). The most prominent antifungal multidrug resistance (MDR) mechanism, encountered against the current classes of antifungals for plants and animals, is efflux pump-mediated resistance (Cowen et al., 2015; Fisher et al., 2018; Holmes et al., 2016).

Fungal genomes can possess a significant number of transport protein-encoding genes. For example, in *S. cerevisiae* the membrane transporter proteins represent 5% of the proteome (341 proteins) (Brohée et al., 2010). In the filamentous fungi *Cryptococcus* sp., *Aspergillus* sp., *Neurospora* sp. and in yeasts; *Saccharomyces* sp., the number of transport proteins per megabase of the genome ranges from 13 to 30 (Ren et al., 2007). This implies the contribution of transport proteins to fungal survival in an environment where they must withstand exposure to a variety of toxins (Barabote et al., 2010).

1.1 Environmental influence on fungi and mitochondrial evolution

1.1.1 Environmental selective pressure

Fungi can thrive in unusual environments as they are plastic in terms of ecology, biology and morphology (Appoloni et al., 2008; Baker et al., 2004; Gilichinsky et al., 2007; Nagai, 1998; Onofri et al., 2011; Selbmann et al., 2005, 2008). Moreover, fungi are environmentally adaptable, and they can easily utilize a range of toxic compounds for their survival, for example in extreme

environments having highly concentrated heavy metals, xenobiotic compounds (Ceci et al., 2012), and radionuclides (Dadachova et al., 2007). Fungi can utilize a range of carbon sources including toxic mixtures of hydrocarbons (Sikkema et al., 1995), petroleum, aromatic compounds, and natural gas (Badali et al., 2011; Kaltseis et al., 2009). One of the well-established model fungal eukaryotes *Neurospora crassa* is a soil microbe that is exposed to many antimicrobial compounds (Blair et al., 2014), and compounds such as phenolic acids and phytosterols (Hamdache et al., 2011). These compounds are present in the burnt plant material (e.g. sugar cane) on which it grows (A. Singh et al., 2015). The xenobiotics, antibiotics, fungicides, pesticides and toxic chemicals in their natural habitat might have selected fungi to develop efflux pumps in mitochondria.

1.1.2 Mitochondrial evolution (Endosymbiosis)

Toxic compounds/antimicrobials have diverse targets in the cell (cell wall, protein synthesis etc.). The focus of this thesis is to investigate the mitochondrial mechanisms involved in dealing with these compounds. It is important to understand the evolutionary history of mitochondria to understand some of their potential resistance mechanisms.

Mitochondria are eukaryotic organelles that reside in the cytoplasm of the cell. They are 0.5- 1.0 μm in diameter and possess a double membrane system, with an ovoid to tubular morphology in some states similar to purple non-sulphur bacteria (Alberts et al., 2007). The French scientist Paul Jules Portier claimed the symbiotic origin of mitochondria in 1918 in his book named '*Les Symbiotes'* (Portier, 1918). Later the theory of the symbiotic origin of mitochondria was supported by Ivan Wallin in the 1920s (I. E. Wallin, 1927; I. E. Wallin, 1923). In 1960, it was discovered that the mitochondria possess DNA (Nass & Nass, 1963), and hsad translation machinery unlike systems in the cytosol (Schatz et al., 1964). These two crucial points, in support of the endosymbiosis theory of organelle origins, were adopted by Lynn Margulis (formerly Sagan) in

her book '*Origin of Eukaryotic Cells'* in 1970 (Margulis, 1970). In this book, the author rejuvenated the endosymbiosis theory that mitochondria and plant plastids originated from prokaryotic bacteria through symbiosis within a eukaryotic host cell (Sagan, 1967).

Comparing mitochondrial and bacterial genomes, it is considered that mitochondria have a bacterial ancestry. Mitochondria have originated from α-Proteobacteria (Yang et al., 1985). However, the mitochondrial genomes have gone through several evolutionary pathways in different eukaryotic lineages, based on comparative mitochondrial genomics studies (Gray et al., 1998, 1999). Comparative mitochondrial proteomics is another way of finding the evolutionary origin of mitochondria (Dreger, 2003; Yan et al., 2009). Genome comparisons of the α-Proteobacteria and eukaryotes found 840 orthologous groups of proteins having α-Proteobacterial signature (Gabaldón & Huynen, 2003, 2007; Szklarczyk & Huynen, 2010), which again supports the clear and specific evolutionary relationship of mitochondria to α-Proteobacterial homologs.

1.1.2.1 Comparison of mtDNA and bacterial DNA

The close homology of mitochondrial and bacterial respiratory complexes is one of the fascinating proofs of their evolutionary relationship. Mitochondria have unique genetic material that is different from their potential bacterial ancestors and eukaryotic hosts (Gray et al., 1998). Additionally, mitochondria have protein translation machinery, which comprises 70S ribosomes, tRNAs and necessary protein factors that resemble those of their bacterial ancestors. However, through the course of evolution, they have lost 99% of their genes, many of which are incorporated into the nucleus. Thus, a majority of the proteins needed to keep the mitochondria functioning are transported from the cytoplasm through a set of mitochondrial membrane translocases (Schmidt et al., 2010).

The mitochondrial genome of the model organism used in these studies, *S. cerevisiae*, contains 30-40 genes that are translated into proteins, or transcribed into small and large subunit rRNAs and tRNAs. A set of conserved genes found in all yeast mtDNA encodes protein subunits involved in oxidative phosphorylation (de Zamaroczy & Bernardi, 1986; Foury et al., 1998; Solieri, 2010; Wolf & Del Giudice, 1988). In *S. cerevisiae*, mtDNA codes for only eight proteins of a total proteome that consists of about 1000 mitochondrial proteins (Malina et al., 2018). Among them, seven proteins are the subunits of the electron transport chain and the ATP synthase, and the other protein is a small subunit of the ribosome (Foury et al., 1998).

1.1.2.2 Physiological functions of mitochondria

The role of mitochondria expands above and beyond the generation of energy in the form of adenosine triphosphate (ATP), and participation in cellular signalling pathways implicated in apoptosis, the progression of mitochondrial diseases, expression patterns of genes, posttranslational modification of proteins and redox balance (the equilibrium state of oxidation and reduction processes).

Mitochondria are the core source of energy conservation inside the cell. The organelle transforms energy derived from oxidative phosphorylation of substrates into chemical energy stored in ATP; the energy-rich compound that is used for the overall maintenance of the cell. Mitochondria have a wide range of essential functions aside from ATP synthesis and cellular respiration, such as regulating membrane biogenesis, synthesizing phospholipids, and participating in the biosynthesis of amino acids, heme groups and iron-sulphur clusters. Moreover, mitochondria are involved in calcium signalling (Rizzuto et al., 2012), stress response (Pellegrino & Haynes, 2015), and a core for cellular signalling (Chandel, 2014). They have a major impact on cellular apoptosis and ageing (Bratic & Larsson, 2013).

1.1.2.3 Distribution and composition of mitochondrial membrane proteins

These double membrane-bound organelles have a mitochondrial outer membrane (MOM) that surrounds the organelle and a mitochondrial inner membrane (MIM), that forms cristae by folding inward to create a large surface membrane area.

To maintain the rigorous signalling and processes, mitochondria have to depend on the cytoplasmic supply of enzymes, ions, ATP, ADP and small metabolites, and the MIM must contain a large number of transporter proteins (Kühlbrandt, 2015; Pebay-Peyroula et al., 2003; Vogel et al., 2006). As expected from its bacterial ancestry, some antibiotics and toxins affect mitochondrial protein synthesis (**Table 1.3**); thus, antibiotic efflux transporters may be present in the MIM of fungal mitochondria.

1.2 Drug efflux pumps in antifungal resistance and their prevalence

1.2.1 Types of drug efflux proteins in *S. cerevisiae*

S. cerevisiae has two major superfamilies of efflux pumps (Sá-Correia et al., 2009) that confer resistance to antifungal drugs using a range of strategies to efflux drugs. The two major groups are the ATP-Binding Cassette (ABC) and the Major Facilitator Superfamily (MFS). Among them, ABC transporters are primary active transporters that utilize energy derived from the hydrolysis of ATP. The core arrangement of the ABCs is a dimer, with each monomer being composed of two domains. One is a nucleotide-binding domain (NBD) located in the cytoplasm and the other is a transmembrane segment (TMS) (**Fig 1.1A**).

MFS proteins are secondary active transporters that rely on an electrochemical gradient of protons as the main driving force to pump substrates across the membrane with the substrate's concentration gradient (Prasad & Rawal, 2014). They are comprised of 12 or 14 TMS, and the

TMSs are connected by cytoplasmic and extracytoplasmic loops (**Fig 1.1B**). The MFS transporters are single sub-unit proteins that are easier to study compared to multi-subunit ABC transporters.

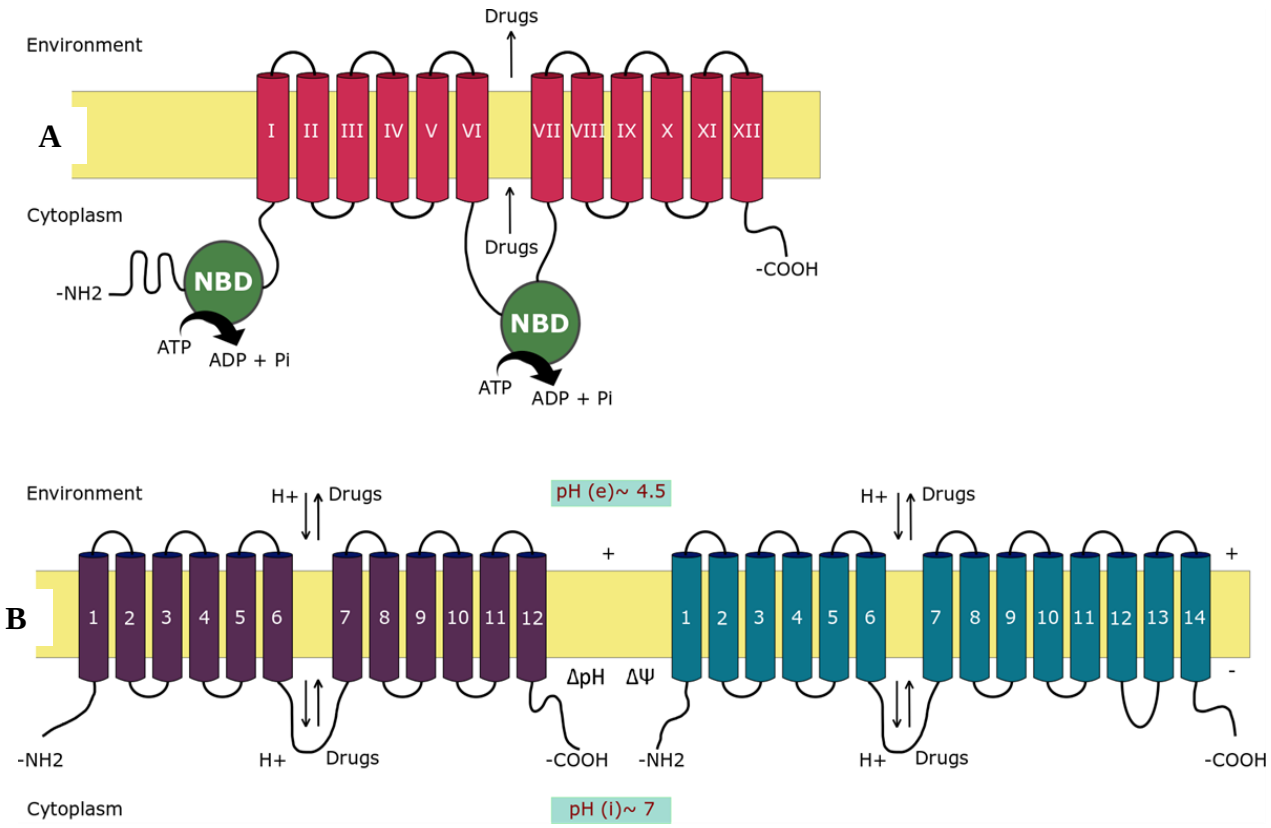
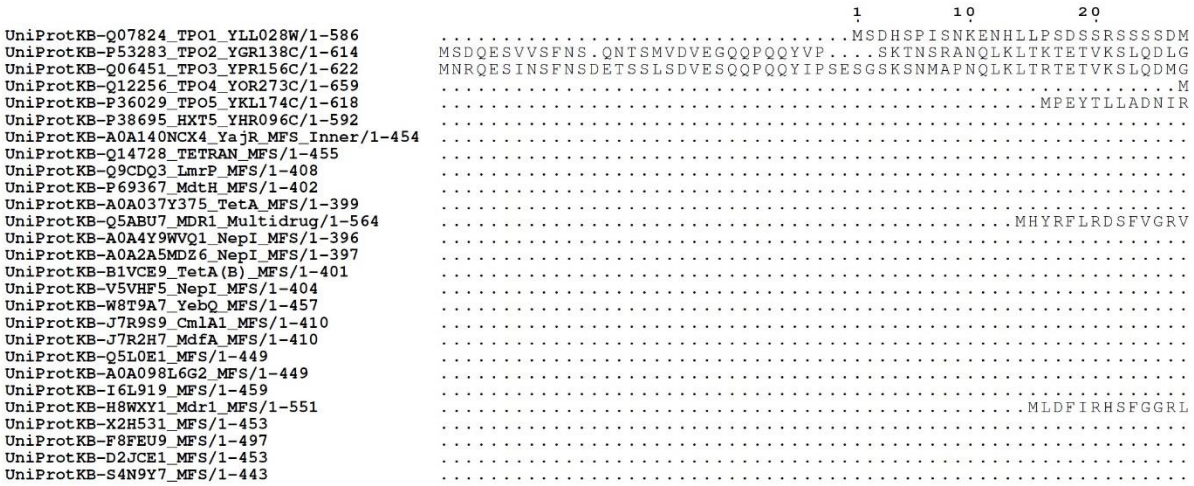


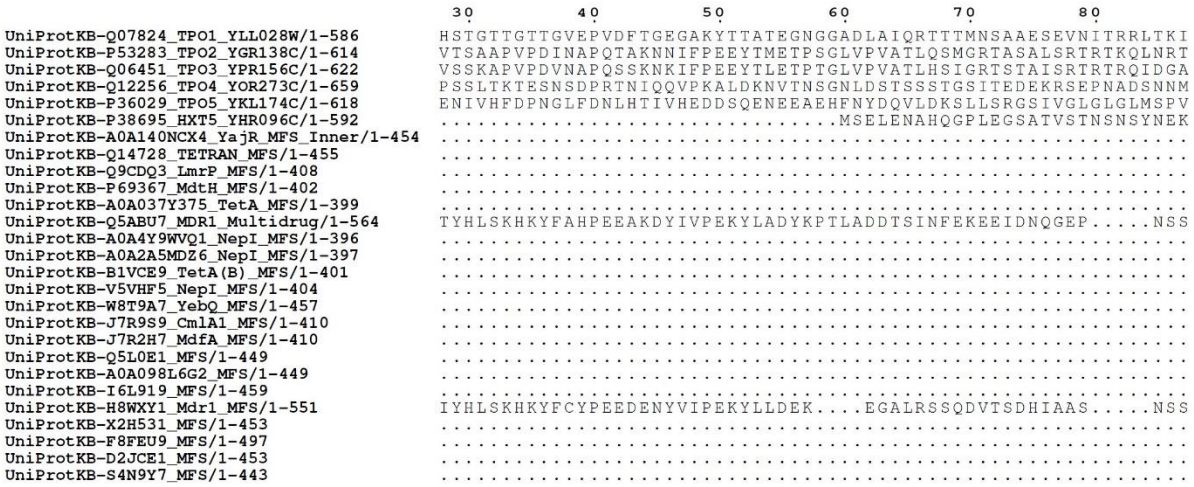
Figure 1.1 Yeast multidrug efflux transporters. Cartoons representing the yeast multidrug transporters. **A)** ABC superfamily and **B)** MFS-MDR transporters of the 12-TMS DHA1 and 14-TMS DHA2. The topologies have been obtained from the *Saccharomyces* Genome Database (SGD) and based on (Sá-Correia et al., 2009). NBD, nucleotide-binding domain.

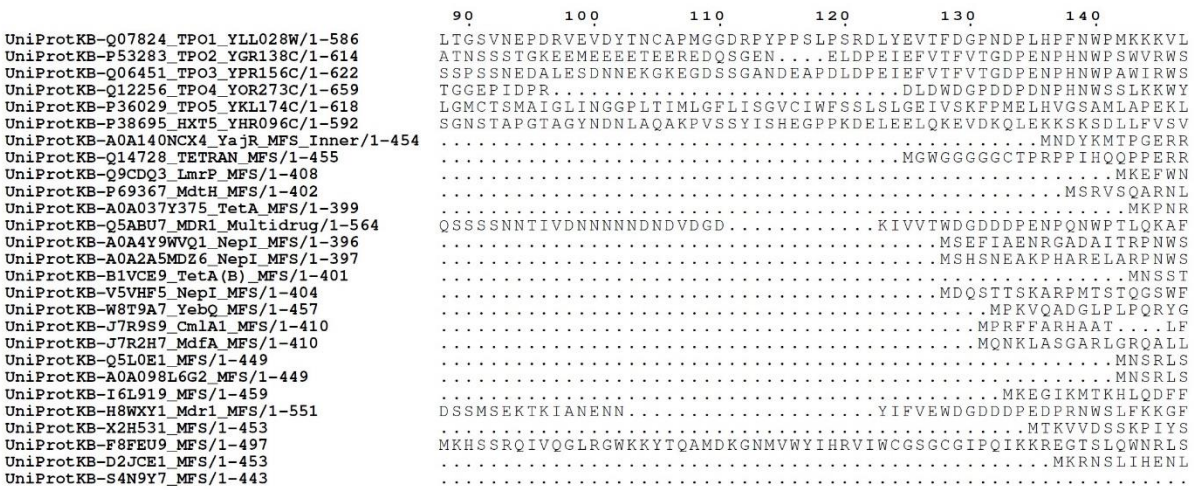
1.2.2 MFS superfamily and conserved sequence motifs

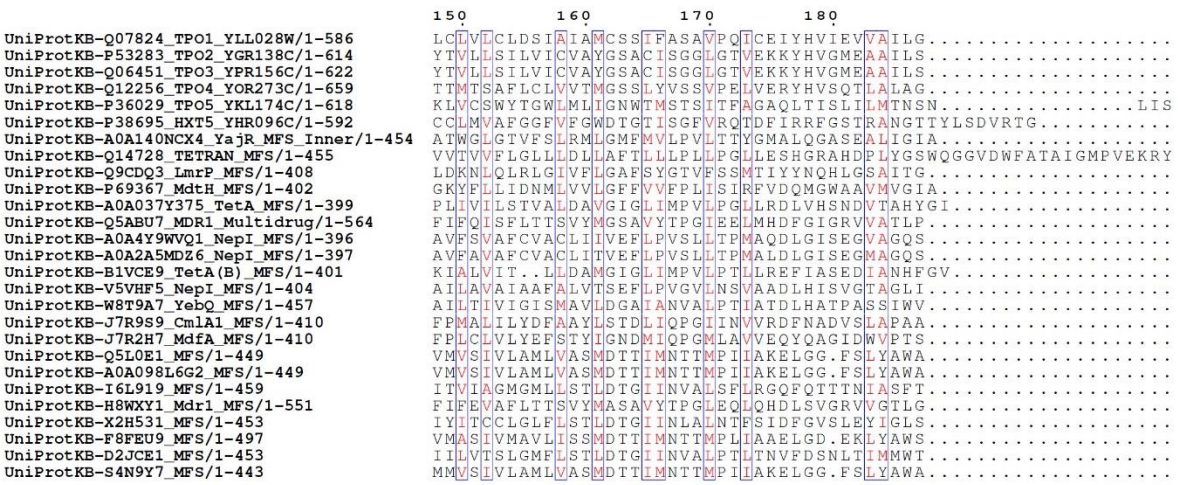
The MFS superfamily was initially subdivided into 74 families, each of which transports a specific type of substrate (Reddy et al., 2012). Members of this family have been found in bacteria, eukaryotes, and archaea. The MFS includes transporters that can function as uniporters, antiporters and symporters (Pao et al., 1998).

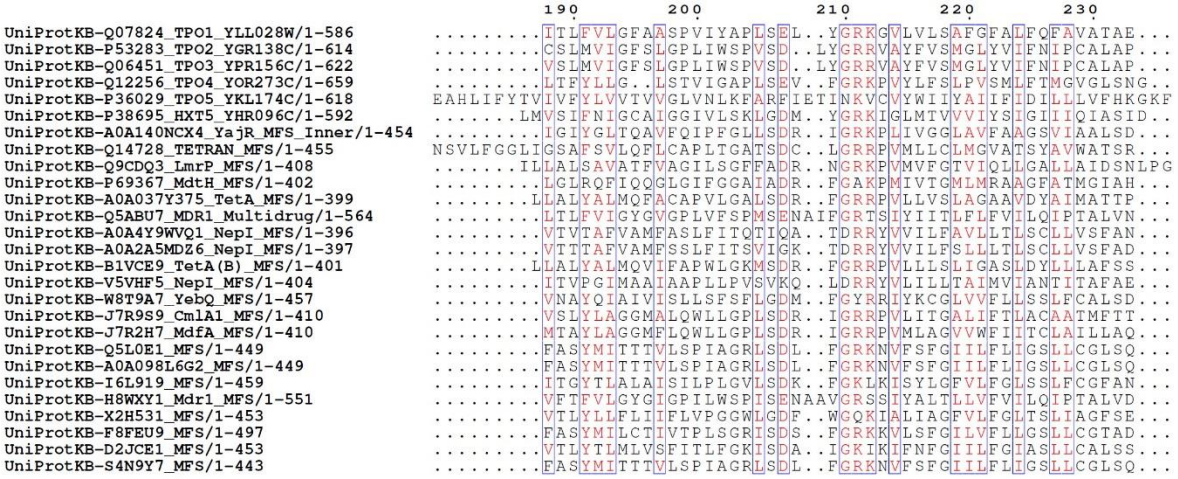
The Multi-Drug Resistant (MDR) transporters of the MFS superfamily (MFS-MDR) are classified into two families depending on the number of TMS. They are the drug:H^+ antiporter family 1 (12 segments; DHA1) and family 2 (14 segments; DHA2) (**Fig 1.1 (B)**) (De Rossi et al., 2002). There is a conserved sequence motif of 5 residues (RXGRR) between the transmembrane 2 (TM2) and transmembrane (TM3) segments in most MFS transporters. In extended form, the motif is [GX3(D/E) (R/K) XG[X](R/K) (R/K)]. It has been shown that each of the families of MFS has its signature sequence motif as well. For example, DHA1 and DHA2 have their unique motifs. The DHA1 motif is (GXLSDRF**GRR**PVL) and the DHA2 motif is (GRLADRF**GRK**RXL) (Pao et al., 1998). The 4 proteins examined in this thesis, Tpo1 to Tpo4, have been aligned to a set of MFS transporters obtained from the BLASTp program in UniProt (Bateman, 2019) (**Fig 1.2**); it shows the presence of DHA1 or DHA2 conserved motifs in Tpo1-Tpo4 protein sequences in this study.

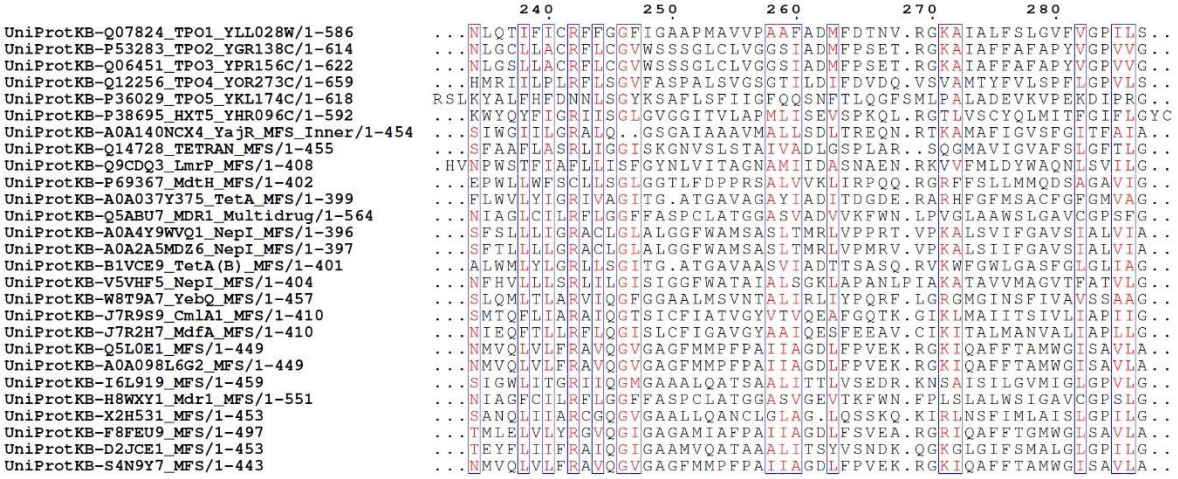

1 10 20
UniProtKB-Q07824_TPO1_YLL028W/1-586 .....MSDHSPISNKENHLLPSDSSRSSSSDM
UniProtKB-P53283_TPO2_YGR138C/1-614 MSDQESVVSFNS.QNTSMVDVEGQQPQQYVP....SKTNSRANQLKLTKTETVKSLQDLG
UniProtKB-Q06451_TPO3_YPR156C/1-622 MNRQESINSFNSDETSSLSDVESQQPQQYIPSESGSKSNMAPNQLKLTRTETVKSLQDMG
UniProtKB-Q12256_TPO4_YOR273C/1-659 .....M
UniProtKB-P36029_TPO5_YKL174C/1-618 .....MPEYTLLADNIR
UniProtKB-P38695_HXT5_YHR096C/1-592 .....
UniProtKB-A0A140NCX4_YajR_MFS_Inner/1-454 .....
UniProtKB-Q14728_TETRAN_MFS/1-455 .....
UniProtKB-Q9CDQ3_LmrP_MFS/1-408 .....
UniProtKB-P69367_MdtH_MFS/1-402 .....
UniProtKB-A0A037Y375_TetA_MFS/1-399 .....
UniProtKB-Q5ABU7_MDR1_Multidrug/1-564 .....MHYRFLRDSFVGRV
UniProtKB-A0A4Y9WVQ1_NepI_MFS/1-396 .....
UniProtKB-A0A2A5MDZ6_NepI_MFS/1-397 .....
UniProtKB-B1VCE9_TetA(B)_MFS/1-401 .....
UniProtKB-V5VHF5_NepI_MFS/1-404 .....
UniProtKB-W8T9A7_YebQ_MFS/1-457 .....
UniProtKB-J7R9S9_CmlA1_MFS/1-410 .....
UniProtKB-J7R2H7_MdfA_MFS/1-410 .....
UniProtKB-Q5L0E1_MFS/1-449 .....
UniProtKB-A0A098L6G2_MFS/1-449 .....
UniProtKB-I6L919_MFS/1-459 .....
UniProtKB-H8WXY1_Mdr1_MFS/1-551 .....MLDFIRHSFGGRL
UniProtKB-X2H531_MFS/1-453 .....
UniProtKB-F8FEU9_MFS/1-497 .....
UniProtKB-D2JCE1_MFS/1-453 .....
UniProtKB-S4N9Y7_MFS/1-443 .....

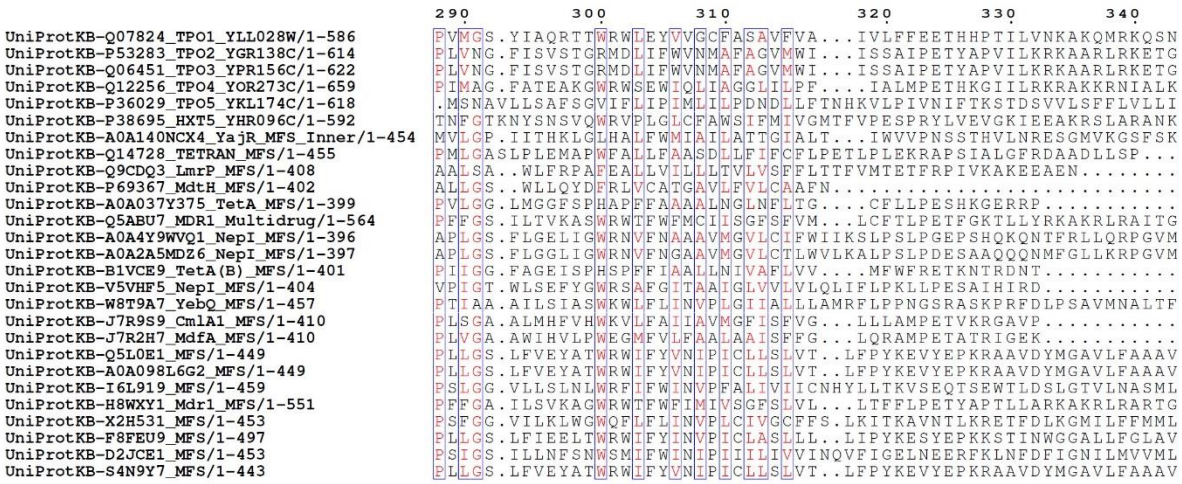

30 40 50 60 70 80
UniProtKB-Q07824_TPO1_YLL028W/1-586 HSTGTTGTTGVEPVDFTGEGAKYTTATEGNGGADLAIQRTTTMNSAAESEVNITRRLTKI
UniProtKB-P53283_TPO2_YGR138C/1-614 VTSAAPVPDINAPQTAKNNIFPEEYTMETPSGLVPVATLQSMGRTASALSRTRTKQLNRT
UniProtKB-Q06451_TPO3_YPR156C/1-622 VSSKAPVPDVNAPQSSKNKIFPEEYTLETPTGLVPVATLHSIGRTSTAISRTRTRQIDGA
UniProtKB-Q12256_TPO4_YOR273C/1-659 PSSLTKTESNSDPRTNIQQVPKALDKNVTNSGNLDSTSSSTGSITEDEKRSEPNADSNNM
UniProtKB-P36029_TPO5_YKL174C/1-618 ENIVHFDPNGLFDNLHTIVHEDDSQENEEAEHFNYDQVLDKSLLSRGSIVGLGLGLMSPV
UniProtKB-P38695_HXT5_YHR096C/1-592 .....MSELENAHQGPLEGSATVSTNSNSYNEK
UniProtKB-A0A140NCX4_YajR_MFS_Inner/1-454 .....
UniProtKB-Q14728_TETRAN_MFS/1-455 .....
UniProtKB-Q9CDQ3_LmrP_MFS/1-408 .....
UniProtKB-P69367_MdtH_MFS/1-402 .....
UniProtKB-A0A037Y375_TetA_MFS/1-399 .....
UniProtKB-Q5ABU7_MDR1_Multidrug/1-564 TYHLSKHKYFAHPEEAKDYIVPEKYLADYKPTLADDTSINFEKEEIDNQGEP.....NSS
UniProtKB-A0A4Y9WVQ1_NepI_MFS/1-396 .....
UniProtKB-A0A2A5MDZ6_NepI_MFS/1-397 .....
UniProtKB-B1VCE9_TetA(B)_MFS/1-401 .....
UniProtKB-V5VHF5_NepI_MFS/1-404 .....
UniProtKB-W8T9A7_YebQ_MFS/1-457 .....
UniProtKB-J7R9S9_CmlA1_MFS/1-410 .....
UniProtKB-J7R2H7_MdfA_MFS/1-410 .....
UniProtKB-Q5L0E1_MFS/1-449 .....
UniProtKB-A0A098L6G2_MFS/1-449 .....
UniProtKB-I6L919_MFS/1-459 .....
UniProtKB-H8WXY1_Mdr1_MFS/1-551 IYHLSKHKYFCYPEEDENYVIPEKYLLDEK....EGALRSSQDVTSDHIAAS.....NSS
UniProtKB-X2H531_MFS/1-453 .....
UniProtKB-F8FEU9_MFS/1-497 .....
UniProtKB-D2JCE1_MFS/1-453 .....
UniProtKB-S4N9Y7_MFS/1-443 .....

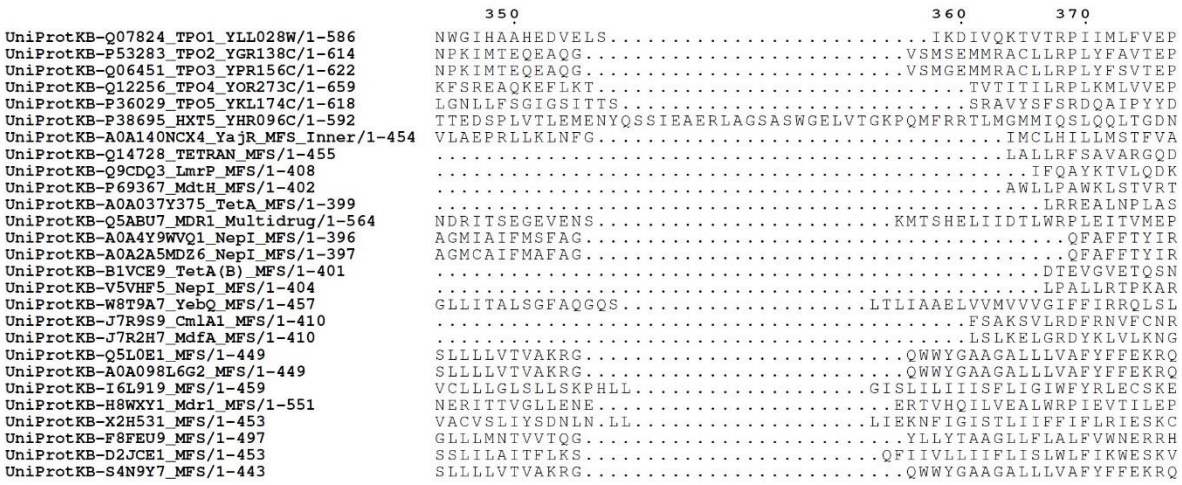

90 100 110 120 130 140
UniProtKB-Q07824_TPO1_YLL028W/1-586 LTGSVNEPDRVEVDYTNCAPMGGDRPYPPSLPSRDLYEVTFDGPNDPLHPFNWPMKKKVL
UniProtKB-P53283_TPO2_YGR138C/1-614 ATNSSSTGKEEMEEEETEEREDQSGEN....ELDPEIEFVTFVTGDPENPHNWPSWVRWS
UniProtKB-Q06451_TPO3_YPR156C/1-622 SSPSSNEDALESDNNEKGKEGDSSGANDEAPDLDPEIEFVTFVTGDPENPHNWPAWIRWS
UniProtKB-Q12256_TPO4_YOR273C/1-659 TGGEPIDPR.....DLDWDGPDDPDNPHNWSSLKKWY
UniProtKB-P36029_TPO5_YKL174C/1-618 LGMCTSMAIGLINGGPLTIMLGFLISGVCIWFSSLSLGEIVSKFPMELHVGSAMLAPEKL
UniProtKB-P38695_HXT5_YHR096C/1-592 SGNSTAPGTAGYNDNLAQAKPVSSYISHEGPPKDELEELQKEVDKQLEKKSKSDLLFVSV
UniProtKB-A0A140NCX4_YajR_MFS_Inner/1-454 .....MNDYKMTPGERR
UniProtKB-Q14728_TETRAN_MFS/1-455 .....MGWGGGGGCTPRPPIHQQPPERR
UniProtKB-Q9CDQ3_LmrP_MFS/1-408 .....MKEFWN
UniProtKB-P69367_MdtH_MFS/1-402 .....MSRVSQARNL
UniProtKB-A0A037Y375_TetA_MFS/1-399 .....MKPNR
UniProtKB-Q5ABU7_MDR1_Multidrug/1-564 QSSSSNNTIVDNNNNNDNDVDGD.....KIVVTWDGDDDPENPQNWPTLQKAF
UniProtKB-A0A4Y9WVQ1_NepI_MFS/1-396 .....MSEFIAENRGADAITRPNWS
UniProtKB-A0A2A5MDZ6_NepI_MFS/1-397 .....MSHSNEAKPHARELARPNWS
UniProtKB-B1VCE9_TetA(B)_MFS/1-401 .....MNSST
UniProtKB-V5VHF5_NepI_MFS/1-404 .....MDQSTTSKARPMTSTQGSWF
UniProtKB-W8T9A7_YebQ_MFS/1-457 .....MPKVQADGLPLPQRYG
UniProtKB-J7R9S9_CmlA1_MFS/1-410 .....MPRFFARHAAT....LF
UniProtKB-J7R2H7_MdfA_MFS/1-410 .....MQNKLASGARLGRQALL
UniProtKB-Q5L0E1_MFS/1-449 .....MNSRLS
UniProtKB-A0A098L6G2_MFS/1-449 .....MNSRLS
UniProtKB-I6L919_MFS/1-459 .....MKEGIKMTKHLQDFF
UniProtKB-H8WXY1_Mdr1_MFS/1-551 DSSMSEKTKIANENN.....YIFVEWDGDDDPEDPRNWSLFKKGF
UniProtKB-X2H531_MFS/1-453 .....MTKVVDSSKPIYS
UniProtKB-F8FEU9_MFS/1-497 MKHSSRQIVQGLRGWKKYTQAMDKGNMVWYIHRVIWCGSGCGIPQIKKREGTSLQWNRLS
UniProtKB-D2JCE1_MFS/1-453 .....MKRNSLIHENL
UniProtKB-S4N9Y7_MFS/1-443 .....

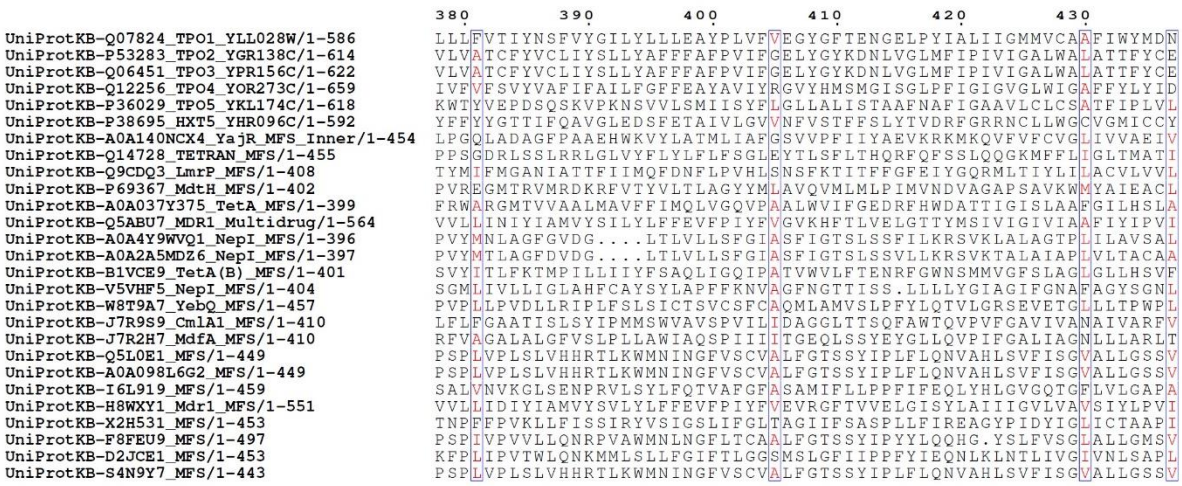

150
160
170
180
UniProtKB-Q07824_TPO1_YLL028W/1-586
UniProtKB-P53283_TPO2_YGR138C/1-614
UniProtKB-Q06451_TPO3_YPR156C/1-622
UniProtKB-Q12256_TPO4_YOR273C/1-659
UniProtKB-P36029_TPO5_YKL174C/1-618
UniProtKB-P38695_HXT5_YHR096C/1-592
UniProtKB-A0A140NCX4_YajR_MFS_Inner/1-454
UniProtKB-Q14728_TETRAN_MFS/1-455
UniProtKB-Q9CDQ3_LmrP_MFS/1-408
UniProtKB-P69367_MdtH_MFS/1-402
UniProtKB-A0A037Y375_TetA_MFS/1-399
UniProtKB-Q5ABU7_MDR1_Multidrug/1-564
UniProtKB-A0A4Y9WVQ1_NepI_MFS/1-396
UniProtKB-A0A2A5MDZ6_NepI_MFS/1-397
UniProtKB-B1VCE9_TetA(B)_MFS/1-401
UniProtKB-V5VHF5_NepI_MFS/1-404
UniProtKB-W8T9A7_YebQ_MFS/1-457
UniProtKB-J7R9S9_CmlA1_MFS/1-410
UniProtKB-J7R2H7_MdfA_MFS/1-410
UniProtKB-Q5L0E1_MFS/1-449
UniProtKB-A0A098L6G2_MFS/1-449
UniProtKB-I6L919_MFS/1-459
UniProtKB-H8WXY1_Mdr1_MFS/1-551
UniProtKB-X2H531_MFS/1-453
UniProtKB-F8FEU9_MFS/1-497
UniProtKB-D2JCE1_MFS/1-453
UniProtKB-S4N9Y7_MFS/1-443

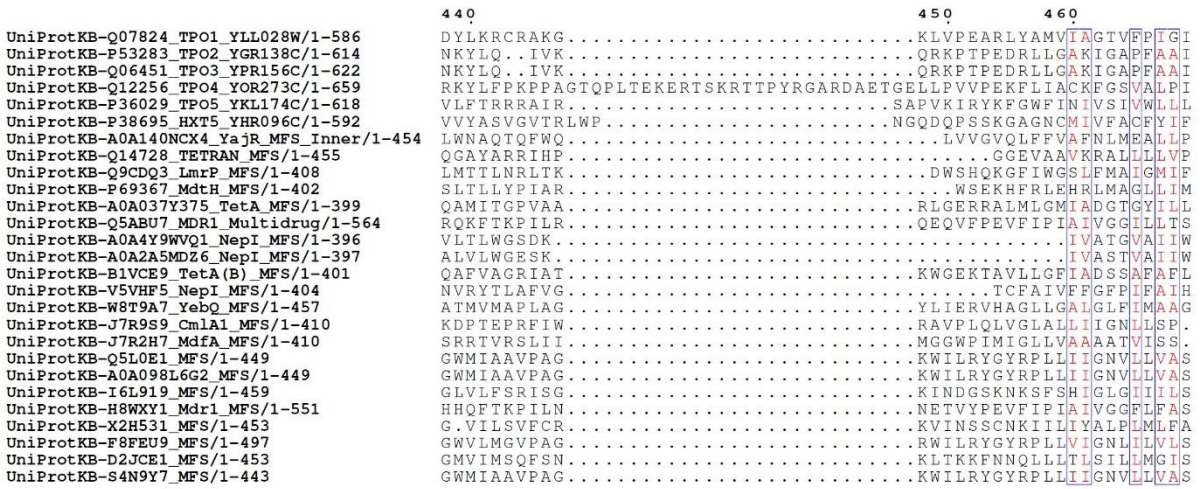

190
200
210
220
230
UniProtKB-Q07824_TPO1_YLL028W/1-586
UniProtKB-P53283_TPO2_YGR138C/1-614
UniProtKB-Q06451_TPO3_YPR156C/1-622
UniProtKB-Q12256_TPO4_YOR273C/1-659
UniProtKB-P36029_TPO5_YKL174C/1-618
UniProtKB-P38695_HXT5_YHR096C/1-592
UniProtKB-A0A140NCX4_YajR_MFS_Inner/1-454
UniProtKB-Q14728_TETRAN_MFS/1-455
UniProtKB-Q9CDQ3_LmrP_MFS/1-408
UniProtKB-P69367_MdtH_MFS/1-402
UniProtKB-A0A037Y375_TetA_MFS/1-399
UniProtKB-Q5ABU7_MDR1_Multidrug/1-564
UniProtKB-A0A4Y9WVQ1_NepI_MFS/1-396
UniProtKB-A0A2A5MDZ6_NepI_MFS/1-397
UniProtKB-B1VCE9_TetA(B)_MFS/1-401
UniProtKB-V5VHF5_NepI_MFS/1-404
UniProtKB-W8T9A7_YebQ_MFS/1-457
UniProtKB-J7R9S9_CmlA1_MFS/1-410
UniProtKB-J7R2H7_MdfA_MFS/1-410
UniProtKB-Q5L0E1_MFS/1-449
UniProtKB-A0A098L6G2_MFS/1-449
UniProtKB-I6L919_MFS/1-459
UniProtKB-H8WXY1_Mdr1_MFS/1-551
UniProtKB-X2H531_MFS/1-453
UniProtKB-F8FEU9_MFS/1-497
UniProtKB-D2JCE1_MFS/1-453
UniProtKB-S4N9Y7_MFS/1-443

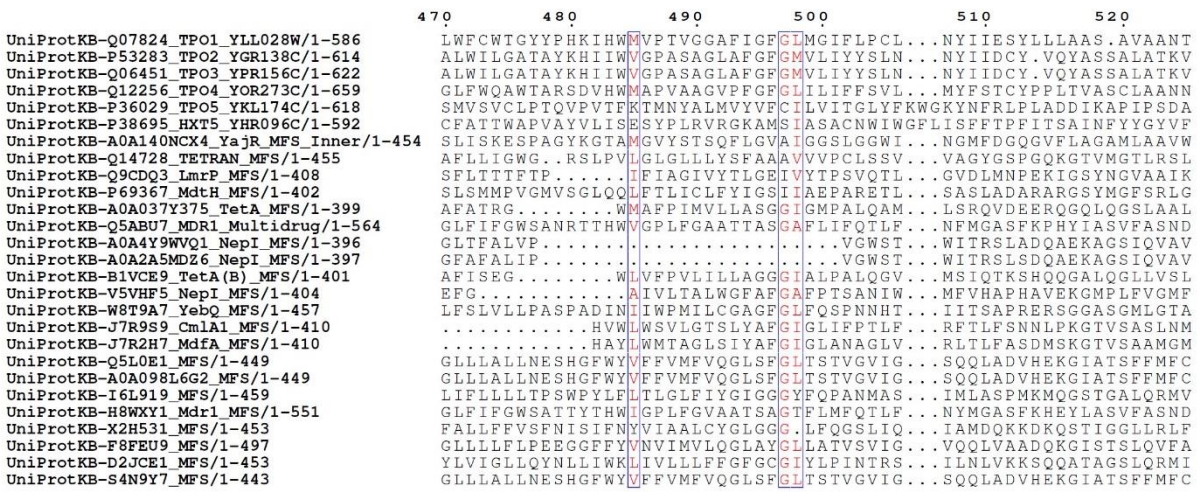

240
250
260
270
280
UniProtKB-Q07824_TPO1_YLL028W/1-586
UniProtKB-P53283_TPO2_YGR138C/1-614
UniProtKB-Q06451_TPO3_YPR156C/1-622
UniProtKB-Q12256_TPO4_YOR273C/1-659
UniProtKB-P36029_TPO5_YKL174C/1-618
UniProtKB-P38695_HXT5_YHR096C/1-592
UniProtKB-A0A140NCX4_YajR_MFS_Inner/1-454
UniProtKB-Q14728_TETRAN_MFS/1-455
UniProtKB-Q9CDQ3_LmrP_MFS/1-408
UniProtKB-P69367_MdtH_MFS/1-402
UniProtKB-A0A037Y375_TetA_MFS/1-399
UniProtKB-Q5ABU7_MDR1_Multidrug/1-564
UniProtKB-A0A4Y9WVQ1_NepI_MFS/1-396
UniProtKB-A0A2A5MDZ6_NepI_MFS/1-397
UniProtKB-B1VCE9_TetA(B)_MFS/1-401
UniProtKB-V5VHF5_NepI_MFS/1-404
UniProtKB-W8T9A7_YebQ_MFS/1-457
UniProtKB-J7R9S9_CmlA1_MFS/1-410
UniProtKB-J7R2H7_MdfA_MFS/1-410
UniProtKB-Q5L0E1_MFS/1-449
UniProtKB-A0A098L6G2_MFS/1-449
UniProtKB-I6L919_MFS/1-459
UniProtKB-H8WXY1_Mdr1_MFS/1-551
UniProtKB-X2H531_MFS/1-453
UniProtKB-F8FEU9_MFS/1-497
UniProtKB-D2JCE1_MFS/1-453
UniProtKB-S4N9Y7_MFS/1-443

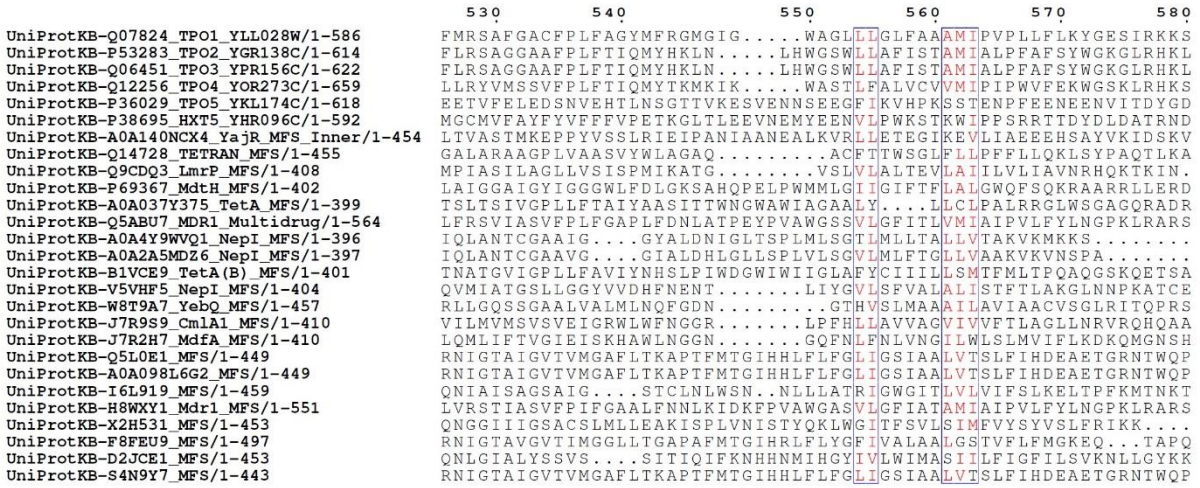

290 300 310 320 330 340
UniProtKB-Q07824_TPO1_YLL028W/1-586 PVMGS.YIAQRTTWRWLEYVVGCFASAVFVA...IVLFFEETHHPTILVNKAKQMRKQSN
UniProtKB-P53283_TPO2_YGR138C/1-614 PLVNG.FISVSTGRMDLIFWVNMAFAGVMWI...ISSAIPETYAPVILKRKAARLRKETG
UniProtKB-Q06451_TPO3_YPR156C/1-622 PLVNG.FISVSTGRMDLIFWVNMAFAGVMWI...ISSAIPETYAPVILKRKAARLRKETG
UniProtKB-Q12256_TPO4_YOR273C/1-659 PIMAG.FATEAKGWRWSEWIQLIAGGLILPF....IALMPETHKGIILRKRAKKRNIALK
UniProtKB-P36029_TPO5_YKL174C/1-618 .MSNAVLLSAFSGVIFLIPIMLILPDNDLLFTNHKVLPIVNIFTKSTDSVVLSFFLVLLI
UniProtKB-P38695_HXT5_YHR096C/1-592 TNFGTKNYSNSVQWRVPLGLCFAWSIFMIVGMTFVPESPRYLVEVGKIEEAKRSLARANK
UniProtKB-A0A140NCX4_YajR_MFS_Inner/1-454 MVLGP.IITHKLGLHALFWMIAILATTGIALT...IWVVPNSSTHVLNRESGMVKGSFSK
UniProtKB-Q14728_TETRAN_MFS/1-455 PMLGASLPLEMAPWFALLFAASDLLFIFCFLPETLPLEKRAPSIALGFRDAADLLSP...
UniProtKB-Q9CDQ3_LmrP_MFS/1-408 AALSA..WLFRPAFEALLVILLLTVLVSFFLTTFVMTETFRPIVKAKEEAEN.....
UniProtKB-P69367_MdtH_MFS/1-402 ALLGS..WLLQYDFRLVCATGAVLFVLCAAFN.....
UniProtKB-A0A037Y375_TetA_MFS/1-399 PVLGG.LMGGFSPHAPFFAAAALNGLNFLTG....CFLLPESHKGERRP.....
UniProtKB-Q5ABU7_MDR1_Multidrug/1-564 PFFGS.ILTVKASWRWTFWFMCIISGFSFVM...LCFTLPETFGKTLLYRKAKRLRAITG
UniProtKB-A0A4Y9WVQ1_NepI_MFS/1-396 APLGS.FLGELIGWRNVFNAAAVMGVLCIFWIIKSLPSLPGEPSHQKQNTFRLLQRPGVM
UniProtKB-A0A2A5MDZ6_NepI_MFS/1-397 APLGS.FLGGLIGWRNVFNGAAVMGVLCTLWVLKALPSLPDESAAQQQNMFGLLKRPGVM
UniProtKB-B1VCE9_TetA(B)_MFS/1-401 PIIGG.FAGEISPHSPFFIAALLNIVAFLVV....MFWFRETKNTRDNT.....
UniProtKB-V5VHF5_NepI_MFS/1-404 VPIGT.WLSEFYGWRSAFGITAAIGLVVLVLQLIFLPKLLPESAIHIRD.....
UniProtKB-W8T9A7_YebQ_MFS/1-457 PTIAA.AILSIASWKWLFLINVPLGIIALLLAMRFLPPNGSRASKPRFDLPSAVMNALTF
UniProtKB-J7R9S9_CmlA1_MFS/1-410 PLSGA.ALMHFVHWKVLFAIIAVMGFISFVG...LLLAMPETVKRGAVP.....
UniProtKB-J7R2H7_MdfA_MFS/1-410 PLVGA.AWIHVLPWEGMFVLFAALAAISFFG...LQRAMPETATRIGEK.....
UniProtKB-Q5L0E1_MFS/1-449 PLLGS.LFVEYATWRWIFYVNIPICLLSLVT..LFPYKEVYEPKRAAVDYMGAVLFAAAV
UniProtKB-A0A098L6G2_MFS/1-449 PLLGS.LFVEYATWRWIFYVNIPICLLSLVT..LFPYKEVYEPKRAAVDYMGAVLFAAAV
UniProtKB-I6L919_MFS/1-459 PSLGG.VLLSLNLWRFIFWINVPFALIVIICNHYLLTKVSEQTSEWTLDSLGTVLNASML
UniProtKB-H8WXY1_Mdr1_MFS/1-551 PFFGA.ILSVKAGWRWTFWFIMIVSGFSLVL...LTFFLPETYAPTLLARKAKRLRARTG
UniProtKB-X2H531_MFS/1-453 PSFGG.VILKLWGWQFLFLINVPLCIVGCFFS.LKITKAVNTLKRETFDLKGMILFFMML
UniProtKB-F8FEU9_MFS/1-497 PLLGS.LFIEELTWRWIFYINVPICLASLLL..LIPYKESYEPKKSTINWGGALLFGLAV
UniProtKB-D2JCE1_MFS/1-453 PSIGS.ILLNFSNWSMIFWINIPIIILIVVINQVFIGELNEERFKLNFDFIGNILMVVML
UniProtKB-S4N9Y7_MFS/1-443 PLLGS.LFVEYATWRWIFYVNIPICLLSLVT..LFPYKEVYEPKRAAVDYMGAVLFAAAV


350 360 370
UniProtKB-Q07824_TPO1_YLL028W/1-586 NWGIHAAHEDVELS.....IKDIVQKTVTRPIIMLFVEP
UniProtKB-P53283_TPO2_YGR138C/1-614 NPKIMTEQEAQG.....VSMSEMMRACLLRPLYFAVTEP
UniProtKB-Q06451_TPO3_YPR156C/1-622 NPKIMTEQEAQG.....VSMGEMMRACLLRPLYFSVTEP
UniProtKB-Q12256_TPO4_YOR273C/1-659 KFSREAQKEFLKT.....TVTITILRPLKMLVVEP
UniProtKB-P36029_TPO5_YKL174C/1-618 LGNLLFSGIGSITTS.....SRAVYSFSRDQAIPYYD
UniProtKB-P38695_HXT5_YHR096C/1-592 TTEDSPLVTLEMENYQSSIEAERLAGSASWGELVTGKPQMFRRTLMGMMIQSLQQLTGDN
UniProtKB-A0A140NCX4_YajR_MFS_Inner/1-454 VLAEPRLLKLNFG.....IMCLHILLMSTFVA
UniProtKB-Q14728_TETRAN_MFS/1-455 .....LALLRFSAVARGQD
UniProtKB-Q9CDQ3_LmrP_MFS/1-408 .....IFQAYKTVLQDK
UniProtKB-P69367_MdtH_MFS/1-402 .....AWLLPAWKLSTVRT
UniProtKB-A0A037Y375_TetA_MFS/1-399 .....LRREALNPLAS
UniProtKB-Q5ABU7_MDR1_Multidrug/1-564 NDRITSEGEVENS.....KMTSHELIIDTLWRPLEITVMEP
UniProtKB-A0A4Y9WVQ1_NepI_MFS/1-396 AGMIAIFMSFAG.....QFAFFTYIR
UniProtKB-A0A2A5MDZ6_NepI_MFS/1-397 AGMCAIFMAFAG.....QFAFFTYIR
UniProtKB-B1VCE9_TetA(B)_MFS/1-401 .....DTEVGVETQSN
UniProtKB-V5VHF5_NepI_MFS/1-404 .....LPALLRTPKAR
UniProtKB-W8T9A7_YebQ_MFS/1-457 GLLITALSGFAQGQS.....LTLIAAELVVMVVVGIFFIRRQLSL
UniProtKB-J7R9S9_CmlA1_MFS/1-410 .....FSAKSVLRDFRNVFCNR
UniProtKB-J7R2H7_MdfA_MFS/1-410 .....LSLKELGRDYKLVLKNG
UniProtKB-Q5L0E1_MFS/1-449 SLLLLVTVAKRG.....QWWYGAAGALLLVAFYFFEKRQ
UniProtKB-A0A098L6G2_MFS/1-449 SLLLLVTVAKRG.....QWWYGAAGALLLVAFYFFEKRQ
UniProtKB-I6L919_MFS/1-459 VCLLLGLSLLSKPHLL.....GISLILIIISFLIGIWFYRLECSKE
UniProtKB-H8WXY1_Mdr1_MFS/1-551 NERITTVGLLENE.....ERTVHQILVEALWRPIEVTILEP
UniProtKB-X2H531_MFS/1-453 VACVSLIYSDNLN.LL.....LIEKNFIGISTLIIFFIFLRIESKC
UniProtKB-F8FEU9_MFS/1-497 GLLLMNTVVTQG.....YLLYTAAGLLFLALFVWNERRH
UniProtKB-D2JCE1_MFS/1-453 SSLILAITFLKS.....QFIIVLLIIFLISLWLFIKWESKV
UniProtKB-S4N9Y7_MFS/1-443 SLLLLVTVAKRG.....QWWYGAAGALLLVAFYFFEKRQ


380 390 400 410 420 430
UniProtKB-Q07824_TPO1_YLL028W/1-586 LLLFVTIYNSFVYGILYLLLEAYPLVFVEGYGFTENGELPYIALIIGMMVCAAFIWYMDN
UniProtKB-P53283_TPO2_YGR138C/1-614 VLVATCFYVCLIYSLLYAFFFAFPVIFGELYGYKDNLVGLMFIPIVIGALWALATTFYCE
UniProtKB-Q06451_TPO3_YPR156C/1-622 VLVATCFYVCLIYSLLYAFFFAFPVIFGELYGYKDNLVGLMFIPIVIGALWALATTFYCE
UniProtKB-Q12256_TPO4_YOR273C/1-659 IVFVFSVYVAFIFAILFGFFEAYAVIYRGVYHMSMGISGLPFIGIGVGLWIGAFFYLYID
UniProtKB-P36029_TPO5_YKL174C/1-618 KWTYVEPDSQSKVPKNSVVLSMIISYFLGLLALISTAAFNAFIGAAVLCLCSATFIPLVL
UniProtKB-P38695_HXT5_YHR096C/1-592 YFFYYGTTIFQAVGLEDSFETAIVLGVVNFVSTFFSLYTVDRFGRRNCLLWGCVGMICCY
UniProtKB-A0A140NCX4_YajR_MFS_Inner/1-454 LPGQLADAGFPAAEHWKVYLATMLIAFGSVVPFIIYAEVKRKMKQVFVFCVGLIVVAEIV
UniProtKB-Q14728_TETRAN_MFS/1-455 PPSGDRLSSLRRLGLVYFLYLFLFSGLEYTLSFLTHQRFQFSSLQQGKMFFLIGLTMATI
UniProtKB-Q9CDQ3_LmrP_MFS/1-408 TYMIFMGANIATTFIIMQFDNFLPVHLSNSFKTITFFGFEIYGQRMLTIYLIILACVLVVL
UniProtKB-P69367_MdtH_MFS/1-402 PVREGMTRVVMRDKRFVTYVLTLAGYYMLAVQVMLMLPIMVNDVAGAPSAVKWMYAIEACL
UniProtKB-A0A037Y375_TetA_MFS/1-399 FRWARGMTVVAALMAVFFIMQLVGQVPAALWVIFGEDRFHWDATTIGISLAAFGILHSLA
UniProtKB-Q5ABU7_MDR1_Multidrug/1-564 VVLLINIYIAMVYSILYLFFEVFPIYFVGVKHFTLVELGTTYMSIVIGIVIAAFIYIPVI
UniProtKB-A0A4Y9WVQ1_NepI_MFS/1-396 PVYMNLAGFGVDG....LTLVLLSFGIASFIGTSLSSFILKRSVKLALAGTPLILAVSAL
UniProtKB-A0A2A5MDZ6_NepI_MFS/1-397 PVYMTLAGFDVDG....LTLVLLSFGIASFIGTSLSSVLLKRSVKTALAIAPLVLTACAA
UniProtKB-B1VCE9_TetA(B)_MFS/1-401 SVYITLFKTMPILLIIYFSAQLIGQIPATVWVLFTENRFGWNSMMVGFSLAGLGLLHSVF
UniProtKB-V5VHF5_NepI_MFS/1-404 SGMLIVLLIGLAHFCAYSYLAPFFKNVAGFNGTTISS.LLLLYGIAGIFGNAFAGYSGNL
UniProtKB-W8T9A7_YebQ_MFS/1-457 PVPLLPVDLLRIPLFSLSICTSVCSFCAQMLAMVSLPFYLQTVLGRSEVETGLLLTPWPL
UniProtKB-J7R9S9_CmlA1_MFS/1-410 LFLFGAATISLSYIPMMSWVAVSPVILIDAGGLTTSQFAWTQVPVFGAVIVANAIVARFV
UniProtKB-J7R2H7_MdfA_MFS/1-410 RFVAGALALGFVSLPLLAWIAQSPIIIITGEQLSSYEYGLLQVPIFGALIAGNLLLARLT
UniProtKB-Q5L0E1_MFS/1-449 PSPLVPLSLVHHRTLKWMNINGFVSCVALFGTSSYIPLFLQNVAHLSVFISGVALLGSSV
UniProtKB-A0A098L6G2_MFS/1-449 PSPLVPLSLVHHRTLKWMNINGFVSCVALFGTSSYIPLFLQNVAHLSVFISGVALLGSSV
UniProtKB-I6L919_MFS/1-459 SALVNVKGLSENPRVLSYLFQTVAFGFASAMIFLLPPFIFEQLYHLGVGQTGFLVLGAPA
UniProtKB-H8WXY1_Mdr1_MFS/1-551 VVLLIDIYIAMVYSVLYLFFEVFPIYFVEVRGFTVVELGISYLAIIIGVLVAVSIYLPVI
UniProtKB-X2H531_MFS/1-453 TNPFFPVKLLFISSIRYVSIGSLIFGLTAGIIFSASPLLFIREAGYPIDYIGLICTAAPI
UniProtKB-F8FEU9_MFS/1-497 PSPIVPVVLLQNRPVAWMNLNGFLTCAALFGTSSYIPYYLQQHG.YSLFVSGLALLGMSV
UniProtKB-D2JCE1_MFS/1-453 KFPLIPVTWLQNKMMLSLLFGIFTLGGSMSLGFIIPPFYIEQNLKLNTLIVGIVNLSAPL
UniProtKB-S4N9Y7_MFS/1-443 PSPLVPLSLVHHRTLKWMNINGFVSCVALFGTSSYIPLFLQNVAHLSVFISGVALLGSSV


440
450
460
UniProtKB-Q07824_TPO1_YLL028W/1-586 DYLKRCRAKG.....KLVPEARLYAMVIAGTVFPIGI
UniProtKB-P53283_TPO2_YGR138C/1-614 NKYLQ..IVK.....QRKPTPEDRLLGAKIGAPFAAI
UniProtKB-Q06451_TPO3_YPR156C/1-622 NKYLQ..IVK.....QRKPTPEDRLLGAKIGAPFAAI
UniProtKB-Q12256_TPO4_YOR273C/1-659 RKYLFPKPPAGTQPLTEKERTSKRTTPYRGARDAETGELLPVVPEKFLIACKFGSVALPI
UniProtKB-P36029_TPO5_YKL174C/1-618 VLFTRRRAIR.....SAPVKIRYKFGWFINIVSIVWLLL
UniProtKB-P38695_HXT5_YHR096C/1-592 VVYASVGVTRLWP.....NGQDQPSSKGAGNCMIVFACFYIF
UniProtKB-A0A140NCX4_YajR_MFS_Inner/1-454 LWNAQTQFWQ.....LVVGVQLFFVAFNLMEALLP
UniProtKB-Q14728_TETRAN_MFS/1-455 QGAYARRIHP.....GGEVAAVKRALLLLVP
UniProtKB-Q9CDQ3_LmrP_MFS/1-408 LMTTLNRLTK.....DWSHQKGFIWGSLFMAIGMIF
UniProtKB-P69367_MdtH_MFS/1-402 SLTLLYPIAR.....WSEKHFRLEHRLMAGLLIM
UniProtKB-A0A037Y375_TetA_MFS/1-399 QAMITGPVAA.....RLGERRALMLGMIADGTGYILL
UniProtKB-Q5ABU7_MDR1_Multidrug/1-564 RQKFTKPILR.....QEQVFPEVFIPIAIVGGILLTS
UniProtKB-A0A4Y9WVQ1_NepI_MFS/1-396 VLTLWGSDK.....IVATGVAIIW
UniProtKB-A0A2A5MDZ6_NepI_MFS/1-397 ALVLWGESK.....IVASTVAIIW
UniProtKB-B1VCE9_TetA(B)_MFS/1-401 QAFVAGRIAT.....KWGEKTAVLLGFIADSSAFAFL
UniProtKB-V5VHF5_NepI_MFS/1-404 NVRYTLAFVG.....TCFAIVFFGFPIFAIH
UniProtKB-W8T9A7_YebQ_MFS/1-457 ATMVMAPLAG.....YLIERVHAGLLGALGLFIMAAG
UniProtKB-J7R9S9_CmlA1_MFS/1-410 KDPTEPRFIW.....RAVPLQLVGLALLIIGNLLSP.
UniProtKB-J7R2H7_MdfA_MFS/1-410 SRRTVRSLII.....MGGWPIMIGLLVAAAATVISS.
UniProtKB-Q5L0E1_MFS/1-449 GWMIAAVPAG.....KWILRYGYRPLLIIGNVLLVAS
UniProtKB-A0A098L6G2_MFS/1-449 GWMIAAVPAG.....KWILRYGYRPLLIIGNVLLVAS
UniProtKB-I6L919_MFS/1-459 GLVLFSRISG.....KINDGSKNKSFSHIGLGIIILS
UniProtKB-H8WXY1_Mdr1_MFS/1-551 HHQFTKPILN.....NETVYPEVFIPIAIVGGFLFAS
UniProtKB-X2H531_MFS/1-453 G.VILSVFCR.....KVINSSCNKIILIYALPLMLFA
UniProtKB-F8FEU9_MFS/1-497 GWVLMGVPAG.....RWILRYGYRPLLVIGNLILVLS
UniProtKB-D2JCE1_MFS/1-453 GMVIMSQFSN.....KLTKKFNNQLLLTLSILLMGIS
UniProtKB-S4N9Y7_MFS/1-443 GWMIAAVPAG.....KWILRYGYRPLLIIGNVLLVAS


470
480
490
500
510
520
UniProtKB-Q07824_TPO1_YLL028W/1-586 LWFCWTGYYPHKIHWMVPTVGGAFIGFGLMGIFLPCL...NYIIESYLLLAAS.AVAANT
UniProtKB-P53283_TPO2_YGR138C/1-614 ALWILGATAYKHIIWVGPASAGLAFGFGMVLIYYSLN...NYIIDCY.VQYASSALATKV
UniProtKB-Q06451_TPO3_YPR156C/1-622 ALWILGATAYKHIIWVGPASAGLAFGFGMVLIYYSLN...NYIIDCY.VQYASSALATKV
UniProtKB-Q12256_TPO4_YOR273C/1-659 GLFWQAWTARSDVHWMAPVAAGVPFGFGLILIFFSVL...MYFSTCYPPLTVASCLAANN
UniProtKB-P36029_TPO5_YKL174C/1-618 SMVSVCLPTQVPVTFKTMNYALMVYVFCILVITGLYFKWGKYNFRLPLADDIKAPIPSDA
UniProtKB-P38695_HXT5_YHR096C/1-592 CFATTWAPVAYVLISESYPLRVRGKAMSIASACNWIWGFLISFFTPFITSAINFYYGYVF
UniProtKB-A0A140NCX4_YajR_MFS_Inner/1-454 SLISKESPAGYKGTAMGVYSTSQFLGVAIGGSLGGWI...NGMFDGQGVFLAGAMLAAVW
UniProtKB-Q14728_TETRAN_MFS/1-455 AFLLIGWG..RSLPVLGLGLLLLYSFAAAVVVPCLSSV...VAGYGSPGQKGTVMGTLRSL
UniProtKB-Q9CDQ3_LmrP_MFS/1-408 SFLTTTFTP.....IFIAGIVYTLGEIVYTPSVQTL...GVDLMNPEKIGSYNGVAAIK
UniProtKB-P69367_MdtH_MFS/1-402 SLSMMPVGMVSGLQQLFTLICLFYIGSIIAEPARETL...SASLADARARGSYMGFSRLG
UniProtKB-A0A037Y375_TetA_MFS/1-399 AFATRG.....WMAFPIMVLLASGGIGMPALQAM...LSRQVDEERQGQLQGSLAAL
UniProtKB-Q5ABU7_MDR1_Multidrug/1-564 GLFIFGWSANRTTHWVGPLFGAATTASGAFLIFQTLF...NFMGASFKPHYIASVFASND
UniProtKB-A0A4Y9WVQ1_NepI_MFS/1-396 GLTFALVP.....VGWST...WITRSLADQAEKAGSIQVAV
UniProtKB-A0A2A5MDZ6_NepI_MFS/1-397 GFAFALIP.....VGWST...WITRSLSDQAEKAGSIQVAV
UniProtKB-B1VCE9_TetA(B)_MFS/1-401 AFISEG.....WLVFPVLILLAGGGIALPALQGV...MSIQTKSHQQGALQGLLVSL
UniProtKB-V5VHF5_NepI_MFS/1-404 EFG.....AIVLTALWGFAFGAFPTSANIW...MFVHAPHAVEKGMPLFVGMF
UniProtKB-W8T9A7_YebQ_MFS/1-457 LFSLVLLPASPADINIIWPMILCGAGFGLFQSPNNHT...IITSAPRERSGGASGMLGTA
UniProtKB-J7R9S9_CmlA1_MFS/1-410 .....HVWLWSVLGTSLYAFGIGLIFPTLF...RFTLFSNNLPKGTVSASLNM
UniProtKB-J7R2H7_MdfA_MFS/1-410 .....HAYLWMTAGLSIYAFGIGLANAGLV...RLTLFASDMSKGTVSAAMGM
UniProtKB-Q5L0E1_MFS/1-449 GLLLALLNESHGFWYVFFVMFVQGLSFGLTSTVGVIG...SQQLADVHEKGIATSFFMFC
UniProtKB-A0A098L6G2_MFS/1-449 GLLLALLNESHGFWYVFFVMFVQGLSFGLTSTVGVIG...SQQLADVHEKGIATSFFMFC
UniProtKB-I6L919_MFS/1-459 LIFLLLLTPSWPYLFLTLGLFIYGIGGGYFQPANMAS...IMLASPMKMQGSTGALQRMV
UniProtKB-H8WXY1_Mdr1_MFS/1-551 GLFIFGWSATTYTHWIGPLFGVAATSAGTFLMFQTLF...NYMGASFKHEYLASVFASND
UniProtKB-X2H531_MFS/1-453 FALLFFVSFNISIFNYVIAALCYGLGGG.LFQGSLIQ...IAMDQKKDKQSTIGGLLRLF
UniProtKB-F8FEU9_MFS/1-497 GLLLLFLPEEGGFFYVNVIMVLQGLAYGLLATVSVIG...VQQLVAADQKGISTSLQVFA
UniProtKB-D2JCE1_MFS/1-453 YLVIGLLQYNLLIWKLIVLLLFFGFGCGIYLPINTRS...ILNLVKKSQQATAGSLQRMI
UniProtKB-S4N9Y7_MFS/1-443 GLLLALLNESHGFWYVFFVMFVQGLSFGLTSTVGVIG...SQQLADVHEKGIATSFFMFC


530
540
550
560
570
580
UniProtKB-Q07824_TPO1_YLL028W/1-586 FMRSAFGACFPLFAGYMFRGMGIG.....WAGLLLGLFAAAMIPVPLLFLKYGESIRKKS
UniProtKB-P53283_TPO2_YGR138C/1-614 FLRSAGGAAFPLFTIQMYHKLN.....LHWGSWLLAFISTAMIALPFAFSYWGKGLRHKL
UniProtKB-Q06451_TPO3_YPR156C/1-622 FLRSAGGAAFPLFTIQMYHKLN.....LHWGSWLLAFISTAMIALPFAFSYWGKGLRHKL
UniProtKB-Q12256_TPO4_YOR273C/1-659 LLRYVMSSVFPLFTIQMYTKMKIK.....WASTLFALVCVVMIPIPWVFEKWGSKLRHKS
UniProtKB-P36029_TPO5_YKL174C/1-618 EETVFELEDSNVEHTLNSGTTVKESVENNSEEGFIKVHPKSSTENPFEENEENVITDYGD
UniProtKB-P38695_HXT5_YHR096C/1-592 MGCMVFAYFYVFFFVPETKGLTLEEVNEMYEENVLPWKSTKWIPPSRRTTDYDLDATRND
UniProtKB-A0A140NCX4_YajR_MFS_Inner/1-454 LTVASTMKEPPYVSSLRIEIPANIAANEALKVRLLETEGIKEVLIAEEEHSAYVKIDSKV
UniProtKB-Q14728_TETRAN_MFS/1-455 GALARAAGPLVAASVYWLAGAQ.....ACFTTWSGLFLLPFFLLQKLSYPAQTLKA
UniProtKB-Q9CDQ3_LmrP_MFS/1-408 MPIASILAGLLVSISPMIKATG.....VSLVLALTEVLAIILVLIAVNRHQKTKIN.
UniProtKB-P69367_MdtH_MFS/1-402 LAIGGAIGYIGGGWLFDLGKSAHQPELPWMMLGIIGIFTFLALGWQFSQKRAARRLLERD
UniProtKB-A0A037Y375_TetA_MFS/1-399 TSLTSIVGPLLFTAIYAASITTWNGWAWIAGAALY....LLCLPALRRGLWSGAGQRADR
UniProtKB-Q5ABU7_MDR1_Multidrug/1-564 LFRSVIASVFPLFGAPLFDNLATPEYPVAWGSSVLGFITLVMIAIPVLFYLNGPKLRARS
UniProtKB-A0A4Y9WVQ1_NepI_MFS/1-396 IQLANTCGAAIG....GYALDNIGLTSPLMLSGTLMLLTALLVTAKVKMKKS.....
UniProtKB-A0A2A5MDZ6_NepI_MFS/1-397 IQLANTCGAAVG....GIALDHLGLLSPLVLSGVLMLFTGLLVAAKVKVNSPA.....
UniProtKB-B1VCE9_TetA(B)_MFS/1-401 TNATGVIGPLLFAVIYNHSLPIWDGWIWIIGLAFYCIIILLSMTFMLTPQAQGSKQETSA
UniProtKB-V5VHF5_NepI_MFS/1-404 QVMIATGSLLGGYVVDHFNENT.....LIYGVLSFVALALISTFTLAKGLNNPKATCE
UniProtKB-W8T9A7_YebQ_MFS/1-457 RLLGQSSGAALVALMLNQFGDN.....GTHVSLMAAAILAVIAACVSGLRITQPRS
UniProtKB-J7R9S9_CmlA1_MFS/1-410 VILMVMSVSVEIGRWLWFNGGR.....LPFHLLAVVAGVIVVFTLAGLLNRVRQHQAA
UniProtKB-J7R2H7_MdfA_MFS/1-410 LQMLIFTVGIEISKHAWLNGGN.....GQFNLFNLVNGILWLSLMVIFLKDKQMGNSH
UniProtKB-Q5L0E1_MFS/1-449 RNIGTAIGVTVMGAFLTKAPTFMTGIHHLFLFGLIGSIAALVTSLFIHDEAETGRNTWQP
UniProtKB-A0A098L6G2_MFS/1-449 RNIGTAIGVTVMGAFLTKAPTFMTGIHHLFLFGLIGSIAALVTSLFIHDEAETGRNTWQP
UniProtKB-I6L919_MFS/1-459 QNIAISAGSAIG....STCLNLWSN..NLLLATRIGWGITLVLVIFSLKELTPFKMTNKT
UniProtKB-H8WXY1_Mdr1_MFS/1-551 LVRSTIASVFPIFGAALFNNLKIDKFPVAWGASVLGFIATAMIAIPVLFYLNGPKLRARS
UniProtKB-X2H531_MFS/1-453 QNGGIIIGSACSLMLLEAKISPLVNISTYQKLWGITFSVLSIMFVYSYVSLFRIKK....
UniProtKB-F8FEU9_MFS/1-497 RNIGTAVGVTIMGGLLTGAPAFMTGIHRLFLYGFIVALAALGSTVFLFMGKEQ...TAPQ
UniProtKB-D2JCE1_MFS/1-453 QNLGIALYSSVS....SITIQIFKNHHNMIHGYIVLWIMASIILFIGFILSVKNLLGYKK
UniProtKB-S4N9Y7_MFS/1-443 RNIGTAIGVTVMGAFLTKAPTFMTGIHHLFLFGLIGSIAALVTSLFIHDEAETGRNTWQP

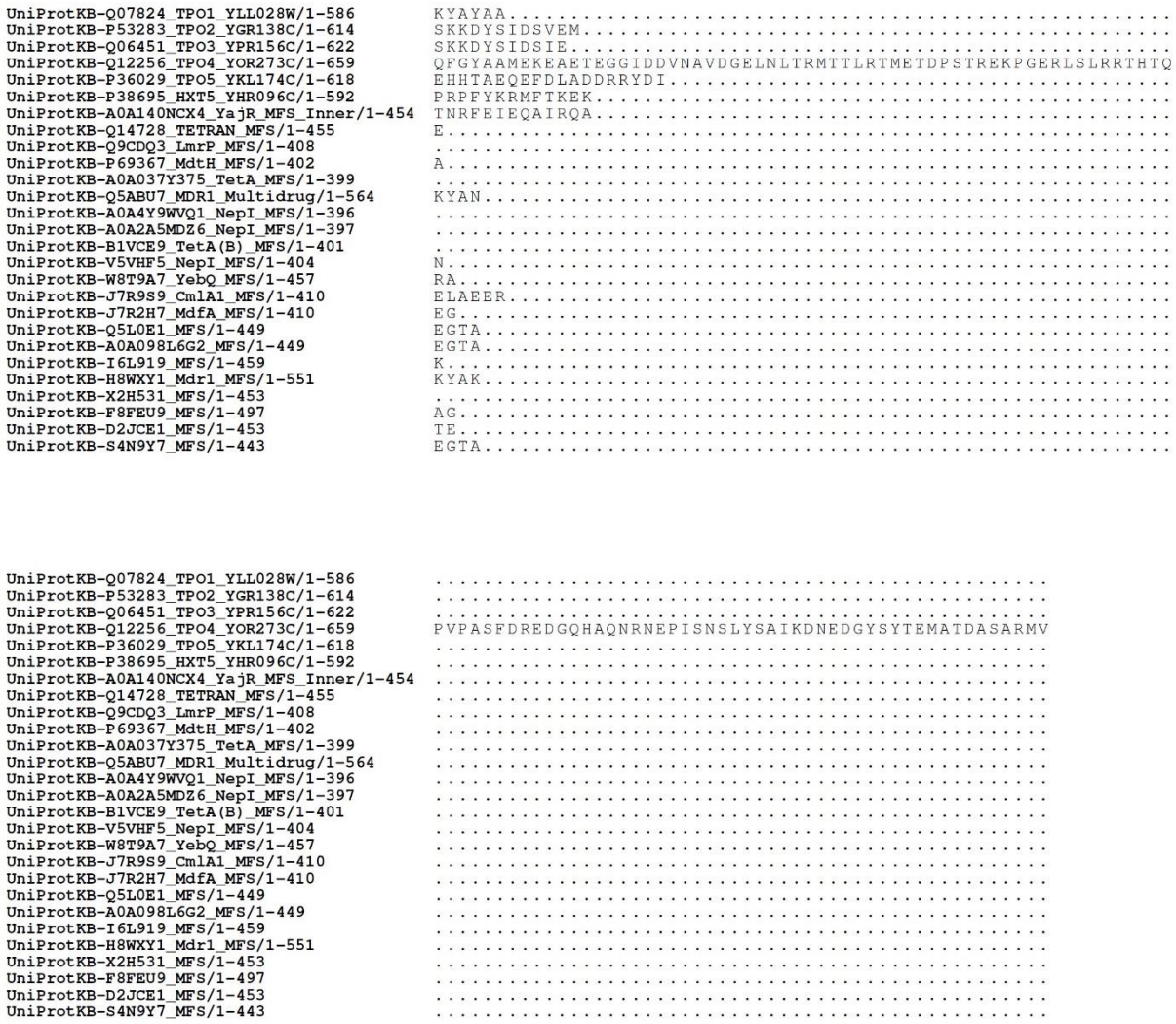


Figure 1.2 Conserved sequence motif of DHA1 and DHA2 among the Tpo proteins of *S. cerevisiae*, prokaryotes, and eukaryotes. Alignment of the Tpo protein sequences of *S. cerevisiae* obtained from SGD, TETRAN; homologue of Tpo1 from *Homo sapiens* (Human) and amino acid sequences obtained from UniProt hit against Tpo1 that include *Escherichia coli*, *Lactobacillus lactis*, *Klebsiella quasipneumoniae*, *Acinetobacter baumannii*, *Geobacillus kaustophius*, *G. thermoleovorans*, *Streptococcus mutans*, *Staphylococcus epidermidis*, *Paenibacillus mucilaginosus* and *Candida albicans*. The protein sequences are mentioned in the figure with their respective UniProtKB IDs and aligned with MAFFT online server (Katoh et al., 2019). The

conserved motif consists of five amino acid residues. The rectangle covering amino acids from 210-212 of the alignment distinguishes the DHA1 (GRR) from DHA2 (GRK) families. The red colour-filled rectangles represent 100% equivalent residues based on their physicochemical properties whereas empty rectangles represent >90% equivalent percentage.

A few of the first studies of MFS transporters encoded by the whole genome of *S. cerevisiae* were examined by (Goffeau et al., 1997; Nelissen et al., 1997; Paulsen et al., 1998). In these studies, 28 MFS proteins were identified as putative MDR-H^+-antiporters and classified into two families considering their predicted 12 or 14 TMS organization (Nelissen et al., 1997). The proton antiport drives the MFS-MDR transporters in yeasts (Marger & Saier, 1993). However, there is evidence that proton antiporters can act as multidrug efflux pumps (EPs). The MdrP of the bacteria *Planococcus maritimus* which is a Na^+ $(Li^+, K^+)/H^+$ antiporter was demonstrated to have multidrug efflux activity. There are several examples of drug efflux pumps which are Na^+/H^+ antiporters too, such as multidrug transporters MdfA and MdtM of *E. coli* (Abdel-Motaal et al., 2018).

1.2.3 Plausibility of finding drug EPs in clinical fungal mitochondria

The currently used classes of antifungals include drugs that target mitochondria. They are used to treat fungal infections of animals and plants. Thus, mitochondria of clinically relevant fungi might have drug efflux pumps. ABC and MFS efflux pumps are widespread among pathogenic fungi. As an example, two proteins Cdr1p and/or CaMdr1p of the ABC and MFS superfamilies respectively were found to be over-expressed in an azole-resistant clinical isolate of *C. albicans* (Fisher et al., 2018).

Among the six main classes of fungicides applied to plant-fungal infections are azoles, succinate dehydrogenase inhibitors (SDHIs), and anilinopyrimidines. SDHIs inhibit complex II (succinate dehydrogenase) of the mitochondrial respiratory components, and anilinopyrimidines may target mitochondrial signalling pathways by targeting NADH kinases (Mosbach et al., 2017). Efflux pump over-expression is one of the resistance mechanisms developed against these fungicides. Among the fungicides that are applied to animals, azoles and pyrimidine analogues (targeting nucleic acid biosynthesis) are mostly evaded through efflux-mediated resistance (Ghannoum & Rice, 1999). Moreover, there is another class of fungicides, the strobilurins (QoIs) which inhibit the cytochrome b of the b-c_1 complex of the mitochondrial electron transfer chain (Fisher et al., 2018). So, it can be speculated that clinical fungal mitochondria might have drug efflux pumps.

1.2.4 Prevalence of MFS compared to ABC transporters

The DHA family of the MFS is more prevalent than the ABC multidrug transporters in *S. cerevisiae* and clinically important fungi (Barabote et al., 2010). To compare their prevalence, a set of pathogenic and non-pathogenic fungi ranging from oomycetes to *Phytophthora infestans* has been shown in **Table 1.1,** in terms of the number of their efflux transporters out of the total transporters.

In these fungi, the efflux transporters comprise more than 50% and up to 75% of all the predicted ABC transporters. In all other fungi, except for *S. cerevisiae*, the MFS-MDR transporters cover from 29 to 39% of all the MFS transporters. 21% of the total 85 MFS transporters found in the *S. cerevisiae* genome are predicted to be involved in efflux activity (Barabote et al., 2010). Thus, the likelihood of finding drug efflux pumps in fungal mitochondria from the MFS superfamily is more than the ABC superfamily.

Table 1.1 Occurrence of putative efflux transporters in a few clinical and non-clinical fungi (based on (Barabote et al., 2010))

Organism	**Total ABC**	**Efflux ABC**	**% Efflux ABC[a]**	**Total MFS**	**Efflux MFS**	**% Efflux MFS[b]**	**N/P[c]**	**Genome size (Megabase)**
S. cerevisiae	24	13	54	85	18	21	N	13
N. crassa	31	17	55	141	55	39	N	40
Aspergillus nidulans	45	35	75	356	99	28	N	31
Aspergillus fumigatus	45	35	75	275	96	35	P	33
Cryptococcus neoformans	29	19	65	192	54	28	P	19
Aspergillus oryzae	72	60	83	507	180	35	P	32
Phytophthora infestans	160	116	72	102	2	<2	P	237

Origin: Transporter Protein Analysis Database (http://www.membranetransport.org/transportDB2/index.html)
[a]Percentage ABC efflux transporters out of the total ABC transporters
[b]Percentage MFS efflux transporters out of the total MFS transporters
[c]N/P, Non-pathogen/Pathogen

1.2.5 The relevance of the non-clinical fungal DHA to those of the clinical fungi

Interestingly, the *S. cerevisiae,* being a non-pathogenic fungus, has several drug efflux pumps (EP) of the DHA1 and DHA2 families. Several antifungal drugs such as fluconazole (ScAzr1, ScQdr1, ScFlr1 and ScYhk8) (Barker et al., 2003; Nunes et al., 2001; Tenreiro et al., 2000), itraconazole (ScYhk8) (Barker et al., 2003), ketoconazole (ScAqr1, ScAzr1, ScQdr1 and ScQdr2) (Tenreiro et al., 2000; Nunes et al., 2001), and caspofungin (ScTpo1) (Markovich et al., 2004a) are involved in the upregulation of these respective EPs mentioned herein. ScAzr1 and ScQdr1 conferred resistance to even multiple antifungal agents (Costa et al., 2014). The *S. cerevisiae* AZR1 gene deletion mutant showed higher susceptibility to azoles like fluconazole and ketoconazole (Tenreiro et al., 2000). Moreover, the ScQDR1 gene deletion mutant showed higher susceptibility to fluconazole and ketoconazole (Nunes et al., 2001).

This phenomenon is further described by (Costa et al., 2014) who performed phylogenetic analyses of DHA1 and DHA2 transporters obtained from *S. cerevisiae* S288C as a reference strain for non-clinical fungus and eight clinically important fungal species - 5 *Candida spp.,* and one each of *Aspergillus fumigatus and Cryptococcus neoformans* (**Figure 1.3**). The *Candida spp*. included in the study were *C. albicans, C. glabrata, C. guilliermondii, C. parapsilosis* and *C. tropicalis* (Paulo Jorge Dias et al., 2010; Paulo J. Dias & Sá-Correia, 2013). These eight fungal species encoded a total of 185 full-length DHA1 and 85 full-length DHA2 transporters. They showed that DHA1 MFSs such as Tpo1, Tpo2, Tpo3 and Tpo4 of the non-clinical *S. cerevisiae* are homologues to the DHA1 MFSs of clinical fungi. This observation indicates that we can use the non-clinical fungi as a model system to study efflux pumps. Thus, it is important to study the DHA MFS in *S. cerevisiae*.

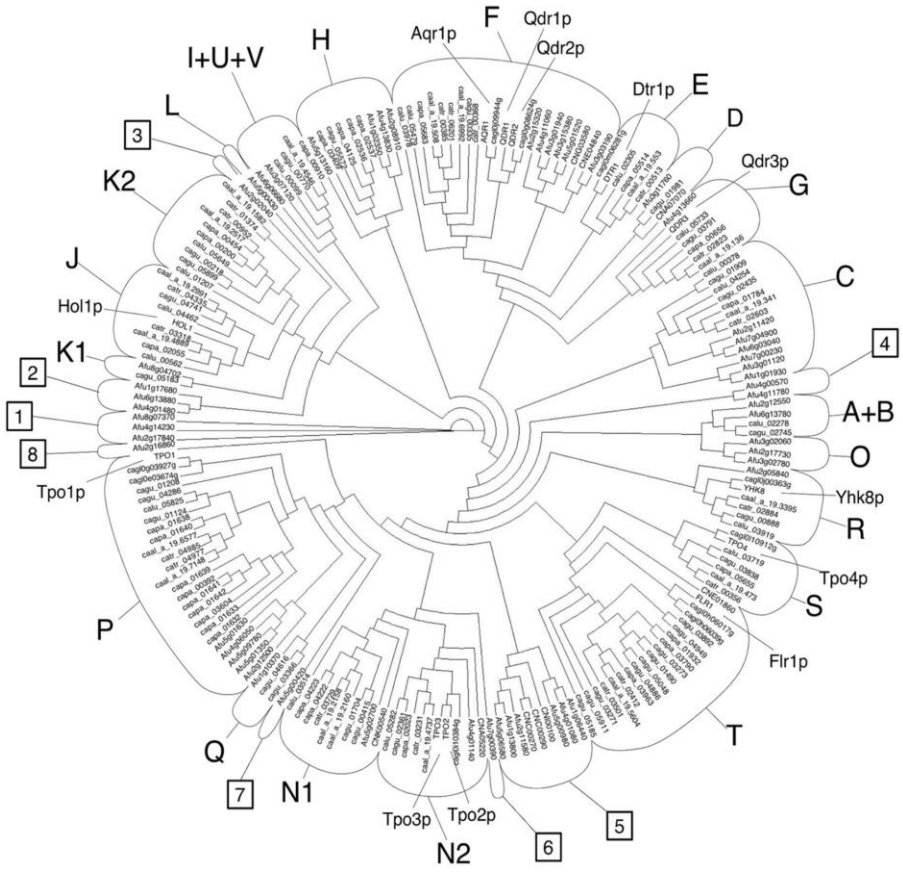


Figure 1.3 A radial phylogenetic tree demonstrating the clustering of DHA1 transporters from the *S. cerevisiae* S288C to the DHA1 of eight clinically important fungal species. Labels A to V indicates the previously reported DHA1 protein phylogenetic clusters. The DHA1s of the *S. cerevisiae* have been singled out of the clusters and mentioned in larger fonts. The newly added clusters 1-4 and 6-7 demonstrate DHA1 genes only from *A. fumigatus,* whereas, cluster 5 demonstrates DHA1 genes from *A. fumigatus* and *C. neoformans.* Adapted from (Costa et al., 2014).

1.3 Characterization of the Transporter of polyamines (Tpo) of *S. cerevisiae*

1.3.1 Physiological functions of Tpo proteins

In *S. cerevisiae,* there are proteins involved in the uptake of polyamines e.g., Gap1 (Uemura, Kashiwagi, et al., 2005), Agp2 (Aouida et al., 2005), Dur3 and Sam3 (Uemura et al., 2007) on plasma membranes and Uga4 (Uemura et al., 2004) on vacuolar membranes, whereas Tpo1-Tpo5 are involved in the excretion of polyamines (Uemura et al., 2007). The above-mentioned proteins are involved in the regulation of polyamine content inside the cell (**Fig 1.4**). Polyamines are organic polycations that include spermine, spermidine and putrescine (Hoyt & Davis, 2004). They have multiple cell physiological roles but are not limited to the regulation of nucleic acid and protein synthesis, and cell growth (Seiler, 1999).

pH is crucial for the transfer of polyamines by Tpo1. It has been shown that Tpo1 catalyzes the uptake of spermine and spermidine at alkaline pH (8.0) and excretion of spermidine at acidic pH (5.0) (Uemura, Tachihara, et al., 2005). Tpo1 has been shown to regulate the timing of expression of stress-response components during oxidative stress through controlled spermine and spermidine export (Krüger et al., 2013). The sorting of the Tpo1 from the endoplasmic reticulum to the plasma membrane and the Tpo1 transport activity are enhanced through phosphorylation (Uemura, Tachihara, et al., 2005).

The identified substrate for Tpo2 and Tpo3 is spermine (Tomitori et al., 2001). The *TPO2* gene is regulated by the *S. cerevisiae* regulator protein Homolog of Ace1 Activator (Haa1). Thus, Haa1 could regulate polyamine transport by Tpo2 (Keller et al., 2001). Identified and characterized substrates for Tpo4 are spermine, spermidine and putrescine (Albertsen et al., 2003).

Tpo5 was found to excrete putrescine effectively and spermidine less effectively (Tachihara et al., 2005). It excretes the putrescine and spermidine out of the cell from Golgi or post-Golgi secretory vesicles through a process that involves both endocytosis and exocytosis (**Fig 1.4**) (Uemura et al., 2007). It is suggested that Tpo5 could lead to the accumulation of polyamines in vesicles and these polyamines then would be excreted through exocytosis, where the Tpo5 proteins are recycled through endocytosis (Tachihara et al., 2005).

1.3.2 Cellular localization of Tpo proteins in *S. cerevisiae*

In *S. cerevisiae*, initially the polyamine transporters Tpo1-Tpo4 were found to be localized in the vacuolar membrane (Tomitori et al., 2001). It was shown that cells overexpressing these proteins can resist polyamine toxicity and have increased polyamine contents in their vacuoles, indicating cytosolic polyamine uptake by these transporters into the vacuoles (Tomitori et al., 2001). Subsequently, it was demonstrated that the Tpo1-Tpo4 are mostly localized on the plasma membrane and fewer molecules were present in the vacuolar membrane (Albertsen et al., 2003) (**Fig 1.4**). Moreover, the overexpression of Tpo1 from a multi-copy vector (Yep351) causes Tpo1 to localize in vacuolar membranes as well as within the plasma membrane. However, expression with a single-copy vector (YCp) demonstrated Tpo1 to be on the plasma membrane (Uemura, Tachihara, et al., 2005). In contrast, Tpo5 is found on the Golgi or post-Golgi secretory vesicles (**Fig 1.4**) determined by immunostaining of hemagglutinin-tagged Tpo5 (Tachihara et al., 2005).

Vögtle et al., 2017 produced a quantitative map of proteins distributed in *S. cerevisiae* mitochondrion and found 206 novel proteins, in highly purified mitochondria, whose mitochondrial localizations were not identified earlier. Among these novel proteins, 3 potential mitochondrial transporters, namely Tpo1, Tpo3 and Hxt5, were identified. We chose these 3

proteins along with Tpo2, Tpo4 and Tpo5 to study in this thesis according to their potential transport properties as *S. cerevisiae* putative mitochondrial drug efflux pumps.

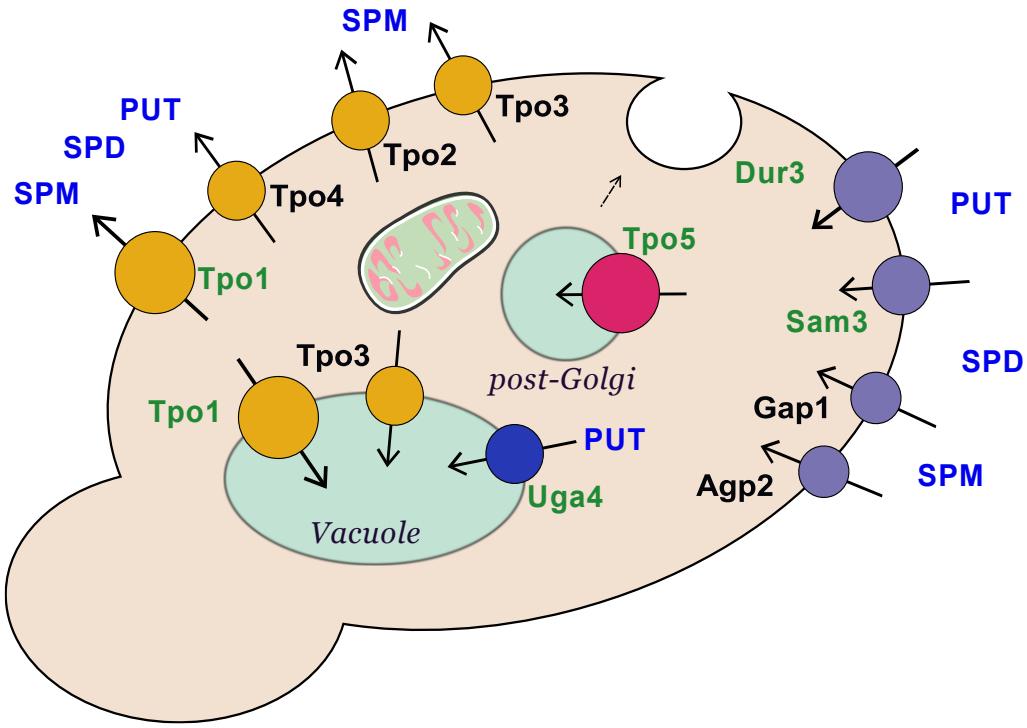


Figure 1.4 Involvement of transporters of polyamine (Tpo) in polyamine regulation and their localization in the *S. cerevisiae* cell. Based on (Uemura et al., 2007). Dur3 and Sam3 are the two main players in polyamine uptake. However, Agp2 uptakes spermine and Gap1 uptakes spermine and putrescine. Moreover, Uga4 sequesters putrescine from the cytoplasm. Tpo1-Tpo5 are involved in the export of polyamines situated either in the plasma membrane, vacuolar or post-Golgi secretory vesicle membranes. The proteins labelled in *green* are more involved in polyamine transport than that of the proteins in *black*. SPM; Spermine, SPD; Spermidine, PUT; Putrescine.

1.3.3 Hexose transporter (Hxt5) of *S. cerevisiae*

In *S. cerevisiae*, the Hexose transporter gene (*HXT5*) encodes the transporter Hxt5, which catalyzes moderate uptake of glucose (Km=10 mM), moderate to low uptake of fructose (Km=40 mM) and low uptake of mannose (Km>100 mM) (Diderich et al., 2001). It was shown that *HXT*-encoded proteins are not essential for the survival of *S. cerevisiae* (Wieczorke et al., 1999). Along with other *HXT* genes (*HXT1-17*), the deletion of *HXT5* is not lethal for the cell (Diderich et al., 2001).

The expression of the Hxt5 is almost undetectable in cells growing on a fermentable carbon source (glucose); however, upon depletion of the glucose, the expression of the Hxt5 is induced (Özcan & Johnston, 1999). In a glucose-depleted state, the Hxt5 was found to be localized on the plasma membrane and some in the cytoplasm when tagged with green fluorescence protein (GFP) (Diderich et al., 2001). The exact subcellular location of Hxt5 is not known.

A few more characteristic properties of the Tpo proteins and Hxt5 are listed in **Table 1.2**.

Table 1.2 Characteristic properties of the Tpo proteins and Hxt5

Gene*	ORF*	Length (bp)*	Protein#	UniProtKB ID	Family$	#TMS$	Length (a.a.)*	Mol. Weight (kDa)*	Median Abundance (molecules/cell)*
TPO1	YLL028W	1761	**Tpo1**	Q07824	Drug:H^+ Antiporter-1 (DHA1)	12	586	64.2	3171 +/- 2243
TPO2	YGR138C	1845	**Tpo2**	P53283	DHA1	12	614	67.6	2938 +/- 911
TPO3	YPR156C	1869	**Tpo3**	Q06451	DHA1	12	622	68.0	3768 +/- 1584
TPO4	YOR273C	1980	**Tpo4**	Q12256	DHA1	12	659	73.2	3846 +/- 2713
TPO5	YKL174C	1857	**Tpo5**	P36029	Amino Acid/Choline Transporter (ACT)	12	618	69.2	764 +/- 376
HXT5	YHR096C	1779	**Hxt5**	P38695	Sugar Porter (SP)	12	592	66.2	1060 +/- 907

*ORF= Open reading frame

*Information adapted from *Saccharomyces* Genome Database (SGD). https://www.yeastgenome.org/

#Information adapted from UniProtKB. https://www.uniprot.org/uniprot/

$Information adapted from Transporter Classification Database (TCDB). https://www.tcdb.org/

1.3.4 Phylogenetic relationship of Tpo and Hxt proteins

S. cerevisiae has undergone a whole-genome duplication (WGD) event from its ancestor (Dujon et al., 2004; Kellis et al., 2004; Wolfe & Shields, 1997). This event generated 551 paralogous gene pairs, meaning 19.6% (1102 of 5516) of the total *S. cerevisiae* genes are identified (Byrne & Wolfe, 2005). The WGD event resulted in paralogs Tpo3 from Tpo2 and Hxt5 from Hxt3, respectively (Byrne & Wolfe, 2005). The relationships among the Tpo and Hxt proteins from a phylogenetic standpoint are shown in **Fig 1.5**. Tpo1-Tpo4 are clustered together whereas the Tpo5 and Hxt proteins share a common ancestor.

1.3.5 Implications of the Tpo proteins in drug resistance

Most of the DHA transporters of *S. cerevisiae* have been implicated in MDR and provide resistance to an array of distinct chemicals (Sá-Correia et al., 2009). In *S. cerevisiae*, the Tpo1 confers resistance to a range of toxic compounds, which is characteristic of multidrug resistance proteins (**section 1.3.6**). It has been shown that Tpo1 is regulated by Pdr1 and Pdr3, both are multidrug efflux pump regulators (Albertsen et al., 2003). Tpo2 and Tpo3 provide resistance to short-chain acetic and propionic acids (Fernandes et al., 2005). Tpo4 confers resistance to quinidine (Delling et al., 1998).

Among the *Candida* species, *C. glabrata* is the most closely related to *S. cerevisiae* at an evolutionary scale (Herrero, 2005; Roetzer et al., 2011). Thus, we can have an understanding of the implications of Tpo proteins in drug resistance from *C. glabrata* too. However, in *C. glabrata*, CgTpo1 and CgTpo3 provide resistance to clotrimazole and fluconazole drugs (Costa et al., 2016). Moreover, in a recent study, CgTpo4 is found to confer resistance to antimicrobial peptides (AMP), e.g., histatin-5 (Cavalheiro et al., 2021).



Figure 1.5: Evolutionary relationships of Tpo proteins. The evolutionary history was inferred using the Neighbor-Joining method (Saitou & Nei, 1987). The optimal tree with the sum of branch length = 7.02585223 is shown. The percentage of replicate trees in which the associated taxa clustered together in the bootstrap test (1000 replicates) is shown next to the branches (Felsenstein, 1985). The tree is drawn to scale, with branch lengths in the same units as those of the evolutionary

distances used to infer the phylogenetic tree. The evolutionary distances were computed using the Poisson correction method (Zuckerkandl & Pauling, 1965) and are in the units of the number of amino acid substitutions per site. This analysis involved 22 amino acid sequences. All ambiguous positions were removed for each sequence pair (pairwise deletion option). There was a total of 795 amino acid positions in the final dataset. Evolutionary analyses were conducted in MEGA X (S. Kumar et al., 2018).

1.3.6 Substrate range of Tpo1

Most of the drug proton antiporters of the total DHA1 and DHA2 subfamilies identified in *S. cerevisiae* are responsible for resistance to multiple growth inhibitory compounds. By far, ScTpo1 transports the widest range of predicted substrates (Sá-Correia et al., 2009). However, several studies showed Tpo1 as a multidrug efflux pump that is presumed to be in the vacuolar or plasma membrane. The expression of Tpo1 conferred resistance to a widely used antimalarial drug; artesunate (Alenquer et al., 2006), Herbicide (2,4 D) (Remy et al., 2017), Cycloheximide (Do Valle Matta et al., 2001; Sá-Correia et al., 2009), Caspofungin (Markovich et al., 2004b), Quinidine (Do Valle Matta et al., 2001) and Non-steroidal anti-inflammatory drugs (NSAIDS); Indomethacin (Mima et al., 2007). Except for NSAIDs, none of these drugs have mitochondrial targets. There are many potential substrates for Tpo1 mentioned in **Tables 6.1** and **6.2** (**Appendix 1**).

To date, no studies have shown Tpo1 taking part in direct drug efflux in fungal mitochondria. Thus, we looked for information about any homologues of Tpo1 in prokaryotes and lower eukaryotes.

1.3.7 Homologues of Tpo1 from Prokaryotes (*E. coli*) and eukaryotes (*Homo sapiens*)

Until 2007, it had not been possible to find any MFS-MDR homologues in the higher eukaryotes by direct amino acid sequence alignment (Mima et al., 2007). However, a study demonstrated a human orthologue of the yeast MFS MDR gene *TPO1*, which is referred to as TETRAN (tetracycline transporter-like protein) (Mima et al., 2007). TETRAN showed 40% identity and 74% similarity to the tetracycline transporter (TetA) of *E. coli*; both of them have 12-TMS and belong to the MFS superfamily (see **Fig. 1.2**) (Duyao et al., 1993; Levy, 1992). Mima et al., 2007 showed that yeast Tpo1 and human TETRAN conferred resistance to indomethacin (a non-steroidal anti-inflammatory drug (NSAID)), in yeast and cultured human cells, respectively.

(Miguel Cacho Teixeira & Sá-Correia, 2002) showed the induction of *TPO1* transcription, in yeast, using herbicides. The researchers in this study performed northern blotting and could demonstrate the induction of *TPO1* mRNA by indomethacin. However, the expression of Tpo2, Tpo3 and Tpo4 (homologues of Tpo1), were found not to contribute to the indomethacin resistance in *S. cerevisiae* (Mima et al., 2007).

The NSAIDs inhibit cyclooxygenase (COX-1 and COX-2) that play important roles in inflammation and pain and are generally found on the endoplasmic reticulum (ER) (Vane & Botting, 1998). However, the COX-2 is found to be localized in the mitochondria of some human cancer cell types (Liou et al., 2005). Specifically, indomethacin is found to uncouple oxidative phosphorylation in isolated rat liver mitochondria (Somasundaram et al., 1997). Moreover, indomethacin impairs human mitochondrial functions in a concentration-dependant and organ-specific way (Herminghaus et al., 2020). Thus, we were curious to find more mitochondrial targeting drugs that could be potential substrates for Tpo proteins.

1.4 Mitochondria targeting drugs

A number of studies showed that bacteriostatic and bactericidal agents target mitochondrial components (Hutchin & Cortopassi, 1994; Lowes et al., 2009; McKee et al., 2006; Pochini et al., 2008; Riesbeck et al., 1990; Tune, 1997). Moreover, from the evolutionary perspective of mitochondria, bacterial antibiotics can impair mammalian mitochondrial functions including oxidative stress and oxidative damage (Duewelhenke et al., 2007; Kalghatgi et al., 2013; Lawrence et al., 1996).

The ribosomal RNA (rRNA) is one of the major targets of bacterial antibiotics to inhibit protein synthesis. There are striking similarities between the ribosomal subunits of bacteria and

mitochondria (Lamb et al., 2015) and bacterial antibiotics target mitochondria and their components (Gootz et al., 1990; Hobbie et al., 2008; Hutchin & Cortopassi, 1994; Lowes et al., 2009; McKee et al., 2006; Pochini et al., 2008). Furthermore, the mutation rate of the mitochondrial rRNA (mt rRNA) is higher than the nuclear rRNA (Singh et al., 2014) and further changes to the mitochondrial rRNA might create more sensitive target sites for bacterial antibiotics.

Chloramphenicol (CAP) interferes with the peptide bond formation, more precisely preventing the aminoacyl-tRNA 3′ end from binding in the peptidyl transferase center (Schlünzen et al., 2001), whereas erythromycin (ERY) hampers the progression of the nascent peptide chain through the ribosomal exit tunnel (Lovmar et al., 2004; Tenson et al., 2003; Tu et al., 2005). Tetracycline (TET) inhibits protein synthesis by interfering with the binding of the aminoacyl-tRNA to the mRNA-ribosome complex (Chopra et al., 1992; Chopra & Roberts, 2001; Goldman et al., 1983; Schnappinger & Hillen, 1996).

Several studies showed antifungal drugs can target fungal mitochondria (**Table 6.1**); however, there are very few studies that demonstrated the effect of antibacterial agents on the fungal mitochondria. Interestingly, one study coined the term ‘Mitoriboscins’ as a group of mitochondrial ribosome inhibitors that have therapeutic potential against cancer stem cells (CSCs) (Ozsvari et al., 2017). Moreover, ‘Mitoriboscins’ can inhibit the growth of pathogenic fungi such as *C. albicans,* and both gram-positive and gram-negative bacteria (Ozsvari et al., 2017). Thus, for our study, several antibiotics have been selected considering their potential of targeting and inhibiting mitochondrial functions (**Table 1.3)**.

Table 1.3 Potential mitochondrial-targeted potential antibiotics and their mode of action (Lamb et al., 2015).

Antibiotics	Targets	Mechanism of action	Comment	References
Erythromycins	39S subunit (large) of the mitochondrial ribosome	Inhibit protein synthesis	Inhibitors of mitochondrial biogenesis	(Lamb et al., 2015)
Azithromycin	39S subunit, mitoribosome	Inhibit protein synthesis		(Lamb et al., 2015)
Chloramphenicol	39S subunit, mitoribosome	Inhibit protein synthesis	Significant inhibitors of mammalian mitochondrial protein synthesis	(Feder, 1986; McKee et al., 2006; Yunis, 1989)
Tetracycline	28 S subunit (small) of the mitochondrial ribosome	Inhibit protein synthesis	Significant inhibitors of mammalian mitochondrial protein synthesis	(Kroon et al., 1984; McKee et al., 2006; Riesbeck et al., 1990; Van den Bogert et al., 1983; van den Bogert & Kroon, 1981)
Glycylcycline	28 S subunit, mitoribosome	Inhibit protein synthesis		(Lamb et al., 2015)

Cefonicid	Carnitine/acylcarnitine transporter	Inhibitors of the transporter	The inhibition is completely competitive for the substrate-binding site; it is the most potent inhibitor	(Pochini et al., 2008)
Ampicillin	Carnitine/acylcarnitine transporter	Inhibitors of the transporter	The inhibition is completely competitive for the substrate-binding site	(Pochini et al., 2008)
Oxazolidinones (Linezolid)	Likely binding to and inhibition of mito ribosomes	Inhibit protein synthesis	Readily enter isolated mitochondria in comparison to bacteria	(McKee et al., 2006)

1.5 Research gap

There is no known evidence of fungal mitochondrial drug efflux pumps to date. Interestingly, one study showed that the *TPO1* gene of the *S. cerevisiae,* which encodes a MFS transporter, causes resistance to indomethacin; a non-steroidal anti-inflammatory drug (NSAID) (Mima et al., 2007). However, the mitochondrial localization of this Tpo1 efflux pump was not demonstrated in this study.

On the other hand, a separate study showed that breast cancer cells acquire doxorubicin (DOX) drug resistance through the mitochondrial drug efflux pumps, which are found to be ATP-dependent, and thus from the ABC superfamily protein. The identified pumps are the breast cancer resistance protein (BCRP) and multidrug resistance-associated protein (MRP1) respectively. Moreover, these pumps were found to be expressed and localized in mitochondria (Dartier et al., 2017). Interestingly, this study confirmed the presence of drug efflux pumps in mammalian mitochondria.

So, we are highly convinced to search for drug efflux pumps in fungal mitochondria. If successful, we anticipate our study to be a starting point for more sophisticated *in-vivo* models to investigate mitochondrial drug accumulation and efflux-mediated resistance in fungi.

1.6 Hypothesis

Fungal mitochondria will contain efflux pumps of the Major Facilitator Superfamily (MFS) that could be involved in antimicrobial resistance.

1.7 Objectives

In this thesis, the transporter of polyamines (Tpo1-Tpo5) and Hexose transporter (Hxt5) of the MFS have been studied.

1. To search for potential candidates of MFS drug efflux pumps and to demonstrate efflux of EtBr, a model compound, from fungal mitochondria

2. To express and examine the putative mitochondrial MFS drug efflux pumps in bacteria in order to study their specificity and mode of action

CHAPTER 2

Chapter 2: Methods and Materials

2.1 Search for putative MFS efflux pumps in fungi and creation of yeast deletion mutants

The potential MFS encoding genes from *N. crassa* 74-OR23-IVA were searched using the TransportDB-Transporter Protein Analysis Database (Elbourne et al., 2017) and from *S. cerevisiae* using the Saccharomyces Genome Database (SGD) (Chervitz et al., 1999). The sequence for a known *Listeria monocytogenes* MFS efflux pump, TetA, (UniProtKB ID A0A0E1RB31) was used to find putative MFS drug efflux pumps in *N. crassa* based on amino acid sequence similarity, using BLASTp in NCBI.

The *S. cerevisiae* deletion mutants in **Table 2.1** were obtained from Dharmacon Inc. Lafayette, Co. USA. We have purchased strains that are missing one of the pumps from Tpo1-Tpo4.

Table 2.1 Commercially obtained deletion mutants.

Strains	**ORF Name**	**Knock out description**	**Background strain/ genotype**	**Required aa¥**
BY4742_ΔTPO1	YLL028W	Yeast MATα Knockout strain YLL028W	BY4742 MATα his3Δ1 leu2Δ0 lys2Δ0 ura3Δ0	Histidine Leucine Lysine
BY4742_ΔTPO2	YGR138C	Yeast MATα Knockout strain YGR138C	BY4742 MATα his3Δ1 leu2Δ0 lys2Δ0 ura3Δ0	Histidine Leucine Lysine

BY4741_ΔTPO3	YPR156C	Yeast MATa Knockout strain YPR156C	BY4741	MATa his3Δ1 leu2Δ0 met15Δ0 ura3Δ0	Histidine Leucine Methionine
BY4741_ΔTPO4	YOR273C	Yeast MATa Knockout strain YOR273C	BY4741	MATa his3Δ1 leu2Δ0 met15Δ0 ura3Δ0	Histidine Leucine Methionine

[¥]Essential amino acids and must be added to the media for the respective strain's selective growth.

2.1.1 Analysis of yeast strains lacking putative pumps.

2.1.1.1 Selection media

The synthetic complete (SC) media+glucose plates supplemented with (+histidine +leucine +lysine +uracil) and (+histidine +leucine +methionine +uracil) were used for the selection of BY4742_ΔTPO1 and BY4742_ΔTPO2, and BY4742_ΔTPO3 and BY4742_ΔTPO4, respectively. Cells were grown at 30 °C in YPG (1% (w/v) yeast extract, 2 % (w/v) peptone and 3 % (v/v) glycerol) to ensure active mitochondria. YPD (1% (w/v) yeast extract, 2% (w/v) peptone, 2% (w/v) dextrose and 1.5% (w/v) agar) medium was used to demonstrate the effect of media on the mitochondrial susceptibility to antibiotics.

2.1.1.2 Chemicals

Chemicals and reagents were purchased from Thermo Fisher Scientific (Mississauga, ON, Canada), Sigma-Aldrich Canada (Oakville, ON, Canada), BioShop Canada (Burlington, ON, Canada), and VWR International (Mississauga, ON, Canada). The antibiotics chloramphenicol (CAP), tetracycline (TET) and erythromycin (ERY) were dissolved in 95% ethanol to prepare the

stock. 95% (v/v) ethanol was added to the YPG control plates at a concentration of 2-3% to normalize the effect of ethanol if there is any.

2.1.1.3 Antibiotic susceptibility assays

The spot plating of yeast was carried out following the protocol of (Ritch et al., 2010) with some modifications. Cells were grown in 15 ml YPG for 72 hours at 30℃ in a shaking water bath to obtain an optical density (OD) of 3.5-4.5 at 600 nm. For the spot plating, cells were diluted to 0.2 OD using MilliQ water to make a total volume of 1 ml in a microcentrifuge tube and serially diluted to 10^{-5}. A volume of 10 µl from each of the dilutions of each of the five strains was spotted on YPG plates containing 50-2000 µg/ml CAP, 3-4000 µg/ml ERY and 50-1000 µg/ml TET, respectively. A volume of 95% ethanol, equal to the volume of antibiotic added onto the highest antibiotic concentration plate of each experiment, was spread onto the 0 µg/ml plate. The ethanol volume was adjusted for the other plates to make the total volume of ethanol the same. Photographs were taken after 3-4 days of incubation at 30 ℃.

For the 96-well microtitre plating, cells were diluted to 0.2 OD with fresh YPG media. Antibiotics CAP and TET were added to the dilutions to a final concentration of 1200-1300 µg/ml and 100-300 µg/ml, respectively. 200 µl from each of the treatment groups was added into the 96-well plate with three technical replicates. The ethanol volume was adjusted to be equal in each well throughout the plate. The cultures were grown for 44-48 hours at 30 ℃ with continuous orbital shaking. The absorbance was recorded every 30 mins using an Epoch™ 2 Microplate Spectrophotometer (BioTek) at 600 nm wavelength. 96-well clear flat bottom polystyrene TC-treated microplates were used for the assay (Corning® #3599).

2.1.2 EtBr efflux from fungal mitochondria

2.1.2.1 *N. crassa* mitochondria extraction

N. crassa strains were obtained from the Fungal Genetics Stock Centre. *N. crassa* strains WT FGSC 9718 (*Δmus-5::bar mat a*) and ΔPor-1 (*Δpor::hph+ Δmus51::bar+* transformant of FGSC 9718) were used in this study (Summers et al., 2012). *N. crassa* mitochondria were isolated according to the method of (Harkness et al., 1994) followed by growth in Vogel's Medium (VM) according to (Davis & de Serres, 1970).

2.1.2.2 *S. cerevisiae* mitochondria extraction

A fresh log phase culture of *S. cerevisiae* BY4741 was taken to produce spheroplasts for crude mitochondria isolation. Yeast crude mitochondria were isolated following the protocol of (Meisinger et al., 2006) with some modifications. Lyticase was used instead of zymolyase. Lyticase needs to be added to the zymolyase buffer (1.2 M sorbitol, 20 mM potassium phosphate, pH 7.4) right before use. Lyticase enzyme with either 1 µl of 2-mercaptoethanol (2-ME) (99%, Sigma-Aldrich) or 10 mM dithiothreitol (DTT) per 100 µl of yeast-enzyme buffer suspension was used to treat the yeast cells. According to (Meisinger et al., 2006), for 1 g wet weight of cells (pellets), 7 ml of lyticase buffer (zymolyase buffer) should be used. The optimum conditions for lyticase activity for *S. cerevisiae* are 30°C at pH 7.5, a minimum of 300 U/ml of lyticase buffer, and incubation with gentle shaking at 100 rpm for 70 to 120 minutes.

The OD at 600 nm was measured before and after the treatment followed by a Sodium dodecyl sulphate (SDS) assay (Ritch et al., 2010) to determine the efficacy of the enzyme, meaning the production of spheroplasts. SDS will pop the spheroplasts (if any are produced) and cause a reduction in OD compared to that from before lyticase treatment. The SDS assay includes 2 ml of

1 M sorbitol, 800 µl of 5% SDS and 200 µl of lyticase-treated yeast suspension to make a total of 3 ml.

2.1.2.3 EtBr efflux assay

Mitochondria were freshly isolated from both the organisms before use in each efflux assay. Tris-Buffered Saline (TBS) (2.4% Tris-Base, 8.8% NaCl, pH 7.6) and F5 buffer were used in the assays. The F5 buffer is prepared according to (Court et al., 1996), and it is important to provide an isotonic environment for the mitochondria.

The EtBr efflux assay was performed following the protocols of (Ammor et al., 2006) and (Kumar A. & Worobec, 2005), with some modifications. This method allows real-time monitoring of the experimental progress. The assay was carried out in a 3-ml cuvette using the Agilent Cary Eclipse fluorescence spectrophotometer. Using an excitation wavelength of 520 nm and emission wavelength of 590 nm with a slit width of 5 nm for excitation and 5 nm for emission, measurements were taken every 15 seconds. This experiment occurred at 25°C.

Initially, a mixture of 2 ml buffer (F5 or TBS) and 5 mg/ml mitochondria was placed in a 3-ml cuvette with magnetic stirrers. After reaching a baseline (roughly after 2 minutes), 10 µl of 1 mg/ml EtBr solution was added to each cuvette. The fluorescence was allowed to be saturated, then 10 µl of 1 M succinate was added followed by 2 µl of 1 mM Oligomycin and 10 µl of 2 mM CCCP. The measurements continued for 15-25 min, measuring every 15 seconds.

Table 2.2 List of strains used in this study.

Strains	Genotype	Reference /source
Saccharomyces cerevisiae		
BY4741	*MATa his3Δ1 leu2Δ0 met15Δ0 ura3Δ0*	(Winston et al., 1995)
S150	*MATa leu2-3 leu2-112 ura3 trpl-289 his3-1*	(Arkinstall et al., 1991)
Escherichia coli		
DH5α	*E. coli* F$^-$ φ80*lac*ZΔM15 Δ(*lac*ZYA-*arg*F) U169 *rec*A1 *end*A1 *hsd*R17(r_K^-, m_K^+) *pho*A *sup*E44 *thi*-1 *gyr*A96 *rel*A1 λ$^-$	Invitrogen #18265017
BL21-CodonPlus™ (DE3)-RIL	*E. coli* BL21 *lac*ZY derivative; contains extra copies of the *arg*U, *ile*Y, and *leu*W tRNA genes	Agilent #230245
SHuffle T7@	*E. coli* K12 cell derivative; enhanced capacity to correctly fold proteins with multiple disulfide bonds	NEB-c3026
OverExpress™ C43(DE3)	*E. coli* F$^-$ *omp*T *hsd*SB (rB- mB-) *gal dcm* (DE3)	Sigma-Aldrich #CMC0019

Table 2.3 List of plasmids used in this study.

Plasmid	Features	Reference
pRS416	Source of *CEN6-ARS4* and *URA3*	(Sikorski & Hieter, 1989)
pET21b(+)	T7 promoter, transcription start, terminator and Tag coding sequence MCS His•Tag coding sequence *lac*I coding sequence. High copy	(McMurry & Levy, 1995)
CEN/pET21b(+)	Yeast-*E. coli* shuttle expression vector	This study
pET22b(+)	T7 promoter *pelB* coding sequence Multiple cloning sites (*Nco*I -*Xho*I) His Tag coding sequence *lac*I coding sequence High copy	(Barilla et al., 2001)
pMS119EH	P*tac*I protmoter-Amp^{R}-*lac*I^{Q} MCS Low copy	(Fürste et al., 1986)

Table 2.4 List of oligonucleotides (primers) and PCR reactions used in this study.

Target gene	Primer	Sequence (5' → 3')	Amplicon size (bp)	Purpose
TPO1 of Sc gDNA	TPO1_F	TAAGCA**GCTAGC**ATGTCGGATCATTCTCCCATTTCTAATAA	1761	Restriction and ligation cloning, at *Nhe*I and *Xho*I sites in pET21b(+)
	TPO1_R	TGCTTA**GAGCTC**AGCGGCGTAAGCATACTTGGATTT		
TPO3 of Sc gDNA	TPO3_F	TAAGCA**GCTAGC**ATGAACAGACAGGAATCCATAAATTC	1869	Restriction and ligation cloning, at *Nhe*I and *Xho*I sites in pET21b(+)
	TPO3_R	TGCTTA**GAGCTC**TTCAATACTATCTATGGAATAATCCTTCTTG		
CEN6-ARS4 and *URA3* of pRS416	CEN6-ARS4/ URA3_F	TAATACGGTTATCCACAGAATCAGGGGATAACGCAGGAAAGAGAAAAGTGCCACCTGGGTCCTTTTCATCACGTG	1807	Yeast-*E. coli* shuttle vector for homologous recombination; homologous to pET21b(+) at *Pci*I site
	CEN6-ARS4/ URA3_R	CGGCCTTTTTACGGTTCCTGGCCTTTTGCTGGCCTTTTGCTCCAGTTTTTTAGTTTTGCTGGCCGCATCTTCTCA		
TPO1 of Sc gDNA	TPO1_recomb_1_F	TGCTCGAGTGCGGCCGCAAGCTTGTCGACGGAGCTCGAATTCATGTCGGATCATTCTCCCATTTCTAATAAGGAAAATCAT	1803	Homologous recombination cloning; homologous to CEN/pET21b(+) at *BamH*I site
	TPO1_recomb_1_R	TATACATATGGCTAGCATGACTGGTGGACAGCAAATGGGTCGTTAATGGTGATGGTGATGGTGAGCGGCGTAAGCATACTTGGATTTCTT		
TPO1 of Sc gDNA	TPO1_extended_F	AAAGGAAACGATCGTAGGAATT	2461	To get a *TPO1* extended PCR product with 350 bp up and downstream of the *TPO1* ORF; used as a template for the recombination primers
	TPO1_extended_R	TACTCTTGTGCTTGTGCAT		

TPO2 of Sc gDNA	TPO2_extended_F	TATACATTGCGCATACACCC	2545	Same as above
	TPO2_extended_R	GATTTTTGAGTTGCATAATGTCAATTA		
TPO3 of Sc gDNA	TPO3_extended_F	CGCCTAAGAACATTTGTCTTT	2569	Same as above
	TPO3_extended_R	AAATTCGTATTCCTCGGTCAA		
TPO4 of Sc gDNA	TPO4_extended_F	GCTCACCTTAAATCCGTGTTA	2680	Same as above
	TPO4_extended_R	AACTGAGAAAAAACTGTTGTTGT		
TPO5 of Sc gDNA	TPO5_extended_F	TTTCTTCTTCATCCGAGTCAA	2557	Same as above
	TPO5_extended_R	ATTTTGATTACTGCCGTTCTC		
HXT5 of Sc gDNA	HXT5_extended_F	ATTAATGGTCGTGTGGATGAATAT	2479	Same as above
	HXT5_extended_R	GTCCTCACTGTTTTATTACCAAG		
TPO1 extended PCR product	TPO1_recomb_2_F	TCTAGAAATAATTTTGTTTAACTTTAAGAA GGAGATATACATATGTCGGATCATTCTCCC ATTTCTAATAAGGAAAATCAT	1803	Homologous recombination and CPEC cloning; homologous to CEN/pET21b(+) at *Nde*I site
	TPO1_recomb_2_R	TCTAGAAATAATTTTGTTTAACTTTAAGAA GGAGATATACATATGTCGGATCATTCTCCC ATTTCTAATAAGGAAAATCAT		
TPO2 extended PCR product	TPO2_recomb_F	TCTAGAAATAATTTTGTTTAACTTTAAGAA GGAGATATACATATGTCGGATCATTCTCCC ATTTCTAATAAGGAAAATCAT	1867	Homologous recombination and CPEC cloning;

	TPO2_recomb_R	TCTAGAAATAATTTTGTTTAACTTTAAGAAGGAGATATACATATGTCGGATCATTCTCCCATTTCTAATAAGGAAAATCAT		homologous to CEN/pET21b(+) at *Nde*I site
TPO3 extended PCR product	TPO3_recomb_F	TCTAGAAATAATTTTGTTTAACTTTAAGAAGGAGATATACATATGTCGGATCATTCTCCCATTTCTAATAAGGAAAATCAT	1912	Homologous recombination and CPEC cloning; homologous to CEN/pET21b(+) at *Nde*I site
	TPO3_recomb_R	TCTAGAAATAATTTTGTTTAACTTTAAGAAGGAGATATACATATGTCGGATCATTCTCCCATTTCTAATAAGGAAAATCAT		
TPO4 extended PCR product	TPO4_recomb_F	TCTAGAAATAATTTTGTTTAACTTTAAGAAGGAGATATACATATGCCTTCTTCTTTGACAAAAACC	2022	Homologous recombination and CPEC cloning; homologous to CEN/pET21b(+) at *Nde*I site
	TPO4_recomb_R	CGGATCCCGACCCATTTGCTGTCCACCAGTCATGCTAGCTTAGTGGTGGTGGTGGTGGTGAACCATTCTGGCGGAAGC		
TPO5 extended PCR product	TPO5_recomb_F	TCTAGAAATAATTTTGTTTAACTTTAAGAAGGAGATATACATATGCCAGAGTATACGCTACT	1900	Homologous recombination and CPEC cloning; homologous to CEN/pET21b(+) at *Nde*I site
	TPO5_recomb_R	CGGATCCCGACCCATTTGCTGTCCACCAGTCATGCTAGCTTAGTGGTGGTGGTGGTGGTGTATATCATATCTACGATCATCGGC		
HXT5 extended PCR product	HXT5_recomb_F	TCTAGAAATAATTTTGTTTAACTTTAAGAAGGAGATATACATATGTCGGAACTTGAAAACG	1822	Homologous recombination and CPEC cloning; homologous to CEN/pET21b(+) at *Nde*I site
	HXT5_recomb_R	CGGATCCCGACCCATTTGCTGTCCACCAGTCATGCTAGCTTAGTGGTGGTGGTGGTGGTGTTTTTCTTTAGTGAACATCCTTTT		

CEN/pET21b (+)	T7 promoter_F	CGCGAAATTAATACGACTCACTATAGG	800-1000	Sequencing
	T7 terminal_R	CAAAAAACCCCTCAAGACCCG		
TPO1/CEN/pET21b(+)	TPO1_Seq1_F	TTTGTAGGCC CCATTTTATC GC	841	Sequencing
	TPO1_Seq2_R	TGTTAACCAA AATGGTAGGG TGA	978	
TPO2/CEN/pET21b(+)	TPO2_Seq1_F	CGCTTTTGCTCCTTACGTTG	900	Sequencing
	TPO2_Seq2_R	CAACAACGGGACCAACGTAAG	911	
TPO3/CEN/pET21b(+)	TPO3_Seq1_F	GCCGATATGTTCCCAAGTGAA	900	Sequencing
	TPO3_Seq2_R	CCAGTTTCCTTTCTTAATCTAGCA	911	
TPO4/CEN/pET21b(+)	TPO4_Seq1_F	TAAGGCCTTTAAAAATGCTTGTCG	920	Sequencing
	TPO4_Seq2_R	AGGTAAAAGAAAGCACCTATCCATAAC	1095	
TPO5/CEN/pET21b(+)	TPO5_Seq1_F	CCACGTGGTATGTCGAATG	874	Sequencing
	TPO5_Seq2_R	TCACGACTAAAACTATATACCGCA	1100	
HXT5/CEN/pET21b(+)	HXT5_Seq1_F	ACTGAAGACTCTCCTTTAGTAACTTTA	910	Sequencing
	HXT5_Seq2_R	TGAATCTTCCAAACCAACAGC	1120	
TPO1 extended PCR product	TPO1_cloning_pMS119EH_v2_F	ATAACAATTTCACACAGGAAACAGATGTCGGATCATTCTCCCATTTCTAATAAGGAAAATCAT	1785	CPEC cloning; homologous to pMS119EH at *EcoR*I site
	TPO1_cloning_pMS119EH_v2_R	AGGATCCCCGGGTACCGAGCTCGAATTTTAGTGGTGGTGGTGGTGAGCGGCGTAAGCATACTT	1779	
TPO2 extended PCR product	TPO2_cloning_pMS119EH_v2_F	ATAACAATTTCACACAGGAAACAGATGAGTGATCAAGAATCTGTTGTTT	1869	CPEC cloning; homologous to pMS119EH at *EcoR*I site
	TPO2_cloning_pMS119EH_v2_R	GGGTACCGAGCTCGAATTTTAGTGGTGGTGGTGGTGGTGCATCTCAACACTGTCGATG	1863	

TPO3 extended PCR product	TPO3_cloning_pMS119EH_v2_F	ATAACAATTTCACACAGGAAACAGATGAACAGACAGGAATCCATAAAT	1893	CPEC cloning; homologous to pMS119EH at *EcoR*I site
	TPO3_cloning_pMS119EH_v2_R	GGGTACCGAGCTCGAATTTTAGTGGTGGTGGTGGTGGTTCAATACTATCTATGGAATAATCCTTC	1887	
TPO4 extended PCR product	TPO4_cloning_pMS119EH_v2_F	ATAACAATTTCACACAGGAAACAGATGCCTTCTTCTTTGACAAAAACC	2004	CPEC cloning; homologous to pMS119EH at *EcoR*I site
	TPO4_cloning_pMS119EH_v2_R	GGGTACCGAGCTCGAATTTTAGTGGTGGTGGTGGTGGTGAACCATTCTGGCGGAAGC	1998	
TPO5 extended PCR product	TPO5_cloning_pMS119EH_v2_F	ATAACAATTTCACACAGGAAACAGATGCCAGAGTATACGCTACT	1881	CPEC cloning; homologous to pMS119EH at *EcoR*I site
	TPO5_cloning_pMS119EH_v2_R	GGGTACCGAGCTCGAATTTTAGTGGTGGTGGTGGTGGTGTATATCATATCTACGATCATCGGC	1875	
HXT5 extended PCR product	HXT5_cloning_pMS119EH_v2_F	ATAACAATTTCACACAGGAAACAGATGTCGGAACTTGAAAACG	1803	CPEC cloning; homologous to pMS119EH at *EcoR*I site
	HXT5_cloning_pMS119EH_v2_R	GGGTACCGAGCTCGAATTTTAGTGGTGGTGGTGGTGGTTTTTCTTTAGTGAACATCCTTTT	1797	

2.2 Expression and examination of the putative drug efflux pumps in bacteria

2.2.1 Oligonucleotides, plasmids, bacterial strains, and growth conditions

The strains, plasmids, and oligonucleotides used in this study are listed in **Table 2.2, Table 2.3** and **Table 2.4**, respectively. All *E. coli* strains were grown routinely in Luria-Bertani (LB) medium (Becton, Dickinson and Company, Mississauga, Canada) at 37 °C with shaking at 250 rpm unless otherwise mentioned. All *E. coli* cells harbouring plasmids were supplemented with antibiotics corresponding to the selection marker (ampicillin, 100 µg/ml; tetracycline, 12.5 µg/ml). SC150 cells were selected with the SC (synthetic complete; his +leu +lys -ura) media (Sigma-Aldrich, Canada) without uracil.

2.2.2 Extraction of genomic DNA (gDNA) and plasmid

S. cerevisiae gDNA was isolated using DNeasy Blood & Tissue Kit (Cat No./ID: 69504) following the manufacturer's protocol. No *E. coli* gDNA was necessary for this study. Yeast plasmid DNA was extracted following the smash & grab protocol by Wickner, 1991. Plasmid DNA from *E. coli* was extracted from the cell pellets of 1-5 ml of overnight grown culture using Monarch® Plasmid DNA Miniprep Kit (NEB# T1010) following the manufacturers' guidelines.

2.2.3 Construction and cloning of putative efflux pump genes.

The restriction enzyme digestion-ligation cloning was tried using the NEB Traditional Cloning Quick Guide followed by preparation of insert and vector, purification and ligation of the components, and transformation into *E. coli* competent cells (DH5α) (Kostylev et al., 2015). The homologous recombination of *TPO1-5* and *HXT5* into pET21b(+) (#69741, Sigma-Aldrich) was attempted following (Chino et al., 2010) in yeast strain S150 (Young & Court, 2008).

The recombinant expression vectors were created by Circular Polymerase Extension Cloning (CPEC) (**Fig. 4.1**) following the method of Quan & Tian, 2009. In summary, extended PCR products (around 350 bp up and downstream of the gene) of *TPO1-5* and *HXT5* were generated using the primers in **Table 2.4**. The target was to create a 2.5-kb template, from the BY4741 gDNA for all the genes, to be used for the second round of PCR of CPEC using the recombination primers in **Table 2.4**. *TPO1-5* and *HXT5* genes were cloned into plasmids CEN/pET21b(+) and pMS119EH. The constructs are listed in **Table 4.1**.

The recombinant plasmid assembly was checked using restriction digestion; the NEBcutter V2.0 (restriction mapping tool) (Vincze et al., 2003) was used to generate a predicted digestion pattern. The restriction enzyme digestion reactions of both the yeast and *E. coli* plasmids were carried out using the enzymes and buffers from NEB Inc. and following the manufacturer's instructions. Moreover, the constructs created were sequenced using Sanger sequencing services from The Centre for Applied Genomics (SickKids, Toronto, ON, Canada), and analyzed to ensure the right open reading frame. Forward and reverse sequencing primers are listed in **Table 2.4**.

2.2.4 Expression and detection of Tpo proteins

The expression induction media, *E. coli* expression strains, vectors and induction parameters tried in this study have been listed in (**Table 7.2**; **Appendix 2**). An autoinduction medium ZYM-5052 (Studier, 2005), a modified LB medium (**Table 7.1**; **Appendix 2**), Terrific broth (TB) and M9 minimal medium (Kangwa et al., 2015) were used for protein expression. For final cultures in Studier's autoinduction medium, growth at 20 °C is recommended over 48 hours. *E. coli* growth media were supplemented with 100 pM to 0.5 mM Isopropyl β-D-1-thiogalactopyranoside (IPTG) as needed (**Table 7.2**; **Appendix 2**).

For reducing the toxicity of the expressed proteins we followed (Qing et al., 2004). Briefly transformed *E. coli* strains were grown at 37 °C. The cultures were shifted to a 16, 20 and 25 °C shaking incubator at the mid-log phase, respectively, and IPTG was added to induce protein expression. The level of expression was monitored over time 0, 12, 24 hours after this cold-shock induction.

The protein was isolated using a small-scale protein expression protocol by Qiagen (The QIAexpressionist™, 2002). The total membrane of *E. coli* expression host strains was isolated following the method of (Ma et al., 2013). The isolated proteins were detected using SDS-PAGE and western blotting, respectively. SDS-PAGE was cast with 0.1% SDS and 12% acrylamide: bisacrylamide (29:1) using a Mini-PROTEAN® 3 Cell kit (Bio-Rad Laboratories, Hercules, CA). Gels were loaded with 10 µl of Blue Prestained Protein Standard, Broad Range (11-250 kDa) (NEB# P7718). Electrophoresis was performed at 175 V for 45 minutes at room temperature and the gel was electroblotted to nitrocellulose. The western blot was probed using the Thermo Scientific HisProbe-HRP conjugate (#15165) and TMB 1-Component Membrane Peroxidase Substrate (#5420-0027) following the manufacturer's protocol.

2.2.5 Functional analysis of the Tpo proteins

2.2.5.1 Antibiotic susceptibility testing assay

The Minimum Inhibitory Concentration (MIC) of CAP and ERY against *E. coli* transformants expressing the genes of interest was determined using the two-fold broth dilution method. This method was carried out in LB medium following the Clinical and Laboratory Standards Institute (CLSI, 2019) with some modifications. Briefly, 100 µl of the overnight culture was used to inoculate fresh 8 ml LB broth and incubated at 37 ℃ with continuous shaking. Strains were grown for another 5 hours to reach an OD of 0.3-0.4 and induced with 5 µM IPTG for 1-2 hours. Cells

were normalized to OD 0.2 with fresh LB+ampicillin+treatment antibiotics in microcentrifuge tubes to a volume of 1 ml. A volume of 200 µl was taken from the microcentrifuge tubes and added to the 96-well plates with 3 technical replicates. The cultures were grown to OD 1.2-1.4 at 37 ℃ with continuous orbital shaking. The concentrations used for CAP and ERY were 16-128 and 0.5-32 µg/ml with a two-fold increase, respectively.

2.2.5.2 EtBr accumulation assay

EtBr accumulation assay was performed following the method of (Miguel Viveiros et al., 2008a) with a few modifications. Briefly, 5 ml of fresh LB broth was inoculated with 100 µl of overnight culture and grown at 37 °C with continuous shaking. Expression of the respective genes was induced by the addition of 5 µM IPTG at 600 nm wavelength absorbance (A600) which is 0.3–0.4 and grown to A600 = 1.0. One ml of culture was pelleted at 10,000 rpm for 5 minutes and washed with 1X PBS. Washed cells were resuspended in 900 µl of 1X PBS and 80 µl of the cell suspension were added to each well of the flat transparent bottom black plate (Greiner bio-one, supplier: Thermo Scientific, Mississauga, ON, Canada).

Using a Spectromax M2 plate reader, A600 was measured for the suspension followed by the fluorescence every 30 seconds, with excitation and emission wavelengths of 518 nm and 605 nm, respectively. After the initial few reads (6 to 8 reads), EtBr was added at a final concentration of 40 µg/ml and then after another 10 to 12 reads, glucose was added at a final concentration of 0.4% to energize the cells. After 25-30 minutes of continuous reading, carbonyl cyanide 3-chlorophenylhydrazone (CCCP) was added at the final concentrations of 5 and 40 µg/ml, and the assay was run to a total of 60 minutes.

CHAPTER 3

Chapter 3: To search for potential candidates of MFS drug efflux pumps and to demonstrate efflux of EtBr, a model compound, from fungal mitochondria.

3.1 Introduction

Eukaryotic cells can tolerate certain levels of antibiotics with mitochondrial targets. This may be in part due to limited uptake of the drugs by mitochondria, and there may be other mechanisms involved. There is evidence for efflux pump activity in mammalian mitochondria but not in fungal mitochondria. We were curious to find evidence of efflux in mitochondria. One of our lab members (*A. McLoughlin, B.Sc. Hons. 2014*) demonstrated EtBr efflux from isolated *N. crassa* mitochondria only when a protonmotive force was established across the membrane using an appropriate substrate. In the EtBr efflux assay, the DNA intercalation of EtBr causes increased fluorescence, while the decrease in fluorescence means the dye is being effluxed out of mitochondria. This phenomenon was succinate-dependent as it creates membrane potential ($\Delta\Psi_m$) across the mitochondrial membrane that can be utilized by secondary active efflux pumps. In **Fig. 8.1** (**Appendix 3**), it can be seen that there is a sharp decrease in fluorescence after the addition of substrate and suggests the presence of proton antiporter efflux pumps. Thus, we started looking for a single sub-unit MFS drug:H^+ antiporters.

We searched for potential MFS encoding genes from *N. crassa* and *S. cerevisiae* (**section 2.1**), two of the model organisms that have been used in our lab. 22 members of the Drug:H^+ Antiporter (DHA) family of the MFS in *S. cerevisiae* were identified, which were also demonstrated by (Sá-Correia et al., 2009). Meanwhile, (Vögtle et al., 2017) produced a quantitative map of proteins

distributed in the *S. cerevisiae* mitochondria. They found 206 novel proteins, in highly purified mitochondria, whose mitochondrial localizations were not identified earlier. Among them, 3 potential mitochondrial transporters, namely Tpo1, Tpo3 and Hxt5 were identified, and we chose them along with Tpo2, Tpo4 and Tpo5 for this study according to their potential transport properties as *S. cerevisiae* putative mitochondrial drug efflux pumps.

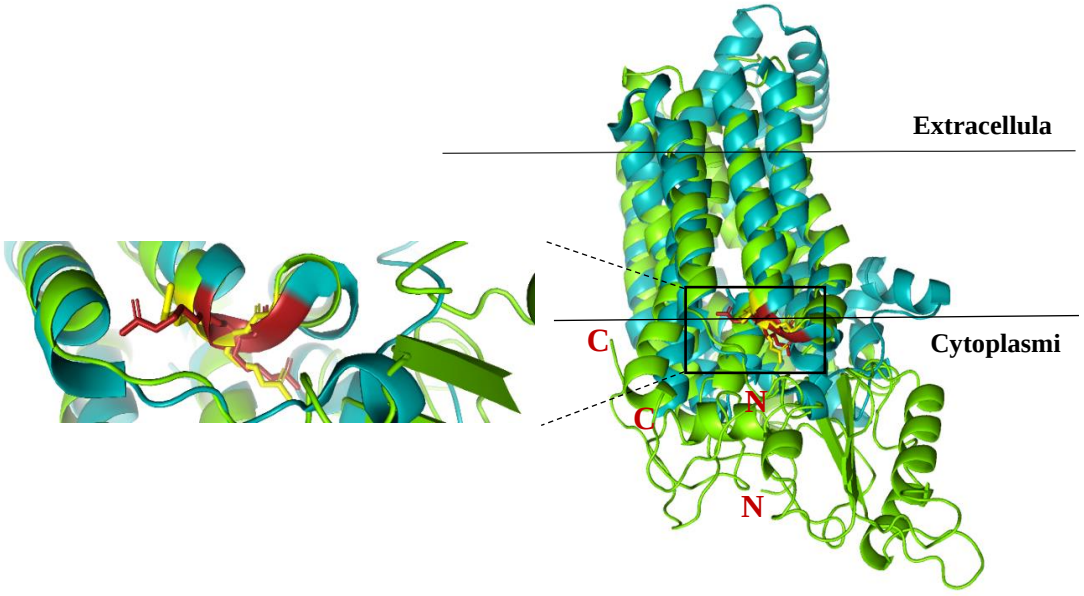
Interestingly, there are additional supports for Tpo1 to be a potential mitochondrial drug efflux pump. Several studies showed Tpo1 to be a multidrug efflux pump localized in the plasma membrane as its expression conferred resistance to several chemical compounds (Albertsen et al., 2003; Costa et al., 2016; Uemura, Tachihara, et al., 2005). However, no studies showed Tpo1 taking part in direct drug efflux from fungal mitochondria. Thus, we looked for any homologues of Tpo1 in prokaryotes and eukaryotes.

3.2 Results

3.2.1 Predicted structural similarity among yeast Tpo1 and homologues in *E. coli* and humans.

We started to investigate the homology between *S. cerevisiae* Tpo1 (ScTpo1) and *Homo sapiens* TETRAN using Phyre2 modelling (Kelley et al., 2015). TETRAN is a human tetracycline transporter-like protein (L11669 [GenBank]; 6S4M [PDB]) and a human orthologue of ScTpo1 (Mima et al., 2007). Both Tpo1 and TETRAN have predicted folding patterns like MFS transporters with similar MFS motifs (**Fig. 3.1**). YajR is predicted to be a drug-efflux pump (Jiang et al., 2013) and the Phyre2 algorithm used the *E. coli* YajR transporter as a template with 100% confidence and 71% coverage of the Tpo1 amino acid sequence.

A)


Extracellula
Cytoplasmi
C
C
N
N

B)

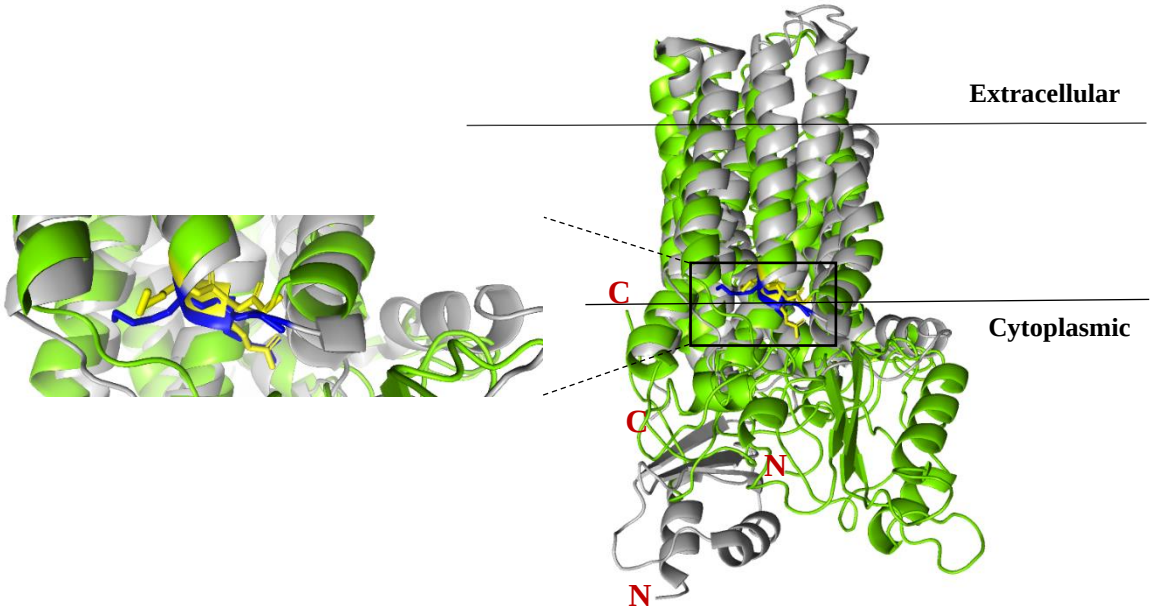

Extracellular
Cytoplasmic
C
C
N
N

Figure 3.1 The homology modelling and structural prediction of Tpo1, and alignment to TETRAN and YajR showing a conserved sequence motif of three amino acid residues. The structures of Tpo1 and TETRAN were predicted using Phyre2 (Kelley et al., 2015) where *E. coli* MFS MDR transporter YajR (3.15 Å) (3WDO [PDB]) was used as a template. Then the structures were aligned and viewed through PyMOL (https://pymol.org/2/). **A)** The Tpo1 structure (Green) aligned against TETRAN (Cyan) and **B)** against *E. coli* YajR (Grey) in PyMOL highlighting the conserved motifs (Zoomed/Unzoomed). The conserved motifs are as follows, Tpo1 (yellow) GRK, TETRAN (red) GRR and YajR (blue) GRK.

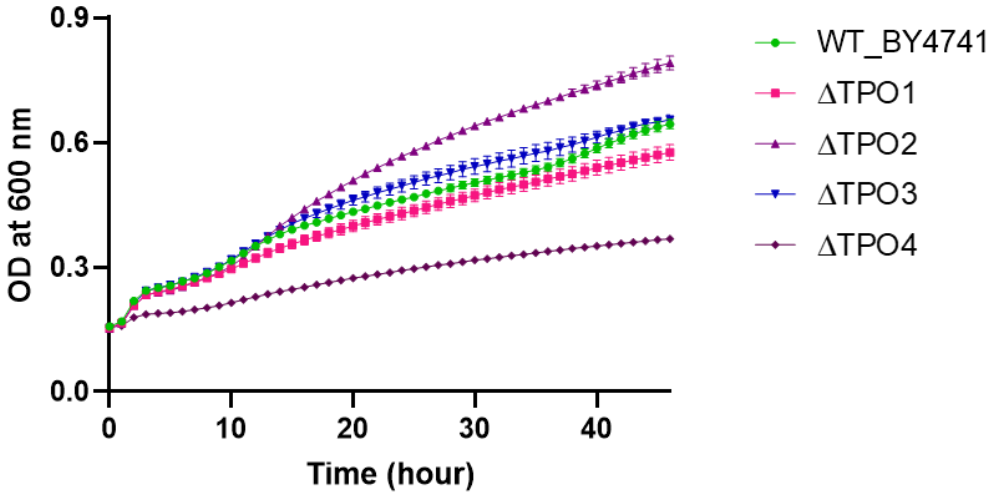
3.2.2 Analysis of yeast strains lacking putative pumps

We tried to determine the effect of *TPO* gene deletion on i) the growth kinetics and ii) mitochondrial efflux capacity of the mutants against several mitochondria-targeted antibiotics. Moreover, the effects of deletion have been compared to the wild-type *S. cerevisiae* BY4741. We have commercially obtained four deletion mutants of BY4741 and BY4742, referred to as ΔTPO1, ΔTPO2, ΔTPO3 and ΔTPO4 listed in (**Table 2.1**).

3.2.2.1 Growth kinetics at the non-selective condition

To determine the general fitness of the mutants, respiratory growth in the YPG medium was analyzed. Glycerol was used as the carbon source to test mitochondrial function under respiratory conditions. The ΔTPO4 strain grew slower (with final OD 3.5) whereas ΔTPO2 grew to a higher optical density (OD 8.1) than the WT (final OD 6.0). The ΔTPO1 and ΔTPO3 strains grew with no statistically significant difference (P-value 0.7066) to the WT (**Fig. 3.2 (A)**). In the presence of 3% ethanol (YPEG), the growth of each deletion strain was statistically indistinguishable with P-value >0.05 from that of the wild type (**Fig. 3.2 (B)**).

A)



B)

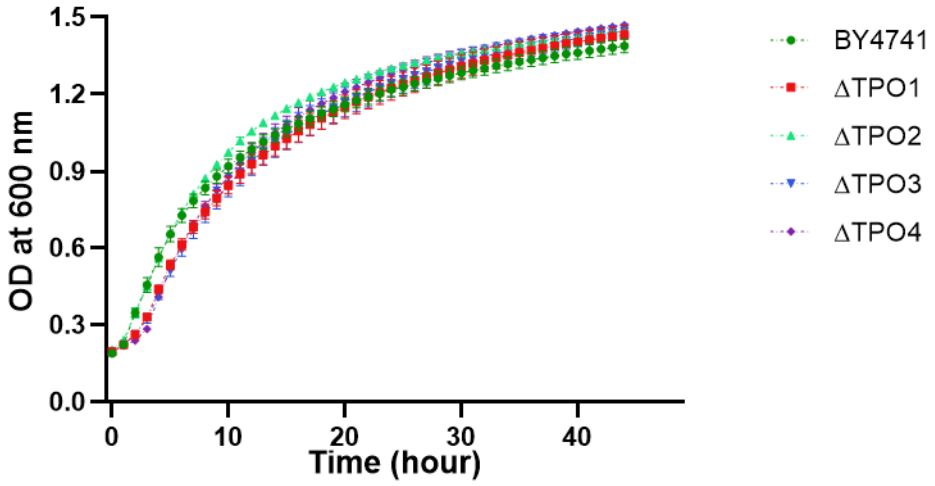


Figure 3.2 Growth of wild-type (BY4741) and deletion strains under non-selective conditions. Yeast WT and the deletion mutants ΔTPO1-4 were grown in YPG without (**A**) and with (**B**) 3% ethanol. They were inoculated at 0.2 OD in 200 µl liquid culture using a 96-well plate and grown for 44-48 hours at 30 ℃ with continuous shaking. The absorbance was recorded every 30 mins using an Epoch 2 plate reader at 600 nm wavelength. The average of three technical replicates at each time point with the standard error mean (SEM) has been plotted. The P-value of each growth curve has been determined using Mann-Whitney U two-tailed analysis.

3.2.2.2 Growth kinetics analysis using spot plating

In the following experiments, the sensitivity and growth properties of deletion mutants were compared to the wild type (WT) BY4741, in the presence of several mitochondria-targeting antibiotics on solid growth media (**Table 1.3**).

Different studies have used different concentrations of antibiotics to inhibit yeast growth. Shockman & Lampen, 1962 tested the effect of the antibacterial antibiotic against protoplasts and log-phase *S. cerevisiae* (LK2G12) cells in liquid culture. They have shown that the minimum inhibitory concentration of CAP, TET, and ERY is >100 µg/ml for both the cell types. Another study has shown MIC values of CAP and ERY against the growth of *S. cerevisiae* L410 in liquid glycerol-containing media are >100 µg/ml (Linnane et al., 1968). Another study by Blackburn & Avery, 2003 showed that *S. cerevisiae* BY4741 remains unaffected with up to 512 µg/ml of tetracycline or oxytetracycline treatment on YEPD agar plates. Therefore, using the agar spot-plating technique, we tested the sensitivity of yeast with 50-2000 µg/ml CAP (**Fig. 3.3)**, 3-4000 µg/ml ERY (**Fig, 3.4**) and 50-1000 µg/ml TET (data not shown except the results for 100, 200 and 300 µg/ml TET in **Fig. 3.5**).

3.2.2.2.1 Response to Chloramphenicol

Multiple concentrations of CAP (50-2000 µg/ml) were tested to determine concentrations of CAP that led to differences in growth among the wild-type and deletion strains. We observed that each of the strains showed reduced growth in 1200-1300 µg/ml CAP compared to the control (0 µg/ml CAP) (**Fig. 3.3**) and no growth with 2000 µg/ml CAP. However, in each of the treatment groups, the ΔTPO1, ΔTPO2 and ΔTPO3 strains were found to have reduced growth compared to the WT, except in the presence of 1250 µg/ml CAP. Remarkably, ΔTPO3, and in particularly ΔTPO4, have

bigger colonies than WT in the presence of chloramphenicol; this also was observed in repeated experiments (data not shown).

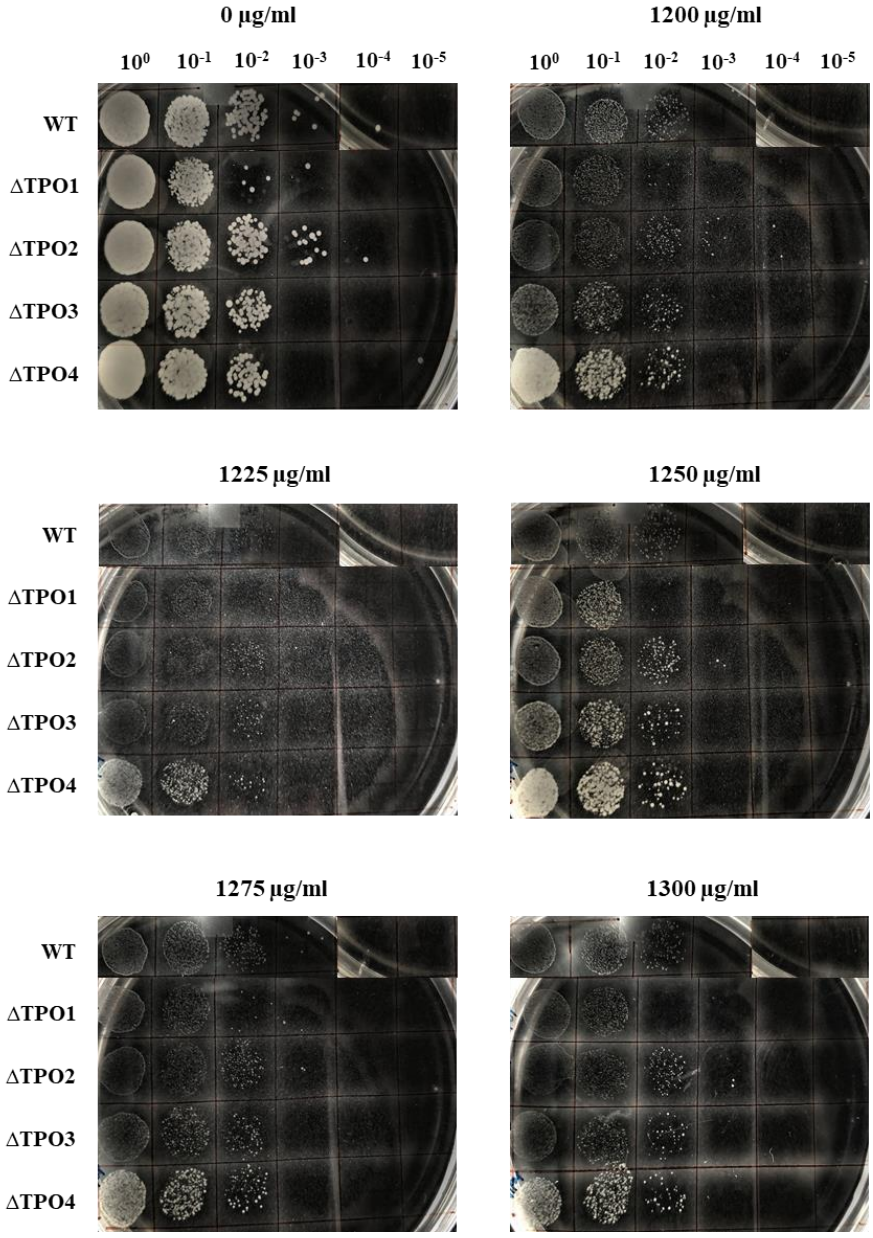


Figure 3.3 Growth of BY4741 and deletion mutants in the presence of chloramphenicol (CAP). The strains were diluted to 0.2 OD from a 72-hour YPG culture and serially diluted to 10^{-5}. A volume of 10 µl from each of the dilutions of each of the five strains was spotted on YPG plates containing 0, 1200, 1225, 1250, 1275 and 1300 µg/ml CAP, respectively. A volume of ethanol, equal to the volume of antibiotic added onto the 1300 µg/ml plate, was spread onto the 0 µg/ml plate. The ethanol volume was adjusted for the other plates to make the total volume of ethanol the same. Plates were incubated at 30 ℃ for 72 hours. The photographs taken were adjusted for a better visualization using ImageJ (https://imagej.net/ImageJ2) (Schneider et al., 2012). Some parts of the image were rearranged to align with the same dilution.

3.2.2.2.2 Response to Erythromycin

All the strains from the treatment groups showed a gradual reduction in growth, with increasing concentration of erythromycin (15-20 µg/ml), in comparison to the wild type BY4741 (**Fig. 3.4**). In the presence of 30 µg/ml ERY (MIC), there was very little growth of any strain, including the WT. Among all the strains, the ΔTPO3 mutant displayed the lowest growth compared to the WT with 20 µg/ml ERY. We have found 20 µg/ml as an optimum concentration of ERY to demonstrate the difference in growth between the deletion mutant and WT.

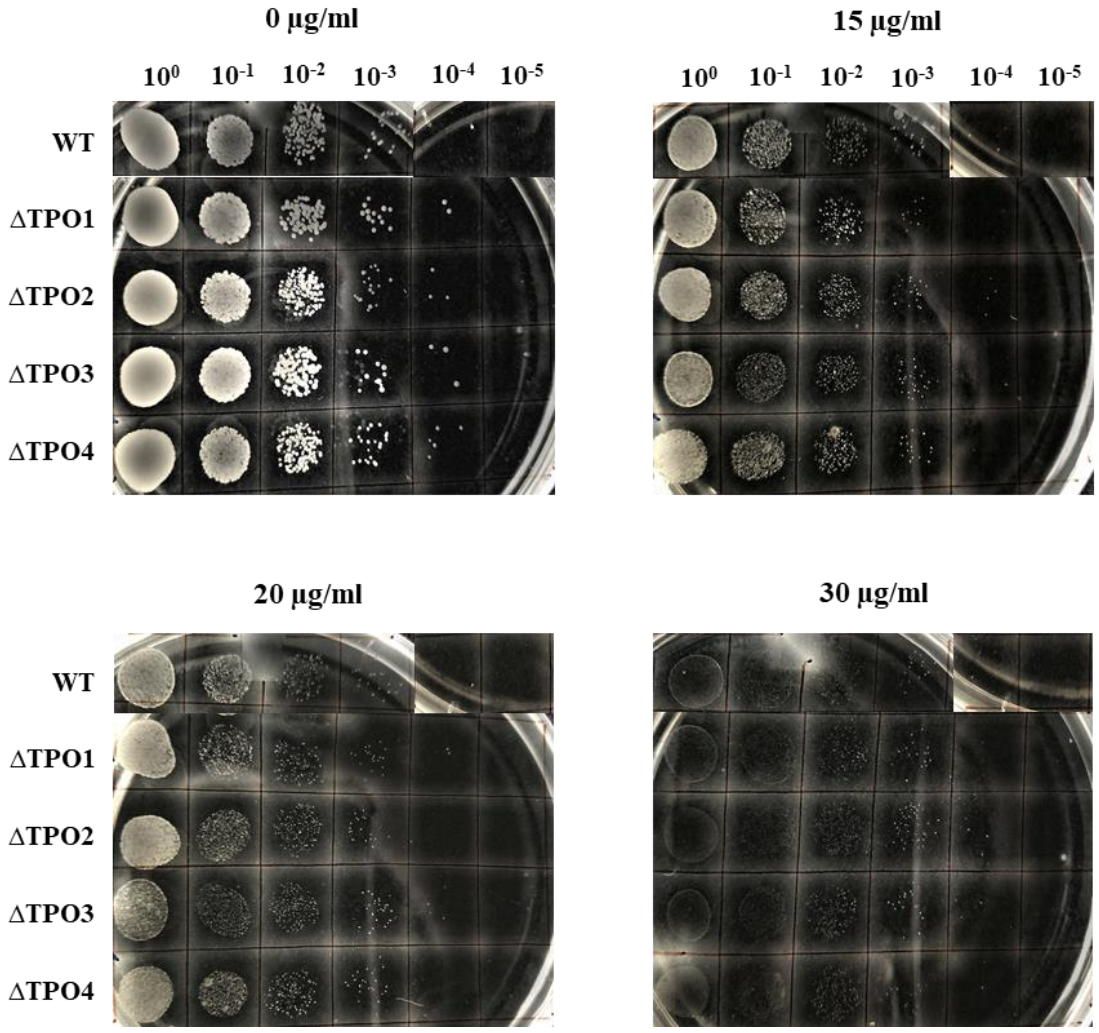


Figure 3.4 Growth of BY4741 and deletion mutants in the presence of erythromycin. The strains were diluted to 0.2 OD from a 72-hour YPG culture and serially diluted to 10^{-5}. A volume of 10 µl from each of the dilutions of each of the five strains was spotted on YPG plates containing 0, 15, 20 and 30 µg/ml ERY, respectively. Equal volume of ethanol, to the volume of antibiotic added onto the 30 µg/ml plate, was spread onto the 0 µg/ml plate. The ethanol volume was adjusted for the other plates to make the total volume equal. Plates were incubated at 30 ℃ for 72 hours. The photographs taken were adjusted for a better visualization using ImageJ (https://imagej.net/ImageJ2) (Schneider et al., 2012). Some parts of the image were rearranged to align with the same dilution.

3.2.2.2.3 Response to Tetracycline

We observed that all the strains from the treatment groups (100 and 200 µg/ml TET) showed reduced growth compared to the control group (0 µg/ml TET) (**Fig. 3.5**). The experiment was carried out twice, and both biological replicates (BR) of the ΔTPO1 (**Fig. 3.5 (A)**) and ΔTPO4 (**Fig. 3.5 (B)**) showed similar growth to the WT in all the treatment groups. The ΔTPO2 of both the BRs of the 300 µg/ml group showed the lowest growth compared to the WT among all the treatment groups. We found that in all the treatment groups, the ΔTPO2 of BR#1 has been more affected by the TET compared to BR#2 (**Fig. 3.5 (A)**). The ΔTPO3 of the BR#1 of the 300 µg/ml group showed the lowest growth compared to the WT among all the treatment groups (**Fig. 3.5 (B)**). More replicates are required to resolve these unexpected differences.

A)

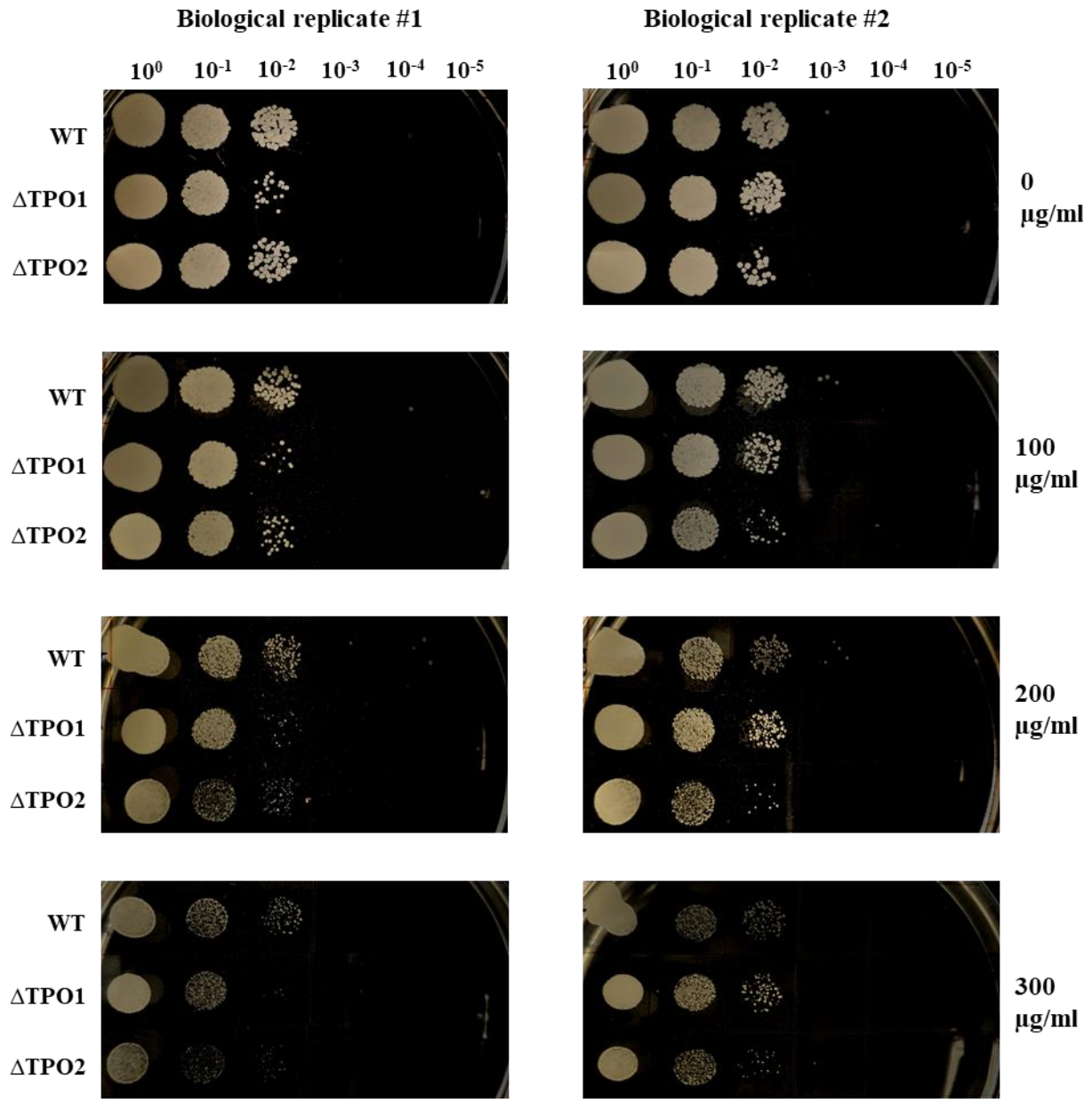


Figure 3.5 (A) Growth of BY4741 and the ΔTPO1-2 deletion mutants in the presence of tetracycline.

B)

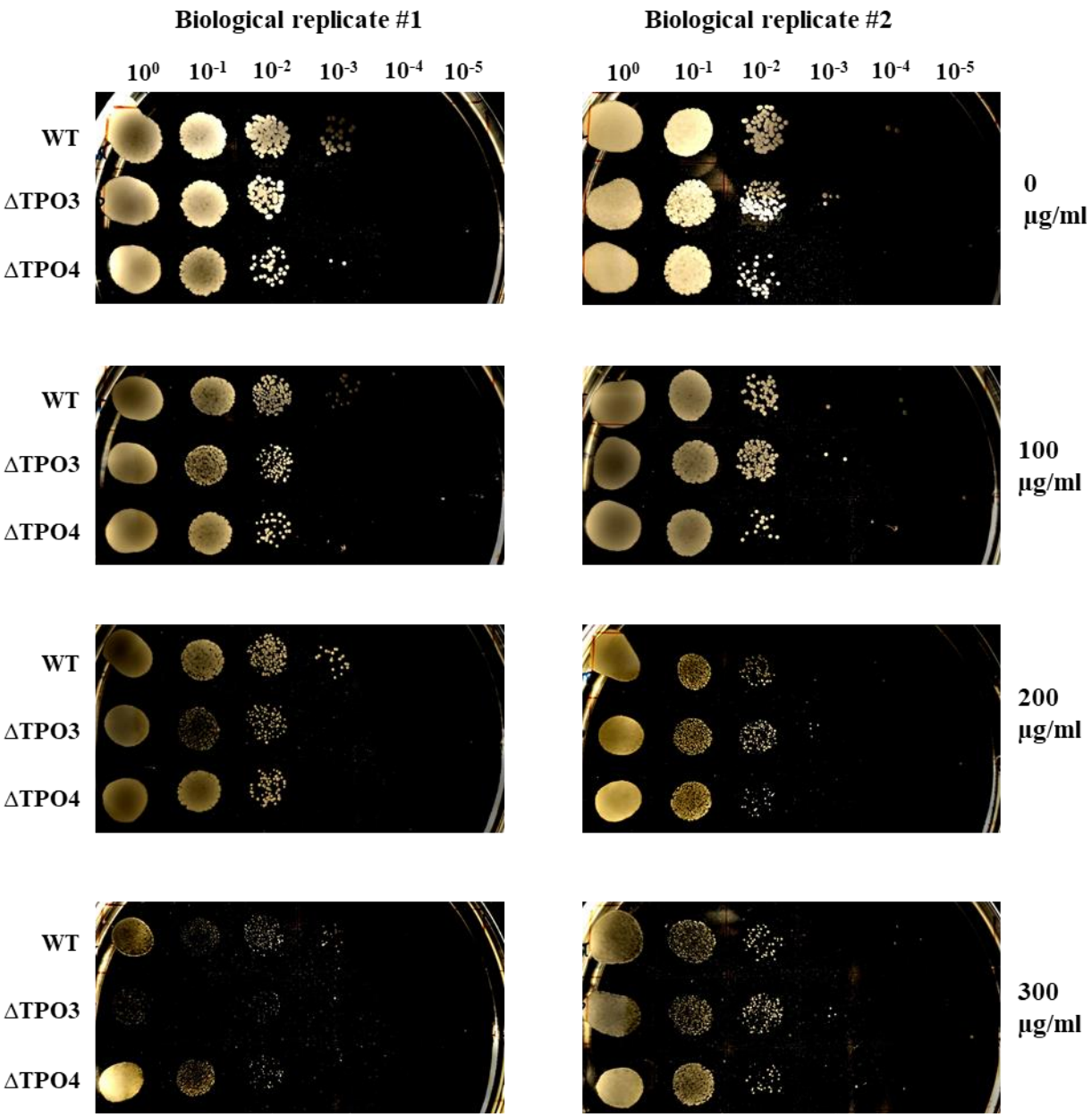


Figure 3.5 (B) Growth of BY4741 and the ΔTPO3-4 deletion mutants in the presence of tetracycline.

Figure 3.5 Growth of BY4741 and the deletion mutants ΔTPO1-2 (A) and ΔTPO3-4 (B) in the presence of tetracycline. Strains of the two biological replicates were diluted to 0.2 OD from a 72-hour YPG culture and serially diluted to 10^{-5}. A volume of 10 µl from each of the dilutions of each of the five strains was spotted on YPG plates containing 0, 100, 200 and 300 µg/ml TET, respectively. Equal volume of ethanol, to the volume of antibiotic added onto the 300 µg/ml plate, was spread onto the 0 µg/ml plate. The ethanol volume was adjusted for the other plates to make the total volume equal. Plates were incubated at 30 ℃ for 72 hours. The photographs taken were adjusted for a better visualization using ImageJ (https://imagej.net/ImageJ2) (Schneider et al., 2012).

3.2.2.3 Effect of growth medium on the antibiotic response

We designed the following experiment to determine whether the effect of the antibiotic on physiology is due to the effect on the mitochondria of the deletion mutants growing in different media. Respiration and mitochondrial function are required for growth on YPG, not on YPD, where fermentation can take place. All the strains of the TET-treatment group showed reduced growth and smaller colonies compared to the control (0 μg/ml TET) group on YPG. The ΔTPO3 mutant showed significantly reduced growth compared to the WT with 300 μg/ml TET on YPG (**Fig. 3.6**), in agreement with one of the BR of the experiment shown in **Fig. 3.5**. There is no obvious difference in growth between the wild-type and the mutants using 100, 200 and 300 μg/ml TET on YPD, in agreement with the hypothesis that these antibiotics are affecting only mitochondrial function.

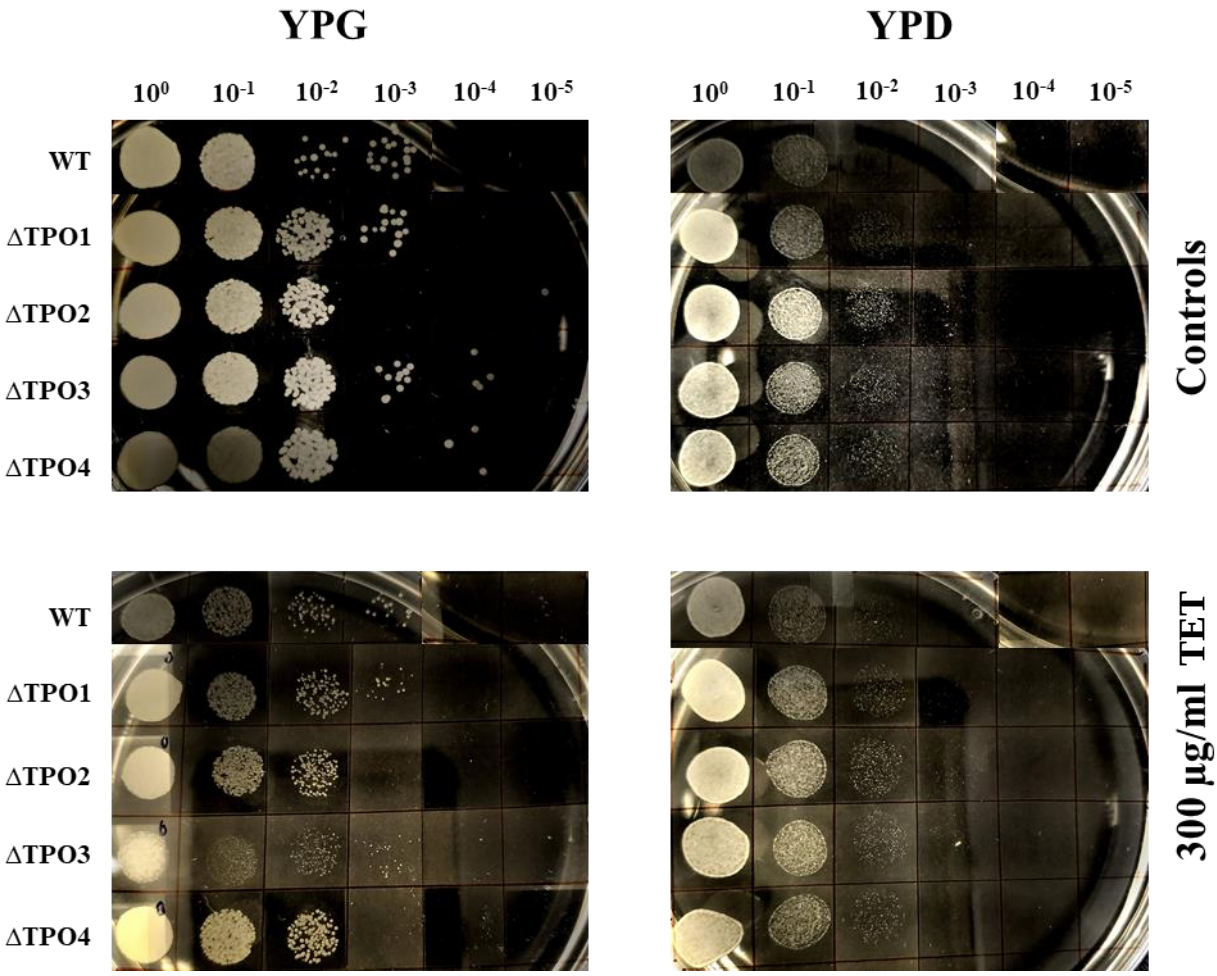


Figure 3.6 Role of growth media on the mitochondrial response to antibiotics. The strains were diluted to 0.2 OD from 72-hour YPG and YPD growth cultures respectively, and serially diluted to 10^{-5}. A volume of 10 µl from each of the dilutions of each of the five strains was spotted on YPG and YPD plates containing 0, 100, 200 and 300 µg/ml TET, respectively. Equal volume of ethanol, to the volume of antibiotic added onto the 300 µg/ml plate, was spread onto the 0 µg/ml (control) plate. The ethanol volume was adjusted for the other plates to make the total volume equal. Plates were incubated at 30 ℃ for 72 hours. Only the plates with the highest concentration of TET have been shown. The photographs taken were adjusted for a better visualization using

ImageJ (https://imagej.net/ImageJ2) (Schneider et al., 2012). Some parts of the image were rearranged to align with the same dilution.

3.2.2.4 Analysis of growth kinetics in the presence of antibiotics, using 96-well plating

The agar spot-plate results presented above are qualitative, thus the growth rates of the cells cannot be measured. Therefore, we have set the following experiments to investigate the growth kinetics of the deletion mutants in the presence of several mitochondria-targeting antibiotics (**Table 1.3**) in liquid growth media.

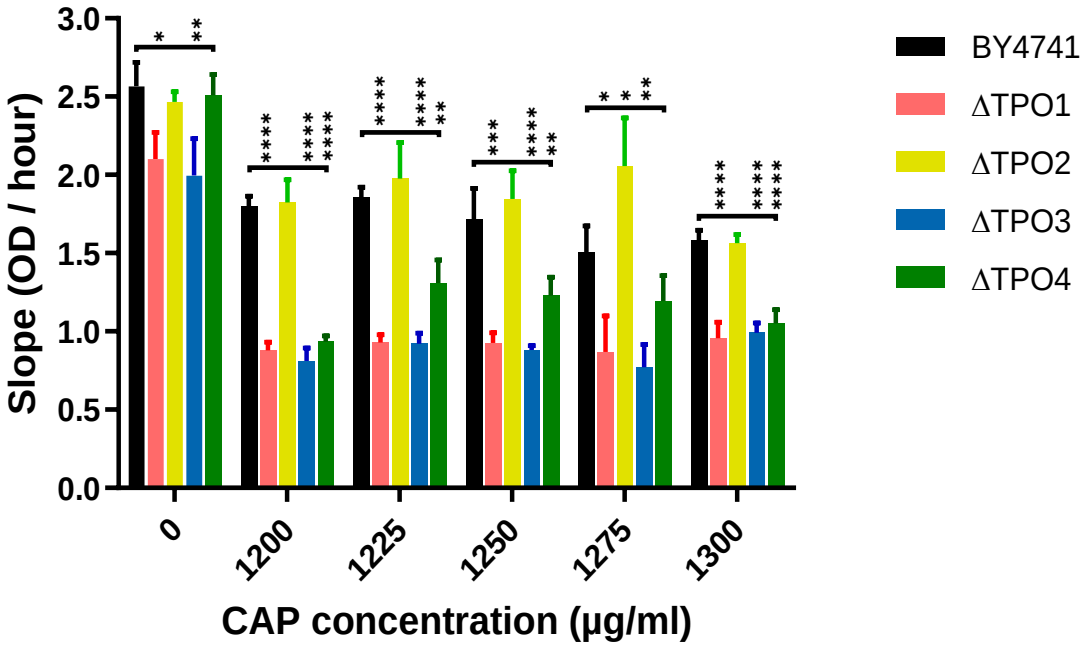
We found the range of concentrations for the mutants as 1200-1300 µg/ml CAP (**Fig. 3.3**), 15-30 µg/ml ERY (**Fig. 3.4**) and 100-300 µg/ml TET (**Fig. 3.5**), respectively. Then we used these values for setting up the 96-well plating experiments.

3.2.2.4.1 Response to Chloramphenicol

We compared the susceptibility of the WT and deletion mutants to CAP in terms of maximum growth rate (OD/hour) and overall growth. In the case of the control group (0 µg/ml CAP), all four mutants grew similar to the WT having a similar final OD and growth phases (**Fig. 3.7 (B)**). Except for the ΔTPO2, all three mutants were much more sensitive than the WT to the presence of CAP, among which the mutant ΔTPO3 exhibited the greatest inhibition (**Fig. 3.7 (A)**). For 1225, 1250 and 1300 µg/ml CAP treatment groups, all three mutants, except for the ΔTPO2, showed a sharp log phase (within 2-12 hours) and reached the stationary phase faster than the WT (**Fig. 3.7 (B)**). The WT reached the stationary phase between 16-24 hours (**Fig. 3.7 (B)**). Among the mutants,

ΔTPO1 demonstrated the lowest average OD for all the treatment groups except for the 1200 µg/ml CAP group.

A)



B)

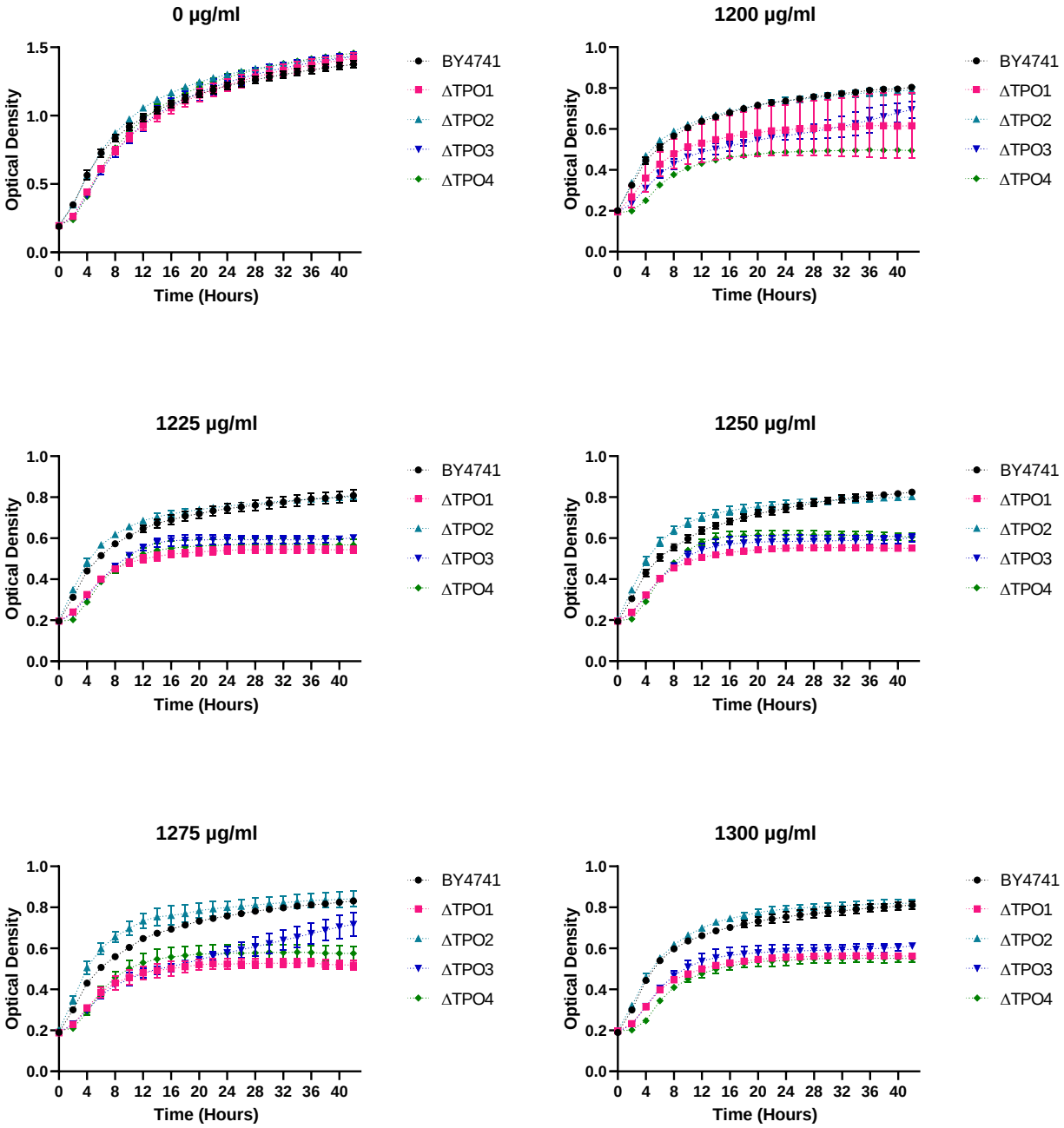

0 µg/ml
1200 µg/ml
1225 µg/ml
1250 µg/ml
1275 µg/ml
1300 µg/ml
Optical Density
Time (Hours)
BY4741
ΔTPO1
ΔTPO2
ΔTPO3
ΔTPO4

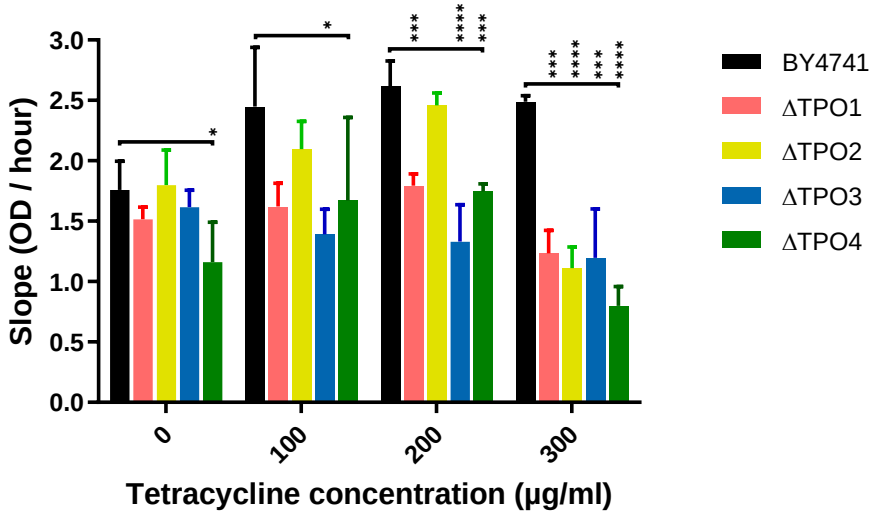
Figure 3.7 Growth of BY4741 and deletion mutants in the presence of CAP. The strains were diluted in fresh YPG to 0.2 OD from a 72-hour YPG culture. A volume of 200 µl of each of the five strains containing 0, 1200, 1225, 1250, 1275 and 1300 µg/ml CAP, respectively, was added onto the 96-well plate. A volume of ethanol, equal to the volume of antibiotic added to the 1300 µg/ml CAP group, was applied to the 0 µg/ml CAP group. The ethanol volume was adjusted for the other groups to make the total volume of ethanol equal. The cultures were grown for 44-48 hours at 30°C with continuous shaking. The absorbance was recorded every 30 mins using an Epoch 2 plate reader at 600 nm wavelength. **A) Comparison of growth rates.** Specific growth rate (slope) was calculated using the change of OD over a specific time (0-12 hours) of the exponential phase of the growth curve. Means and standard deviations are shown. The average slope of the 3 technical replicates of each of the mutants from each treatment group was compared to their respective WT using one-way ANOVA at 95% CI to indicate statistical significance. *P < 0.05, **P < 0.01, ***P < 0.001, ****P < 0.0001. **B) Comparison of growth kinetics.** Growth kinetics was followed by plotting the average OD of the 3 replicates against each time point. The growth kinetics of each of the mutants from each treatment group was compared to their respective WT using an XY plot. All the data were presented using GraphPad Prism 9.0.0 (121) (https://www.graphpad.com/scientific-software/prism/).

3.2.2.4.2 Response to Tetracycline

In this experiment, the susceptibility of the WT and deletion mutants to TET was compared in terms of growth rate (OD/hour) and kinetics. In the control group (0 µg/ml TET), there is no significant difference in growth rate between the WT and the mutants, except for the ΔTPO4 strain, which grows more slowly (**Fig. 3.8 (A)**). The 300 µg/ml TET demonstrated the highest inhibition of growth of all the mutants compared to the WT (**Fig. 3.8 (A)**).

When the entire growth curve was considered, in the case of the control group (0 µg/ml TET), besides ΔTPO1, all the mutants grew similar to the WT having similar final OD of 1.0 and a late log phase (6-12 hours) followed by other phases of growth (**Fig. 3.8 (B)**). For the control and all the treatment groups, the strains experienced no lag phase, which might result if the overnight cultures were not in the stationary phase. There was a sharp log phase (0-8 hours) and the deletion strains reached stationary phase at a lower OD (at <0.9) than did the control group (at >0.9) (**Fig. 3.8 (B)**).

A)


Slope (OD / hour)
3.0
2.5
2.0
1.5
1.0
0.5
0.0
0
100
200
300
Tetracycline concentration (µg/ml)
*
*
***
****
***
***
****
****
BY4741
ΔTPO1
ΔTPO2
ΔTPO3
ΔTPO4

B)

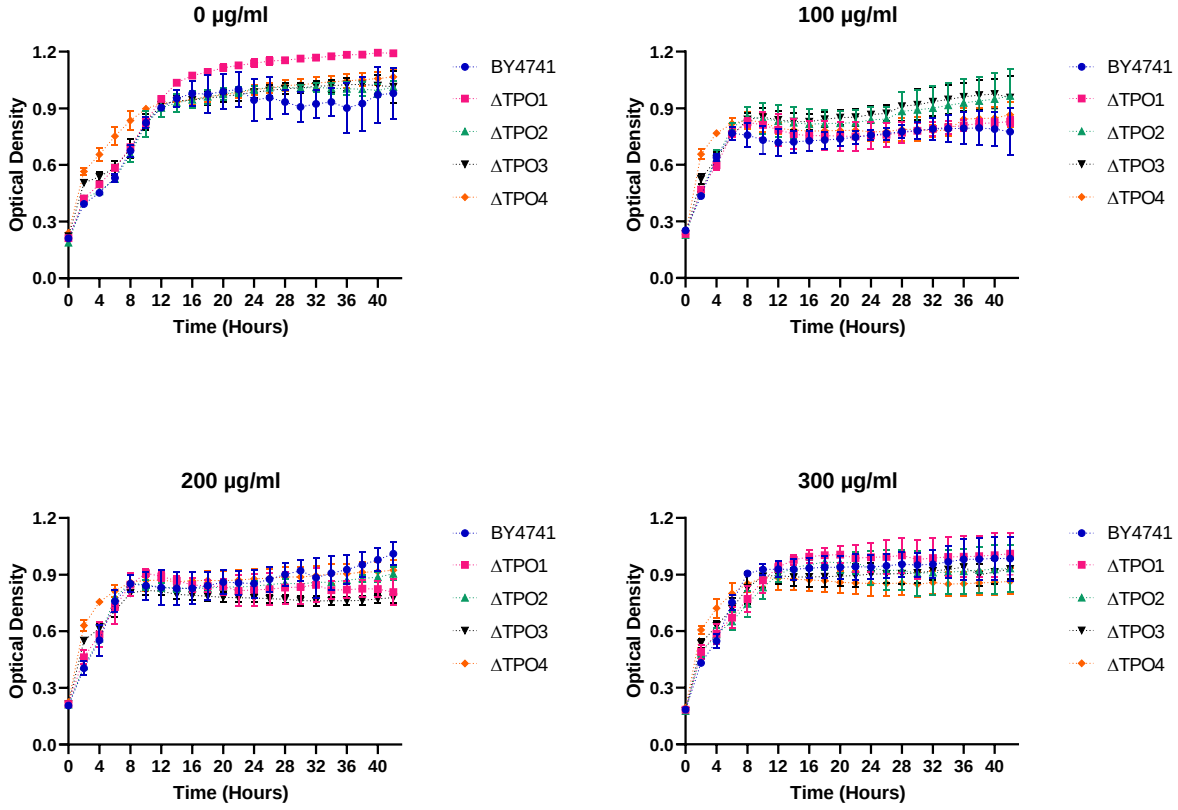

0 µg/ml
100 µg/ml
200 µg/ml
300 µg/ml
Optical Density
Time (Hours)
0.0
0.3
0.6
0.9
1.2
0 4 8 12 16 20 24 28 32 36 40
BY4741
ΔTPO1
ΔTPO2
ΔTPO3
ΔTPO4

Figure 3.8 Growth of BY4741 and deletion mutants in the presence of TET. The strains were diluted to 0.2 OD from a 72-hour YPG culture. A final volume of 200 µl culture of each of the five strains containing 0, 100, 200 and 300 µg/ml TET, respectively, were added onto the 96-well plate. Equal volume of ethanol, to the volume of antibiotic added to the 300 µg/ml TET group, was applied to the 0 µg/ml TET group. The ethanol volume was adjusted for the other groups to make the total volume equal. The cultures were grown for 44-48 hours at 30 ℃ with continuous shaking. The absorbance was recorded every 30 mins using an Epoch 2 plate reader at 600 nm wavelength. **A) Comparison of growth rates.** Specific growth rate (slope) was calculated using the change of OD over a specific time of the exponential phase of the growth curve. The average slope of the 3 technical replicates of each of the mutants from each treatment group was compared to their respective WT using one-way ANOVA at 95% CI to indicate statistical significance. *$P < 0.05$, ***$P < 0.001$, ****$P < 0.0001$. **B) Comparison of growth kinetics.** Growth kinetics (change of biomass) was calculated by plotting the average OD of the 3 replicates against each time point. The growth kinetics of each of the mutants from each treatment group was compared to their respective WT using an XY plot. Means and standard deviations are shown. All the data were presented using GraphPad Prism 9.0.0 (121) (https://www.graphpad.com/scientific-software/prism/).

3.2.3 EtBr efflux from fungal mitochondria

We hypothesized that if the efflux pumps are deleted, the mutants' mitochondria (mito) will show less efflux compared to WT. The objective of the experiments was to look for evidence of efflux activity by assessing EtBr efflux in *TPO* mutant and WT mitochondria. For the initial experiments, isolated mitochondria from WT *Neurospora crassa* were used, as they are easy to obtain in large amounts. Putative drug efflux pumps are located in the inner membrane and would pump drugs into the intermembrane space. A strain of *N. crassa,* which lacks the outer membrane porin (ΔPor-1) was also studied, to determine if this protein is involved in the release of EtBr from the intermembrane space. Once the experiment was established for these mitochondria, the experiments were repeated with those of WT *S. cerevisiae.*

3.2.3.1 EtBr efflux from *N. crassa* mitochondria

The experiment involves measuring the fluorescence of EtBr in the presence of mitochondria with membrane potential (induced by succinate) or membrane potential dissipated by the drug CCCP.

First, EtBr was added to mitochondria in buffer, and a baseline of fluorescence was established. In **Fig. 3.9 (A)**, the WT (*N. crassa*) and ΔPor-1 mito showed a similar accumulation of EtBr. For the WT, there was a small decrease in relative fluorescence after the putative mitochondrial pumps were energized by using succinate. This suggests that some of the EtBr are being pumped out of mitochondria, where its fluorescence would be reduced. A partial increase in fluorescence was observed after the addition of ADP, which would drive ATP synthesis and therefore, consume some of the membrane potentials. This supports the idea that the membrane potential is required for keeping EtBr out of mitochondria. The addition of oligomycin, which blocks the ATP synthase, did not change the level of EtBr fluorescence, which is expected if it is not an ATP-dependant

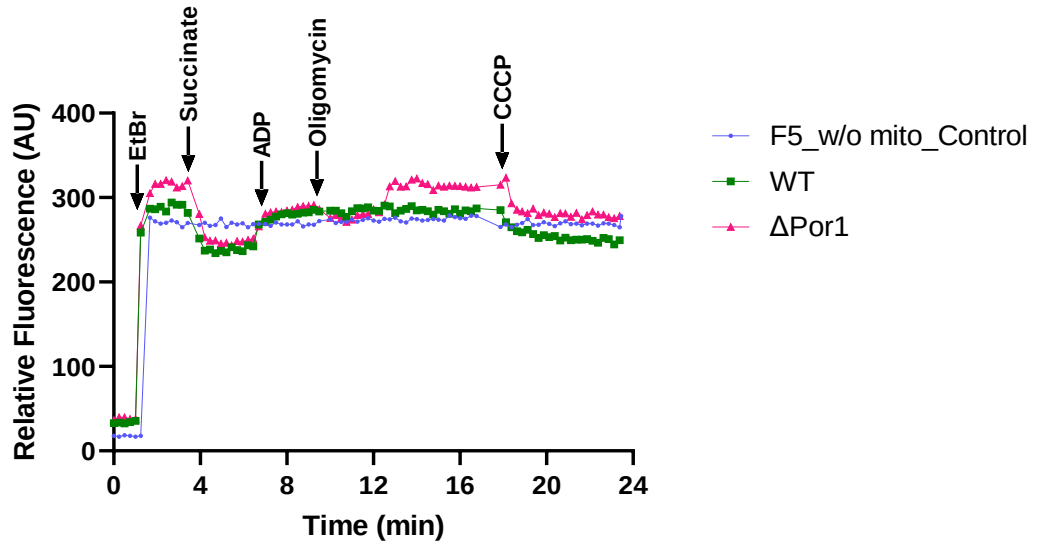
pump. However, as expected, EtBr fluorescence decreased after the addition of CCCP, which dissipates the potential. The results were somewhat different for ΔPor-1 mitochondria in this experiment. After a delay, there was an increase in EtBr fluorescence after the addition of oligomycin. Nonetheless, the addition of CCCP did increase fluorescence, indicating a role of the membrane potential in effluxing EtBr.

In a second experiment, shown in **Fig. 3.9 (B)**, the ΔPor-1 strain appeared to accumulate 25% more EtBr compared to the WT. However, we will need more replicates to establish this result. In this experiment, ΔPor-1 and the WT behaved similarly in the presence of succinate, ADP, oligomycin and multiple amounts of CCCP. ΔPor-1 mitochondria were found to be more sensitive to increasing concentrations of CCCP considering the relative fluorescence intensity.

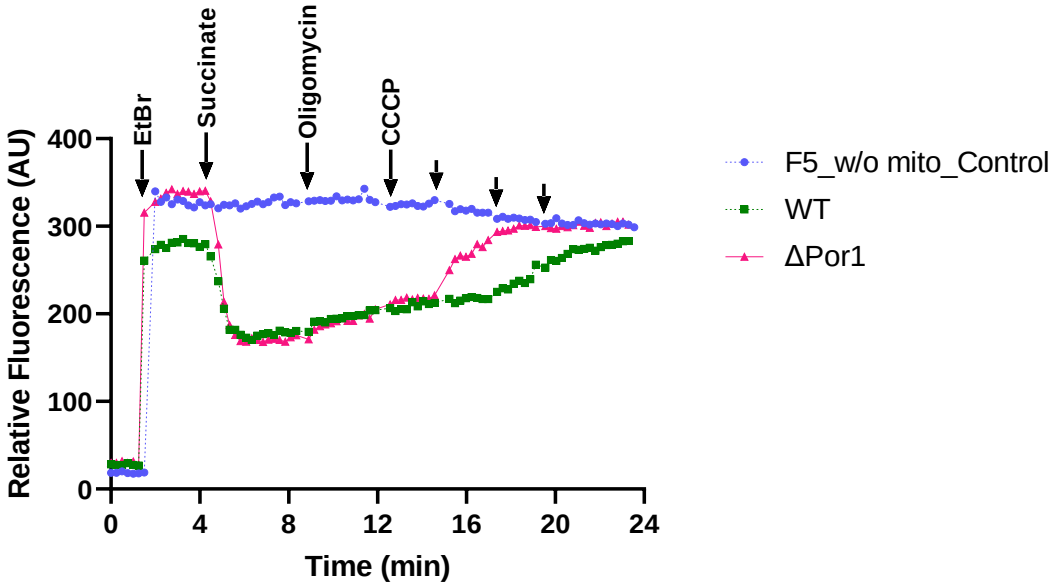
The fluorescence of EtBr between the F5 buffer (control) and F5 buffer+mito (treatment) was found to be similar. To determine if this was related to the BSA in the F5 buffer, two controls were used. In **Fig. 3.9 (A and B)**, the background fluorescence of EtBr of the F5 buffer (without mito), WT and ΔPor-1 groups was found to be similar. However, a clear difference in background fluorescence of EtBr has been observed between the F5 (+BSA) and TBS (Tris-buffered saline (-BSA)) buffers.

In this third experiment, **Fig. 3.9 (C)**, the WT and ΔPor-1 mitochondria showed similar accumulation and efflux of EtBr, and an increase in fluorescence after the energy is dissipated using CCCP.

A)


Relative Fluorescence (AU)
400
300
200
100
0
EtBr
Succinate
ADP
Oligomycin
CCCP
0
4
8
12
16
20
24
Time (min)
F5_w/o mito_Control
WT
ΔPor1

B)


Relative Fluorescence (AU)
400
300
200
100
0
EtBr
Succinate
Oligomycin
CCCP
0
4
8
12
16
20
24
Time (min)
F5_w/o mito_Control
WT
ΔPor1

C)

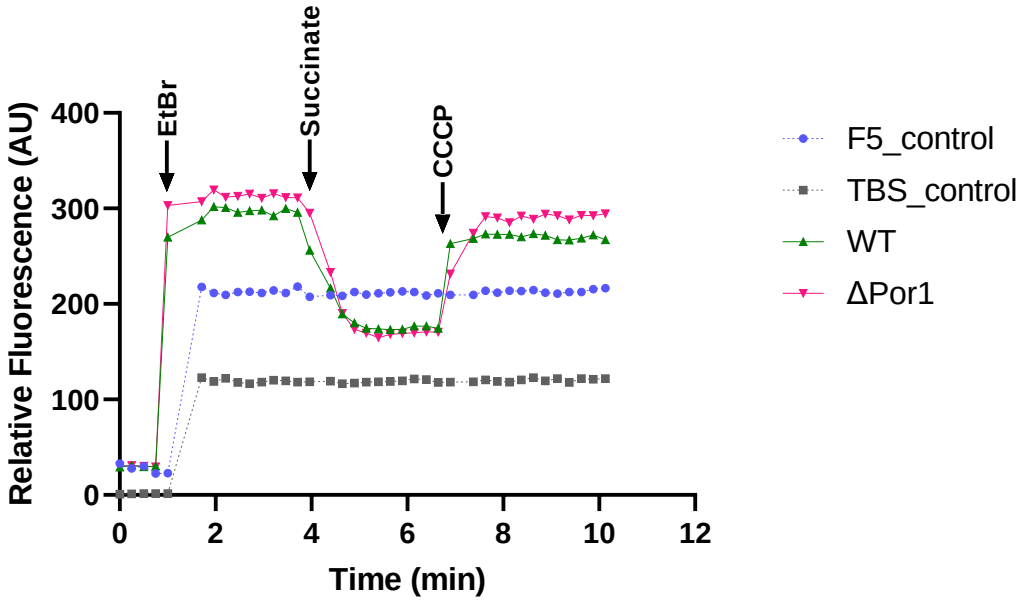


Figure 3.9 Optimization of EtBr efflux from *N. crassa* mitochondria. The relative fluorescence (arbitrary units) was recorded every 0.25 mins using a 'Cary Eclipse' fluorescence reader following an excitation and emission wavelength of 520 and 590 nm respectively, and a slit width of 5 nm. In these experiments, EtBr, succinate and oligomycin were added at 1-, 4- and 9-min points respectively, in a total volume of 3 ml. 2 mM CCCP was added as indicated by arrows at the given time points on the graph. Concentrations are as indicated in Chapter 2. About 0.24 mg/ml mito protein and F5 buffer were used for A) and B). **A) With ADP and oligomycin.** The ADP and CCCP were added at 7- and 18-min points, respectively. **B) With oligomycin.** The CCCP was added at 12.5-, 15-, 17.5- and 19.5-min points with an increasing volume of 10 µl each time. **C) Test without ADP and oligomycin.** 0.1 mg/ml mito was used, and the additions of ADP and oligomycin were omitted. The fluorescence of EtBr +/- BSA was examined in buffer with (F5) and without (TBS, Tris-buffered saline) BSA.

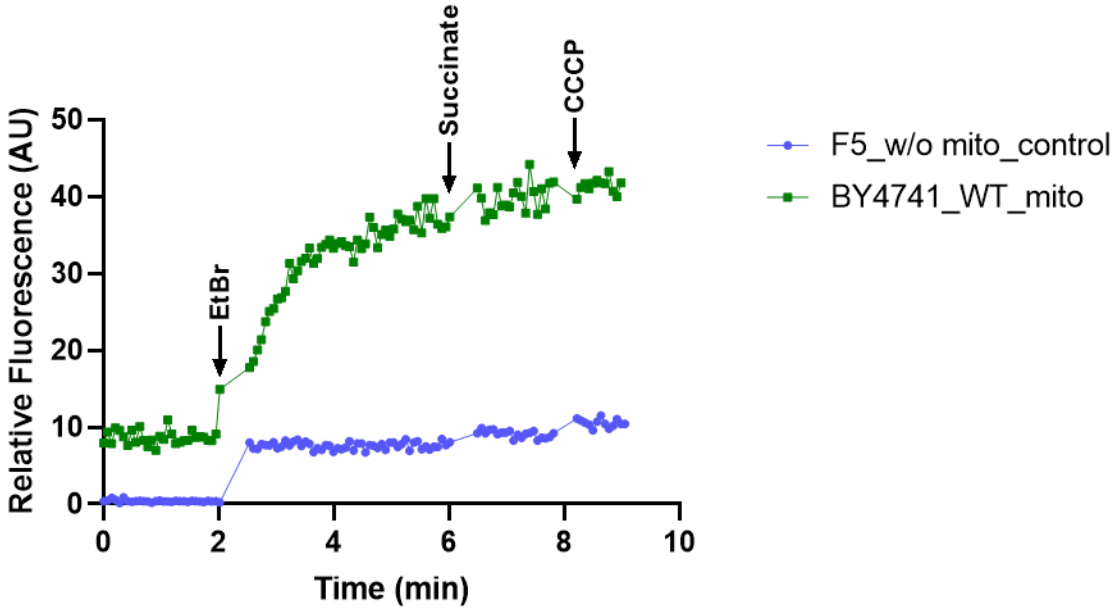
3.2.3.2 EtBr efflux from *S. cerevisiae* mitochondria

The next step was to repeat the experiment using yeast mitochondria, which were isolated according to our lab procedure which uses dithiothreitol (DTT) with lyticase enzyme. The yeast WT mito showed a very low accumulation of EtBr and there was no change in fluorescence even after the addition of succinate F**ig. 3.10 (A)**.

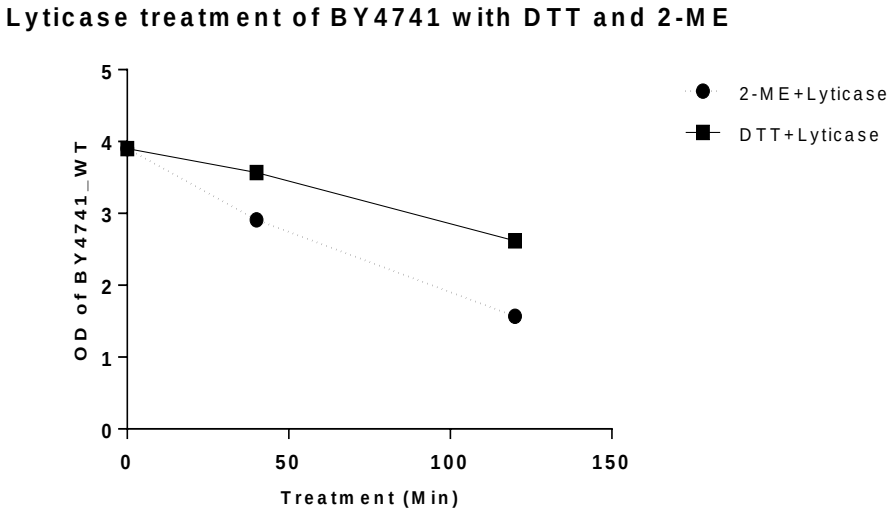
In an attempt to increase the yield of mitochondria, the effectiveness of two denaturing agents, 2-mercaptoethanol (2-ME) or DTT was tested along with the lyticase enzyme. Spheroplast production was measured by the decrease in OD that accompanies the lysis of yeast cells. As seen in **Fig. 3.10 (B)**, lyticase enzyme with 2-mercaptoethanol (2-ME) produced more spheroplasts compared to the enzyme with dithiothreitol (DTT). For both groups, the lyticase treatment started with yeast cells of an OD of 4. After the treatment, the OD was reduced to 1.57 and 2.62 for lyticase+2-ME and lyticase+DTT, respectively.

The next experiment utilized mitochondria produced from spheroplasts generated with 2-ME (WT2) or DTT (WT1) (**Fig. 3.10 (C)**). The WT2 mito demonstrated a higher accumulation of EtBr compared to WT1. However, we did not see any evidence of efflux activity in the presence of succinate and the WT mito seems insensitive to CCCP.

A)


Relative Fluorescence (AU)
50
40
30
20
10
0
0
2
4
6
8
10
Time (min)
EtBr
Succinate
CCCP
F5_w/o mito_control
BY4741_WT_mito

B)


Lyticase treatment of BY4741 with DTT and 2-ME
OD of BY4741_WT
5
4
3
2
1
0
0
50
100
150
Treatment (Min)
2-ME+Lyticase
DTT+Lyticase

C)

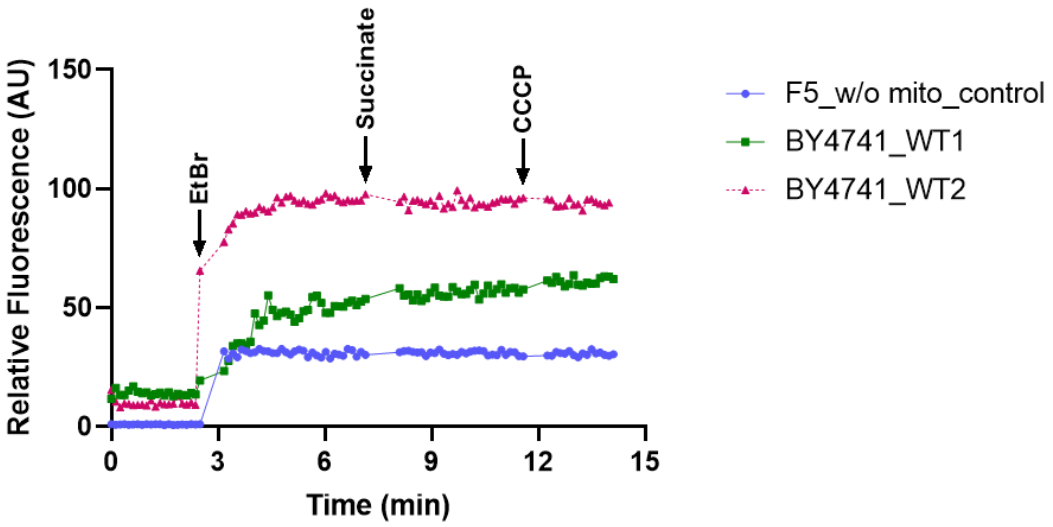


Figure 3.10 Optimization of EtBr efflux from *S. cerevisiae* mitochondria. The relative fluorescence (AU) was recorded every 0.25 mins using a 'Cary Eclipse' fluorescence reader following an excitation and emission wavelength of 520 and 590 nm respectively, and a slit width of 5 nm. In these experiments, EtBr was added at a 2-min point, in a total volume of 3 ml. The succinate and CCCP were added as shown on the graph, after the stabilization of the signal. Mito from the +DTT and +2-ME spheroplasts preparation (SP) were used at concentrations of 0.01 and 0.045 mg/ml, respectively, in the 3 ml reaction. **A) Before optimizing the SP (+DTT).** The succinate and CCCP are added at 6- and 8.5-min points. **B) Comparison of efficacy of 2-ME or DTT with lyticase to make spheroplasts**. 300 Units/ml of Lyticase, 1 µl of 2-ME per 100 µl of yeast-enzyme buffer suspension or 10 mM DTT were used to treat the yeast cells. The treatment was carried out at pH 7.5, 30 ℃ and 100 rpm for 70-120 minutes. The OD was measured before, during and at the end of the treatment to determine the efficacy of the enzyme. **C) Comparison of EtBr accumulation using mito obtained by DTT or 2-ME treatment**. The succinate and CCCP were added at 7- and 11.5-min points.

3.3 Discussion

In our study, we looked for evidence of putative fungal mitochondrial efflux pumps and tried to establish them as potential drug efflux pumps. To date, no studies have shown Tpo1-5 and Hxt5 in the fungal mitochondria taking part in direct drug efflux, but several studies show Tpo1 to be a multidrug efflux pump localized in the plasma membrane. It can efflux the widest range of substrates compared to Tpo2-5 and Hxt5 (Alenquer et al., 2006; Do Valle Matta et al., 2001; Markovich et al., 2004a; Remy et al., 2017; Sá-Correia et al., 2009). Thus, we looked for information about any homologues of Tpo1 in prokaryotes and lower eukaryotes.

One study investigated a human orthologue of the yeast MFS MDR gene *TPO1*, which is referred to as TETRAN (tetracycline transporter-like protein) (Mima et al., 2007). TETRAN has a similarity to the tetracycline transporter (TetA) of *E. coli;* both of them have 12-TMS and belong to the MFS superfamily (Duyao et al., 1993; Levy, 1992). (Mima et al., 2007) showed that yeast Tpo1 and human TETRAN conferred resistance to Indomethacin, which is a non-steroidal anti-inflammatory drug (NSAID), in yeast and human cells, respectively. The researchers performed northern blotting and demonstrated the induction of *TPO1* transcription, which herbicides can induce the transcription in *S. cerevisiae* (Miguel Cacho Teixeira & Sá-Correia, 2002). However, the expression of the homologues of Tpo1, namely Tpo2, Tpo3 and Tpo4, was not found to be proportional to the concentration of indomethacin (Mima et al., 2007). To support the hypothesis that Tpo1 might be able to efflux drugs, in our study, we confirmed that Tpo1, TETRAN and YajR contain similar predicted motifs of the drug:H^+ antiporter families (**Fig. 3.1**). YajR is a multidrug efflux pump of the MFS superfamily having 12 TMS (Jiang et al., 2014). Thus, we can speculate Tpo1 as a putative mitochondrial MFS drug efflux pump.

We then wanted to analyze the effect of different mitochondrial-targeted antibiotics on the commercially obtained BY4741 and BY4742 deletion mutants of *TPO1-4*. In our study, ethanol was used as a solvent to dissolve the antibiotics, so the mutants were grown in YPG media with and without ethanol to demonstrate the effect of ethanol on their growth. The WT and mutants have shown faster growth and a shorter lag phase with ethanol compared to without ethanol (**Fig. 3.2**). Several studies highlighted the growth inhibitory effect of ethanol during fermentation by yeast (Kubota et al., 2004). However, a study showed the growth complementary effect of ethanol where up to 1% Ethanol was shown to enhance the growth when added to the media in batch culture (Wasungu & Simard, 1982). Thus, in our case, 3% ethanol might have augmented the growth of the strains.

Glycerols taken up by yeast cells using a membrane transporter encoded by *STL1 (sugar transporter-like protein)*, whereas ethanol is proposed to be transported through passive diffusion (Turcotte et al., 2010). The ethanol is converted to Acetyl-CoA in fewer steps compared to glycerol and enters the TCA cycle (Turcotte et al., 2010). Thus, the addition of ethanol along with glycerol could trigger the cells to grow faster with a shorter lag phase. Both ethanol and glycerol are nonfermentable carbon sources, meaning the cells can utilize them by oxidative phosphorylation (respiratory pathway) in mitochondria. Moreover, in **Fig. 8.2** (**Appendix 3**), we have shown that cellular growth increased with 3% ethanol compared to 0% ethanol, whereas growth reduced with increasing concentration of tetracycline even with ethanol.

We hypothesized that the bacterial antibiotics would inhibit the *S. cerevisiae* growth, as the mitochondria have antibiotic target sites similar to bacteria. In our study, we demonstrated the effect of chloramphenicol, erythromycin and tetracycline on the growth of the mutants compared to the WT, as they inhibit the yeast mitochondrial protein synthesis both *in vivo* (Clark-Walker &

Linnane, 1966) and *in vitro* (Linnane et al., 1968). CAP and ERY bind to the bacterial 50S subunit of ribosomal RNA (Schlünzen et al., 2001; Tu et al., 2005).

To investigate the effect of growth medium on the efficacy of an antibiotic, we used both spot plating and liquid cultures in 96-well plates. Hung et al., 2018 compared the sensitivity of several *S. cerevisiae* mutants against the cell wall binding toxin calcofluor white (CFW) using traditional spot plating and 96-well liquid assay. They found that the MIC value of the CFW is higher for the yeast growing on solid media compared to the liquid media. It was hypothesized that the difference in MIC value could result from the difference in exposure of cells to CFW in liquid versus on a plate. The cells are exposed to drugs more homogenously in the liquid media than on the plate. However, in this study, the overall results of CAP and TET treatments obtained through spot plating and 96-well plating were found to be similar. The specific differences are discussed in detail in the following paragraphs.

In the spot-plating experiments, we found that ΔTPO3 is the most sensitive mutant, compared to the WT, to all three antibiotics (**Fig. 3.3-3.5**). In contrast, the ΔTPO4 was found to have more visible growth compared to those of the other mutants and WT under the treatment of CAP only (**Fig. 3.3**). One possibility is that the deletion of the *TPO4* gene causes an upregulation of the other *TPO* genes, so ΔTPO4 has more of the other putative pumps (Tpo1-3) in effluxing CAP as a specific substrate than WT.

Tetracycline has been shown to inhibit mitochondrial protein synthesis because of the presence of the 70S ribosome in this organelle (Riesbeck et al., 1990). In this study, we could hypothesize that Tpo2 and Tpo3 are the putative tetracycline efflux pumps (**Fig. 3.5**), because the ΔTpo2 and ΔTpo3

strains are highly sensitive to 300 μg/ml TET and lack the respective efflux pumps compared to WT, ΔTpo1 and ΔTpo4, which retain Tpo2 and Tpo3 pumps.

An experiment was needed to show that the effects of the drug on the cell were due to interference with mitochondrial activity. Thus, we compared the effect of antibiotics on yeast mitochondria growing in a fermentable (YPD) and nonfermentable (YPG) media, respectively. We have found no difference between the mutants and WT growth on YPD plates containing tetracycline (TET) (**Fig. 3.6**). They do not need mitochondrial activity under those conditions. The yeasts could utilize the energy produced through the fermentative pathway. Thus, we can say that the effect of TET is due to its effect on the respiring mitochondria in the YPG medium.

The spot plating method is helpful to observe the effect of an antibiotic on the phenotype of yeast; however, there are limitations in interpreting the results and the experiments are less cost-effective (Hung et al., 2018). Thus, to overcome the limitations of spot-plating and to observe the growth kinetics of yeast we adopted liquid culture in 96-well plates, as this method has been demonstrated by different groups (Ho et al., 2009; Olsen et al., 2010). It provides options to reduce the experimental volume, incubation time, antibiotic inactivation, and increase the throughput. More importantly, using 96-well plates generates reproducible quantitative measures of the effects of the antibiotics on the yeasts' growth rate.

In the 96-well experiments, we found that all the mutants except for ΔTPO2 are sensitive to 1200-1300 μg/ml of CAP (**Fig. 3.7**). Thus, yeast mitochondria might not need Tpo2 to efflux CAP, whereas it can utilize Tpo1, Tpo3 and Tpo4 to efflux CAP. It is also possible that there is differential expression of other *TPO* genes when one is missing, and that the resulting combination is useful, except when Tpo2 is missing. Unexpectedly, the mutants and WT from the tetracycline

treatment groups have a very short lag phase and sharp log phase, meaning a faster growth rate compared to the strains in the absence of TET (**Fig. 3.8 (A)**). It was shown that *Candida albicans* grows with a modest, unexplained, increase during the early log phase (in the first 6 hours) at a sublethal concentration (<150 µg/ml) of TET (Larsen et al., 2008). In our case, the lower concentrations of TET might have triggered a signal for a faster growth rate, however, it needs to be investigated further. On the other hand, the ΔTPO3 exhibited the highest inhibition of growth among the mutants compared to WT with CAP and TET (**Fig. 3.7-8**). Thus, Tpo3 could be a putative CAP and TET efflux pump.

The abundance (**Table 1.2**) and localization (section **1.3.2)** of the Tpo proteins vary inside the *S. cerevisiae* cell. Tpo1 and Tpo3 are localized in the plasma membrane (Albertsen et al., 2003), vacuolar membrane (Tomitori et al., 2001) and mitochondria (Vögtle et al., 2017), whereas Tpo2 and Tpo4 are found in the plasma and vacuolar membrane. Low levels of Tpo1 and Tpo3 have been detected in mitochondria (Vögtle et al., 2017).

As we know the CAP and TET are mitochondria targeting antibiotics, and thus do not have any effect on the yeast cytoplasmic ribosomes. As illustrated in **Fig. 1.4**, CAP and TET could be removed out of the WT cell through the plasma membrane, or into vacuoles, or out of the mitochondria into the cytosol where they do no damage. These antibiotics might not affect mitochondria at lower concentrations that could be maintained by a combination of pumps.

Now, if we consider ΔTPO2 cells, which resemble WT in terms of sensitivity to these drugs, Tpo2 would be absent from the plasma and vacuolar membranes. However, these antibiotics might not have any effect on whether the cells have the Tpo2 or not, because Tpo1 and/or Tpo3 in mitochondria might efflux the antibiotics from mitochondria, as well as from the cytoplasm via

the plasma membrane or through vacuoles. The same could be true for ΔTPO4 cells. Now, if we look at the ΔTPO3 cells, Tpo3 would be absent from all three possible locations. So, there could be reduced antibiotic detoxification by transporting into the vacuoles (Albertsen et al., 2003) or efflux out of the mitochondria and out of cells in the absence of Tpo3. However, Tpo1 may be able to partially compensate for the lack of Tpo3, because it is localized to the same set of membranes. To test this possibility, the resistance of a ΔTPO1/ΔTPO3 strain should be examined. Similarly, it might be expected that Tpo3 could compensate for the lack of Tpo1in ΔTPO1 cells. However, we observed that ΔTPO3 cells are the most sensitive to antibiotics. It could be due to the higher abundance (molecules/cell) of Tpo3 versus Tpo1, which is observed in WT *S. cerevisiae* cells (**Table 1.2**). The regulation of this family of genes is not understood, and it is also possible that the absence of a single Tpo protein leads to altered expression levels of the others. The relative abundances of the Tpo family mRNA should be investigated to address this possibility.

We then wished to find any evidence of efflux from fungal mitochondria *in vitro*. We started with the *N. crassa* as the yield of mitochondria extraction is high; that is 2-3 mg/g wet weight of cells (Sebald et al., 1979). Moreover, our lab has demonstrated EtBr efflux from *N. crassa* mitochondria (**Fig. 8.1**; **Appendix 3**).

The use of a fluorophore agent that promotes a significant substrate accumulation is crucial for a demonstration of efflux activity (Lomovskaya & Bostian, 2006; M. Viveiros et al., 2008). EtBr binds to mitochondrial DNA, with the highest accumulation in *S. cerevisiae* compared to other available cationic fluorophores (Sayas et al., 2015). The opposite charges of the EtBr (+) and mitochondrial matrix (-) might enhance the movement into mitochondria (Khan et al., 2007). Moreover, mtDNA is more accessible to EtBr binding compared to the nuclear DNA that is

compacted with histones and other nuclear proteins (Kanki et al., 2004). Thus, we chose EtBr for our efflux experiments.

In the efflux experiments with *N. crassa* mitochondria, we added ADP to enhance the generation of ATP to see whether it is utilized by the putative pumps, Oligomycin, which interferes with the ATPase, was used to inhibit the synthesis of new ATP, and prevent consumption of the membrane potential. We demonstrated that the putative efflux pumps are not ATP-dependent; rather they are membrane potential-dependent because a reduction in fluorescence was seen in the absence of ADP, which is required for ATP synthesis (**Fig. 3.9**). We noted that the background fluorescence of the control group having F5 buffer was found to be similar to the treatment groups (**Fig. 3.9 A and B**). This could indicate that only a small amount of the EtBr was taken up by mitochondria. However, the F5 buffer contains bovine serum albumin (BSA) (66 430 Da, Sigma). This protein has isoelectric point ranging from *p*H 5.1 to 5.5; thus the protein has an overall negative charge (−18*e*) at *p*H 7 (Fologea et al., 2007), whereas EtBr is a cationic compound. So, this interaction of oppositely charged compounds might hinder the accumulation of EtBr inside mitochondria, making the background fluorescence similar for both groups, with and without mitochondria. However, in a BSA-free buffer (TBS) the background fluorescence was reduced (**Fig. 3.9 (C)**), thus, the best control for further experiments would be F5 with no BSA.

The isolation of mitochondria from *S. cerevisiae* is tricky and the yield is very low compared to *N. crassa*. The crude mitochondria extracted generally is 200-250 µg protein/g wet weight of yeast cells (Liao et al., 2018). In the first experiment, we observed that the relative fluorescence of EtBr accumulation is very low, implying that the concentration of mitochondria was too low (**Fig. 3.10 (A)**). We optimized the production of spheroplasts from vegetative yeast cells with lyticase enzyme to obtain an increased concentration of mitochondria. We have shown that lyticase enzyme

in the presence of 2-mercaptoethanol can turn >50% of the cells into spheroplasts (**Fig. 3.10 (B)**). This optimization enabled us to show a higher accumulation of EtBr but there was no evidence of efflux after energizing with succinate (**Fig. 3.10 (C)**). However, the total yield of mitochondria was still about 10% of that from *N. crassa*, so it could be that the number of mitochondria was still insufficient and there was not enough fluorescence to show efflux. Moreover, it could be due to the absence of any efflux pumps in yeast mitochondria. If that were the case, the experiments from the TPO deletion strains reflect the presence of plasma membrane and vacuolar pumps. However, the question remains open until we can produce more yeast mitochondria to repeat the experiment.

In summary, even though several studies and homology predictions supported Tpo1 to be the best candidate for a potential mitochondrial drug efflux pump, we have shown that Tpo3 could be the one most likely involved in protecting yeast cells from CAP and ERY, supported by the qualitative result of the growth phenotype and quantitative result of growth kinetics. We could demonstrate the evidence for efflux in *N. crassa* WT mitochondria but could not do so for *S. cerevisiae* BY4741 mitochondria yet.

CHAPTER 4

Chapter 4: To express and examine the putative mitochondrial MFS drug efflux pumps in bacteria in order to study their specificity and mode of action

4.1 Introduction

To study the functions of the putative efflux pumps, it is important to express them in a suitable host/vector system. We need an expression system that can yield a high amount of protein, can multiply in a shorter time with high biomass, simple regulation of process scale and is overall cost-effective. As the organism of choice, *E. coli* satisfies all the above-mentioned options to be a suitable heterologous expression system.

Even though there are concerns regarding the lack of post-translational modification *in E. coli*, many eukaryotic proteins can be expressed and analyzed in this organism (Deniaud et al., 2011; Griffiths et al., 1999). For example, studies have shown that single mitochondrial-type ADP/ATP carriers (AACs) can be functionally expressed in *E. coli* (Haferkamp et al., 2002). Moreover, the putative drug efflux pumps considered for our studies are single-subunit MFS transporters, meaning they should be much easier to study compared to multi-subunit ABC transporters in *E. coli*.

In this chapter, we will express the putative efflux pumps namely *TPO1-TPO5* and *HXT5* in *E. coli* and analyze the functions in terms of mitochondria-targeted antibiotic (**Table 1.3**) efflux *in vivo*.

4.2 Results

4.2.1 Cloning of *TPO* genes

The first attempt to clone each *TPO* gene involved a recombination-based approach in yeast (Colot et al., 2006). To use this approach, we first needed a shuttle-vector with the following i) origins of replication in *E. coli* and *S. cerevisiae* ii) selectable markers for both organisms iii) a promoter system to allow overexpression of the cloned gene in *E. coli*. We were successful in the development of a pET21b(+)-based shuttle expression vector denoted as 'CEN/pET21b(+)' shown in **Fig. 4.1 (A)**. It contains the yeast origin of replication (CEN/ARS) and yeast auxotrophic marker (URA3) from pRS416 and pET21b(+) sequences that encoded the elements needed from *E. coli*. It was created by homologous recombination in yeast using a 1799-bp fragment of the *S. cerevisiae CEN6* centromere fused to an autonomously replicating sequence (to create a CEN/ARS sequence) and auxotrophic marker, *URA3* encoding orotidine-5'-phosphate decarboxylase, required for uracil biosynthesis.

The basic cloning strategy was to amplify a *TPO* gene with primers sharing terminal homology with the *BamH*I-cut shuttle vector and to transform both pieces into *S. cerevisiae*. Successful homologous recombination would generate a circular plasmid. However, this approach was not successful because we could not clone the genes of interest into this shuttle vector.

For subsequent cloning, we followed the method of Quan & Tian, 2009. This is a simple cloning method that uses a one-step polymerase chain reaction (PCR) to assemble and clone multiple inserts with any vector in-vitro (**Fig. 4.1**). We cloned *TPO1-5* and *HXT5* genes into a high copy number plasmid CEN/pET21b(+) to create expression plasmid constructs shown in **Fig. 4.2 (C)**. The constructs are listed in **Table 4.1**.

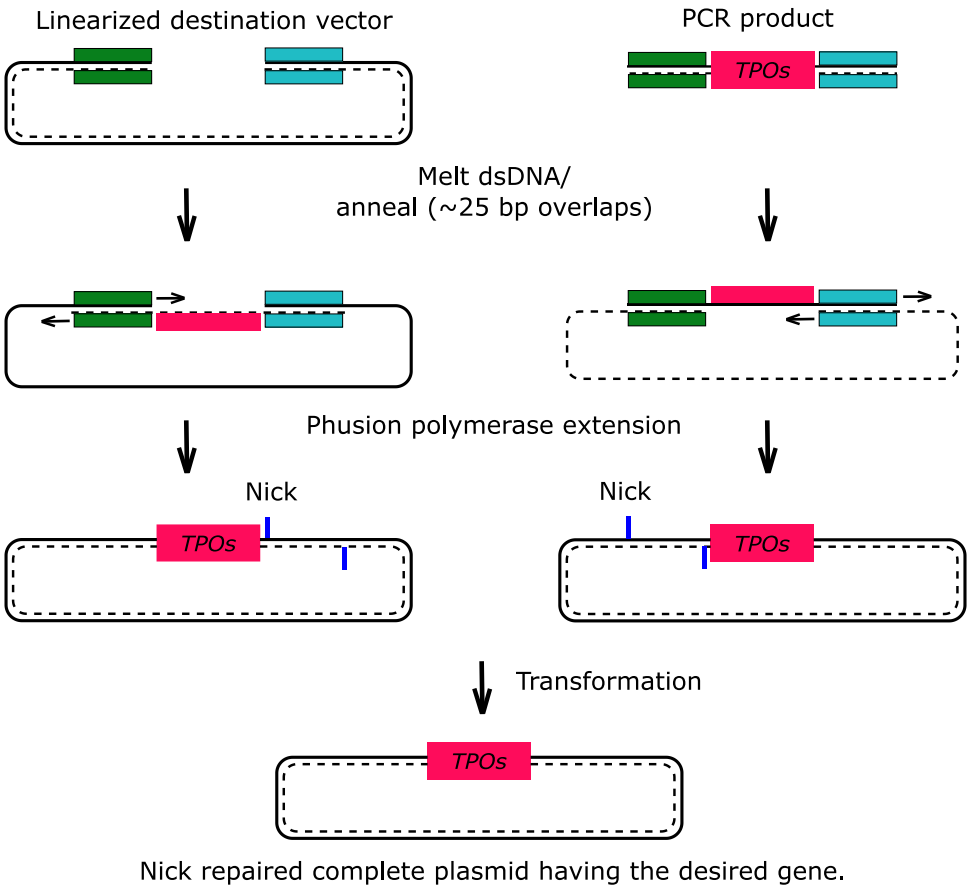
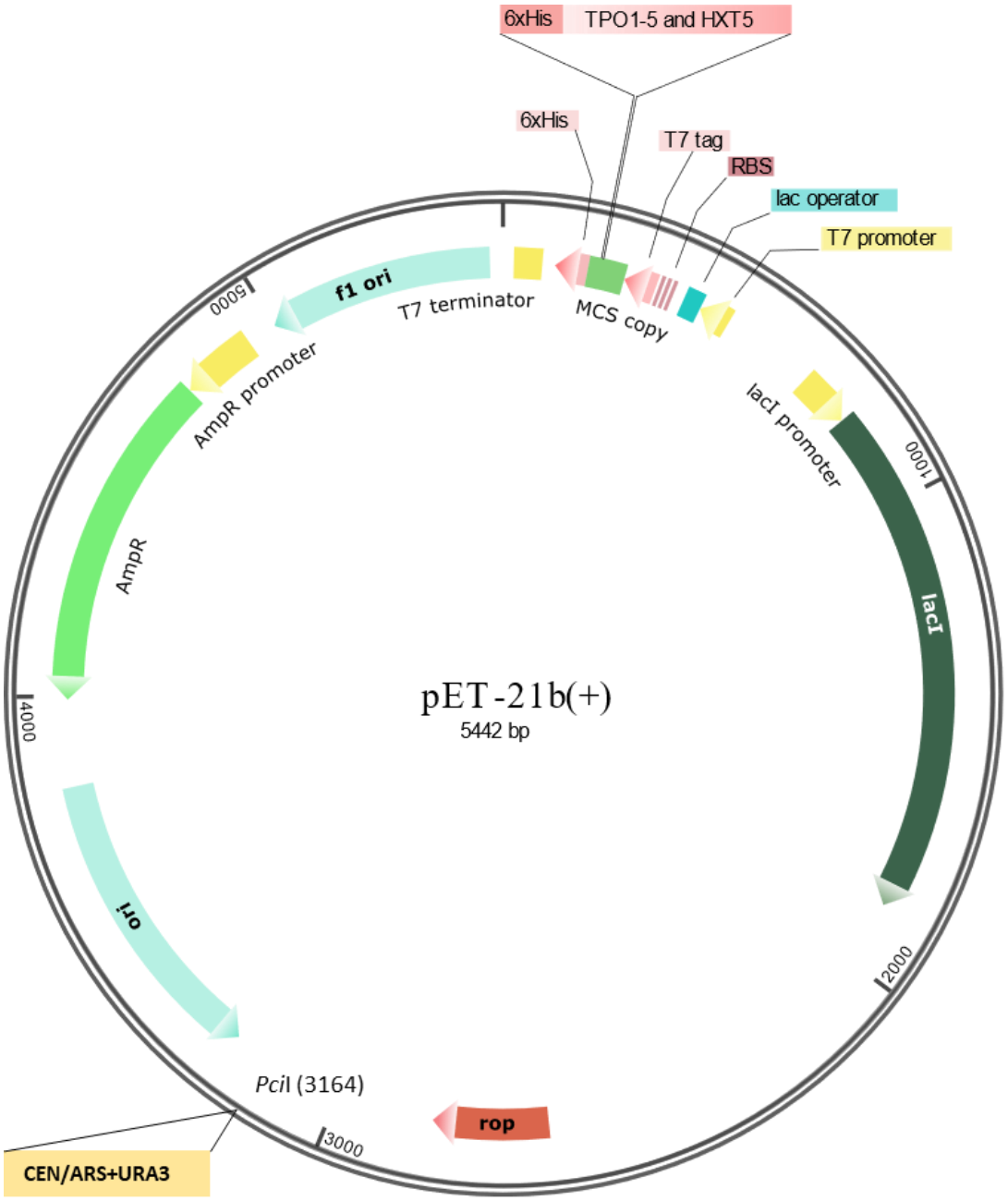


Figure 4.1 A schematic diagram of the Circular Polymerase Extension Cloning (CPEC) mechanism for cloning an individual gene. The insert and the vector are designed to have overlapping sequences at the ends. After denaturation and annealing, the overlapping sequences help the vector and the insert to hybridize. After hybridization, they work as a template for each other and keep incorporating new nucleotides until they reach their 5'-end. The nascent plasmid carries a nick on each strand. The nicks are shown by blue lines. This nicked plasmid was used for transformation to be repaired and multiplied in copy numbers (Quan & Tian, 2009).

A)


6xHis
TPO1-5 and HXT5
6xHis
T7 tag
RBS
lac operator
T7 promoter
f1 ori
T7 terminator
MCS copy
6000
AmpR promoter
AmpR
4000
ori
PciI (3164)
rop
3000
CEN/ARS+URA3
lacI promoter
lacI
1000
2000
pET-21b(+)
5442 bp

B) **C)**

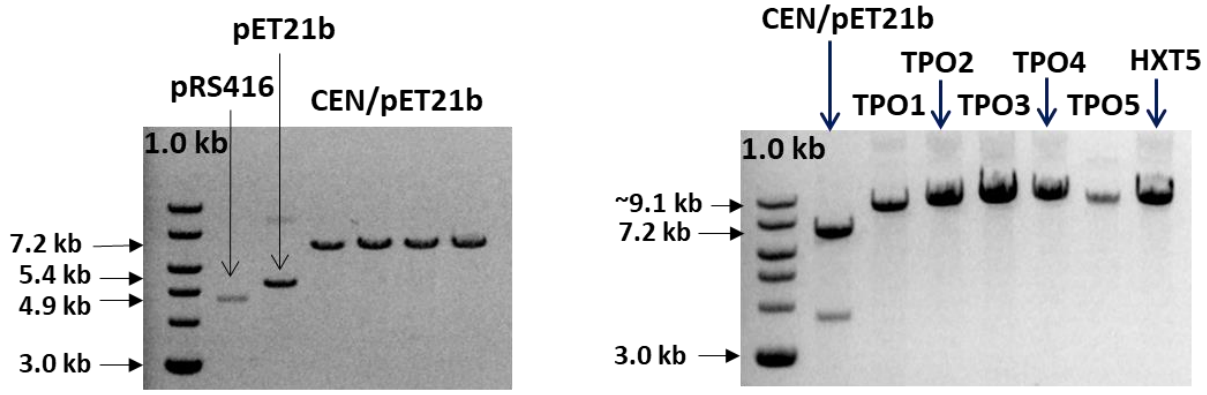


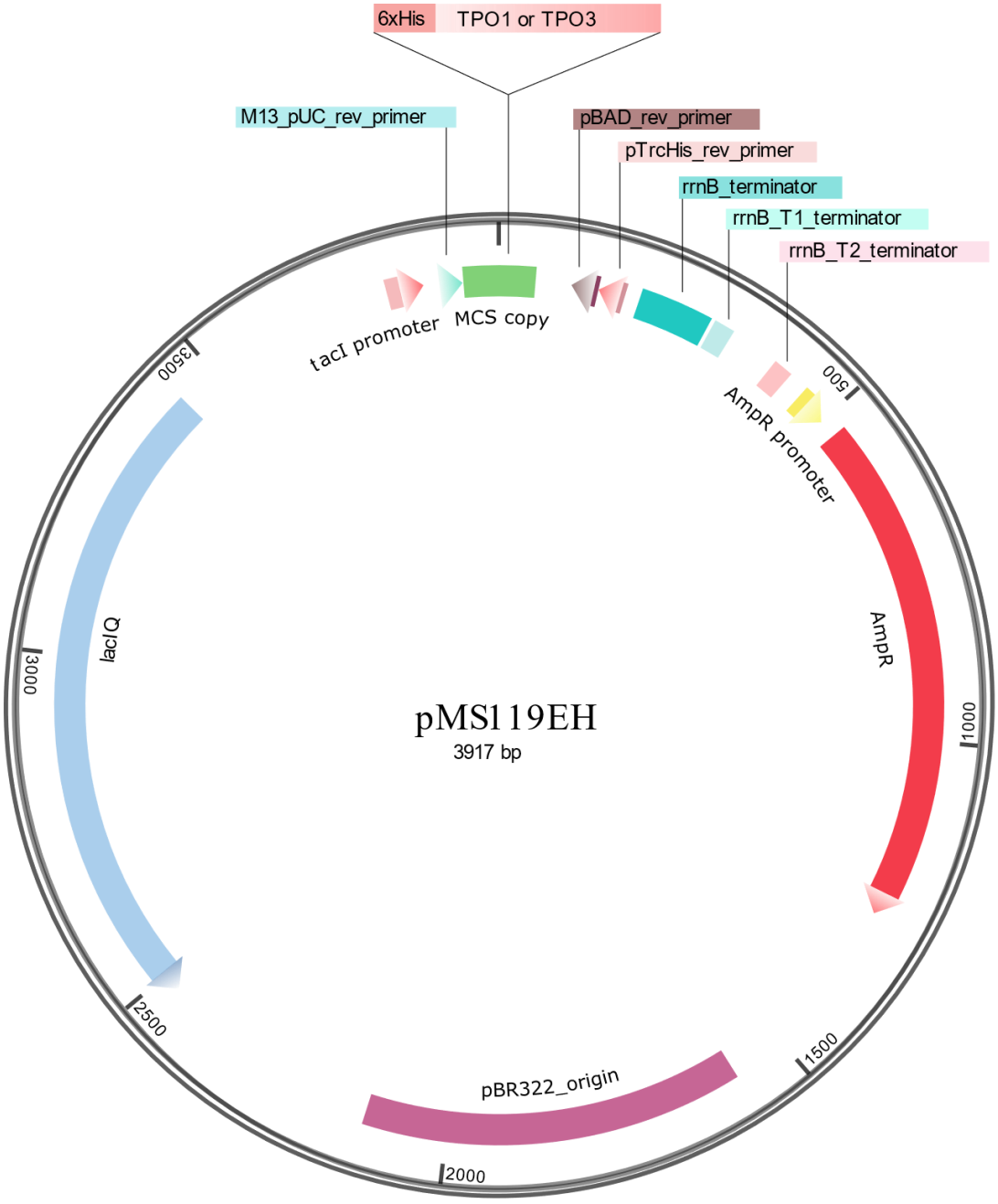
Figure 4.2 Cloning in the expression vector pET21b(+). A) The pET21b(+)-based shuttle vector, CEN/pET21b(+). The *CEN/ARS* and *URA3* fragments were obtained from a yeast-based plasmid pRS416 (NovoPro V010220#, (Sikorski & Hieter, 1989)) and cloned at the *Pci*I (3164 bp) site of pET21b(+). **B)** Lanes 2 and 3 on the gel show the two fragments used in the transformation to produce the shuttle vectors (independent clones shown in lanes 4-7). All these vectors were *BamH*I-cut to be linearized. **A)** The *TPO1-5* and *HXT5* genes with the His-tag and a stop codon after that were cloned separately into the multiple cloning site (MCS) at *Nde*I of the CEN/pET21b(+) by CPEC. **C**) Confirming all the constructs created by CPEC. The constructs and the empty vector were digested with *Xho*I. The expected constructs will produce bands at 9.1 kb. The molecular weight marker used in this figure was NEB 1 kb+ DNA ladder (1st lane).

Also, we have recently cloned *TPO1* and *TPO3* in the plasmid pMS119EH using CPEC to create expression plasmid constructs listed in **Table 4.1**. This is a low copy number vector with the hybrid promoter *tac*I that regulates the expression of a protein with allolactose and IPTG induction (Fürste et al., 1986).

Table 4.1 All the constructs created with the circular polymerase extension cloning (CPEC) method are listed in the table below.

Construct code	Renamed as	Comments
TPO1r2/CEN/pET21b	TPO1_pET	TPO1 gene with the yeast replication origin CEN/ARS in vector pET21b(+)
TPO2r/CEN/pET21b	TPO2_pET	TPO2 gene with the yeast replication origin CEN/ARS in vector pET21b(+)
TPO3r/CEN/pET21b	TPO3_pET	TPO3 gene with the yeast replication origin CEN/ARS in vector pET21b(+)
TPO4r/CEN/pET21b	TPO4_pET	TPO4 gene with the yeast replication origin CEN/ARS in vector pET21b(+)
TPO5r/CEN/pET21b	TPO5_pET	TPO5 gene with the yeast replication origin CEN/ARS in vector pET21b(+)
HXT5r/CEN/pET21b	HXT5_pET	HXT5 gene with the yeast replication origin CEN/ARS in vector pET21b(+)
TPO1/pMS119EH	TPO1_pMS	TPO1 gene in vector pMS119EH
TPO3/pMS119EH	TPO3_pMS	TPO3 gene in vector pMS119EH

A)


6xHis
TPO1 or TPO3
M13_pUC_rev_primer
pBAD_rev_primer
pTrcHis_rev_primer
rrnB_terminator
rrnB_T1_terminator
rrnB_T2_terminator
tacI promoter
MCS copy
AmpR promoter
AmpR
lacIQ
pBR322_origin
pMS119EH
3917 bp
500
1000
1500
2000
2500
3000
3500

B)

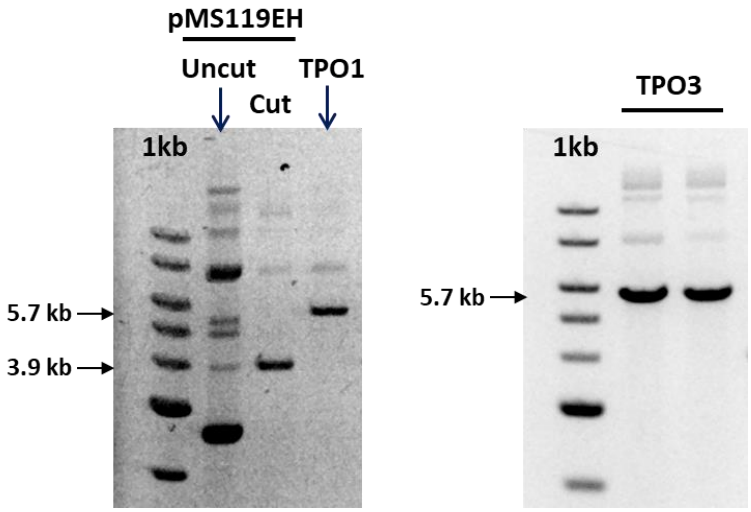


Figure 4.3 Cloning in the expression vector pMS119EH. A) The pMS119EH vector design. *TPO1* and *TPO3* were cloned into the MCS at the *EcoR*I site, with a His-tag coding sequence and a stop codon after that. **B) Confirmation of the constructs on an agarose gel.** The construct TPO1_pMS119EH was digested with *BamH*I (left panel), whereas the TPO3_pMS119EH (right panel) and the empty pMS119EH vector (left panel) were digested with *EcoR*I. The expected constructs will produce bands at ~5.7 kb. The molecular weight marker used in this figure was NEB 1 kb+ DNA ladder (1st lane).

All the constructs created in the pET21b(+) background were sequenced using Sanger sequencing services from The Centre for Applied Genomics (SickKids, Toronto, ON, Canada), and analyzed to ensure they contained the correct open reading frame. We checked for the correct ribosome binding site, start codon, His-tag sequence and stop codon for all the constructs. Forward and reverse sequencing primers for pET21b(+), PT7, and His-tag regions are listed in **Table 2.4**. The pMS119EH constructs will be sequenced in near future.

We also wanted to investigate the effect of *E. coli* N-terminal PelB signal sequence for periplasmic localization, and codon optimization on the expression of the genes, so that if the signal sequence is required, we could clone all prepared lab constructs into a *pelB* vector that encodes this signal sequence. We obtained a commercially cloned and *E. coli* codon-optimized *TPO1* with *E. coli* plasma membrane-targeted signal sequence, already cloned into a pET-22b(+) expression vector and the construct is denoted as 'Sc Tpo1 Opt_pET-22b(+)'.

4.2.2 Expression of Tpo proteins

4.2.2.1 Optimization of expression parameters

50% of therapeutic drugs target membrane proteins (MP), and the MPs are only 1% of total cellular proteins. Overexpression of the MPs is pivotal for their functional and structural characterization. Thus, selecting an appropriate overexpression system is critical and often time-consuming (Bernaudat et al., 2011). For example, the induction with IPTG may need to be carried out under different parameters such as temperature, media, induction time and different expression cell types. To determine the optimum temperature and IPTG concentration for gene expression, we grew different cell types having one of the following expression vectors pET21b(+), pET22b(+) and pMS119EH respectively. The parameters we have followed in this study are listed in **Table 4.2**.

Table 4.2 Summary of conditions tested for the expression of native and commercially codon-optimized proteins (*please refer to Appendix 2*).

Protein name	**Expression vector**	**Cell type (*E. coli*)**	**Antibiotic selections**	**Induction temperature (°C)**	**Induction time (Hours)**	**IPTG concentration**
Tpo1, Tpo2, Tpo3, Tpo4, Tpo5 and Hxt5_cons[#]	pET21b+	RIL[¥]	Tetracycline	16, 20, 30 and 37	0.5 to 24	100 pM to 0.5 mM
		SHuffle T7[@]	Ampicillin			
		C43				
Tpo1_opt[*] and Mdm10_opt*	pET22b+	RIL	Tetracycline			
		SHuffle T7	Ampicillin			
		C43				
Tpo1 and Tpo3	pMS119EH	C43	Ampicillin	20 and 37	24	5 µM to 5 mM

opt[*]= codon-optimized, **cons[#]**= constructs

RIL[¥]= *E. coli* BL21-CodonPlus™ (DE3)-RIL competent cell contains extra copies of the argU, ileY, and leuW tRNA genes (Agilent #230245), **SHuffle T7[@]**= *E. coli* K12 cells suitable for T7 protein expression with enhanced capacity to correctly fold proteins with multiple disulfide bonds (NEB-c3026).

We found that inducing expression in *E. coli* C43 from the 'Sc Tpo1 Opt_pET-22b(+)' with 0.5 mM IPTG likely was toxic for the cells because the cells grew very little following induction (**Fig. 4.4**). In contrast, overexpression of two other codon-optimized genes of yeast proteins, namely mitochondrial porins (voltage-dependent anion channels or VDAC) and mitochondrial division and morphology protein (Mdm10) in pET22b(+) didn't affect the cellular growth similar to cells expressing Tpo1.

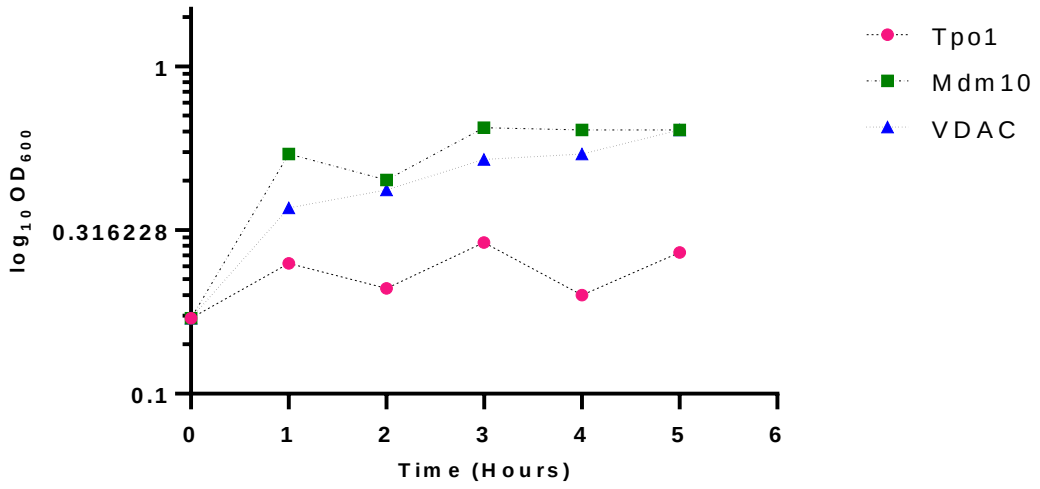


Figure 4.4 Comparison of growth of *E. coli* C43 expressing codon-optimized proteins from pET vectors. Cells were induced with 0.5 mM IPTG and incubated at 37 ºC for 5 hours. The VDAC, Mdm10 and Tpo1 genes were commercially cloned and codon-optimized for expression in *E. coli* from the pET22(+) vector.

The C41 (DE3) and C43 (DE3) strains have improved membrane protein overproduction characteristics (Miroux & Walker, 1996). The *E. coli* BL21 (DE3) mutants such as C41 (DE3) and C43 (DE3) have mutations in the *lacZ* promoter that drives the low-level expression of T7 RNA polymerase; thus there is a reduced rate of transcription of a gene cloned behind a T7 promoter, compared to the case where the T7 RNA polymerase is expressed from a wild-type *lacZ* (Miroux & Walker, 1996) and the synthesis of the toxic proteins is perhaps more tolerated (Wagner et al., 2008). The pMS119EH utilizes a strong P*tac* promoter (a hybrid of the *E. coli trp* and *lac* promoters). The expression of P*tac* is repressed by the LacI protein. The $lacI^q$ allele has a promoter mutation that increases the intracellular concentration of the LacI repressor, resulting in the strong repression of P*tac*. The addition of the inducer IPTG inactivates the LacI repressor. Thus, the amount of expression from P*tac* is proportional to the concentration of IPTG added: low concentrations of IPTG result in relatively low expression and high concentrations of IPTG result in high expression from P*tac*. By varying the IPTG concentration the amount of gene product cloned downstream from P*tac* can be varied over several orders of magnitude.

The high level of overexpression of Tpo1 might cause cellular toxicity. Therefore, *E. coli* C43 with a low copy number plasmid TPO1_pMS119EH was studied. IPTG was used at concentrations ranging from 5 μM to 5 mM, to generate different levels of protein expression and allow us to find a non-toxic level of expression. We saw optimum growth, compared to the empty vector control, at 5 μM IPTG, indicating that Tpo1 production might be occurring at low levels that are not toxic (**Fig. 4.5**). In contrast, C43/TPO1_pMS cells induced with 50, 500 μM or 5 mM IPTG showed the least growth in comparison to the control, indicating that toxic levels of the protein were produced.

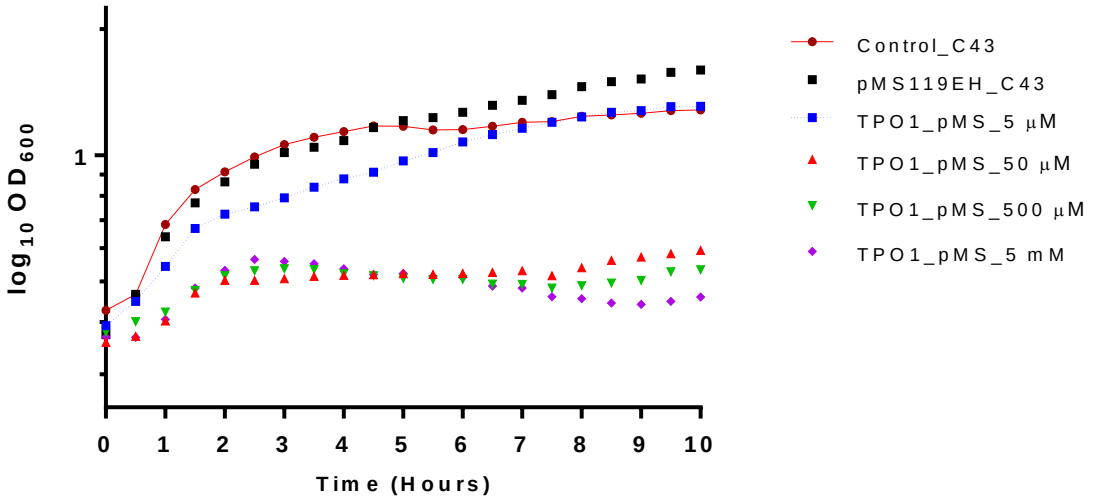


Figure 4.5 Determining the optimum concentration of IPTG for induction of *TPO1*. *E. coli* C43 carrying the TPO1_pMS119EH expression vector was induced at 0.6 OD with a range of IPTG concentrations from 5 µM to 5 mM. The control C43 cells were grown in the absence of IPTG. The cultures were grown in a 96-well plate at 37 ºC. Growth kinetics is shown by plotting the average OD of the 3 replicates against each time point in a semilogarithmic fashion.

4.2.2.2 Detection of the expressed protein

As an initial screening of protein expression, we attempted to extract the proteins via the His-tag. After this first step of confirming the presence of the proteins through Ni-NTA resin binding and SDS-PAGE, and subsequently, through western blot, confirmation of proteins' integration into the plasma membrane will be required (**Fig. 4.6**).

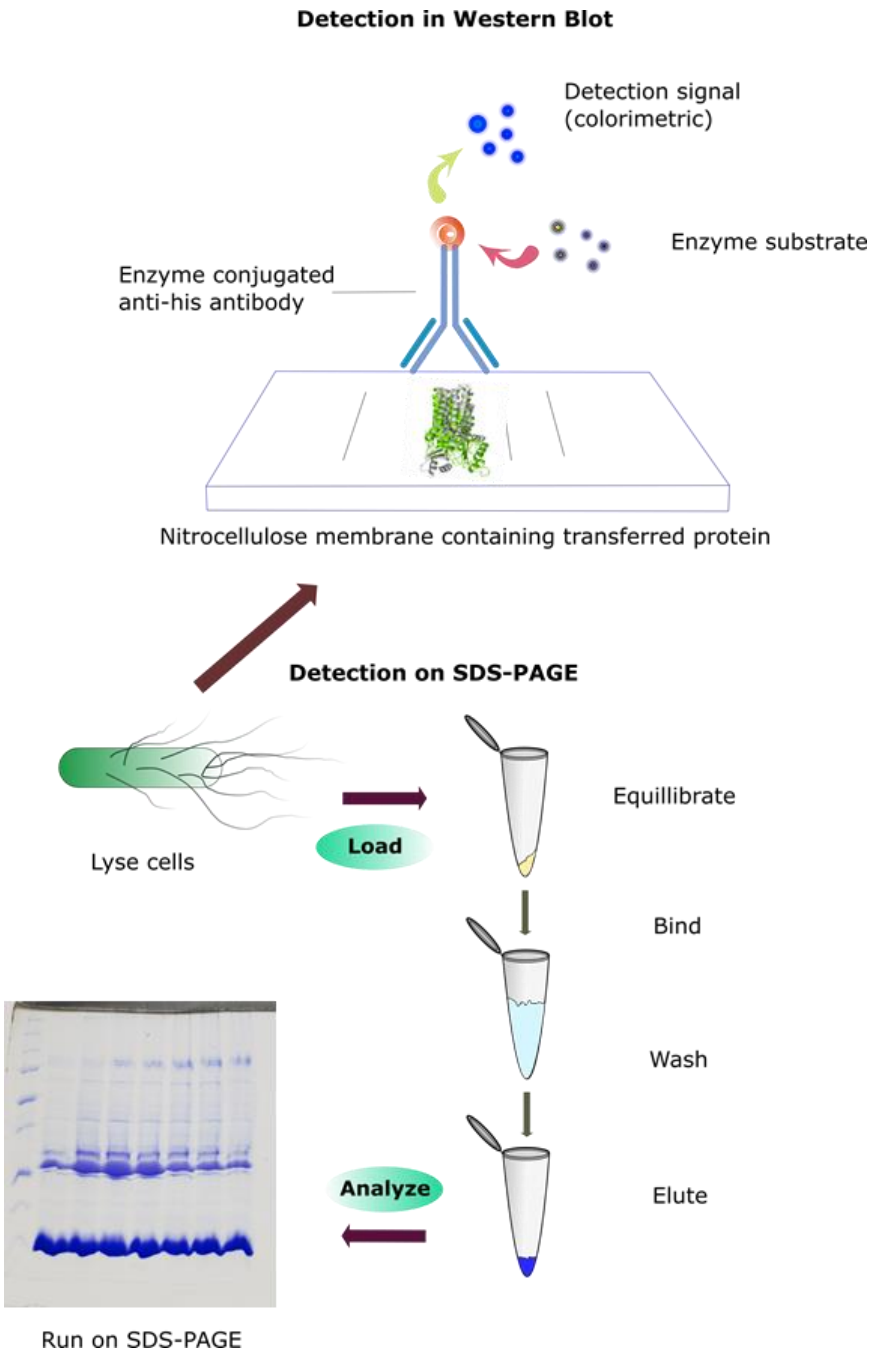


Fig. 4.6 Workflow for testing expression in *E. coli*. After the induction of the cells, a small cell pellet of ~75 µl is collected for protein extraction using Qiagen small-scale protein preparation protocol and lysed. The protein sample can be run on SDS-PAGE or directly taken for western

blot (WB) detection. For WB, an enzyme-linked anti-his antibody and substrates are used to detect the color on the blotting membrane for protein expression confirmation.

First, we looked for expression of the Tpo proteins from 'Sc Tpo1 Opt_pET-22b(+)', the commercially cloned and codon-optimized His-tagged Tpo1. Expression was induced with IPTG, the cells were lysed, and the resulting extract was mixed with Ni-NTA-agarose. Any bound proteins were eluted and analyzed by SDS-PAGE (**Fig. 4.7 (A)**). No additional bands were observed. Similarly, no differences were found between the IPTG-induced and uninduced fractions of Tpo1 and Tpo3 expressed from the pET21b or pMS119EH vectors (**Fig. 4.7 (B)**).

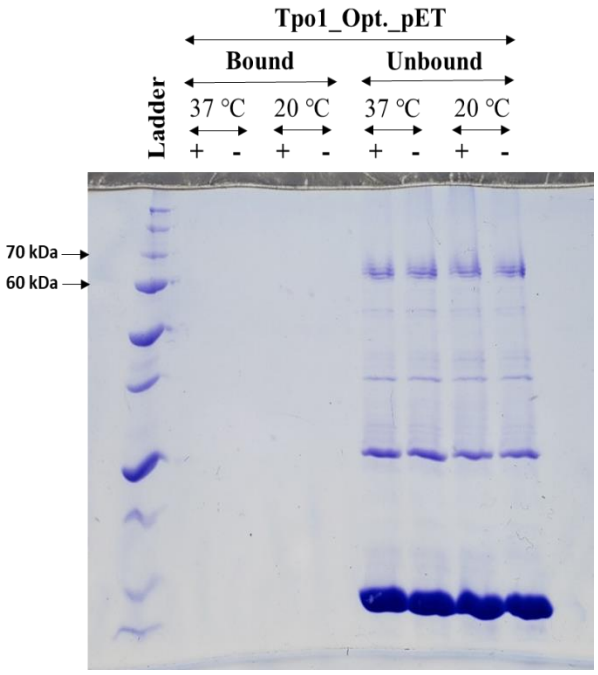
We predicted the formation of inclusion bodies (IB), which might hide the His-tag site of the Tpo proteins. The formation of IBs could be prevented by changing the promoter, host strain, and combinations thereof; controlling the growth conditions (especially the pH of the culture); adding non-metabolizable sugars such as sucrose and sorbitol to the fermentation medium, and changing the temperature of induction, usually by lowering it (Baneyx, 1999; Schein, 1989; Wetzel, 1992). Cold shock treatment might reduce the chance of IB formation described by (Qing et al., 2004) (see method **2.2.4**). We tried with the recommended induction temperatures between 16-25°C (**Table 4.2**) with a longer induction time up to 24 hours that should allow the cells to grow at a slower rate and help prevent protein aggregation.

As the Tpo1_opt was found to be toxic, we took precautions to reduce basal level induction from the pET-based vectors. To achieve a tighter control, we used an LB-modified medium with glycerol as a carbon source, as LB is a rich medium that contains tryptone or peptone that could have lactose in it (**section 2.2.4**). Moreover, we used an autoinduction medium named ZYM-5052

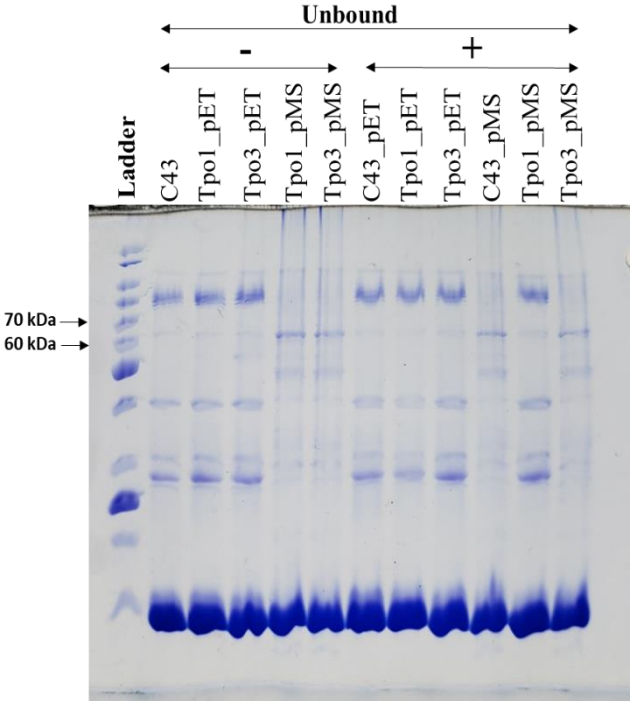
(Studier, 2005) containing three carbon sources as glucose, lactose and glycerol. The glucose amount present in the media is sufficient to boost the growth to a high density, whereas the lactose is present in a small amount and comes into play right after the exhaustion of glucose. It induces transcription, and the expression of the target protein precedes the next round of cell growth. Finally, glycerol extends the supply of carbon sources after induction. Autoinduction replaces the need for the addition of IPTG at the log phase (Studier, 2005). However, for all the lab constructs we could not see proteins in the bound fractions. For the unbound fraction there were bands in all the +/- IPTG columns, but no significant difference among them (data not shown). This suggests that the His-tag on Tpo1 might be hidden.

The Tpo proteins might have been expressed in amounts too low for detection on SDS-PAGE. Assuming that these proteins were in the *E. coli* membranes, an attempt was made to enrich for them by isolating membranes. The small-scale isolation of the membrane from *E. coli* was done following the protocol of Ma et al., 2013. However, bands of the expected sizes (64-73 kDa) for the Tpo proteins were not seen in the membrane fractions on the SDS-PAGE gels (**Fig. 4.7 (C)**). Attempts to detect Tpo proteins from the whole-cell lysed fraction (without Ni-NTA step) using an anti-his antibody in western blot were unsuccessful (data not shown).

A)


Tpo1_Opt._pET
Bound
Unbound
Ladder
37 °C
20 °C
37 °C
20 °C
+ - + - + - + -
70 kDa
60 kDa

B)


Unbound
-
+
Ladder
C43
Tpo1_pET
Tpo3_pET
Tpo1_pMS
Tpo3_pMS
C43_pET
Tpo1_pET
Tpo3_pET
C43_pMS
Tpo1_pMS
Tpo3_pMS
70 kDa
60 kDa

C)

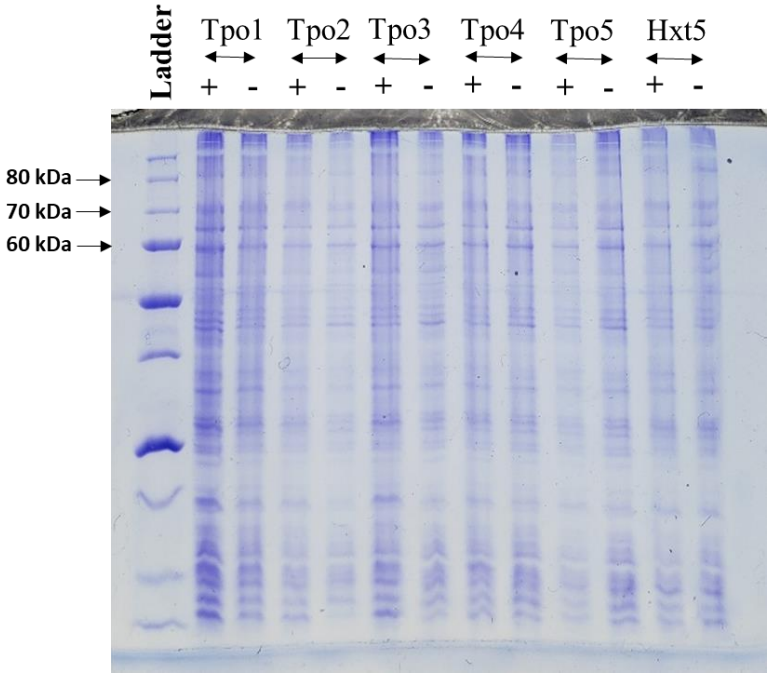

Ladder
Tpo1
Tpo2
Tpo3
Tpo4
Tpo5
Hxt5
+ - + - + - + - + - + -
80 kDa
70 kDa
60 kDa

Figure 4.7 SDS-PAGE analysis of proteins produced in induced and un-induced cells. A) Screening via purification on Ni-NTA. The C43 (DE3) *E. coli* cells with the optimized *TPO1* gene in the pET22b(+) plasmid were induced with 0.5 mM IPTG in LB at 37 and 20℃, respectively, for 30 mins. The protein preps were run through the Ni-NTA column to trap proteins with His-tags. The bound (elute of Ni-NTA) and unbound (Ni-NTA flow-through) fractions of the preps were run on SDS-PAGE gels to confirm the Tpo1 at 64.2 kDa size. **B)** The C43 cells carrying *TPO1* and *TPO3* genes in the pET21b(+) and pMS119EH background respectively, were induced with 5 µM IPTG in LB at 20℃ for 18 hours. The cell lysates were not run through the Ni-NTA column; rather these lysate fractions were run on SDS-PAGE gels directly after the lysis step. Tpo1 and Tpo3 are 64.2 and 68.06 kDa, respectively. **C) Screening by membrane purification.** The BL21-CodonPlus (DE3)-RIL_*E. coli* cells having *TPO1-5* and *HXT5* genes in pET21b(+) were induced with 0.5 mM IPTG in LB at 20℃ for 30 mins. The membrane preps were run on SDS-PAGE gels to confirm the proteins at the 64-73 kDa range. '+' and '-' indicate with and without IPTG, respectively.

4.2.3 Functional analysis of putative pumps

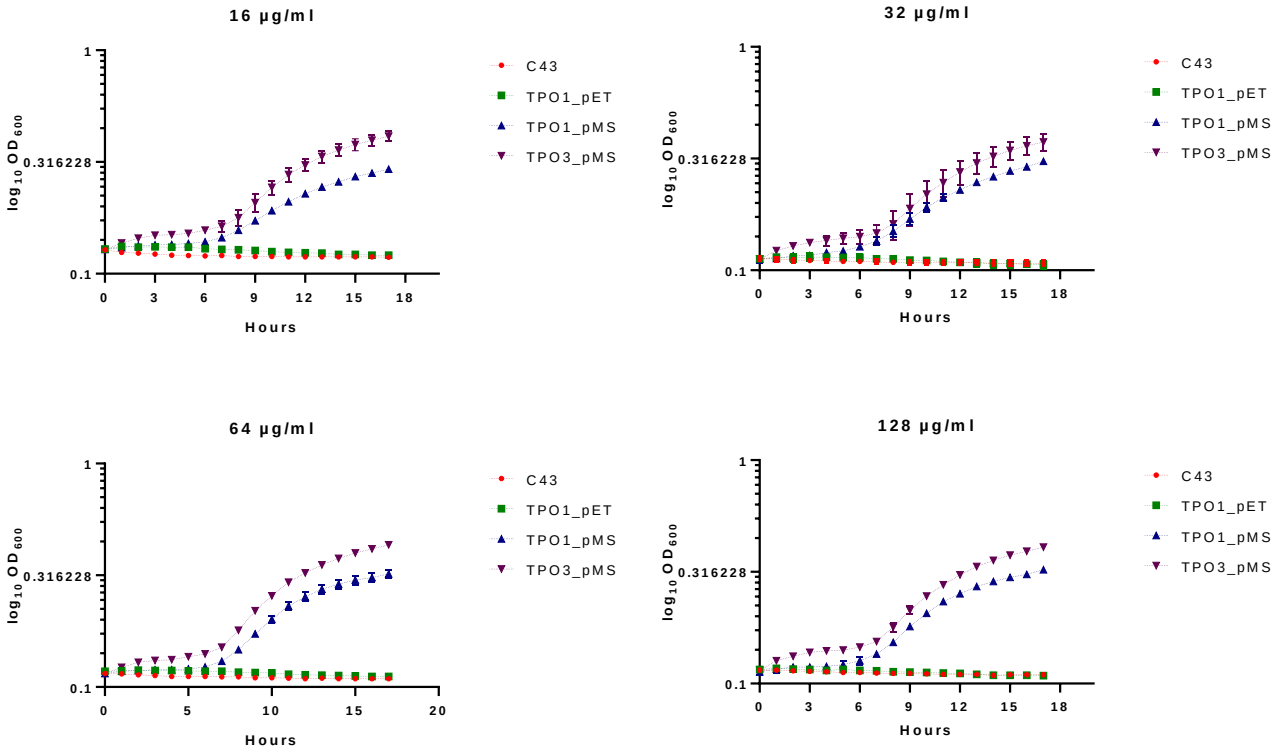
Although we were unable to detect the Tpo proteins on gels, it remained possible that a sufficient amount of these proteins was present in the cell membrane to affect antibiotic resistance. We set up the following experiments to determine the resistance of the Tpo expressing *E. coli* to several mitochondria-targeting antibiotics (**Table 1.3**).

4.2.3.1 Response to Chloramphenicol

We compared the resistance of the WT C43 cells with those of C43/TPO1_pET, C43/TPO1_pMS and C43/TPO3_pMS to CAP in terms of specific growth rate (μ) (OD minutes^{-1}) and kinetics, after IPTG induction. Untransformed C43 cells were sensitive to all concentrations of CAP tested. For all treatment groups, we found the induced C43/TPO1_pMS and C43/TPO3_pMS cells had an extended period of lag phase (around 7 hours) followed by a steady log phase (**Fig. 4.8 (A)**). On the other hand, the C43/TPO1_pET cells did not grow and maintained similar OD throughout the growth period. Among the treatment groups, the C43/TPO1_pMS and C43/TPO3_pMS cells demonstrated the highest final OD in the presence of 64 μg/ml CAP (**Fig. 4.8 (A)**).

The specific growth rate (μ) of C43 and C43/TPO1_pET was almost zero, whereas the C43/TPO1_pMS and C43/TPO3_pMS cells exhibited a significant higher growth rate (**Fig. 4.8 (B)**). Among them, C43/TPO3_pMS cells showed the highest growth rate (**Fig. 4.8 (B)**).

A)


16 µg/ml
32 µg/ml
64 µg/ml
128 µg/ml
log10 OD600
1
0.316228
0.1
Hours
C43
TPO1_pET
TPO1_pMS
TPO3_pMS

B)

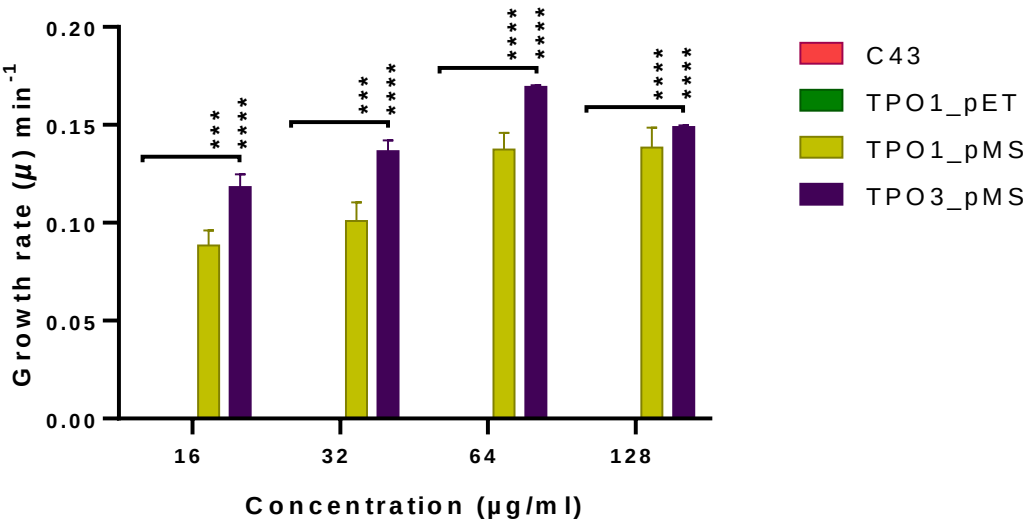

Growth rate (µ) min-1
0.20
0.15
0.10
0.05
0.00
16
32
64
128
Concentration (µg/ml)
***
****
C43
TPO1_pET
TPO1_pMS
TPO3_pMS

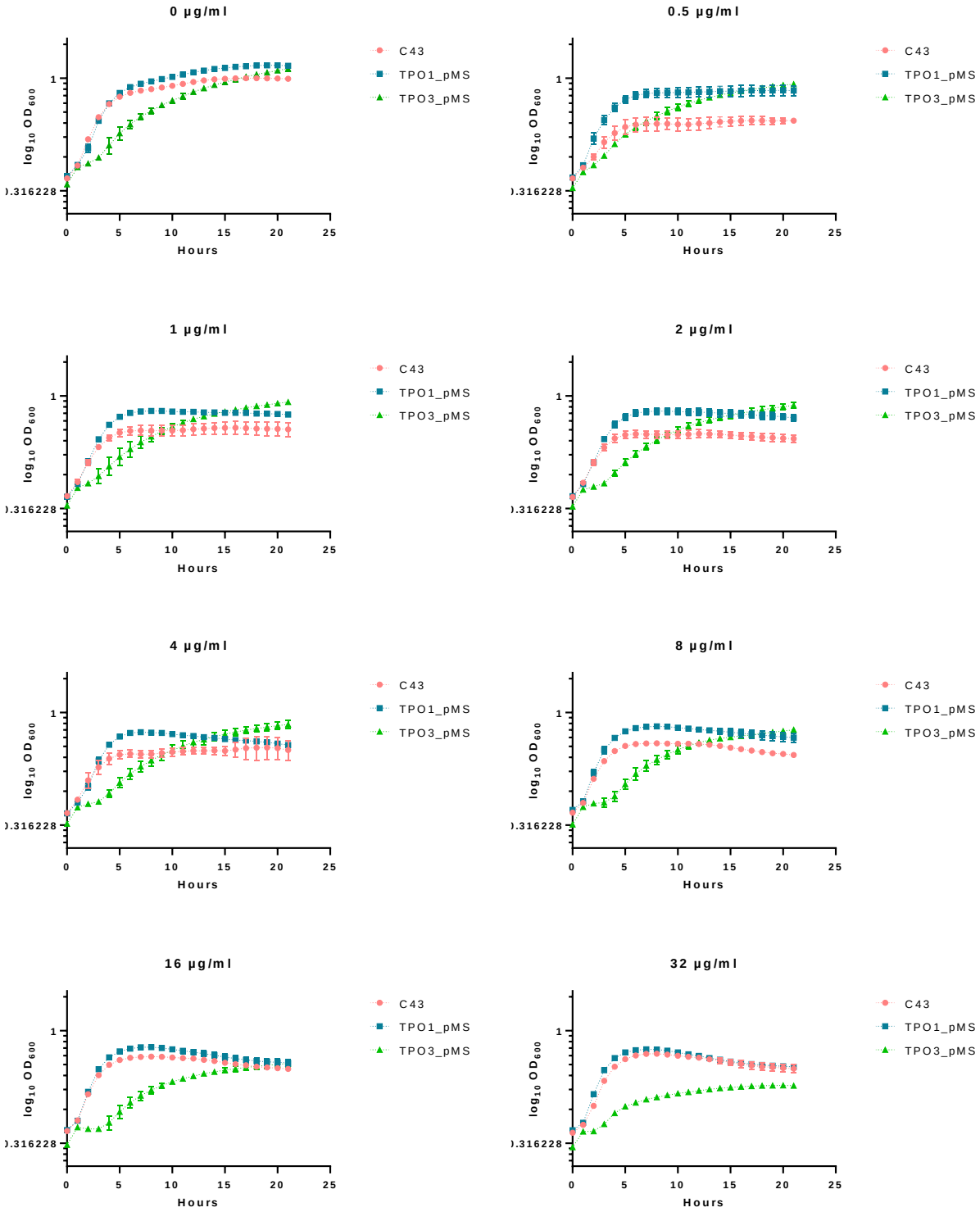
Figure 4.8 Growth of wild-type C43 and the Tpo1- or Tpo3-expressing strains in the presence of Chloramphenicol. Overnight cultures of strains were transferred to fresh LB+Ampicillin and grown to OD 0.3-0.4. 5 µM IPTG was added and induction occurred for about 60-80 mins. After the induction, the OD of the cultures was adjusted to be the same for the starting point. A volume of 200 µl culture of each of the four strains containing 16, 32, 64 and 128 µg/ml CAP, respectively, were added onto the 96-well plate. The ethanol volume was adjusted for all the groups to make the total volume equal. The cultures were grown for 18 hours at 37 ℃ with continuous shaking. The absorbance was recorded every 15 mins using an Epoch 2 plate reader at 600 nm wavelength. **A) Comparison of growth kinetics.** Growth kinetics is shown by plotting the average OD of the 3 replicates against each time point in a semilogarithmic fashion. The growth kinetics of each of the strains from each treatment group was compared to their respective WT using an XY graph. **B) Comparison of growth rates.** The specific growth rate (μ) was calculated using the change of OD over a specific time of the exponential phase of the semilogarithmic growth curve. The average slope of the 3 technical replicates of each of the strains from each treatment group was compared to their respective WT using one-way ANOVA at 95% CI to indicate statistical significance. *P < 0.05, **P < 0.01, ***P < 0.001, ****P < 0.0001. Means and standard deviations are shown. All the data were presented using GraphPad Prism 9.0.0 (121) (https://www.graphpad.com/scientific-software/prism/).

4.2.3.2 Response to Erythromycin

We compared the resistance of the WT C43 cells and those with plasmids, C43/TPO1_pMS and C43/TPO3_pMS to ERY in terms of specific growth rate (μ) (minutes^{-1}) and kinetics. Besides C43/TPO3_pMS, in the case of the control group (0 µg/ml), the C43/TPO1_pMS grew like C43 having a similar OD and phases of growth (**Fig. 4.9 (A)**). The C43 and C43/TPO1_pMS cells had a shorter period of rapid growth followed by a stationary phase, whereas the C43/TPO3_pMS cells had continuous slow growth (which is not exponential). Except for the 32 µg/ml group, in all the treatment groups even though the C43/TPO3_pMS cells demonstrated a longer lag phase with slower growth but reached a similar final OD compared to the C43 and C43/TPO1_pMS cells (**Fig. 4.9 (A)**). With 0.5 µg/ml erythromycin, the C43/TPO1_pMS cells showed the highest resistance difference compared to the C43 (**Fig. 4.9 (A)**).

We then investigated the specific growth rate (μ) of the strains in response to ERY. The C43/TPO1_pMS cells exhibited a significantly higher growth rate compared to C43 in each of the treatment groups, but not in the absence of antibiotics (**Fig. 4.9 (B)**). However, the C43/TPO3_pMS cells grew slowly compared to others under every condition. Among the treatment groups, C43/TPO1_pMS cells showed a higher growth rate compared to C43 at 4 µg/ml ERY (**Fig. 4.9 (B)**).

A)


0 µg/ml
0.5 µg/ml
1 µg/ml
2 µg/ml
4 µg/ml
8 µg/ml
16 µg/ml
32 µg/ml
C43
TPO1_pMS
TPO3_pMS
log10 OD600
Hours
0
5
10
15
20
25
1
0.316228

B)

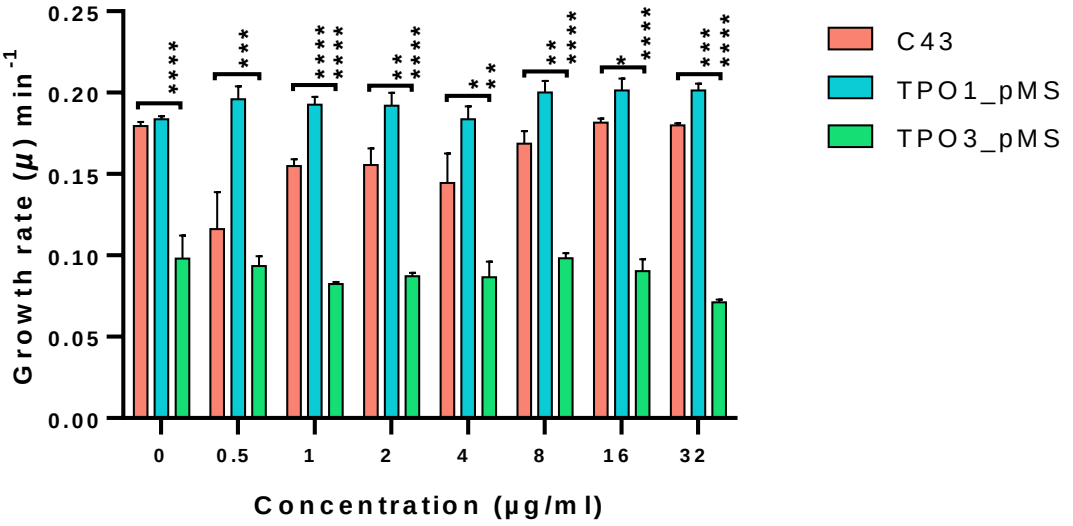


Figure 4.9 Growth of wild-type C43 and the Tpo1- or Tpo3-expressing strains in the presence of Erythromycin. Overnight cultures of strains were transferred to fresh LB+Ampicillin to let it grow up to OD 0.3-0.4. Added 5 µM IPTG and induced for about 60-80 mins. After the induction, the OD of the cultures was adjusted to be the same for the starting point. A volume of 200 µl culture of each of the five strains containing 0, 0.5, 1, 2, 4, 8, 16 and 32 µg/ml Ery, respectively, were added onto the 96-well plate. A volume of ethanol, equal to the volume of antibiotic added to the 32 µg/ml Ery group, was applied to the 0 µg/ml Ery group. The ethanol volume was adjusted for the other groups to make the total volume equal. The cultures were grown for 21-22 hours at 37 ℃ with continuous shaking. The absorbance was recorded every 15 mins using an Epoch 2 plate reader at 600 nm wavelength. **A) Comparison of growth kinetics.** Growth kinetics is shown by plotting the average OD of the 3 replicates against each time point in a semilogarithmic fashion. The growth kinetics of each of the mutants from each treatment group was compared to their respective WT using an XY graph. **B) Comparison of growth rates.** The specific growth rate (μ)

was calculated using the change of OD over a specific time of the exponential phase of the growth curve. The average slope of the 3 technical replicates of each of the mutants from each treatment group was compared to their respective WT using one-way ANOVA at 95% CI to indicate statistical significance. *$P < 0.05$, **$P < 0.01$, ***$P < 0.001$, ****$P < 0.0001$. Means and standard deviations are shown. All the data were presented using GraphPad Prism 9.0.0 (121) (https://www.graphpad.com/scientific-software/prism/).

4.2.4 EtBr accumulation assay using cloned *E. coli*

Unfortunately, the fold changes of bacterial sensitivity to drugs rarely correlate exactly with the results (growth rates, kinetics or any physiological change) obtained in experiments, which cannot determine efflux activity directly. So, it is hard to be confident that the differences in the drug sensitivities are due to efflux. Therefore, a direct way of assessing efflux activity such as EtBr accumulation assay in bacteria is necessary. This is a widely used functional assay for energy-dependent efflux pumps (Blair & Piddock, 2016).

We carried out the EtBr accumulation assay to obtain further evidence for the functionality of each of the expressed proteins. In this assay, cells first accumulate EtBr in the absence of glucose; this leads to an increase in EtBr fluorescence. Upon the addition of glucose, respiration can begin, generating a membrane potential, which should allow MSF pumps to be active. If this allows efflux of EtBr, the fluorescence should decrease. To confirm that the effect is related to the membrane potential, CCCP is added to dissipate the potential; at this point, EtBr should again accumulate in the cells and fluorescence should increase (M. Singh et al., 2020).

We have optimized the assay for C43 with different concentrations of glucose, EtBr and CCCP (data not shown). Moreover, to find the optimum concentration of CCCP causing better accumulation of EtBr by the cells expressing the constructs, we compared the effect of 5 and 40 µg/ml CCCP (**Fig. 4.10**). In both the experiments with 5 and 40 µg/ml CCCP, the C43 accumulated EtBr up to 250 relative fluorescence units (RFU). After energy generation using glucose, the C43 did not efflux EtBr; thus the RFU kept increasing slowly. Then after CCCP addition, the EtBr accumulation in C43 continued.

Our data shows that the C43/TPO1_pMS cells could not efflux EtBr, whereas the C43/TPO3_pMS cells could efflux EtBr compared to the C43 (**Fig. 4.10**). In both the experiments with 5 and 40 µg/ml CCCP, the C43/TPO3_pMS cells accumulated EtBr up to 300 RFU. After energy generation using glucose, the C43/TPO3_pMS cells could efflux EtBr; thus the relative fluorescence decreased up to 220 RFU. Then after CCCP addition, the EtBr accumulation in C43/TPO3_pMS cells continued. There is no significant difference in the fluorescence patterns between the IPTG-induced and uninduced TPO3_pMS constructs.

In all cases, after the addition of 5 µg/ml CCCP, the relative fluorescence reduced more, before starting to accumulate EtBr, compared to the addition of 40 µg/ml CCCP (**Fig. 4.10**). However, there is no difference in the final RFU of EtBr accumulation.

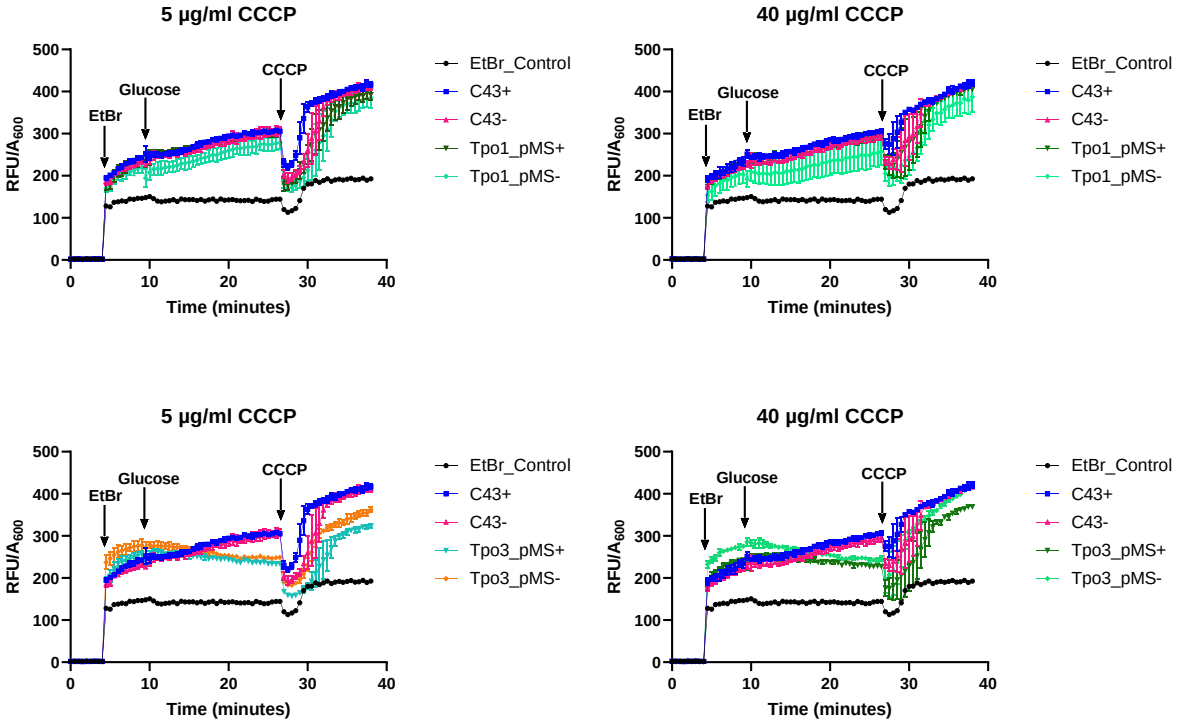


Fig. 4.10 Ethidium bromide accumulation assay of cells with pMS119EH-based constructs. Kinetics of ethidium bromide accumulation with time was measured and compared between IPTG-induced and uninduced C43, C43/TPO1_pMS and C43/TPO3_pMS cells. EtBr fluorescence was measured at excitation and emission wavelengths of 518 nm and 605 nm, respectively and normalized with cell density measured at 600 nm. The cells were induced with 5 µM IPTG for 3 hours. Glucose 0.4 %, EtBr 40 µg/ml, and CCCP 5 and 40 µg/ml have been used in this experiment; replicate experiments are shown. The EtBr control contains all the components except for cells. '+' and '-' indicate with and without IPTG induction, respectively.

4.3 Discussion

In this study, we analyzed the expression and functions of the polyamine transporters in *E. coli* expression hosts. At the beginning of cloning work, we tried restriction enzyme digestion and ligation of genes and pET21b(+) plasmid, and their subsequent amplification in *E. coli* DH5α following the Traditional Cloning Quick Guide | NEB. However, we failed to clone with this technique (data not shown). Then, we tried homologous recombination in yeast strain SC150 following the method of Chino et al., 2010. This procedure consists of co-transforming yeast cells with a mixture of the linear vector and PCR fragments, both having common flanking sequences. The idea was to develop a shuttle expression vector that can be used simultaneously for homologous recombination of the genes of interest in the SC150 and the expression in *E. coli*. We successfully developed the shuttle expression vector CEN/pET21b(+) but failed in subsequent cloning of the genes in this background (**Fig. 4.2 (A)**).

After failing we looked for alternative methods and had success with circular polymerase extension cloning (CPEC), the method of Quan & Tian, 2009. This is a simple cloning method that uses a one-step polymerase chain reaction (PCR) to assemble and clone multiple inserts with any vector *in-vitro* (**Fig. 4.1**). We cloned *TPO1-5* and *HXT5* into the shuttle expression vector CEN/pET21b(+) using CPEC (**Table 4.1**).

To study a eukaryotic protein in bacteria, it is essential to design the system such that it can produce as large an amount of protein as possible. One of the exogenous protein overproducing systems is the two-step expression vector-based system (Griffiths et al., 1999), where a copy of the bacteriophage T7 RNA polymerase is recombined into the *E. coli* chromosomal DNA under the control of strong *lac* promoter, and the gene of interest in the pET-based vector under the control

of late *lac* promoter (**Fig. 4.2**). This high copy vector pET21b(+) can provide a high level of expression of the genes of interest (*TPO1-5* and *HXT5*) with the lactose analog IPTG (isopropyl β-d-thiogalactoside) induction. First, the T7 RNA polymerase is synthesized which then transcribes the genes at a very high level at T7 promoter on the pET21b(+).

The ready manipulation, rapid growth and inexpensive culturing have advantaged the *E. coli* as the first choice of host for the initial screening of recombinant protein expression (Khow & Suntrarachun, 2012; Rosano & Ceccarelli, 2014). We started the expression studies with three commercially cloned and *E. coli* codon-optimized genes in pET22b(+), *VDAC_opt* and *Mdm10_opt* that were previously used in our lab, and *TPO1_opt* to investigate the effect of codon-optimization and the presence of plasma membrane targeting signal sequence *pelB* on expression. These genes were induced with 0.5-2 mM IPTG for 20 mins to 5 hours at 16 to 37 ºC in C43. Several other parameters were altered and are included in **Table 7.2** (**Appendix 2**).

As an initial screening of protein expression, we have performed the rapid screening of small-scale expression culture (a protocol by Qiagen) to determine whether a protein is expressed, as it allows protein with the His-tag expressed anywhere in the cell to be extracted. We found that VDAC_opt is expressed and bound to Ni-NTA using Qiagen protocol with urea buffers (**section 2.2.4**), whereas Mdm10_opt and Tpo1_opt were not found using this protocol (data not shown). However, the Mdm10_opt was found in the unbound fraction (not bound by the His-tag on the Ni-NTA) using Qiagen protocol with NPI buffers (**section 2.2.4**). On the other hand, Tpo1_opt was found to be toxic after 0.5 mM IPTG induction (**Fig. 4.4**), and the cells began dying after about one generation time, so there was no chance to observe the effect of codon optimization and signal sequence on the Tpo1_opt expression. However, we could determine the point of application of IPTG depending on the range of exponential phases found (**Fig. 4.4**). The VDAC and Mdm10 are

outer membrane proteins, whereas Tpo1 is the inner membrane protein (Vögtle et al., 2017). The overexpression of Tpo1 might upset the membrane potential, which is essential for cell survival. Too much might also prevent other essential proteins from utilizing the protein secretion system, which would also be fatal.

Several limitations of the *E. coli*-based host system could be the potential causes behind the toxicity of the Tpo1_opt. These include inclusion body formation, protein inactivity, and lack of post-translational modification. Recently, numerous host strains and vector types have been introduced to overcome these limitations (Khow & Suntrarachun, 2012; Mathieu et al., 2019). We adopted several modifications to overcome the toxicity of the expressed protein (**Table 4.3**).

Table 4.3 Strategies adopted in this study to address the toxicity of the Tpo proteins expression in *E. coli*

Possible reasons	**Strategies to resolve**
Protein may be toxic before the induction	Control basal level induction:
	• Controlling induction temperature (Cold shock up to 16℃ lower) and longer time (up to 24 hours)
	• Using defined media; LB modified media with glycerol as carbon source
	• Autoinduction media; ZYM 5052 with glucose, lactose, and glycerol as carbon source
Protein may be toxic after the induction	Control level of induction:
	• Low copy vector pMS119EH with tunable Ptac promoter
	• Using strain to improve protein stability; *E. coli* SHuffle T7
	• Using strain that is better for the expression of toxic proteins C43(DE3).

The frequency of codon usage and abundance of tRNA in a particular organism varies. In this study, the genes of interest are checked for the Codon Adaptation Index (CAI) (**Table 9.2**; **Appendix 4**) and found to have codons synonymous with the *E. coli* rare or very low abundant tRNAs. Thus it is crucial in expressing the genes in hosts that support an additional supply of tRNA to reduce codon-biases. Thus, we started the expression of *TPO1-5* and *HXT5* in CEN/pET21b(+) along with the codon-optimized *Mdm10_opt* and *TPO1_opt* using the *E. coli* BL21-CodonPlus (DE3)-RIL (J. S. Lewis et al., 2020). Moreover, we found the Tpos to have cysteine residues (**Table 9.3**; **Appendix 4**). So, we considered *E. coli* Shuffle T7 cells (Lobstein

et al., 2012) with an enhanced capacity to express and correctly fold Tpo proteins with multiple disulfide bonds. We found the Mdm10_opt in the Ni-NTA bound fraction using RIL cells with very low IPTG induction (100 pM to 50 μM) at 20 ℃ for 4 hours (data not shown). However, no signs of Tpo expressed from the lab constructs or Tpo1_opt with and without IPTG in the bound or unbound fraction were found on the SDS-PAGE (**Fig. 4.7 (A))**.

The small-scale isolation of the membrane from the *E. coli* was done following the protocol from (Ma et al., 2013). However, we did not find bands of the expected sizes for the Tpo proteins from the membrane fraction, on the SDS-PAGE gels (**Fig. 4.7 (C)**). Even after trying with all the above-mentioned parameters, we could not find the protein in the detectable range on the SDS-PAGE. Together, these data suggest that the expression of the optimized clones from a high-expression plasmid is toxic to cells. Thus, we considered a low copy vector pMS119EH and a host cell C43 to allow for reduced production. TPO1 and TPO3 were cloned into pMS119EH using the CPEC (**Fig. 4.3**). Furthermore, we could determine the optimum IPTG concentration as 5 μg/ml for the expression of TPO1_pMS in C43 (**Fig. 4.5**). This result reflects the fine-tuning of the IPTG induction. However, we still could not see on the SDS-PAGE (**Fig. 4.7 (B)**) and western blot (data not shown).

Even though we failed to detect the Tpo proteins, we performed functional studies of cells putatively expressing these proteins. We thought that the amount of protein produced inside the cells might not be sufficient for detection, but that it might be sufficient to generate a phenotype. The protein concentration might have reached a toxic level for the cells before reaching the threshold concentration of protein detection. Moreover, the fine-tuning of IPTG induction indicated that the reduced expression of the toxic protein was well tolerated by the cells, thus they grew slowly (**Fig. 4.5**).

According to the hypothesis, if the genes of interest encode efflux pumps, expression in *E. coli* might give bacteria antibiotic resistance. In this study, we demonstrated the effect of chloramphenicol (CAP) and erythromycin (ERY) on the growth of C43, C43/TPO1_pET, C43/TPO1_pMS and C43/TPO3_pMS using the 96-well plating technique, as these drugs inhibit bacterial protein synthesis (Lovmar et al., 2004; Schlünzen et al., 2001; Siibak et al., 2009; Tenson et al., 2003; Tu et al., 2005). When studying the efflux of antimicrobial substrates, it has been commonplace to use drug susceptibility measurements (such as the MIC) to reveal differences in drug efflux activity. We hypothesized that the low-level expression of an additional pump might cause a change in susceptibility to CAP and ERY than its WT counterpart.

We observed that the C43/TPO1_pMS and C43/TPO3_pMS cells are significantly resistant to CAP up to 128 µg/ml compared to the C43 or TPO1_pET that are sensitive (**Fig. 4.8 (B)**). However, the expression of efflux pumps is exhausting for the cells, thus, reducing growth and causes a fitness cost (Langevin & Dunlop, 2018; Siu et al., 2018). So, the extended lag phase of 7 hours could be the time, when cells were more involved in expressing the efflux pumps compared to cellular growth (**Fig. 4.8 (A)**). After reaching the threshold of producing enough pumps to tackle the CAP, the cells started accumulating biomass.

The C43/TPO3_pMS cells demonstrated slower growth rate compared to the C43 and C43/TPO1_pMS without ERY (0 µg/ml) (**Fig. 4.9 (A)**). It could be due to Tpo3 toxicity if the expression is leaky; this is suggested by the similar phenotypes in the presence and absence of IPTG. Thus, with increasing concentration of ERY, the C43/TPO3_pMS cells might have to tackle both the toxicity of Tpo3 and ERY, which results in the slower accumulation of biomass over a longer time (20 hours). However, we found the C43/TPO3_pMS cells more tolerant, considering the final OD reached, with increasing concentration of ERY (0.5-8 µg/ml) compared to C43 or

C43/TPO1_pMS (**Fig. 4.9 (A)**). In contrast, the C43/TPO1_pMS cells were the quickest responder, considering the very short/absent lag phase, to increasing concentration of ERY (**Fig. 4.9 (A)**). It could be due to the faster expression and integration of Tpo1 in the membrane.

For the EtBr accumulation assay, we hypothesized that 3 hours of induction with IPTG will produce enough Tpos without reaching the toxic level for the cells (**Fig. 4.5**). The assay needs physiologically active cells to demonstrate the efflux. In the assay, EtBr is introduced to the C43 *E. coli*, and it diffuses through the membrane to be preloaded for the efflux to start followed by the addition of glucose and CCCP. The difference in the efflux of EtBr between C43/TPO1_pMS and C43/TPO3_pMS could be because the C43/TPO1_pMS cells are likely unable to efflux of EtBr, as it reaches the stationary phase within the 3 hours of induction (**Fig. 4.9 (B)**). However, TPO3_pMS is active even after 15 hours of growth (**Fig. 4.9 (B)**) and thus could show the efflux of EtBr.

In summary, we have shown CAP and ERY may be potential substrates of Tpo1 and Tpo3 in indirect assays (antibiotic susceptibility assays). However, we were unable to establish these proteins as efflux pumps using a direct assay yet (EtBr accumulation assay).

CHAPTER 5

5.1 Conclusions

In this thesis work, two approaches were used to further the understanding of fungal mitochondrial membrane proteins as drug efflux pumps. These two complementary approaches produced data that led to the following conclusions:

1. *E. coli* YajR and *Homo sapiens* TETRAN could be the homologues to ScTpo1 (**Fig. 3.1**).
2. In spot plate assays, the ΔTPO3 strain has shown the highest sensitivity to all three antibiotics CAP, ERY and TET compared to other mutants (**Fig. 3.3-5**).
3. The effect of the mitochondria targeting antibiotics on the physiology of the deletion mutants is albeit due to the effect on the respiring mitochondria of the mutants growing in YPG media (**Fig. 3.6**).
4. In 96-well plating assays, the ΔTPO3 yeast strain has shown the highest sensitivity to CAP and TET compared to other mutants (**Fig. 3.7-3.8**).
5. The *N. crassa* mitochondria have shown efflux of EtBr (**Fig. 3.9 (C)**).
6. Inducing expression from the 'Sc Tpo1 Opt_pET-22b(+)' with 0.5 mM IPTG was found to be toxic for *E. coli* cells (**Fig. 4.4**).
7. In indirect assays (antibiotic susceptibility tests), the CAP and ERY are found to be potential substrates of Tpo1 and Tpo3 in *E. coli* (**Fig. 4.8-4.9**).

In this thesis, the development of a prokaryotic host system will provide a platform for the functional analysis of eukaryotic mitochondrial inner membrane proteins *in vitro*. Due to the difficulties in the study of these proteins, this work will function as a guide to making the accessible characterization of putative mitochondrial efflux pumps.

5.2 Future Directions

Considering the results obtained in this study, several experiments need to be addressed in future focusing on the following objectives to complete the story.

1. Further investigation of the physiology of the BY4741 deletion mutants
2. Improve the characterization of the Tpo proteins' functions.

We demonstrated the effect of CAP, TET and ERY on BY4741 WT and the deletion mutants ΔTPO1-4 through spot plating, however, could not demonstrate the effect of ERY through 96-well plating. We also need to investigate the effect of other fungicides and toxic chemicals on the deletion mutants. This might let us find novel substrates for Tpo1, Tpo2, Tpo3 and Tpo4.

We found that Tpo3 could be a putative CAP and TET efflux pump **(Fig. 3.7-3.8).** However, to confirm the statement we need to create double/triple deletion mutants of *TPO* genes. Such as creating double mutants of Tpo1 and Tpo3 to prove that they are the pumps responsible for CAP and TET efflux in mitochondria. In the case of single deletion, the effect of Tpo1 deletion might be diminished by the efflux by Tpo3 or vice versa.

Demonstration of ethidium bromide (EtBr) efflux from yeast mitochondria is pivotal for establishing the hypothesis that fungal mitochondria have drug efflux pumps. However, we could not establish the efflux of EtBr from yeast mitochondria due to the insufficient yield of mitochondria extraction. Thus, we need to continue improving yeast mitochondria extraction to perform a successful EtBr efflux assay.

Even though we could not see the Tpo proteins on the SDS-PAGE we performed the functional assays in *E. coli* expression strains. However, determination of expression at the transcript level

using qRT-PCR will bolster the results obtained in the functional studies. The qRT-PCR results will confirm the validity of the sequence and design our constructs.

The growth of wild-type *E. coli* C43 complemented with TPO1_pMS or TPO3_pMS has not been observed in the presence of TET in this study. Thus, it is important to investigate the sensitivity of the C43 expressing TPO1_pMS or TPO3_pMS, to TET and other mitochondria targeting drugs. Moreover, *E. coli* K12 and *E. coli* AG100TET strains will be used as positive controls according to (Martins et al., 2013), because of their previous well-characterized expression of efflux pumps system. These positive controls will validate the experiments.

EtBr accumulation assay with C43 expressing Tpo proteins is a direct way of assessing efflux activity. Even though we showed EtBr efflux from C43 expressing Tpo3, there was no obvious difference in efflux between the +/- IPTG samples. We need to continue and optimize the EtBr accumulation assay in future. So, this assay will allow us to establish Tpo proteins as efflux pumps.

5.3 Significance of this study

The functional analysis of the *S. cerevisiae* DHA transporters (Tpo proteins under investigation) will provide clues on the function of homologous transporters from pathogenic yeast and filamentous fungi.

Drug resistance in human cells is common, and studies showed drugs targeting the prokaryotes eventually might hamper mitochondria functions. Thus studies targeting the fungal mitochondrial drug efflux pumps might potentially find human orthologs of these pumps. This finding will help design chemotherapeutic drugs which would not harm human mitochondria (could be pumped out of the mitochondria) but will affect the prokaryotes.

6. Appendix 1: Supporting Information for Chapter 1

Table 6.1 The list of antifungal substrates of Tpo1

Name of herbicides	Group name	Mode of action	Change of physiology in yeast	Concentration used for optimum resistance	Solvent used to dissolve	Comments	Reference
Mancozeb	Dithiocarbamate	Able to inactivate sulfhydryl groups of amino acids of redox-sensitive proteins.	Affected oxidative stress, protein translation initiation and protein folding disassembling of protein aggregates and degradation of damaged proteins.	0.1 mM	1% dimethyl sulfoxide (DMSO)	Overexpression of Tpo1 in *Arabidopsis thaliana* to confer tolerance to Mancozeb	(Remy et al., 2017; Roede & Jones, 2014; Santos et al., 2009; Miguel Cacho Teixeira et al., 2008)
Mycophenolic acid	Morpholinoethyl ester prodrug	It is a potent and specific inhibitor of inosine 5 monophosphate (IMP) dehydrogenase, the first committed step of GMP synthesis.	Microscopic observation revealed inhibition of growth, increase in cell size and a multinucleate or puffy DNA content.	100 mg/l	1% dimethyl sulfoxide (DMSO) or dimethylformamide (DMF)	Overexpression of Tpo1in BY4742 results in increased resistance to MPA	(Desmoucelles et al., 2002)

Caspofungin	Echinocandins	It inhibits the synthesis of the fungal cell wall component beta-(1,3)-D-glucan.	Affects fungal cell wall integrity, inhibits cell wall synthesis and osmotic disruption of the fungal cell.	0.063 to 0.5 µg/ml for *S. cerevisiae*	1% dimethyl sulfoxide (DMSO) or dimethylformamide (DMF)		(Formosa et al., 2013; Markovich et al., 2004b; McCormack & Perry, 2005)
Azoles, polyenes, and allylamine/thiocarbamates	Azole based compounds	Inhibition of synthesis of or direct interaction with ergosterol; a predominant component of the fungal cell membrane.	The target of the azoles, the product of ERG11, is an essential component of the ergosterol biosynthetic pathway. The hyphal structure gets more affected than the yeast vegetative cells.	10 µg/ml as MIC for fluconazole	Organic solvents		(Ghannoum & Rice, 1999; Ha & White, 1999)
Amphotericin B and nystatin	Polyene	Act by binding to sterols in the plasma membrane, disrupting membrane function.	Induce programmed cell death (PCD) in *Saccharomyces cerevisiae.*	0.5 µM as the MIC for Amphotericin B	Methanol and dichloromethane, ethanol, and slightly soluble in water		(Ghannoum & Rice, 1999; Ha & White, 1999; Morton et al., 2007),

Table 6.2 The list of herbicide substrates of Tpo1

Name of herbicides	Group name	Mode of action	Change of physiology in yeast	Concentration used for optimum resistance	The solvent used to dissolve	Comments	Reference
2,4-dichlorophenoxyacetic acid (2,4-D)	Phenoxy herbicides and defoliants	Acts by mimicking the action of the plant growth hormone auxin, which results in uncontrolled growth and eventually death in susceptible plants.	Dissipation of the physiological H+-gradients across vacuolar and plasma membranes occurring under 2,4-D and oxidative stress.	Accumulation of radiolabeled [14C] 2,4-D with a final concentration of 7.5 μM	1% dimethyl sulfoxide (DMSO)	Overexpression of Tpo1 in *Arabidopsis thaliana* to confer tolerance, pH needs to be 3.5 of the media for the susceptibility assay.	(Remy et al., 2017; Miguel C. Teixeira et al., 2004; Miguel Cacho Teixeira & Sá-Correia, 2002; Viegas et al., 2005),
2-methyl-4-chlorophenoxyacetic acid (MCPA)	Phenoxy alkanoic acids	Auxin-like herbicide and may also lead to the acidification of the cell interior as the result of the dissociation.	Moderate toxicity led to a period of latency before the eventual resumption of inhibited growth.	1–1.5 mM	1% dimethyl sulfoxide (DMSO)		(Cabral et al., 2004; Miguel Cacho Teixeira & Sá-Correia, 2002)
Barban (4-chloro-2-butynyl (3-chlorophenyl) carbamate)	Carbamate	Herbicidal action is due to anti-mitotic effects, reducing plant cellular division and so retarding shoot growth (https://sitem.herts.ac.uk/aeru/ppdb/en/Reports/1108.htm)		>20 μM	Acetone	Tpo1p has been shown to confer yeast resistance to the herbicide Barban	(K. A. Lewis et al., 2016; Remy et al., 2017)

Alachlor (2-chloro-N-2,6-diethyl phenyl-N-methoxymethyl acetamide)	Aniline herbicide (chloroacetanilide)	Inhibition of lipid biosynthesis (e.g., very long fatty acid formation) in target plants and nontarget aquatic primary producers.	Decrease in the cellular iron content.	0.41 to 1.1 mM	0.2% DMSO		(Gil et al., 2017; Remy et al., 2017)
Metolachlor [2-chloro-N-(2-methoxy-1-methylethyl)-2′-ethyl-6′-methyl ac-etanilide]	Chloroacetanilide family	Inhibition of elongases and of the geranylgeranyl pyrophosphate (GGPP) cyclases, which are part of the gibberellin pathway (https://en.wikipedia.org/wiki/Metolachlor#cite_note-9).	Affects cell division and consequently yeast growth even in complete fermentative media (DOI:10.1023/A:1008943914292)	288 µg/mL	Acetone		(Remy et al., 2017; Sanyal & Kulshrestha, 2002)
Cycloheximide	Actidione	Blocks the elongation-factor-2-mediated translocation of peptidyl-tRNA from the A site to the P site on the 60s ribosomal subunit.	Inhibition of protein translation	50 nM to 50 µg/mL	1% dimethyl sulfoxide (DMSO)		(Dehoux et al., 1993; Do Valle Matta et al., 2001), (Fried & Warner, 1982; Schneider-Poetsch et al., 2010)
Quinidine	class I antiarrhythmic agent	Acts as a blocker of voltage-gated sodium channels.	Leads to slight global acidification of the cell interior and plasma membrane permeabilization with a consequent increase in the H+ influx rate.	3 mM	70% Ethanol	Extremely hazardous substance	(De Lera Ruiz & Kraus, 2015; Do Valle Matta et al., 2001; Nunes et al., 2001)

7. Appendix 2: Supporting Information for Chapter 2

Table 7.1 The composition of a modified LB medium (for 1 litre)

Components	**Amount**
Tryptone	12 g
Yeast Nitrogen Base	6.7 g
Glycerol	40 mL
Milli-Q water	Up to 1 L

*Adjust the pH to 7.5-8.0 with KOH.

Table 7.2 Parameters tested for protein expression in this study

No. of tests	Name of proteins	$Cell types	#Media used	1st incubation		2nd incubation in fresh media	IPTG induction			*Lysis buffer used	Comments
				Temp. (ºC)	Time (hours)	Temp. (ºC)	Conc. used	Temp. (ºC)	Time (hours)		
1	VDAC_Opt	C43	LB	37	O/N@	37	0.5 mM	37	4	Tris-Urea	VDAC was found with Ni-NTA fraction with urea buffers and Qiagen protocol. Mdm10 and Tpo1 could not be found in Ni-NTA bound/unbound fractions with urea buffer
	Mdm10_Opt	C43	LB	37	O/N	37	0.5 mM	37	4	Tris-Urea	
	Tpo1_Opt	C43	LB	37	O/N	37	0.5 mM	37	4	Tris-Urea	
2	VDAC_Opt	C43	LB	37	O/N	37	0.5 mM	37	4	NPI-10	Only Mdm10 in unbound fraction
	Mdm10_Opt	C43	LB	37	O/N	37	0.5 mM	37	4	NPI-10	
	Tpo1_Opt	C43	LB	37	O/N	37	0.5 mM	37	4	NPI-10	
3	VDAC_Opt	C43	LB	37	O/N	37	0.5 mM	37	4	GuHCl	Only VDAC in both +/- NaCl
	Mdm10_Opt	C43	LB	37	O/N	37	0.5 mM	37	4	GuHCl	
	Tpo1_Opt	C43	LB	37	O/N	37	0.5 mM	37	4	GuHCl	
4	Mdm10_Opt	RIL	LB	37	O/N	37	0.5 mM	20	4	NPI-10	No desired sized bands found
	Tpo1_Opt	RIL	LB	37	O/N	37	0.5 mM	20	4	NPI-10	
	Mdm10_Opt	T7	LB	37	O/N	37	0.5 mM	20	4	NPI-10	
	Tpo1_Opt	T7	LB	37	O/N	37	0.5 mM	20	4	NPI-10	
	Mdm10_Opt	RIL	LB	37	O/N	37	50 µM	20	4	NPI-10	
	Tpo1_Opt	RIL	LB	37	O/N	37	50 µM	20	4	NPI-10	

	Mdm10_Opt	T7	LB	37	O/N	37	50 µM	20	4	NPI-10	
	Tpo1_Opt	T7	LB	37	O/N	37	50 µM	20	4	NPI-10	
5	Tpo1_pET	RIL	LB	37	7	20	0.5 mM	16	24	NPI-10	For both IPTG conc. in bound fractions of all proteins, a similar-sized band is found
	Tpo2_pET	RIL	LB	37	7	20	0.5 mM	16	24	NPI-10	
	Tpo3_pET	RIL	LB	37	7	20	0.5 mM	16	24	NPI-10	
	Tpo4_pET	RIL	LB	37	7	20	0.5 mM	16	24	NPI-10	
	Tpo5_pET	RIL	LB	37	7	20	0.5 mM	16	24	NPI-10	
	Hxt5_pET	RIL	LB	37	7	20	0.5 mM	16	24	NPI-10	
	Tpo1_pET	RIL	LB	37	7	20	50 µM	16	24	NPI-10	
	Tpo2_pET	RIL	LB	37	7	20	50 µM	16	24	NPI-10	
	Tpo3_pET	RIL	LB	37	7	20	50 µM	16	24	NPI-10	
	Tpo4_pET	RIL	LB	37	7	20	50 µM	16	24	NPI-10	
	Tpo5_pET	RIL	LB	37	7	20	50 µM	16	24	NPI-10	
	Hxt5_pET	RIL	LB	37	7	20	50 µM	16	24	NPI-10	
6	VDAC_Opt	RIL	LB	37	O/N	25	0.5 mM	20	17	NPI-10	VDAC not found with Ni-NTA bound or unbound fractions
	VDAC_Opt	RIL	LB	37	O/N	25	50 µM	20	17	NPI-10	
	VDAC_Opt	T7	LB	37	O/N	25	0.5 mM	20	17	NPI-10	
	VDAC_Opt	T7	LB	37	O/N	25	50 µM	20	17	NPI-10	
7	RIL WT cells	RIL	LB	37	O/N	16	0.5 mM	16	24	NPI-10	No distinct difference in +/- IPTG fractions
	RIL WT cells	RIL	LB	37	O/N	16	0	16	24	NPI-10	
	Tpo1_pET	RIL	LB	37	O/N	16	0.5 mM	16	24	NPI-10	
	Tpo1_pET	RIL	LB	37	O/N	16	0	16	24	NPI-10	
	Tpo3_pET	RIL	LB	37	O/N	16	0.5 mM	16	24	NPI-10	
	Tpo3_pET	RIL	LB	37	O/N	16	0	16	24	NPI-10	
	Mdm10_Opt	RIL	LB	37	O/N	16	0.5 mM	16	24	NPI-10	
	Mdm10_Opt	RIL	LB	37	O/N	16	0	16	24	NPI-10	
	Mdm10_Opt	T7	LB	37	O/N	16	0.5 mM	16	24	NPI-10	

	Mdm10_Opt	T7	LB	37	O/N	16	0	16	24	NPI-10	
8	Tpo1_pET	RIL	LB	37	O/N	20	0.5 mM	16	24	NPI-10	No bands on the Ni-NTA bound fractions
	Tpo1_pET	RIL	LB	37	O/N	20	0	16	24	NPI-10	
	Tpo3_pET	RIL	LB	37	O/N	20	0.5 mM	16	24	NPI-10	
	Tpo3_pET	RIL	LB	37	O/N	20	0	16	24	NPI-10	
9	Tpo1_pET	RIL	LB	37	O/N	20	0	16	4	NPI-10	No distinct bands were found on bound fractions of the +IPTG, but 4 bands on all +/- IPTG. *E. coli* native proteins with high histidine might be bound to the Ni-NTA. **Mdm10** bands found on the bound fractions with all four +IPTG conc. compared to -IPTG
	Tpo1_pET	RIL	LB	37	O/N	20	50 µM	16	4	NPI-10	
	Tpo1_pET	RIL	LB	37	O/N	20	25 µM	16	4	NPI-10	
	Tpo1_pET	RIL	LB	37	O/N	20	1 µM	16	4	NPI-10	
	Tpo1_pET	RIL	LB	37	O/N	20	100 pM	16	4	NPI-10	
	Tpo3_pET	RIL	LB	37	O/N	20	0	16	4	NPI-10	
	Tpo3_pET	RIL	LB	37	O/N	20	50 µM	16	4	NPI-10	
	Tpo3_pET	RIL	LB	37	O/N	20	25 µM	16	4	NPI-10	
	Tpo3_pET	RIL	LB	37	O/N	20	1 µM	16	4	NPI-10	
	Tpo3_pET	RIL	LB	37	O/N	20	100 pM	16	4	NPI-10	
	Mdm10_Opt	RIL	LB	37	O/N	20	0	16	4	NPI-10	
	Mdm10_Opt	RIL	LB	37	O/N	20	50 µM	16	4	NPI-10	
	Mdm10_Opt	RIL	LB	37	O/N	20	25 µM	16	4	NPI-10	
	Mdm10_Opt	RIL	LB	37	O/N	20	1 µM	16	4	NPI-10	
	Mdm10_Opt	RIL	LB	37	O/N	20	100 pM	16	4	NPI-10	
10	Tpo1_pET	RIL	LB	37	O/N	20	0.5 mM	20	1	NPI-10	No bands were found on the bound fractions of both the +/- IPTG cells
	Tpo1_pET	RIL	LB	37	O/N	20	0	20	1	NPI-10	
	Tpo3_pET	RIL	LB	37	O/N	20	0.5 mM	20	1	NPI-10	
	Tpo3_pET	RIL	LB	37	O/N	20	0	20	1	NPI-10	
	Hxt5_pET	RIL	LB	37	O/N	20	0.5 mM	20	1	NPI-10	
	Hxt5_pET	RIL	LB	37	O/N	20	0	20	1	NPI-10	

11	Tpo1_pET	RIL	LB	37	6	20	25 µM	16	1	NPI-10	Only with TPO1 bands were found. But they were present in both the +/- IPTG RIL and C43 cells
	Tpo1_pET	RIL	LB	37	6	20	0	16	1	NPI-10	
	Tpo3_pET	RIL	LB	37	6	20	25 µM	16	1	NPI-10	
	Tpo3_pET	RIL	LB	37	6	20	0	16	1	NPI-10	
	Hxt5_pET	RIL	LB	37	6	20	25 µM	16	1	NPI-10	
	Hxt5_pET	RIL	LB	37	6	20	0	16	1	NPI-10	
	Tpo1_Opt	C43	LB	37	6	20	25 µM	16	1	NPI-10	
	Tpo1_Opt	C43	LB	37	6	20	0	16	1	NPI-10	
¥12	Tpo1_pET	RIL	LB	37	O/N	37	0.5 mM	16	1	Sucrose-lysozyme	Very nice membrane prep. But there is no difference in band patterns between +/- IPTG
	Tpo1_pET	RIL	LB	37	O/N	37	0	16	1	Sucrose-lysozyme	
	Tpo3_pET	RIL	LB	37	O/N	37	0.5 mM	16	1	Sucrose-lysozyme	
	Tpo3_pET	RIL	LB	37	O/N	37	0	16	1	Sucrose-lysozyme	
13	Tpo1_pET	RIL	LB	37	O/N	37	0.5 mM	16	0.75	NPI-10	All clear in the bound fractions. For the sup fraction there were bands in all the +/- IPTG columns, but no significant difference. This indicates TPO's his-tag might be hidden in the membrane.
	Tpo1_pET	RIL	LB	37	O/N	37	0	16	0.75	NPI-10	
	Tpo2_pET	RIL	LB	37	O/N	37	0.5 mM	16	0.75	NPI-10	
	Tpo2_pET	RIL	LB	37	O/N	37	0	16	0.75	NPI-10	
	Tpo3_pET	RIL	LB	37	O/N	37	0.5 mM	16	0.75	NPI-10	
	Tpo3_pET	RIL	LB	37	O/N	37	0	16	0.75	NPI-10	
	Tpo4_pET	RIL	LB	37	O/N	37	0.5 mM	16	0.75	NPI-10	
	Tpo4_pET	RIL	LB	37	O/N	37	0	16	0.75	NPI-10	
	Tpo5_pET	RIL	LB	37	O/N	37	0.5 mM	16	0.75	NPI-10	
	Tpo5_pET	RIL	LB	37	O/N	37	0	16	0.75	NPI-10	
	Hxt5_pET	RIL	LB	37	O/N	37	0.5 mM	16	0.75	NPI-10	
	Hxt5_pET	RIL	LB	37	O/N	37	0	16	0.75	NPI-10	
¥14	Tpo1_pET	RIL	LB	37	O/N	37	0.5 mM	20	0.5	Sucrose-lysozyme	Very nice band patterns, the prep is good. But, there is no difference in band patterns between +/- IPTG.
	Tpo1_pET	RIL	LB	37	O/N	37	0	20	0.5	Sucrose-lysozyme	
	Tpo2_pET	RIL	LB	37	O/N	37	0.5 mM	20	0.5	Sucrose-lysozyme	
	Tpo2_pET	RIL	LB	37	O/N	37	0	20	0.5	Sucrose-lysozyme	

	Tpo3_pET	RIL	LB	37	O/N	37	0.5 mM	20	0.5	Sucrose-lysozyme	
	Tpo3_pET	RIL	LB	37	O/N	37	0	20	0.5	Sucrose-lysozyme	
	Tpo4_pET	RIL	LB	37	O/N	37	0.5 mM	20	0.5	Sucrose-lysozyme	
	Tpo4_pET	RIL	LB	37	O/N	37	0	20	0.5	Sucrose-lysozyme	
	Tpo5_pET	RIL	LB	37	O/N	37	0.5 mM	20	0.5	Sucrose-lysozyme	
	Tpo5_pET	RIL	LB	37	O/N	37	0	20	0.5	Sucrose-lysozyme	
	Hxt5_pET	RIL	LB	37	O/N	37	0.5 mM	20	0.5	Sucrose-lysozyme	
	Hxt5_pET	RIL	LB	37	O/N	37	0	20	0.5	Sucrose-lysozyme	
15	Tpo1_Opt	C43	LB	37	O/N	37	0.5 mM	37	0.5	NPI-10	All clear in the bound fractions. For the sup fraction there were bands in all the +/- IPTG columns, but no significant difference. This indicates TPO's his-tag might be hidden in the membrane.
	Tpo1_Opt	C43	LB	37	O/N	37	0	37	0.5	NPI-10	
	Tpo1_Opt	C43	LB	37	O/N	37	0.5 mM	20	0.5	NPI-10	
	Tpo1_Opt	C43	LB	37	O/N	37	0	20	0.5	NPI-10	
¥16	Tpo1_Opt	C43	LB	37	O/N	37	0.5 mM	37	0.5	Sucrose-lysozyme	There was no difference. All the wells were smeary, maybe C43 doesn't provide good membrane prep
	Tpo1_Opt	C43	LB	37	O/N	37	0	37	0.5	Sucrose-lysozyme	
	Tpo1_Opt	C43	LB	37	O/N	37	0.5 mM	20	0.5	Sucrose-lysozyme	
	Tpo1_Opt	C43	LB	37	O/N	37	0	20	0.5	Sucrose-lysozyme	
17	Tpo1_Opt	C43	LB modified	37	O/N	37	25 µM	20	1	NPI-10	All clear in the bound fractions. For the sup fraction there were bands but no difference in band patterns between the +/- IPTG columns.
	Tpo1_Opt	C43	LB modified	37	O/N	37	0	20	1	NPI-10	
18	Tpo1_pET	C43	TB	37	O/N	37	0.5 mM	37	0.5	NPI-10	All clear in the bound fractions. For the sup fraction there were more bands than before, in all the +/-
	Tpo1_pET	C43	TB	37	O/N	37	0	37	0.5	NPI-10	
	Tpo2_pET	C43	TB	37	O/N	37	0.5 mM	37	0.5	NPI-10	
	Tpo2_pET	C43	TB	37	O/N	37	0	37	0.5	NPI-10	

	Tpo3_pET	C43	TB	37	O/N	37	0.5 mM	37	0.5	NPI-10	IPTG columns, but no significant difference between them.
	Tpo3_pET	C43	TB	37	O/N	37	0	37	0.5	NPI-10	
¥19	Tpo1_pET	C43	TB	37	O/N	37	0.5 mM	37	0.5	Sucrose-lysozyme	There was no difference. All the wells were smeary, maybe C43 doesn't provide good membrane prep. Moreover, the buffers were old. Need to try another membrane prep with C43 and a new buffer.
	Tpo1_pET	C43	TB	37	O/N	37	0	37	0.5	Sucrose-lysozyme	
	Tpo2_pET	C43	TB	37	O/N	37	0.5 mM	37	0.5	Sucrose-lysozyme	
	Tpo2_pET	C43	TB	37	O/N	37	0	37	0.5	Sucrose-lysozyme	
	Tpo3_pET	C43	TB	37	O/N	37	0.5 mM	37	0.5	Sucrose-lysozyme	
	Tpo3_pET	C43	TB	37	O/N	37	0	37	0.5	Sucrose-lysozyme	
20	Tpo1_Opt	C43	ZYM-5052	37	O/N	37	0	37	15	NPI-10	
	Tpo1_pET	C43	ZYM-5052	37	O/N	37	0	37	15	NPI-10	Ni-NTA bound fraction (after the binding step and final elution)
	Tpo2_pET	C43	ZYM-5052	37	O/N	37	0	37	15	NPI-10	
	Tpo3_pET	C43	ZYM-5052	37	O/N	37	0	37	15	NPI-10	No desired size band found
	Tpo4_pET	C43	ZYM-5052	37	O/N	37	0	37	15	NPI-10	
	Tpo5_pET	C43	ZYM-5052	37	O/N	37	0	37	15	NPI-10	The supernatant (from the binding step that remains from Ni-NTA)
	Hxt5_pET	C43	ZYM-5052	37	O/N	37	0	37	15	NPI-10	
¥21	Tpo1_Opt	C43	ZYM-5052	37	O/N	37	0	37	15	Sucrose-lysozyme	Membrane prep showed smeary bands, decided to treat the prep with DNase and RNase
	Tpo1_pET	C43	ZYM-5052	37	O/N	37	0	37	15	Sucrose-lysozyme	
	Tpo2_pET	C43	ZYM-5052	37	O/N	37	0	37	15	Sucrose-lysozyme	

	Tpo3_pET	C43	ZYM-5052	37	O/N	37	0	37	15	Sucrose-lysozyme	
	Tpo4_pET	C43	ZYM-5052	37	O/N	37	0	37	15	Sucrose-lysozyme	
	Tpo5_pET	C43	ZYM-5052	37	O/N	37	0	37	15	Sucrose-lysozyme	
	Hxt5_pET	C43	ZYM-5052	37	O/N	37	0	37	15	Sucrose-lysozyme	
22	pMS	C43	LB	37	O/N	37	5 mM	37	24	NPI-10	No bands in bound fractions, but nice bands in unbound fractions. However, no difference in band patterns between +/- IPTG columns.
	pMS	C43	LB	37	O/N	37	0	37	24	NPI-10	
	Tpo1_pMS	C43	LB	37	O/N	37	5 mM	37	24	NPI-10	
	Tpo1_pMS	C43	LB	37	O/N	37	0	37	24	NPI-10	
23	C43	C43	LB	37	O/N	37	0	20	24	NPI-10	All clear in the bound fractions. For the sup fraction there were more bands than before, in all the +/- IPTG columns, but no significant difference between them.
	pET21b+	C43	LB	37	O/N	37	0	20	24	NPI-10	
	Tpo1_pET	C43	LB	37	O/N	37	0	20	24	NPI-10	
	Tpo1_pET	C43	LB	37	O/N	37	5 µM	20	24	NPI-10	
	Tpo3_pET	C43	LB	37	O/N	37	0	20	24	NPI-10	
	Tpo3_pET	C43	LB	37	O/N	37	5 µM	20	24	NPI-10	
	pMS119EH	C43	LB	37	O/N	37	0	20	24	NPI-10	
	Tpo1_pMS	C43	LB	37	O/N	37	0	20	24	NPI-10	
	Tpo1_pMS	C43	LB	37	O/N	37	5 µM	20	24	NPI-10	
	Tpo3_pMS	C43	LB	37	O/N	37	0	20	24	NPI-10	
	Tpo3 _pMS	C43	LB	37	O/N	37	5 µM	20	24	NPI-10	
	VDAC	C43	LB	37	O/N	37	0	20	24	NPI-10	
	VDAC	C43	LB	37	O/N	37	5 µM	20	24	NPI-10	

***Lysis buffers: NPI-10 =** 50 mM NaH_2PO_4, 300 mM NaCl and 10 mM Imidazole. **Tris-Urea** = 5M Urea, 0.05M Tris HCl, 2% SDS and 1% 2-mercaptoethnol. **GuHCl** (Guanidine hydrochloride) = 6 M GuHCl; 0.1 M NaH_2PO_4; 0.01 M Tris·Cl; pH 8.0. **Sucrose-lysozyme = i)** 0.2M Tris-HCl + 1M Sucrose + 1mM EDTA, ph 8.0, **ii)** 10 mg/ml Lysozyme. **[¥]Membrane preparations**. Tests 1, 2 and 3 are done by **Kelsey Weshnoweski.**

[$]Cell types: RIL = *E. coli* BL21-CodonPlus™ (DE3)-RIL, **SHuffle T7 =** *E. coli* K12 cells, **C43** = OverExpress™ *E. coli* C43(DE3).

[#]Media used: LB = Lysogeny broth, TB = Terrific broth, ZYM-5052 = Autoinduction media. **O/N[@]** = Over night (around 18 hours).

8. Appendix 3: Supporting Information for Chapter 3

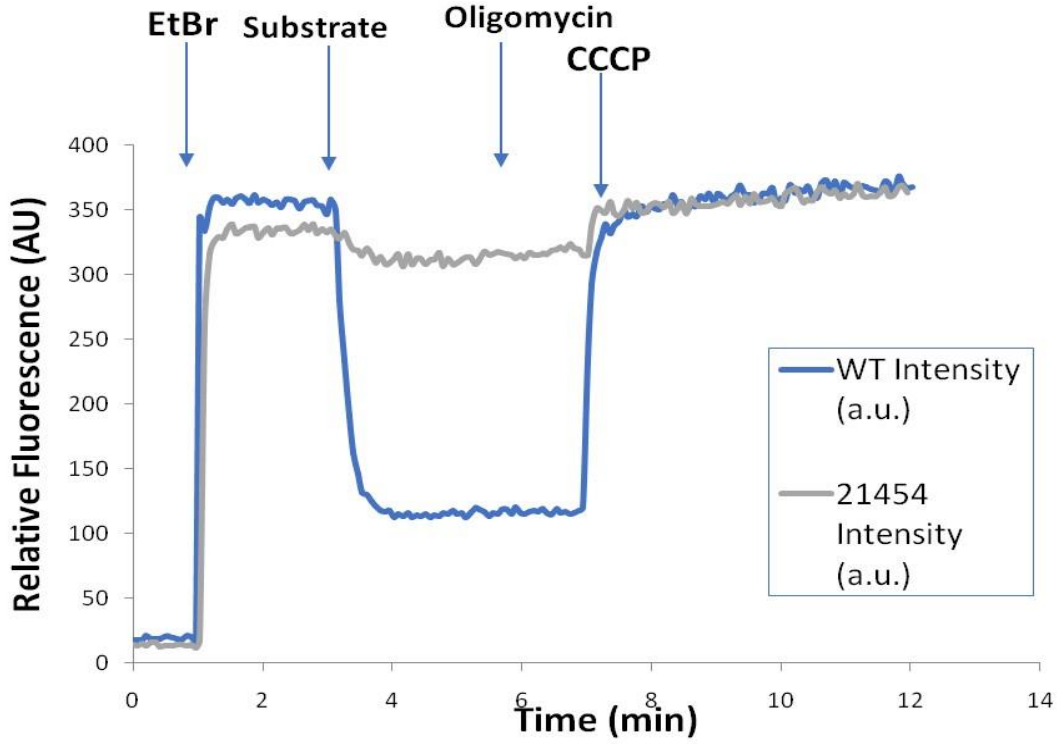


Figure 8.1: EtBr fluorescence in the presence and absence of membrane potential in *N. crassa* mitochondria. Two strains were analyzed, the WT (FGSC 9718) and a mutant strain that doesn't express a protein with homology to ABC proteins (Scp1). EtBr was added to isolated mitochondria and after 2 min, EtBr was added. Substrate (Glutamate/Malate/Succinate) was added to induce a membrane potential, and after 6 minutes, oligomycin was added to block ATP synthesis, and then CCCP was added to dissipate the potential. Deletion mutant (21454) didn't show EtBr efflux, whereas the WT showed efflux only when membrane potential ($\Delta\Psi_m$) was created by succinate. The putative MFS pumps under consideration are Drug/H+ antiporters, not ABC transporters.

*Courtesy of *A. McLoughlin*

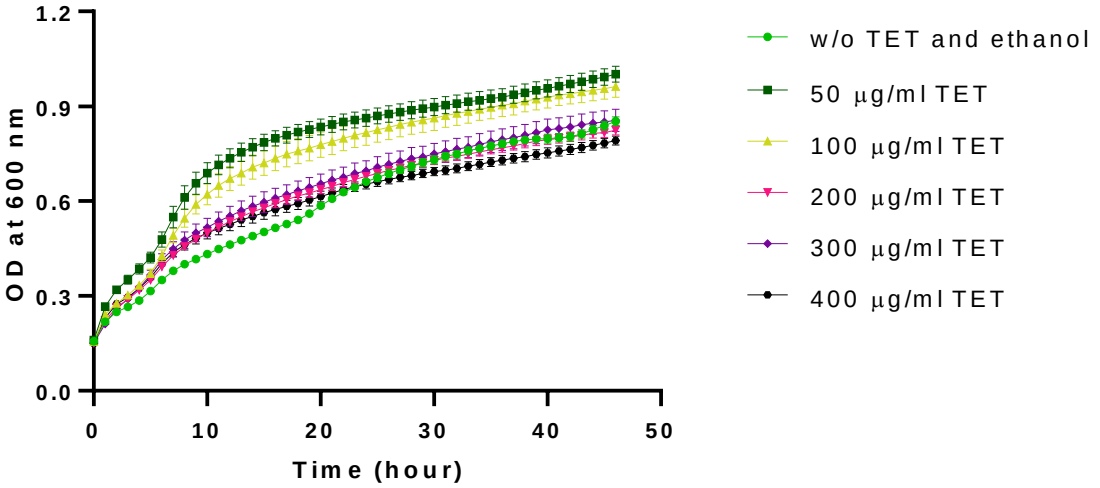


Figure 8.2: Yeast WT_BY4741 was grown in YPG with and without 3% ethanol. BY4741 was treated with tetracycline, increasing concentration of TET, and compared with the 'w/o TET and ethanol' group. They were inoculated at 0.2 OD in 200 µl liquid culture using a 96-well plate and grown for 44-48 hours at 30 ℃ with continuous shaking. The absorbance was recorded every 30 mins using an Epoch 2 plate reader at 600 nm wavelength. The average of three technical replicates at each time point with the standard error mean (SEM) has been plotted.

9. Appendix 4: Supporting Information for Chapter 4

Table 9.1 Glycosylation percentage of the Tpo proteins and Hxt5.

Protein	Total amino acids	Glycosylated amino acids	Glycosylation percentage (%)
Tpo1	586	39	6.65
Tpo2	614	51	8.30
Tpo3	618	39	6.65
Tpo4	622	48	7.71
Tpo5	592	38	6.41
Hxt5	659	56	8.49

*The information has been gathered using the online tool (https://comp.chem.nottingham.ac.uk/glyco/) (Hamby & Hirst, 2008).

Table 9.2 The Codon Adaptation Index (CAI) of the Tpo proteins and Hxt5.

Protein	Ideal Value	CAI
Tpo1	0.8-1.0	0.63
Tpo2		0.64
Tpo3		0.64
Tpo4		0.61
Tpo5		0.62
Hxt5		0.65

*The lower the value, the greater the chance that the protein will be poorly expressed. The information is gathered using the online tool (https://www.genscript.com/tools/rare-codon-analysis).

Table 9.3 Distribution of cysteine residues (C) among the Tpo proteins and Hxt5.

Protein	Total amino acids	Cystein residue	Percentage (%)
Tpo1	586	12	2.04
Tpo2	614	13	2.11
Tpo3	618	11	1.77
Tpo4	622	5	0.80
Tpo5	592	8	1.35
Hxt5	659	15	2.27

*Information adapted from *Saccharomyces* Genome Database (SGD). https://www.yeastgenome.org/

10. References

Abdel-Motaal, H., Meng, L., Zhang, Z., Abdelazez, A. H., Shao, L., Xu, T., Meng, F., Abozaed, S., Zhang, R., & Jiang, J. (2018). An uncharacterized major facilitator superfamily transporter from *Planococcus maritimus* exhibits dual functions as a Na+(Li+, K+)/H+ antiporter and a multidrug efflux pump. *Frontiers in Microbiology*, *9*(JUL). https://doi.org/10.3389/fmicb.2018.01601

Alberts, B., Johnson, A., Lewis, J., Raff, M., Roberts, K., & And Walter, P. (2007). Molecular Biology of the Cell - NCBI Bookshelf. In *Amino Acids* (Third, Vol. 54, Issue 2, p. 1392). http://www.ncbi.nlm.nih.gov/books/NBK20684/

Albertsen, M., Bellahn, I., Krämer, R., & Waffenschmidt, S. (2003). Localization and function of the yeast multidrug transporter Tpo1p. *Journal of Biological Chemistry*, *278*(15), 12820–12825. https://doi.org/10.1074/jbc.M210715200

Alenquer, M., Tenreiro, S., & SÃ¡-Correia, I. (2006). Adaptive response to the antimalarial drug artesunate in yeast involves Pdr1p/Pdr3p-mediated transcriptional activation of the resistance determinants *TPO1* and *PDR5*. *FEMS Yeast Research*, *6*(8), 1130–1139. https://doi.org/10.1111/j.1567-1364.2006.00095.x

Ammor, M. S., Flórez, A. B., Margolles, A., & Mayo, B. (2006). Fluorescence spectroscopy: A rapid tool for assessing tetracycline resistance in *Bifidobacterium longum*. *Canadian Journal of Microbiology*, *52*(8), 740–746. https://doi.org/10.1139/W06-031

Aouida, M., Leduc, A., Poulin, R., & Ramotar, D. (2005). AGP2 encodes the major permease for high-affinity polyamine import in *Saccharomyces cerevisiae*. *Journal of Biological Chemistry*, *280*(25), 24267–24276. https://doi.org/10.1074/jbc.M503071200

Appoloni, S., Lekberg, Y., Tercek, M. T., Zabinski, C. A., & Redecker, D. (2008). Molecular

community analysis of arbuscular mycorrhizal fungi in roots of geothermal soils in Yellowstone National Park (USA). *Microbial Ecology*, *56*(4), 649–659. https://doi.org/10.1007/s00248-008-9384-9

Arkinstall, S. J., Papasavvas, S. G., & Payton, M. A. (1991). Yeast α-matching factor receptor-linked G-protein signal transduction suppresses Ras-dependent activity. *FEBS Letters*, *284*(1), 123–128. https://doi.org/10.1016/0014-5793(91)80777-Z

Badali, H., Prenafeta-Boldu, F. X., Guarro, J., Klaassen, C. H., Meis, J. F., & De Hoog, G. S. (2011). *Cladophialophora psammophila*, a novel species of Chaetothyriales with a potential use in the bioremediation of volatile aromatic hydrocarbons. *Fungal Biology*, *115*(10), 1019–1029. https://doi.org/10.1016/j.funbio.2011.04.005

Baker, B. J., Lutz, M. A., Dawson, S. C., Bond, P. L., & Banfield, J. F. (2004). Metabolically active eukaryotic communities in extremely acidic mine drainage. *Applied and Environmental Microbiology*, *70*(10), 6264–6271. https://doi.org/10.1128/AEM.70.10.6264-6271.2004

Baneyx, F. (1999). Recombinant protein expression in *Escherichia coli.* In *Current Opinion in Biotechnology* (Vol. 10, Issue 5, pp. 411–421). Current Biology Ltd. https://doi.org/10.1016/S0958-1669(99)00003-8

Barabote, R. D., Thekkiniath, J., Strauss, R. E., Vediyappan, G., Fralick, J. A., & Francisco, M. J. S. (2010). Xenobiotic efflux in bacteria and fungi: A genomics update. *Advances in Enzymology and Related Areas of Molecular Biology*, *77 1*, 237–306. https://doi.org/10.1002/9780470920541.ch6

Barilla, D., Lee, B. A., & Proudfoot, N. J. (2001). Cleavage/polyadenylation factor IA associates with the carboxyl-terminal domain of RNA polymerase II in *Saccharomyces cerevisiae*.

Proceedings of the National Academy of Sciences, *98*(2), 445–450. https://doi.org/10.1073/pnas.98.2.445

Barker, K. S., Pearson, M. M., & Rogers, P. D. (2003). Identification of genes differentially expressed in association with reduced azole susceptibility in *Saccharomyces cerevisiae*. *Journal of Antimicrobial Chemotherapy*, *51*(5), 1131–1140. https://doi.org/10.1093/jac/dkg217

Bateman, A. (2019). UniProt: A worldwide hub of protein knowledge. *Nucleic Acids Research*, *47*(D1), D506–D515. https://doi.org/10.1093/nar/gky1049

Bernaudat, F., Frelet-Barrand, A., Pochon, N., Dementin, S., Hivin, P., Boutigny, S., Rioux, J. B., Salvi, D., Seigneurin-Berny, D., Richaud, P., Joyard, J., Pignol, D., Sabaty, M., Desnos, T., Pebay-Peyroula, E., Darrouzet, E., Vernet, T., & Rolland, N. (2011). Heterologous expression of membrane proteins: Choosing the appropriate host. *PLoS ONE*, *6*(12), e29191–e29191. https://doi.org/10.1371/journal.pone.0029191

Blackburn, A. S., & Avery, S. V. (2003). Genome-wide screening of *Saccharomyces cerevisiae* to identify genes required for antibiotic insusceptibility of eukaryotes. *Antimicrobial Agents and Chemotherapy*, *47*(2), 676–681. https://doi.org/10.1128/AAC.47.2.676-681.2003

Blair, J. M. A., & Piddock, L. J. V. (2016). How to measure export via bacterial multidrug resistance efflux pumps. *MBio*, *7*(4). https://doi.org/10.1128/mBio.00840-16

Blair, J. M. A., Richmond, G. E., & Piddock, L. J. V. (2014). Multidrug efflux pumps in Gram-negative bacteria and their role in antibiotic resistance. In *Future Microbiology* (Vol. 9, Issue 10, pp. 1165–1177). Future Medicine Ltd. https://doi.org/10.2217/FMB.14.66

Bratic, A., & Larsson, N. G. (2013). The role of mitochondria in aging. In *Journal of Clinical Investigation* (Vol. 123, Issue 3, pp. 951–957). https://doi.org/10.1172/JCI64125

Brohée, S., Barriot, R., Moreau, Y., & André, B. (2010). YTPdb: a wiki database of yeast membrane transporters. *Biochimica et Biophysica Acta*, *1798*(10), 1908–1912. https://doi.org/10.1016/J.BBAMEM.2010.06.008

Byrne, K. P., & Wolfe, K. H. (2005). The Yeast Gene Order Browser: Combining curated homology and syntenic context reveals gene fate in polyploid species. *Genome Research*, *15*(10), 1456–1461. https://doi.org/10.1101/gr.3672305

Cabral, M. G., Sá-Correia, I., & Viegas, C. A. (2004). Adaptative responses in yeast to the herbicide 2-methyl-4- chlorophenoxyacetic acid at the level of intracellular pH homeostasis. *Journal of Applied Microbiology*, *96*(3), 603–612. https://doi.org/10.1111/j.1365-2672.2004.02199.x

Cavalheiro, M., Romão, D., Santos, R., Mil-Homens, D., Pais, P., Costa, C., Galocha, M., Pereira, D., Takahashi-Nakaguchi, A., Chibana, H., Fialho, A. M., & Teixeira, M. C. (2021). Role of cgtpo4 in polyamine and antimicrobial peptide resistance: determining virulence in *Candida glabrata*. *International Journal of Molecular Sciences*, *22*(3), 1–15. https://doi.org/10.3390/ijms22031376

Ceci, A., Maggi, O., Pinzari, F., & Persiani, A. M. (2012). Growth responses to and accumulation of vanadium in agricultural soil fungi. *Applied Soil Ecology*, *58*, 1–11. https://doi.org/10.1016/j.apsoil.2012.02.022

Chandel, N. S. (2014). Mitochondria as signaling organelles. In *BMC Biology* (Vol. 12, p. 34). BioMed Central Ltd. https://doi.org/10.1186/1741-7007-12-34

Chervitz, S. A., Hester, E. T., Ball, C. A., Dolinski, K., Dwight, S. S., Harris, M. A., Juvik, G., Malekian, A., Roberts, S., Roe, T., Scafe, C., Schroeder, M., Sherlock, G., Weng, S., Zhu, Y., Cherry, J. M., & Botstein, D. (1999). Using the Saccharomyces Genome Database

(SGD) for analysis of protein similarities and structure. *Nucleic Acids Research*, *27*(1), 74–78. https://doi.org/10.1093/NAR/27.1.74

Chino, A., Watanabe, K., & Moriya, H. (2010). Plasmid construction using recombination activity in the fission yeast *Schizosaccharomyces pombe*. *PLoS ONE*, *5*(3), e9652–e9652. https://doi.org/10.1371/journal.pone.0009652

Chopra, I., Hawkey, P. M., & Hinton, M. (1992). Tetracyclines, molecular and clinical aspects. In *Journal of Antimicrobial Chemotherapy* (Vol. 29, Issue 3, pp. 245–277). *J Antimicrob Chemother*. https://doi.org/10.1093/jac/29.3.245

Chopra, Ian, & Roberts, M. (2001). Tetracycline Antibiotics: Mode of Action, Applications, Molecular Biology, and Epidemiology of Bacterial Resistance. *Microbiology and Molecular Biology Reviews*, *65*(2), 232–260. https://doi.org/10.1128/mmbr.65.2.232-260.2001

Clark-Walker, G. D., & Linnane, A. W. (1966). In vivo differentiation of yeast cytoplasmic and mitochondrial protein synthesis with antibiotics. *Biochemical and Biophysical Research Communications*, *25*(1), 8–13. https://doi.org/10.1016/0006-291X(66)90631-0

Colot, H. V., Park, G., Turner, G. E., Ringelberg, C., Crew, C. M., Litvinkova, L., Weiss, R. L., Borkovich, K. A., & Dunlap, J. C. (2006). A high-throughput gene knockout procedure for *Neurospora* reveals functions for multiple transcription factors. *Proceedings of the National Academy of Sciences of the United States of America*, *103*(27), 10352–10357. https://doi.org/10.1073/pnas.0601456103

Costa, C., Dias, P. J., Sá-Correia, I., & Teixeira, M. C. (2014). MFS multidrug transporters in pathogenic fungi: Do they have real clinical impact? In *Frontiers in Physiology: Vol. 5 MAY*. https://doi.org/10.3389/fphys.2014.00197

Costa, C., Ribeiro, J., Miranda, I. M., Silva-Dias, A., Cavalheiro, M., Costa-de-Oliveira, S., Rodrigues, A. G., & Teixeira, M. C. (2016). Clotrimazole drug resistance in *Candida glabrata* clinical isolates correlates with increased expression of the drug: H+ antiporters CgAqr1, CgTpo1_1, CgTpo3, and CgQdr2. *Frontiers in Microbiology*, *7*(APR). https://doi.org/10.3389/fmicb.2016.00526

Court, D. A., Kleene, R., Neupert, W., & Lill, R. (1996). Role of the N- and C-termini of porin in import into the outer membrane of *Neurospora* mitochondria. *FEBS Letters*, *390*(1), 73–77. https://doi.org/10.1016/0014-5793(96)00629-1

Cowen, L. E., Sanglard, D., Howard, S. J., Rogers, P. D., & Perlin, D. S. (2015). Mechanisms of antifungal drug resistance. *Cold Spring Harbor Perspectives in Medicine*, *5*(7). https://doi.org/10.1101/cshperspect.a019752

Dadachova, E., Bryan, R. A., Huang, X., Moadel, T., Schweitzer, A. D., Aisen, P., Nosanchuk, J. D., & Casadevall, A. (2007). Ionizing radiation changes the electronic properties of melanin and enhances the growth of melanized fungi. *PLoS ONE*, *2*(5). https://doi.org/10.1371/journal.pone.0000457

Dartier, J., Lemaitre, E., Chourpa, I., Goupille, C., Servais, S., Chevalier, S., Mahéo, K., & Dumas, J. F. (2017). ATP-dependent activity and mitochondrial localization of drug efflux pumps in doxorubicin-resistant breast cancer cells. *Biochimica et Biophysica Acta - General Subjects*, *1861*(5), 1075–1084. https://doi.org/10.1016/j.bbagen.2017.02.019

Davis, R. H., & de Serres, F. J. (1970). Genetic and Microbiological Research Techniques for *Neurospora crassa*. *Methods in Enzymology*, *17*, 79–143. https://doi.org/10.1016/0076-6879(71)17168-6

De Lera Ruiz, M., & Kraus, R. L. (2015). Voltage-Gated Sodium Channels: Structure, Function,

Pharmacology, and Clinical Indications. In *Journal of Medicinal Chemistry* (Vol. 58, Issue 18, pp. 7093–7118). American Chemical Society. https://doi.org/10.1021/jm501981g

De Rossi, E., Arrigo, P., Bellinzoni, M., Silva, P. E. A., Martín, C., Aínsa, J. A., Guglierame, P., & Riccardi, G. (2002). The multidrug transporters belonging to major facilitator superfamily (MFS) in *Mycobacterium tuberculosis*. *Molecular Medicine*, *8*(11), 714–724. https://doi.org/10.1007/bf03402035

de Zamaroczy, M., & Bernardi, G. (1986). The primary structure of the mitochondrial genome of *Saccharomyces cerevisiae* - a review. *Gene*, *47*(2–3), 155–177. https://doi.org/10.1016/0378-1119(86)90060-0

Dehoux, P., Davies, J., & Cannon, M. (1993). Natural cycloheximide resistance in yeast: The role of ribosomal protein L41. *European Journal of Biochemistry*, *213*(2), 841–848. https://doi.org/10.1111/j.1432-1033.1993.tb17827.x

Delling, U., Raymond, M., & Schurr, E. (1998). Identification of *Saccharomyces cerevisiae* genes conferring resistance to quinoline ring-containing antimalarial drugs. *Antimicrobial Agents and Chemotherapy*, *42*(5), 1034–1041. https://doi.org/10.1128/aac.42.5.1034

Deniaud, A., Bernaudat, F., Frelet-Barrand, A., Juillan-Binard, C., Vernet, T., Rolland, N., & Pebay-Peyroula, E. (2011). Expression of a chloroplast ATP/ADP transporter in E. coli membranes: Behind the Mistic strategy. *Biochimica et Biophysica Acta - Biomembranes*, *1808*(8), 2059–2066. https://doi.org/10.1016/j.bbamem.2011.04.011

Desmoucelles, C., Pinson, B., Saint-Marc, C., & Daignan-Fornier, B. (2002). Screening the yeast "Disruptome" for mutants affecting resistance to the immunosuppressive drug, mycophenolic acid. *Journal of Biological Chemistry*, *277*(30), 27036–27044. https://doi.org/10.1074/jbc.M111433200

Dias, Paulo J., & Sá-Correia, I. (2013). The drug: H+ antiporters of family 2 (DHA2), siderophore transporters (ARN) and glutathione: H+ antiporters (GEX) have a common evolutionary origin in hemiascomycete yeasts. *BMC Genomics*, *14*(1). https://doi.org/10.1186/1471-2164-14-901

Dias, Paulo Jorge, Seret, M. L., Goffeau, A., Correia, I. S., & Baret, P. V. (2010). Evolution of the 12-spanner drug:H+ antiporter DHA1 family in hemiascomycetous yeasts. *OMICS A Journal of Integrative Biology*, *14*(6), 701–710. https://doi.org/10.1089/omi.2010.0104

Diderich, J. A., Schuurmans, J. M., Van Gaalen, M. C., Kruckeberg, A. L., & Van Dam, K. (2001). Functional analysis of the hexose transporter homologue HXT5 in *Saccharomyces cerevisiae*. *Yeast*, *18*(16), 1515–1524. https://doi.org/10.1002/yea.779

Do Valle Matta, M. A., Jonniaux, J. L., Balzi, E., Goffeau, A., & Van Den Hazel, B. (2001). Novel target genes of the yeast regulator Pdr1p: A contribution of the TPO1 gene in resistance to quinidine and other drugs. *Gene*, *272*(1–2), 111–119. https://doi.org/10.1016/S0378-1119(01)00558-3

Dreger, M. (2003). Proteome analysis at the level of subcellular structures. In *European Journal of Biochemistry* (Vol. 270, Issue 4, pp. 589–599). Eur J Biochem. https://doi.org/10.1046/j.1432-1033.2003.03426.x

Duewelhenke, N., Krut, O., & Eysel, P. (2007). Influence on mitochondria and cytotoxicity of different antibiotics administered in high concentrations on primary human osteoblasts and cell lines. *Antimicrobial Agents and Chemotherapy*, *51*(1), 54–63. https://doi.org/10.1128/AAC.00729-05

Dujon, B., Sherman, D., Fischer, G., Durrens, P., Casaregela, S., Lafentaine, I., De Montigny, J., Marck, C., Neuvéglise, C., Talla, E., Goffard, N., Frangeul, L., Algie, M., Anthouard, V.,

Babour, A., Barbe, V., Barnay, S., Blanchin, S., Beckerich, J. M., … Souciet, J. L. (2004). Genome evolution in yeasts. *Nature*, *430*(6995), 35–44. https://doi.org/10.1038/nature02579

Duyao, M. P., Taylor, S. A. M., Buckler, A. J., Ambrose, C. M., Lin, C., Groot, N., Church, D., Barnes, G., Wasmuth, J. J., Housman, D. E., Macdonald, M. E., & Gusella, J. F. (1993). A gene from chromosome 4p 16.3 with similarity to a superfamily of transporter proteins. *Human Molecular Genetics*, *2*(6), 673–676. https://doi.org/10.1093/hmg/2.6.673

Elbourne, L. D. H., Tetu, S. G., Hassan, K. A., & Paulsen, I. T. (2017). TransportDB 2.0: a database for exploring membrane transporters in sequenced genomes from all domains of life. *Nucleic Acids Research*, *45*(Database issue), D320. https://doi.org/10.1093/NAR/GKW1068

Feder, H. M. (1986). Chloramphenicol: What we have learned in the last decade. *Southern Medical Journal*, *79*(9), 1129–1134. https://doi.org/10.1097/00007611-198609000-00022

Felsenstein, J. (1985). Confidence limits on phylogenies: an approach using the bootstrap. *Evolution*, *39*(4), 783–791. https://doi.org/10.1111/j.1558-5646.1985.tb00420.x

Fernandes, A. R., Mira, N. P., Vargas, R. C., Canelhas, I., & Sá-Correia, I. (2005). *Saccharomyces cerevisiae* adaptation to weak acids involves the transcription factor Haa1p and Haa1p-regulated genes. *Biochemical and Biophysical Research Communications*, *337*(1), 95–103. https://doi.org/10.1016/j.bbrc.2005.09.010

Fisher, M. C., Hawkins, N. J., Sanglard, D., & Gurr, S. J. (2018). Worldwide emergence of resistance to antifungal drugs challenges human health and food security. In *Science* (Vol. 360, Issue 6390, pp. 739–742). American Association for the Advancement of Science. https://doi.org/10.1126/science.aap7999

Fologea, D., Ledden, B., McNabb, D. S., & Li, J. (2007). Electrical characterization of protein molecules by a solid-state nanopore. *Applied Physics Letters*, *91*(5), 053901–1. https://doi.org/10.1063/1.2767206

Formosa, C., Schiavone, M., Martin-Yken, H., François, J. M., Duval, R. E., & Dague, E. (2013). Nanoscale effects of caspofungin against two yeast species, *Saccharomyces cerevisiae* and *Candida albicans*. *Antimicrobial Agents and Chemotherapy*, *57*(8), 3498–3506. https://doi.org/10.1128/AAC.00105-13

Foury, F., Roganti, T., Lecrenier, N., & Purnelle, B. (1998). The complete sequence of the mitochondrial genome of *Saccharomyces cerevisiae*. *FEBS Letters*, *440*(3), 325–331. https://doi.org/10.1016/S0014-5793(98)01467-7

Fried, H. M., & Warner, J. R. (1982). Molecular cloning and analysis of yeast gene for cycloheximide resistance and ribosomal protein L29. *Nucleic Acids Research*, *10*(10), 3133–3148. https://doi.org/10.1093/nar/10.10.3133

Fürste, J. P., Pansegrau, W., Frank, R., Blöcker, H., Scholz, P., Bagdasarian, M., & Lanka, E. (1986). Molecular cloning of the plasmid RP4 primase region in a multi-host-range tacP expression vector. *Gene*, *48*(1), 119–131. https://doi.org/10.1016/0378-1119(86)90358-6

Gabaldón, T., & Huynen, M. A. (2003). Reconstruction of the proto-mitochondrial metabolism. *Science*, *301*(5633), 609. https://doi.org/10.1126/science.1085463

Gabaldón, T., & Huynen, M. A. (2007). From endosymbiont to host-controlled organelle: The hijacking of mitochondrial protein synthesis and metabolism. *PLoS Computational Biology*, *3*(11), 2209–2218. https://doi.org/10.1371/journal.pcbi.0030219

Ghannoum, M. A., & Rice, L. B. (1999). Antifungal agents: Mode of action, mechanisms of resistance, and correlation of these mechanisms with bacterial resistance. In *Clinical*

Microbiology Reviews (Vol. 12, Issue 4, pp. 501–517). American Society for Microbiology. https://doi.org/10.1128/cmr.12.4.501

Gil, F. N., Bellí, G., & Viegas, C. A. (2017). The *Saccharomyces cerevisiae* response to stress caused by the herbicidal active substance alachlor requires the iron regulon transcription factor Aft1p. *Environmental Microbiology*, *19*(2), 485–499. https://doi.org/10.1111/1462-2920.13439

Gilichinsky, D. A., Wilson, G. S., Friedmann, E. I., McKay, C. P., Sletten, R. S., Rivkina, E. M., Vishnivetskaya, T. A., Erokhina, L. G., Ivanushkina, N. E., Kochkina, G. A., Scherbakova, V. A., Soina, V. S., Spirina, E. V., Vorobyova, E. A., Frodorov-Davydov, D. G., Hallet, B., Ozerskaya, S. M., Sorokovikov, V. A., Laurinavichyus, K. S., … Tiedje, J. M. (2007). Microbial populations in Antarctic permafrost: Biodiversity, stage, age, and implication for astrobiology. *Astrobiology*, *7*(2), 275–311. https://doi.org/10.1089/ast.2006.0012

Goffeau, A., Park, J., Paulsen, I. T., Jonniaux, J. L., Dinh, T., Mordant, P., & Saier, M. H. (1997). Multidrug-resistant transport proteins in yeast: Complete inventory and phylogenetic characterization of yeast open reading frames within the major facilitator superfamily. *Yeast*, *13*(1), 43–54. https://doi.org/10.1002/(SICI)1097-0061(199701)13:1<43::AID-YEA56>3.0.CO;2-J

Goldman, R. A., Hasan, T., Hall, C. C., Cooperman, B. S., Strycharz, W. A., & Strycharz, W. A. (1983). Photoincorporation of Tetracycline into *Escherichia coli* Ribosomes. Identification of the Major Proteins Photolabeled by Native Tetracycline and Tetracycline Photoproducts and Implications for the Inhibitory Action of Tetracycline on Protein Synthesis. *Biochemistry*, *22*(2), 359–368. https://doi.org/10.1021/bi00271a020

Gootz, T. D., Barrett, J. F., & Sutcliffe, J. A. (1990). Inhibitory effects of quinolone antibacterial

agents on eucaryotic topoisomerases and related test systems. In *Antimicrobial Agents and Chemotherapy* (Vol. 34, Issue 1, pp. 8–12). Antimicrob Agents Chemother. https://doi.org/10.1128/AAC.34.1.8

Gray, M. W., Burger, G., & Lang, B. F. (1999). Mitochondrial evolution. In *Science* (Vol. 283, Issue 5407, pp. 1476–1481). Science. https://doi.org/10.1126/science.283.5407.1476

Gray, M. W., Lang, B. F., Cedergren, R., Golding, G. B., Lemieux, C., Sankoff, D., Turmel, M., Brossard, N., Delage, E., Littlejohn, T. G., Plante, I., Rioux, P., Saint-Louis, D., Zhu, Y., & Burger, G. (1998). Genome structure and gene content in protist mitochondrial DNAs. *Nucleic Acids Research*, *26*(4), 865–878. https://doi.org/10.1093/nar/26.4.865

Griffiths, A., Gelbart, W., Miller, J., & Lewontin, R. (1999). Expressing Eukaryotic Genes in Bacteria. In *Modern Genetic Analysis*. W. H. Freeman. https://www.ncbi.nlm.nih.gov/books/NBK21359/

Ha, K. C., & White, T. C. (1999). Effects of azole antifungal drugs on the transition from yeast cells to hyphae in susceptible and resistant isolates of the pathogenic yeast *Candida albicans*. *Antimicrobial Agents and Chemotherapy*, *43*(4), 763–768. https://doi.org/10.1128/aac.43.4.763

Haferkamp, I., Hackstein, J. H. P., Voncken, F. G. J., Schmit, G., & Tjaden, J. (2002). Functional integration of mitochondrial and hydrogenosomal ADP/ATP carriers in the *Escherichia coli* membrane reveals different biochemical characteristics for plants, mammals and anaerobic chytrids. *European Journal of Biochemistry*, *269*(13), 3172–3181. https://doi.org/10.1046/j.1432-1033.2002.02991.x

Hamby, S. E., & Hirst, J. D. (2008). Prediction of glycosylation sites using random forests. *BMC Bioinformatics*, *9*(1), 1–13. https://doi.org/10.1186/1471-2105-9-500

Hamdache, A., Lamarti, A., Aleu, J., & Collado, I. G. (2011). Non-peptide metabolites from the genus bacillus. *Journal of Natural Products, 74*(4), 893–899. https://doi.org/10.1021/np100853e

Harkness, T. A. A., Nargang, F. E., Van Der Klei, I., Neupert, W., & Lill, R. (1994). A crucial role of the mitochondrial protein import receptor MOM19 for the biogenesis of mitochondria. *Journal of Cell Biology, 124*(5), 637–648. https://doi.org/10.1083/jcb.124.5.637

Herminghaus, A., Buitenhuis, A. J., Schulz, J., Truse, R., Vollmer, C., Relja, B., Bauer, I., & Picker, O. (2020). Indomethacin Increases the Efficacy of Oxygen Utilization of Colonic Mitochondria and Uncouples Hepatic Mitochondria in Tissue Homogenates From Healthy Rats. *Frontiers in Medicine, 7*. https://doi.org/10.3389/fmed.2020.00463

Herrero, E. (2005). Evolutionary relationships between *Saccharomyces cerevisiae* and other fungal species as determined from genome comparisons. In *Revista Iberoamericana de Micologia* (Vol. 22, Issue 4, pp. 217–222). Asociacion Espanola de Micologia. https://doi.org/10.1016/S1130-1406(05)70046-2

Ho, C. H., Magtanong, L., Barker, S. L., Gresham, D., Nishimura, S., Natarajan, P., Koh, J. L. Y., Porter, J., Gray, C. A., Andersen, R. J., Giaever, G., Nislow, C., Andrews, B., Botstein, D., Graham, T. R., Yoshida, M., & Boone, C. (2009). A molecular barcoded yeast ORF library enables mode-of-action analysis of bioactive compounds. *Nature Biotechnology, 27*(4), 369–377. https://doi.org/10.1038/nbt.1534

Hobbie, S. N., Akshay, S., Kalapala, S. K., Bruell, C. M., Shcherbakov, D., & Böttger, E. C. (2008). Genetic analysis of interactions with eukaryotic rRNA identify the mitoribosome as target in aminoglycoside ototoxicity. *Proceedings of the National Academy of Sciences of*

the United States of America, *105*(52), 20888–20893. https://doi.org/10.1073/pnas.0811258106

Holmes, A. R., Cardno, T. S., Strouse, J. J., Ivnitski-Steele, I., Keniya, M. V., Lackovic, K., Monk, B. C., Sklar, L. A., & Cannon, R. D. (2016). Targeting efflux pumps to overcome antifungal drug resistance. In *Future Medicinal Chemistry* (Vol. 8, Issue 12, pp. 1485–1501). Future Science. https://doi.org/10.4155/fmc-2016-0050

Hovsepian, J., Defenouillère, Q., Albanèse, V., Váchová, L., Garcia, C., Palková, Z., & Léon, S. (2017). Multilevel regulation of an α-arrestin by glucose depletion controls hexose transporter endocytosis. *Journal of Cell Biology*, *216*(6), 1811–1831. https://doi.org/10.1083/jcb.201610094

Hoyt, M. A., & Davis, R. H. (2004). Polyamines in Fungi. In *Biochemistry and Molecular Biology* (pp. 335–347). Springer Berlin Heidelberg. https://doi.org/10.1007/978-3-662-06064-3_16

Hung, C. W., Martínez-Márquez, J. Y., Javed, F. T., & Duncan, M. C. (2018). A simple and inexpensive quantitative technique for determining chemical sensitivity in *Saccharomyces cerevisiae. Scientific Reports*, *8*(1), 1–16. https://doi.org/10.1038/s41598-018-30305-z

Hutchin, T., & Cortopassi, G. (1994). Proposed molecular and cellular mechanism for aminoglycoside ototoxicity. In *Antimicrobial Agents and Chemotherapy* (Vol. 38, Issue 11, pp. 2517–2520). American Society for Microbiology. https://doi.org/10.1128/AAC.38.11.2517

Jiang, D., Zhao, Y., Fan, J., Liu, X., Wu, Y., Feng, W., & Zhang, X. C. (2014). Atomic resolution structure of the *E. coli* YajR transporter YAM domain. *Biochemical and Biophysical Research Communications*, *450*(2), 929–935.

https://doi.org/10.1016/j.bbrc.2014.06.053

Jiang, D., Zhao, Y., Wang, X., Fan, J., Heng, J., Liu, X., Feng, W., Kang, X., Huang, B., Liu, J., & Zhang, X. C. (2013). Structure of the YajR transporter suggests a transport mechanism based on the conserved motif A. *Proceedings of the National Academy of Sciences of the United States of America*, *110*(36), 14664–14669. https://doi.org/10.1073/pnas.1308127110

K, K., J, R., & KD, Y. (2019). MAFFT online service: multiple sequence alignment, interactive sequence choice and visualization. *Briefings in Bioinformatics*, *20*(4), 1160–1166. https://doi.org/10.1093/BIB/BBX108

Kalghatgi, S., Spina, C. S., Costello, J. C., Liesa, M., Morones-Ramirez, J. R., Slomovic, S., Molina, A., Shirihai, O. S., & Collins, J. J. (2013). Bactericidal antibiotics induce mitochondrial dysfunction and oxidative damage in mammalian cells. *Science Translational Medicine*, *5*(192). https://doi.org/10.1126/scitranslmed.3006055

Kaltseis, J., Rainer, J., & De Hoog, G. S. (2009). Ecology of Pseudallescheria and Scedosporium species in human-dominated and natural environments and their distribution in clinical samples. *Medical Mycology*, *47*(4), 398–405. https://doi.org/10.1080/13693780802585317

Kangwa, M., Yelemane, V., Polat, A. N., Gorrepati, K. D. D., Grasselli, M., & Fernández-Lahore, M. (2015). High-level fed-batch fermentative expression of an engineered Staphylococcal protein A based ligand in *E. coli*: purification and characterization. *AMB Express*, *5*(1), 1–10. https://doi.org/10.1186/s13568-015-0155-y

Kanki, T., Nakayama, H., Sasaki, N., Takio, K., Alam, T. I., Hamasaki, N., & Kang, D. (2004). Mitochondrial Nucleoid and Transcription Factor A. In *Mitochondrial Pathogenesis* (pp. 61–68). Springer Berlin Heidelberg. https://doi.org/10.1007/978-3-662-41088-2_7

Keller, G., Ray, E., Brown, P. O., & Winge, D. R. (2001). Haa1, a Protein Homologous to the

Copper-regulated Transcription Factor Ace1, is a Novel Transcriptional Activator. *Journal of Biological Chemistry*, *276*(42), 38697–38702. https://doi.org/10.1074/jbc.M107131200

Kelley, L. A., Mezulis, S., Yates, C. M., Wass, M. N., & Sternberg, M. J. E. (2015). The Phyre2 web portal for protein modeling, prediction and analysis. *Nature Protocols*, *10*(6), 845–858. https://doi.org/10.1038/nprot.2015.053

Kellis, M., Birren, B. W., & Lander, E. S. (2004). Proof and evolutionary analysis of ancient genome duplication in the yeast *Saccharomyces cerevisiae*. *Nature*, *428*(6983), 617–624. https://doi.org/10.1038/nature02424

Khan, S. M., Smigrodzki, R. M., & Swerdlow, R. H. (2007). Cell and animal models of mtDNA biology: progress and prospects. *American Journal of Physiology-Cell Physiology*, *292*(2), C658–C669. https://doi.org/10.1152/ajpcell.00224.2006

Khow, O., & Suntrarachun, S. (2012). Strategies for production of active eukaryotic proteins in bacterial expression system. *Asian Pacific Journal of Tropical Biomedicine*, *2*(2), 159–162. https://doi.org/10.1016/S2221-1691(11)60213-X

Kostylev, M., Otwell, A. E., Richardson, R. E., & Suzuki, Y. (2015). Cloning should be simple: *Escherichia coli* DH5á-mediated assembly of multiple DNA fragments with short end homologies. *PLoS ONE*, *10*(9). https://doi.org/10.1371/journal.pone.0137466

Kroon, A. M., Dontje, B. H. J., Holtrop, M., & Van Den Bogert, C. (1984). The mitochondrial genetic system as a target for chemotherapy: Tetracyclines as cytostatics. *Cancer Letters*, *25*(1), 33–40. https://doi.org/10.1016/S0304-3835(84)80023-3

Krüger, A., Vowinckel, J., Mülleder, M., Grote, P., Capuano, F., Bluemlein, K., & Ralser, M. (2013). Tpo1-mediated spermine and spermidine export controls cell cycle delay and times antioxidant protein expression during the oxidative stress response. *EMBO Reports*, *14*(12),

1113–1119. https://doi.org/10.1038/embor.2013.165

Kubota, S., Takeo, I., Kume, K., Kanai, M., Shitamukai, A., Mizunuma, M., Miyakawa, T., Shimoi, H., Iefuji, H., & Hirata, D. (2004). Bioscience, Biotechnology, and Biochemistry Effect of Ethanol on Cell Growth of Budding Yeast: Genes That Are Important for Cell Growth in the Presence of Ethanol. *Effect of Ethanol on Cell Growth of Budding Yeast: Genes That Are Important for Cell Growth in the Presence of Ethanol*, *68*(4), 968–972. https://doi.org/10.1271/bbb.68.968

Kühlbrandt, W. (2015). Structure and function of mitochondrial membrane protein complexes. *BMC Biology*, *13*(1), 1–11. https://doi.org/10.1186/s12915-015-0201-x

Kumar, A., & Worobec, E. A. (2005). HasF, a TolC-homolog of *Serratia marcescens*, is involved in energy-dependent efflux. *Canadian Journal of Microbiology*, *51*(6), 497–500. https://doi.org/10.1139/w05-029

Kumar, S., Stecher, G., Li, M., Knyaz, C., & Tamura, K. (2018). MEGA X: Molecular evolutionary genetics analysis across computing platforms. *Molecular Biology and Evolution*, *35*(6), 1547–1549. https://doi.org/10.1093/molbev/msy096

Lamb, R., Ozsvari, B., Lisanti, C. L., Tanowitz, H. B., Howell, A., Martinez-Outschoorn, U. E., Sotgia, F., & Lisanti, M. P. (2015). Antibiotics that target mitochondria effectively eradicate cancer stem cells, across multiple tumor types: Treating cancer like an infectious disease. *Oncotarget*, *6*(7), 4569–4584. https://doi.org/10.18632/oncotarget.3174

Langevin, A. M., & Dunlop, M. J. (2018). Stress introduction rate alters the benefit of AcrABTolC efflux pumps. *Journal of Bacteriology*, *200*(1). https://doi.org/10.1128/JB.00525-17

Larsen, B., McCool, L., Mai, H., & Essmann, M. (2008). Tetracycline effects on *Candida*

albicans virulence factors. *Infectious Diseases in Obstetrics and Gynecology*, *2008*. https://doi.org/10.1155/2008/493508

Lawrence, J. W., Claire, D. C., Weissig, V., & Rowe, T. C. (1996). Delayed cytotoxicity and cleavage of mitochondrial DNA in ciprofloxacin- treated mammalian cells. *Molecular Pharmacology*, *50*(5), 1178–1188.

Levy, S. B. (1992). Active efflux mechanisms for antimicrobial resistance. In *Antimicrobial Agents and Chemotherapy* (Vol. 36, Issue 4, pp. 695–703). Antimicrob Agents Chemother. https://doi.org/10.1128/AAC.36.4.695

Lewis, J. S., Spenkelink, L. M., Schauer, G. D., Yurieva, O., Mueller, S. H., Natarajan, V., Kaur, G., Maher, C., Kay, C., O'Donnell, M. E., & van Oijen, A. M. (2020). Tunability of DNA Polymerase Stability during Eukaryotic DNA Replication. *Molecular Cell*, *77*(1), 17-25.e5. https://doi.org/10.1016/j.molcel.2019.10.005

Lewis, K. A., Tzilivakis, J., Warner, D. J., & Green, A. (2016). An international database for pesticide risk assessments and management. *Human and Ecological Risk Assessment*, *22*(4), 1050–1064. https://doi.org/10.1080/10807039.2015.1133242

Liao, P. C., Boldogh, I. R., Siegmund, S. E., Freyberg, Z., & Pon, L. A. (2018). Isolation of mitochondria from *Saccharomyces cerevisiae* using magnetic bead affinity purification. *PLoS ONE*, *13*(4), e0196632. https://doi.org/10.1371/journal.pone.0196632

Linnane, A. W., Lamb, A. J., Christodoulou, C., & Lukins, H. B. (1968). The biogenesis of mitochondria, VI. Biochemical basis of the resistance of *Saccharomyces cerevisiae* toward antibiotics which specifically inhibit mitochondrial protein synthesis. *Proceedings of the National Academy of Sciences of the United States of America*, *59*(4), 1288–1293. https://doi.org/10.1073/pnas.59.4.1288

Liou, J. Y., Aleksic, N., Chen, S. F., Han, T. J., Shyue, S. K., & Wu, K. K. (2005). Mitochondrial localization of cyclooxygenase-2 and calcium-independent phospholipase A2 in human cancer cells: Implication in apoptosis resistance. *Experimental Cell Research*, *306*(1), 75–84. https://doi.org/10.1016/j.yexcr.2005.01.011

Lobstein, J., Emrich, C. A., Jeans, C., Faulkner, M., Riggs, P., & Berkmen, M. (2012). SHuffle, a novel *Escherichia coli* protein expression strain capable of correctly folding disulfide bonded proteins in its cytoplasm. *Microbial Cell Factories*, *11*(1), 753. https://doi.org/10.1186/1475-2859-11-56

Lomovskaya, O., & Bostian, K. A. (2006). Practical applications and feasibility of efflux pump inhibitors in the clinic - A vision for applied use. *Biochemical Pharmacology*, *71*(7), 910–918. https://doi.org/10.1016/j.bcp.2005.12.008

Lovmar, M., Tenson, T., & Ehrenberg, M. (2004). Kinetics of macrolide action: The josamycin and erythromycin cases. *Journal of Biological Chemistry*, *279*(51), 53506–53515. https://doi.org/10.1074/jbc.M401625200

Lowes, D. A., Wallace, C., Murphy, M. P., Webster, N. R., & Galley, H. F. (2009). The mitochondria targeted antioxidant MitoQ protects against fluoroquinolone-induced oxidative stress and mitochondrial membrane damage in human Achilles tendon cells. *Free Radical Research*, *43*(4), 323–328. https://doi.org/10.1080/10715760902736275

Ma, P., Varela, F., Magoch, M., Silva, A. R., RosÃ¡rio, A. L., Brito, J., Oliveira, T. F., Nogly, P., Pessanha, M., Stelter, M., Kletzin, A., Henderson, P. J. F., & Archer, M. (2013). Correction: An Efficient Strategy for Small-Scale Screening and Production of Archaeal Membrane Transport Proteins in Escherichia coli. *PLoS ONE*, *8*(11), e76913. https://doi.org/10.1371/annotation/ba41a7db-2c22-4ffc-b603-526534594a51

Malina, C., Larsson, C., & Nielsen, J. (2018). Yeast mitochondria: An overview of mitochondrial biology and the potential of mitochondrial systems biology. In *FEMS Yeast Research* (Vol. 18, Issue 5, p. 40). Oxford University Press. https://doi.org/10.1093/femsyr/foy040

Marger, M. D., & Saier, M. H. (1993). A major superfamily of transmembrane facilitators that catalyse uniport, symport and antiport. *Trends in Biochemical Sciences*, *18*(1), 13–20. https://doi.org/10.1016/0968-0004(93)90081-W

Margulis, L. (1970). *Origin of Eukaryotic Cells.* New Haven, CT: Yale University Press. https://doi.org/10.2307/3241538

Markovich, S., Yekutiel, A., Shalit, I., Shadkchan, Y., & Osherov, N. (2004a). Genomic approach to identification of mutations affecting caspofungin susceptibility in *Saccharomyces cerevisiae*. *Antimicrobial Agents and Chemotherapy*, *48*(10), 3871–3876. https://doi.org/10.1128/AAC.48.10.3871-3876.2004

Markovich, S., Yekutiel, A., Shalit, I., Shadkchan, Y., & Osherov, N. (2004b). Genomic approach to identification of mutations affecting caspofungin susceptibility in *Saccharomyces cerevisiae. Antimicrobial Agents and Chemotherapy*, *48*(10), 3871–3876. https://doi.org/10.1128/AAC.48.10.3871-3876.2004

Martins, M., McCusker, M. P., Viveiros, M., Couto, I., Fanning, S., Pagès, J.-M., & Amaral, L. (2013). A Simple Method for Assessment of MDR Bacteria for Over-Expressed Efflux Pumps. *The Open Microbiology Journal*, *7*(1), 72–82. https://doi.org/10.2174/1874285801307010072

Mathieu, K., Javed, W., Vallet, S., Lesterlin, C., Candusso, M. P., Ding, F., Xu, X. N., Ebel, C., Jault, J. M., & Orelle, C. (2019). Functionality of membrane proteins overexpressed and purified from *E. coli* is highly dependent upon the strain. *Scientific Reports*, *9*(1), 1–15.

https://doi.org/10.1038/s41598-019-39382-0

McCormack, P. L., & Perry, C. M. (2005). Caspofungin: A review of its use in the treatment of fungal infections. In *Drugs* (Vol. 65, Issue 14, pp. 2049–2068). Drugs. https://doi.org/10.2165/00003495-200565140-00009

McKee, E. E., Ferguson, M., Bentley, A. T., & Marks, T. A. (2006). Inhibition of mammalian mitochondrial protein synthesis by oxazolidinones. *Antimicrobial Agents and Chemotherapy*, *50*(6), 2042–2049. https://doi.org/10.1128/AAC.01411-05

McMurry, L. M., & Levy, S. B. (1995). The NH2-terminal half of the TN10-specified tetracycline efflux protein TetA contains a dimerization domain. *Journal of Biological Chemistry*, *270*(39), 22752–22757. https://doi.org/10.1074/jbc.270.39.22752

Meisinger, C., Pfanner, N., & Truscott, K. N. (2006). Isolation of yeast mitochondria. *Methods in Molecular Biology (Clifton, N.J.)*, *313*, 33–39. https://doi.org/10.1385/1-59259-958-3:033

Mima, S., Ushijima, H., Hwang, H. J., Tsutsumi, S., Makise, M., Yamaguchi, Y., Tsuchiya, T., Mizushima, H., & Mizushima, T. (2007). Identification of the TPO1 gene in yeast, and its human orthologue TETRAN, which cause resistance to NSAIDs. *FEBS Letters*, *581*(7), 1457–1463. https://doi.org/10.1016/j.febslet.2007.03.001

Miroux, B., & Walker, J. E. (1996). Over-production of proteins in *Escherichia coli*: Mutant hosts that allow synthesis of some membrane proteins and globular proteins at high levels. In *Journal of Molecular Biology* (Vol. 260, Issue 3, pp. 289–298). Academic Press. https://doi.org/10.1006/jmbi.1996.0399

Morton, C. O., Dos Santos, S. C., & Coote, P. (2007). An amphibian-derived, cationic, α-helical antimicrobial peptide kills yeast by caspase-independent but AIF-dependent programmed cell death. *Molecular Microbiology*, *65*(2), 494–507. https://doi.org/10.1111/j.1365-

2958.2007.05801.x

Mosbach, A., Edel, D., Farmer, A. D., Widdison, S., Barchietto, T., Dietrich, R. A., Corran, A., & Scalliet, G. (2017). Anilinopyrimidine resistance in *Botrytis cinerea* is linked to mitochondrial function. *Frontiers in Microbiology*, *8*(NOV). https://doi.org/10.3389/fmicb.2017.02361

Nagai, K. (1998). Studies on the distribution of alkalophilic and alkali-tolerant soil fungi II: Fungal flora in two limestone caves in Japan. *Mycoscience*, *39*(3), 293–298. https://doi.org/10.1007/bf02464011

Nass, M. M., & Nass, S. (1963). Intramitochondrial fibers with DNA characteristics. *The Journal of Cell Biology*, *19*(3), 593–611. https://doi.org/10.1083/jcb.19.3.593

Nelissen, B., De Wachter, R., & Goffeau, A. (1997). Classification of all putative permeases and other membrane plurispanners of the major facilitator superfamily encoded by the complete genome of *Saccharomyces cerevisiae*. *FEMS Microbiology Reviews*, *21*(2), 113–134. https://doi.org/10.1016/S0168-6445(97)00053-3

Nunes, P. A., Tenreiro, S., & Sá-Correia, I. (2001). Resistance and adaptation to quinidine in *Saccharomyces cerevisiae*: Role of QDR1 (YIL120w), encoding a plasma membrane transporter of the major facilitator superfamily required for multidrug resistance. *Antimicrobial Agents and Chemotherapy*, *45*(5), 1528–1534. https://doi.org/10.1128/AAC.45.5.1528-1534.2001

Olsen, B., Murakami, C. J., & Kaeberlein, M. (2010). YODA: Software to facilitate high-throughput analysis of chronological life span, growth rate, and survival in budding yeast. *BMC Bioinformatics*, *11*. https://doi.org/10.1186/1471-2105-11-141

Onofri, S., Anastasi, A., Del Frate, G., Di Piazza, S., Garnero, N., Guglielminetti, M., Isola, D.,

Panno, L., Ripa, C., Selbmann, L., Varese, G. C., Voyron, S., Zotti, M., & Zucconi, L. (2011). Biodiversity of rock, beach and water fungi in Italy. *Plant Biosystems, 145*(4), 978–987. https://doi.org/10.1080/11263504.2011.633117

Özcan, S., & Johnston, M. (1999). Function and Regulation of Yeast Hexose Transporters. *Microbiology and Molecular Biology Reviews*, *63*(3), 554–569. https://doi.org/10.1128/mmbr.63.3.554-569.1999

Ozsvari, B., Fiorillo, M., Bonuccelli, G., Cappello, A. R., Frattaruolo, L., Sotgia, F., Trowbridge, R., Foster, R., & Lisanti, M. P. (2017). Mitoriboscins: Mitochondrial-based therapeutics targeting cancer stem cells (CSCs), bacteria and pathogenic yeast. *Oncotarget*, *8*(40), 67457–67472. https://doi.org/10.18632/oncotarget.19084

Paixão, L., Rodrigues, L., Couto, I., Martins, M., Fernandes, P., de Carvalho, C. C. C. R., Monteiro, G. A., Sansonetty, F., Amaral, L., & Viveiros, M. (2009). Fluorometric determination of ethidium bromide efflux kinetics in *Escherichia coli*. *Journal of Biological Engineering*, *3*. https://doi.org/10.1186/1754-1611-3-18

Pao, S. S., Paulsen, I. A. N. T., & Saier, M. H. (1998). Major Facilitator Superfamily-1.pdf. *Microbiology and Molecular Biology Reviews*, *62*(1), 1–34. https://doi.org/1092-2172/98

Paulsen, I. T., Sliwinski, M. K., Nelissen, B., Goffeau, A., & Saier, M. H. (1998). Unified inventory of established and putative transporters encoded within the complete genome of *Saccharomyces cerevisiae*. *FEBS Letters*, *430*(1–2), 116–125. https://doi.org/10.1016/S0014-5793(98)00629-2

Pebay-Peyroula, E., Dahout-Gonzalez, C., Kahn, R., Trézéguet, V., Lauquin, G. J. M., & Brandolin, G. (2003). Structure of mitochondrial ADP/ATP carrier in complex with carboxyatractyloside. *Nature*, *426*(6962), 39–44. https://doi.org/10.1038/nature02056

Pellegrino, M. W., & Haynes, C. M. (2015). Mitophagy and the mitochondrial unfolded protein response in neurodegeneration and bacterial infection. In *BMC Biology* (Vol. 13, Issue 1, p. 22). BioMed Central Ltd. https://doi.org/10.1186/s12915-015-0129-1

Pochini, L., Galluccio, M., Scumaci, D., Giangregorio, N., Tonazzi, A., Palmieri, F., & Indiveri, C. (2008). Interaction of β-lactam antibiotics with the mitochondrial carnitine/acylcarnitine transporter. *Chemico-Biological Interactions*, *173*(3), 187–194. https://doi.org/10.1016/j.cbi.2008.03.003

Portier, P. (1918). *Les Symbiotes*. Paris, France: Masson et Cie. https://en.wikipedia.org/wiki/Symbiogenesis#cite_ref-8

Prasad, R., & Rawal, M. K. (2014). Efflux pump proteins in antifungal resistance. In *Frontiers in Pharmacology: Vol. 5 AUG* (p. 202). Frontiers Research Foundation. https://doi.org/10.3389/fphar.2014.00202

Qing, G., Ma, L. C., Khorchid, A., Swapna, G. V. T., Mal, T. K., Takayama, M. M., Xia, B., Phadtare, S., Ke, H., Acton, T., Montelione, G. T., Ikura, M., & Inouye, M. (2004). Cold-shock induced high-yield protein production in *Escherichia coli*. *Nature Biotechnology*, *22*(7), 877–882. https://doi.org/10.1038/nbt984

Quan, J., & Tian, J. (2009). Circular polymerase extension cloning of complex gene libraries and pathways. *PLoS ONE*, *4*(7), e6441. https://doi.org/10.1371/journal.pone.0006441

Reddy, V. S., Shlykov, M. A., Castillo, R., Sun, E. I., & Saier, M. H. (2012). The major facilitator superfamily (MFS) revisited. *FEBS Journal*, *279*(11), 2022–2035. https://doi.org/10.1111/j.1742-4658.2012.08588.x

Remy, E., Niño-González, M., Godinho, C. P., Cabrito, T. R., Teixeira, M. C., Sá-Correia, I., & Duque, P. (2017). Heterologous expression of the yeast Tpo1p or Pdr5p membrane

transporters in Arabidopsis confers plant xenobiotic tolerance. *Scientific Reports*, *7*(1). https://doi.org/10.1038/s41598-017-04534-7

Ren, Q., Chen, K., & Paulsen, I. T. (2007). TransportDB: A comprehensive database resource for cytoplasmic membrane transport systems and outer membrane channels. *Nucleic Acids Research*, *35*(SUPPL. 1), D274. https://doi.org/10.1093/nar/gkl925

Riesbeck, K., Bredberg, A., & Forsgren, A. (1990). Ciprofloxacin does not inhibit mitochondrial functions but other antiboitics do. *Antimicrobial Agents and Chemotherapy*, *34*(1), 167–169. https://doi.org/10.1128/AAC.34.1.167

Ritch, J. J., Davidson, S. M., Sheehan, J. J., & Austriaco, O.P., N. (2010). Ritch, J. J., Davidson, S. M., Sheehan, J. J., & Austriaco, O.P., N. (2010). The *Saccharomyces* SUN gene, UTH1 , is involved in cell wall biogenesis. FEMS Yeast Research, 10(2), 168–176. https://doi.org/10.1111/j.1567-1364.2009.00601.xThe Saccharomyces SUN. *FEMS Yeast Research*, *10*(2), 168–176. https://doi.org/10.1111/j.1567-1364.2009.00601.x

Rizzuto, R., De Stefani, D., Raffaello, A., & Mammucari, C. (2012). Mitochondria as sensors and regulators of calcium signalling. In *Nature Reviews Molecular Cell Biology* (Vol. 13, Issue 9, pp. 566–578). https://doi.org/10.1038/nrm3412

Roede, J. R., & Jones, D. P. (2014). Thiol-reactivity of the fungicide maneb. *Redox Biology*, *2*(1), 651–655. https://doi.org/10.1016/j.redox.2014.04.007

Roetzer, A., Gabaldón, T., & Schüller, C. (2011). From *Saccharomyces cerevisiae* to *Candida glabrata* in a few easy steps: Important adaptations for an opportunistic pathogen. In *FEMS Microbiology Letters* (Vol. 314, Issue 1, pp. 1–9). Wiley-Blackwell. https://doi.org/10.1111/j.1574-6968.2010.02102.x

Rosano, G. L., & Ceccarelli, E. A. (2014). Recombinant protein expression in *Escherichia coli*:

Advances and challenges. In *Frontiers in Microbiology* (Vol. 5, Issue APR). Frontiers Research Foundation. https://doi.org/10.3389/fmicb.2014.00172

Sá-Correia, I., dos Santos, S. C., Teixeira, M. C., Cabrito, T. R., & Mira, N. P. (2009). Drug:H+ antiporters in chemical stress response in yeast. In *Trends in Microbiology* (Vol. 17, Issue 1, pp. 22–31). Trends Microbiol. https://doi.org/10.1016/j.tim.2008.09.007

Sagan, L. (1967). On the origin of mitosing cells. *Journal of Theoretical Biology*, *14*(3). https://doi.org/10.1016/0022-5193(67)90079-3

Saitou, N., & Nei, M. (1987). The neighbor-joining method: a new method for reconstructing phylogenetic trees. *Molecular Biology and Evolution*, *4*(4), 406–425. https://doi.org/10.1093/oxfordjournals.molbev.a040454

Santos, P. M., Simões, T., & Sá-Correia, I. (2009). Insights into yeast adaptive response to the agricultural fungicide mancozeb: A toxicoproteomics approach. *Proteomics*, *9*(3), 657–670. https://doi.org/10.1002/pmic.200800452

Sanyal, D., & Kulshrestha, G. (2002). Metabolism of metolachlor by fungal cultures. *Journal of Agricultural and Food Chemistry*, *50*(3), 499–505. https://doi.org/10.1021/jf010850d

Sayas, E., García-López, F., & Serrano, R. (2015). Toxicity, mutagenicity and transport in *Saccharomyces cerevisiae* of three popular DNA intercalating fluorescent dyes. *Yeast*, *32*(9), 595–606. https://doi.org/10.1002/yea.3081

Schatz, G., Haslbrunner, E., & Tuppy, H. (1964). Deoxyribonucleic acid associated with yeast mitochondria. *Biochemical and Biophysical Research Communications*, *15*(2), 127–132. https://doi.org/10.1016/0006-291X(64)90311-0

Schein, C. H. (1989). Production of soluble recombinant proteins in bacteria. *Nature Biotechnology*, *7*(11), 1141–1149. https://doi.org/10.1038/nbt1189-1141

Schlünzen, F., Zarivach, R., Harms, J., Bashan, A., Tocilj, A., Albrecht, R., Yonath, A., & Franceschi, F. (2001). Structural basis for the interaction of antibiotics with the peptidyl transferase centre in eubacteria. *Nature*, *413*(6858), 814–821. https://doi.org/10.1038/35101544

Schmidt, O., Pfanner, N., & Meisinger, C. (2010). Mitochondrial protein import: From proteomics to functional mechanisms. In *Nature Reviews Molecular Cell Biology* (Vol. 11, Issue 9, pp. 655–667). https://doi.org/10.1038/nrm2959

Schnappinger, D., & Hillen, W. (1996). Tetracyclines: Antibiotic action, uptake, and resistance mechanisms. In *Archives of Microbiology* (Vol. 165, Issue 6, pp. 359–369). Springer Verlag. https://doi.org/10.1007/s002030050339

Schneider-Poetsch, T., Ju, J., Eyler, D. E., Dang, Y., Bhat, S., Merrick, W. C., Green, R., Shen, B., & Liu, J. O. (2010). Inhibition of eukaryotic translation elongation by cycloheximide and lactimidomycin. *Nature Chemical Biology*, *6*(3), 209–217. https://doi.org/10.1038/nchembio.304

Schneider, C. A., Rasband, W. S., & Eliceiri, K. W. (2012). NIH Image to ImageJ: 25 years of image analysis. In *Nature Methods* (Vol. 9, Issue 7, pp. 671–675). NIH Public Access. https://doi.org/10.1038/nmeth.2089

Sebald, W., Neupert, W., & Weiss, H. (1979). Preparation of Neurospora Crassa Mitochondria. *Methods in Enzymology*, *55*(C), 144–148. https://doi.org/10.1016/0076-6879(79)55020-4

Seiler, N. (1999). A Guide to the Polyamines . Seymour S. Cohen. *The Quarterly Review of Biology*, *74*(3), 342–343. https://doi.org/10.1086/393192

Selbmann, L., De Hoog, G. S., Mazzaglia, A., Friedmann, E. I., & Onofri, S. (2005). Fungi at the edge of life: Cryptoendolithic black fungi from Antarctic desert. *Studies in Mycology*, *51*,

1–32.

Selbmann, L., de Hoog, G. S., Zucconi, L., Isola, D., Ruisi, S., Gerrits van den Ende, A. H. G., Ruibal, C., De Leo, F., Urzì, C., & Onofri, S. (2008). Drought meets acid: three new genera in a dothidealean clade of extremotolerant fungi. *Studies in Mycology*, *61*, 1–20. https://doi.org/10.3114/sim.2008.61.01

Shockman, G. D., & Lampen, J. O. (1962). Inhibition by antibiotics of the growth of bacterial and yeast protoplasts. *Journal of Bacteriology, 84*(3), 508–512. https://doi.org/10.1128/jb.84.3.508-512.1962

Siibak, T., Peil, L., Xiong, L., Mankin, A., Remme, J., & Tenson, T. (2009). Erythromycin- and chloramphenicol-induced ribosomal assembly defects are secondary effects of protein synthesis inhibition. *Antimicrobial Agents and Chemotherapy*, *53*(2), 563–571. https://doi.org/10.1128/AAC.00870-08

Sikkema, J., De Bont, J. A. M., & Poolman, B. (1995). Mechanisms of membrane toxicity of hydrocarbons. In *Microbiological Reviews* (Vol. 59, Issue 2, pp. 201–222). American Society for Microbiology. https://doi.org/10.1128/mmbr.59.2.201-222.1995

Sikorski, R. S., & Hieter, P. (1989). A system of shuttle vectors and yeast host strains designed for efficient manipulation of DNA in *Saccharomyces cerevisiae*. *Genetics*, *122*(1), 19–27. https://doi.org/10.1093/genetics/122.1.19

Singh, A., Lal, U. R., Mukhtar, H. M., Singh, P. S., Shah, G., & Dhawan, R. K. (2015). Phytochemical profile of sugarcane and its potential health aspects. In *Pharmacognosy Reviews* (Vol. 9, Issue 17, pp. 45–54). Medknow Publications. https://doi.org/10.4103/0973-7847.156340

Singh, M., Sykes, E. M. E., Li, Y., & Kumar, A. (2020). Mexxy rnd pump of pseudomonas

aeruginosa pa7 effluxes bi-anionic β-lactams carbenicillin and sulbenicillin when it partners with the outer membrane factor opra but not with oprm. *Microbiology (United Kingdom)*, *166*(11), 1095–1106. https://doi.org/10.1099/mic.0.000971

Singh, R., Sripada, L., & Singh, R. (2014). Side effects of antibiotics during bacterial infection: Mitochondria, the main target in host cell. *Mitochondrion*, *16*, 50–54. https://doi.org/10.1016/j.mito.2013.10.005

Siu, Y., Fenno, J., Lindle, J. M., & Dunlop, M. J. (2018). Design and Selection of a Synthetic Feedback Loop for Optimizing Biofuel Tolerance. *ACS Synthetic Biology*, *7*(1), 16–23. https://doi.org/10.1021/acssynbio.7b00260

Solieri, L. (2010). Mitochondrial inheritance in budding yeasts: Towards an integrated understanding. In *Trends in Microbiology* (Vol. 18, Issue 11, pp. 521–530). Elsevier. https://doi.org/10.1016/j.tim.2010.08.001

Somasundaram, S., Rafi, S., Hayllar, J., Sigthorsson, G., Jacob, M., Price, A. B., Macpherson, A., Mahmod, T., Scott, D., Wrigglesworth, J. M., & Bjarnason, I. (1997). Mitochondrial damage: A possible mechanism of the "topical" phase of NSAID induced injury to the rat intestine. *Gut*, *41*(3), 344–353. https://doi.org/10.1136/gut.41.3.344

Studier, F. W. (2005). Protein production by auto-induction in high density shaking cultures. *Protein Expression and Purification*, *41*(1), 207–234. https://doi.org/10.1016/j.pep.2005.01.016

Summers, W. A. T., Wilkins, J. A., Dwivedi, R. C., Ezzati, P., & Court, D. A. (2012). Mitochondrial dysfunction resulting from the absence of mitochondrial porin in *Neurospora crassa*. *Mitochondrion*, *12*(2), 220–229. https://doi.org/10.1016/j.mito.2011.09.002

Szklarczyk, R., & Huynen, M. A. (2010). Mosaic origin of the mitochondrial proteome. In

Proteomics (Vol. 10, Issue 22, pp. 4012–4024). Proteomics. https://doi.org/10.1002/pmic.201000329

Tachihara, K., Uemura, T., Kashiwagi, K., & Igarashi, K. (2005). Excretion of putrescine and spermidine by the protein encoded by YKL174c (TPO5) in *Saccharomyces cerevisiae*. *Journal of Biological Chemistry*, *280*(13), 12637–12642. https://doi.org/10.1074/jbc.M410778200

Teixeira, Miguel C., Telo, J. P., Duarte, N. F., & Sá-Correia, I. (2004). The herbicide 2,4-dichlorophenoxyacetic acid induces the generation of free-radicals and associated oxidative stress responses in yeast. *Biochemical and Biophysical Research Communications*, *324*(3), 1101–1107. https://doi.org/10.1016/j.bbrc.2004.09.158

Teixeira, Miguel Cacho, Dias, P. J., Simões, T., & Sá-Correia, I. (2008). Yeast adaptation to mancozeb involves the up-regulation of FLR1 under the coordinate control of Yap1, Rpn4, Pdr3, and Yrr1. *Biochemical and Biophysical Research Communications*, *367*(2), 249–255. https://doi.org/10.1016/j.bbrc.2007.12.056

Teixeira, Miguel Cacho, & Sá-Correia, I. (2002). *Saccharomyces cerevisiae* resistance to chlorinated phenoxyacetic acid herbicides involves Pdr1p-mediated transcriptional activation of TPO1 and PDR5 genes. *Biochemical and Biophysical Research Communications*, *292*(2), 530–537. https://doi.org/10.1006/bbrc.2002.6691

Tenreiro, S., Rosa, P. C., Viegas, C. A., & Sá-Correia, I. (2000). Expression of the AZR1 gene (ORF YGR224w), encoding a plasma membrane transporter of the major facilitator superfamily, is required for adaptation to acetic acid and resistance to azoles in *Saccharomyces cerevisiae*. *Yeast*, *16*(16), 1469–1481. https://doi.org/10.1002/1097-0061(200012)16:16<1469::AID-YEA640>3.0.CO;2-A

Tenson, T., Lovmar, M., & Ehrenberg, M. (2003). The mechanism of action of macrolides, lincosamides and streptogramin B reveals the nascent peptide exit path in the ribosome. *Journal of Molecular Biology, 330*(5), 1005–1014. https://doi.org/10.1016/S0022-2836(03)00662-4

Thyagarajan, D., Bressman, S., Bruno, C., Przedborski, S., Shanske, S., Lynch, T., Fahn, S., & Dimauro, S. (2000). A novel mitochondrial 12SrRNA point mutation in parkinsonism, deafness, and neuropathy. *Annals of Neurology, 48*(5), 730–736. https://doi.org/10.1002/1531-8249(200011)48:5<730::AID-ANA6>3.0.CO;2-0

Tomitori, H., Kashiwagi, K., Asakawa, T., Kakinuma, Y., Michael, A. J., & Igarashi, K. (2001). Multiple polyamine transport systems on the vacuolar membrane in yeast. *Biochemical Journal*, *353*(3), 681–688. https://doi.org/10.1042/0264-6021:3530681

Tu, D., Blaha, G., Moore, P. B., & Steitz, T. A. (2005). Structures of MLSBK antibiotics bound to mutated large ribosomal subunits provide a structural explanation for resistance. *Cell*, *121*(2), 257–270. https://doi.org/10.1016/j.cell.2005.02.005

Tune, B. M. (1997). Nephrotoxicity of beta-lactam antibiotics: Mechanisms and strategies for prevention. *Pediatric Nephrology*, *11*(6), 768–772. https://doi.org/10.1007/s004670050386

Turcotte, B., Liang, X. B., Robert, F., & Soontorngun, N. (2010). Transcriptional regulation of nonfermentable carbon utilization in budding yeast. In *FEMS Yeast Research* (Vol. 10, Issue 1, pp. 2–13). https://doi.org/10.1111/j.1567-1364.2009.00555.x

Uemura, T., Kashiwagi, K., & Igarashi, K. (2005). Uptake of putrescine and spermidine by Gap1p on the plasma membrane in *Saccharomyces cerevisiae*. *Biochemical and Biophysical Research Communications*, *328*(4), 1028–1033. https://doi.org/10.1016/j.bbrc.2005.01.064

Uemura, T., Kashiwagi, K., & Igarashi, K. (2007). Polyamine uptake by DUR3 and SAM3 in

Saccharomyces cerevisiae. *Journal of Biological Chemistry*, *282*(10), 7733–7741. https://doi.org/10.1074/jbc.M611105200

Uemura, T., Tachihara, K., Tomitori, H., Kashiwagi, K., & Igarashi, K. (2005). Characteristics of the polyamine transporter TPO1 and regulation of its activity and cellular localization by phosphorylation. *Journal of Biological Chemistry*, *280*(10), 9646–9652. https://doi.org/10.1074/jbc.M410274200

Uemura, T., Tomonari, Y., Kashiwagi, K., & Igarashi, K. (2004). Uptake of GABA and putrescine by UGA4 on the vacuolar membrane in *Saccharomyces cerevisiae*. *Biochemical and Biophysical Research Communications*, *315*(4), 1082–1087. https://doi.org/10.1016/j.bbrc.2004.01.162

van den Bogert, C., & Kroon, A. M. (1981). Tissue distribution and effects on mitochondrial protein synthesis of tetracyclines after prolonged continuous intravenous administration to rats. *Biochemical Pharmacology*, *30*(12), 1706–1709. https://doi.org/10.1016/0006-2952(81)90403-2

Van den Bogert, C., Lont, M., Mojet, M., & Kroon, A. M. (1983). Impairment of liver regeneration during inhibition of mitochondrial protein synthesis by oxytetracycline. *BBA - Bioenergetics*, *722*(3), 393–400. https://doi.org/10.1016/0005-2728(83)90054-3

Vane, J. R., & Botting, R. M. (1998). Mechanism of action of antiinflammatory drugs. In *International Journal of Tissue Reactions* (Vol. 20, Issue 1, pp. 3–15). Scand J Rheumatol Suppl. https://doi.org/10.3109/03009749609097226

Viegas, C. A., Cabral, M. G., Teixeira, M. C., Neumann, G., Heipieper, H. J., & Sá-Correia, I. (2005). Yeast adaptation to 2,4-dichlorophenoxyacetic acid involves increased membrane fatty acid saturation degree and decreased OLE1 transcription. *Biochemical and Biophysical*

Research Communications, *330*(1), 271–278. https://doi.org/10.1016/j.bbrc.2005.02.158

Vincze, T., Posfai, J., & Roberts, R. J. (2003). NEBcutter: A program to cleave DNA with restriction enzymes. *Nucleic Acids Research*, *31*(13), 3688–3691. https://doi.org/10.1093/nar/gkg526

Viveiros, M., Martins, M., Couto, I., Rodrigues, L., Spengler, G., Martins, A., Kristiansen, J., Molnar, J., & Amaral, L. (2008). New Methods for the Identification of Efflux Mediated MDR Bacteria, Genetic Assessment of Regulators and Efflux Pump Constituents, Characterization of Efflux Systems and Screening for Inhibitors of Efflux Pumps. *Current Drug Targets*, *9*(9), 760–778. https://doi.org/10.2174/138945008785747734

Viveiros, Miguel, Martins, A., Paixão, L., Rodrigues, L., Martins, M., Couto, I., Fähnrich, E., Kern, W. V., & Amaral, L. (2008a). Demonstration of intrinsic efflux activity of *Escherichia coli* K-12 AG100 by an automated ethidium bromide method. *International Journal of Antimicrobial Agents*, *31*(5), 458–462. https://doi.org/10.1016/j.ijantimicag.2007.12.015

Vogel, F., Bornhövd, C., Neupert, W., & Reichert, A. S. (2006). Dynamic subcompartmentalization of the mitochondrial inner membrane. *Journal of Cell Biology*, *175*(2), 237–247. https://doi.org/10.1083/jcb.200605138

Vögtle, F. N., Burkhart, J. M., Gonczarowska-Jorge, H., Kücükköse, C., Taskin, A. A., Kopczynski, D., Ahrends, R., Mossmann, D., Sickmann, A., Zahedi, R. P., & Meisinger, C. (2017). Landscape of submitochondrial protein distribution. *Nature Communications*, *8*(1). https://doi.org/10.1038/s41467-017-00359-0

Wagner, S., Klepsch, M. M., Schlegel, S., Appel, A., Draheim, R., Tarry, M., Högbom, M., Van Wijk, K. J., Slotboom, D. J., Persson, J. O., & De Gier, J. W. (2008). Tuning *Escherichia*

coli for membrane protein overexpression. *Proceedings of the National Academy of Sciences of the United States of America*, *105*(38), 14371–14376. https://doi.org/10.1073/pnas.0804090105

Wallin, I. E. (1927). *Symbionticism and the origin of species*. Waverly press; Baltimore, USA: Williams & Wilkins Company. https://archive.org/details/symbionticismori00wall/page/n5/mode/2up?view=theater

Wallin, Ivan E. (1923). The Mitochondria Problem. *The American Naturalist*, *57*(650), 255–261. https://doi.org/10.1086/279919

Warringer, J., Ericson, E., Fernandez, L., Nerman, O., & Blomberg, A. (2003). High-resolution yeast phenomics resolves different physiological features in the saline response. *Proceedings of the National Academy of Sciences of the United States of America*, *100*(26), 15724–15729. https://doi.org/10.1073/pnas.2435976100

Wasungu, K. M., & Simard, R. E. (1982). Growth characteristics of bakers' yeast in ethanol. *Biotechnology and Bioengineering*, *24*(5), 1125–1134. https://doi.org/10.1002/bit.260240509

Wetzel, R. (1992). Principles of protein stability. In editors. In: Rees, AR.; Sternberg, MJE; Wetzel, R. (Ed.), *Protein Engineering: A Practical Approach.* (pp. 191–216). Oxford: IRL Press;

Wickner, R. B. (1991). Methods in yeast genetics: A laboratory course manual. *Analytical Biochemistry*, *197*(1), 273–274. https://doi.org/10.1016/0003-2697(91)90389-b

Wieczorke, R., Krampe, S., Weierstall, T., Freidel, K., Hollenberg, C. P., & Boles, E. (1999). Concurrent knock-out of at least 20 transporter genes is required to block uptake of hexoses in *Saccharomyces cerevisiae*. *FEBS Letters*, *464*(3), 123–128.

https://doi.org/10.1016/S0014-5793(99)01698-1

Winston, F., Dollard, C., & Ricupero-Hovasse, S. L. (1995). Construction of a set of convenient *Saccharomyces cerevisiae* strains that are isogenic to S288C. *Yeast*, *11*(1), 53–55. https://doi.org/10.1002/yea.320110107

Wolf, K., & Del Giudice, L. (1988). The Variable Mitochondrial Genome of Ascomycetes: Organization, Mutational Alterations, and Expression. *Advances in Genetics*, *25*(C), 185–308. https://doi.org/10.1016/S0065-2660(08)60460-5

Wolfe, K. H., & Shields, D. C. (1997). Molecular evidence for an ancient duplication of the entire yeast genome. *Nature*, *387*(6634), 708–713. https://doi.org/10.1038/42711

Yan, W., Aebersold, R., & Raines, E. W. (2009). Evolution of organelle-associated protein profiling. In *Journal of Proteomics* (Vol. 72, Issue 1, pp. 4–11). J Proteomics. https://doi.org/10.1016/j.jprot.2008.11.017

Yang, D., Oyaizu, Y., Oyaizu, H., Olsen, G. J., & Woese, C. R. (1985). Mitochondrial origins. *Proceedings of the National Academy of Sciences of the United States of America*, *82*(13), 4443–4447. https://doi.org/10.1073/pnas.82.13.4443

Young, M. J., & Court, D. A. (2008). Effects of the S288c genetic background and common auxotrophic markers on mitochondrial DNA function in *Saccharomyces cerevisiae*. *Yeast*, *25*(12), 903–912. https://doi.org/10.1002/yea.1644

Yunis, A. A. (1989). Chloramphenicol toxicity: 25 years of research. In *American Journal of Medicine* (Vol. 87, Issue 3 N).

Zuckerkandl, E., & Pauling, L. (1965). Evolutionary Divergence and Convergence in Proteins. In *Evolving Genes and Proteins* (pp. 97–166). https://doi.org/10.1016/b978-1-4832-2734-4.50017-6